Please type a plus sign (+) inside this box → [+] PTO/SB/21 (6-99)

4-14-08   IK AF

TRANSMITTAL FORM

(to be used for all correspondence after initial filing)

Application Number	09/941,992
Filing Date	August 28, 2001
First Named Inventor	Avi, ASHKENAZI, et al.
Group/Art Unit	1646
Examiner Name	Elizabeth, KEMMERER

Total Number of Pages in This Submission		**Attorney Docket Number**	123851-181895P1C1 (formerly 39780-2730-P1C1)

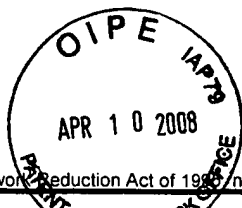## ENCLOSURES *(check all that apply)*

- ☒ Fee Transmittal Form
  - ☐ Fee Attached
- ☐ Amendment / Response
  - ☐ After Final
  - ☐ Version With Markings Showing Changes
  - ☐ Affidavits/declaration(s)
- ☒ Extension of Time Request – 2 months
- ☐ Information Disclosure Statement
- ☐ Certified Copy of Priority Document(s)
- ☐ Response to Missing Parts/ Incomplete Application
  - ☐ Response to Missing Parts under 37 CFR 1.52 or 1.53
  - ☐ Copy of Notice

- ☐ Copy of Assignment
- ☐ Amendment Under 37 CFR §1.48(b)
- ☐ Licensing-related Papers
- ☐ Petition Routing Slip (PTO/SB/69) and Accompanying Petition
- ☐ Petition to Convert to a Provisional Application
- ☐ Power of Attorney, by Assignee to Exclusion of Inventor Under 37 C.F.R. §3.71 With Revocation of Prior Powers
- ☐ Terminal Disclaimer
- ☐ Small Entity Statement
- ☐ Request for Refund

- ☐ After Allowance Communication to Group
- ☐ Appeal Communication to Board of Appeals and Interferences
- ☒ **APPEAL COMMUNICATION TO GROUP** *(APPEAL NOTICE, BRIEF, REPLY BRIEF)*
- ☐ Proprietary Information
- ☐ Status Letter
- ☒ Additional Enclosure(s) *(Please Identify Below):*
- ☒ **EVIDENCE APPENDIX ITEMS 1-9**

Remarks

AUTHORIZATION TO CHARGE DEPOSIT ACCOUNT 07-1700 FOR ANY FEES DUE IN CONNECTION WITH THIS PAPER, REFERENCING ATTORNEY'S DOCKET NO. 39780-2730 P1C1.

SIGNATURE OF APPLICANT, ATTORNEY OR AGENT

Firm *or* Individual name	GOODWIN PROCTER LLP	PANPAN GAO (Reg. No. 43,626)	
	135 Commonwealth Drive, Menlo Park, California 94025	Telephone: (650) 752-3100	Facsimile: (650) 853-1038
Signature			
Date	APRIL 10, 2008	Customer Number:	77845

FILED VIA EXPRESS MAIL NO. EB 985 660 876 US
ON APRIL 10, 2008

PTO/SB/17 (12-04)
Approved for use through 07/31/2006. OMB 0651-0032
U.S. Patent and Trademark Office; U.S. DEPARTMENT OF COMMERCE
Under the Paperwork Reduction Act of 1995, no persons are required to respond to a collection of information unless it displays a valid OMB control number.

OIPE APR 1 0 2008

FEE TRANSMITTAL
for FY 2008
Effective 10/01/2003. Patent fees are subject to annual revision.

Complete if Known	
Application Number	**09/941,992**
Filing Date	**August 28, 2001**
First Named Inventor	**Avi, ASHKENAZI, et al.**
Examiner Name	**Elizabeth, KEMMERER**
Art Unit	**1646**
Attorney Docket No.	**123851-181895 (39780-2730P1C1)**

☐ Applicant claims small entity status. See 37 CFR 1.27

TOTAL AMOUNT OF PAYMENT	($) 970.00

METHOD OF PAYMENT (check all that apply)

☐ Check ☐ Credit card ☐ Money Order ☐ Other ☐ None

☑ Deposit Account:

Deposit Account Number: **07-1700**

Deposit Account Name: **GOODWIN PROCTER LLP**

The Director is authorized to: *(check all that apply)*

☑ Charge fee(s) indicated below   ☑ Credit any overpayments

☑ Charge any additional fee(s) or any underpayment of fee(s)

☐ Charge fee(s) indicated below, **except for the filing fee**
to the above-identified deposit account.

FEE CALCULATION

1. BASIC FILING FEE

Large Entity Fee Code	Fee ($)	Small Entity Fee Code	Fee ($)	Fee Description	Fee Paid
1001	810	2001	405	Utility filing fee	
1002	360	2002	180	Design filing fee	
1003	570	2003	285	Plant filing fee	
1004	810	2004	405	Reissue filing fee	
1005	210	2005	105	Provisional filing fee	

SUBTOTAL (1) ($)

2. EXTRA CLAIM FEES FOR UTILITY AND REISSUE

	Extra Claims	Fee from below	Fee Paid
Total Claims	-20** =	X	=
Independent Claims	- 3** =	X	=
Multiple Dependent			=

Large Entity Fee Code	Fee ($)	Small Entity Fee Code	Fee ($)	Fee Description
1202	50	2202	25	Claims in excess of 20
1201	210	2201	105	Independent claims in excess of 3
1203	370	2203	185	Multiple dependent claim, if not paid
1204	210	2204	105	** Reissue independent claims over original patent
1205	50	2205	25	** Reissue claims in excess of 20 and over original patent

SUBTOTAL (2) ($)

**or number previously paid, if greater; For Reissues, see above

FEE CALCULATION (continued)

3. ADDITIONAL FEES

Large Entity Fee Code	Fee ($)	Small Entity Fee Code	Fee ($)	Fee Description	Fee Paid
1051	130	2051	65	Surcharge - late filing fee or oath	
1052	50	2052	25	Surcharge - late provisional filing fee or cover sheet	
1053	130	1053	130	Non-English specification	
1812	2,520	1812	2,520	For filing a request for *ex parte* reexamination	
1804	920*	1804	920*	Requesting publication of SIR prior to Examiner action	
1805	1,840*	1805	1,840*	Requesting publication of SIR after Examiner action	
1251	120	2251	60	Extension for reply within first month	
1252	460	2252	230	Extension for reply within second month	460.00
1253	1,050	2253	525	Extension for reply within third month	
1254	1,640	2254	820	Extension for reply within fourth month	
1255	2,230	2255	1,115	Extension for reply within fifth month	
1401	510	2401	255	Notice of Appeal	
1402	510	2402	255	Filing a brief in support of an appeal	510.00
1403	1,030	2403	515	Request for oral hearing	
1451	1,510	1451	1,510	Petition to institute a public use proceeding	
1452	510	2452	255	Petition to revive - unavoidable	
1453	1,540	2453	770	Petition to revive - unintentional	
1501	1,440	2501	720	Utility issue fee (or reissue)	
1502	820	2502	410	Design issue fee	
1503	1,130	2503	565	Plant issue fee	
1460	130	1460	130	Petitions to the Commissioner	
1807	50	1807	50	Processing fee under 37 CFR 1.17(q)	
1806	180	1806	180	Submission of Information Disclosure Stmt	
8021	40	8021	40	Recording each patent assignment per property (times number of properties)	
1809	810	2809	405	Filing a submission after final rejection (37 CFR 1.129(a))	
1810	810	2810	405	For each additional invention to be examined (37 CFR 1.129(b))	
1801	810	2801	405	Request for Continued Examination (RCE)	
1802	900	1802	900	Request for expedited examination of a design application	

Other fee (specify) _____

*Reduced by Basic Filing Fee Paid

SUBTOTAL (3) ($) 970.00

SUBMITTED BY

	(Complete *(if applicable)*)		
Name (Print/Type) **PANPAN GAO**	Registration No. (Attorney/Agent) **43,626**	Telephone **(650) 752-3100**
Signature	Date **APRIL 10, 2008**

WARNING: Information on this form may become public. Credit card information should not be included on this form. Provide credit card information and authorization on PTO-2038.

If you need assistance in completing the form, call 1-800-PTO-9199 and select option 2.

THE UNITED STATES PATENT AND TRADEMARK OFFICE

In re application of:)	Examiner: Kemmerer, Elizabeth
)	
Avi ASHKENAZI, *et al.*)	Art Unit: 1646
)	
Application Serial No. 09/941,992)	Confirmation No: 8312
)	
Filed: August 28, 2001)	Attorney's Docket No. 123851-181895
)	(formerly 39780-2730 P1C1)
For: **SECRETED AND TRANSMEMBRANE**)	
POLYPEPTIDES AND NUCLEIC)	**Customer No. 77845**
ACIDS ENCODING THE SAME)	

EXPRESS MAIL LABEL NO: EB 985 660 876 US
DATE MAILED: APRIL 10, 2008

ON APPEAL TO THE BOARD OF PATENT APPEALS AND INTERFERENCES
APPELLANTS' BRIEF

MAIL STOP APPEAL BRIEF - PATENTS
Commissioner for Patents
P.O. Box 1450
Alexandria, Virginia 22313-1450

Dear Sir:

This Appeal Brief, filed in connection with the above captioned patent application, is responsive to the Final Office Actions mailed on September 10, 2007. A Notice of Appeal was filed herein on December 10, 2007. A request for a two-months extension of time is requested herewith. Appellants hereby appeal to the Board of Patent Appeals and Interferences from the final rejection in this case.

The following constitutes the Appellants' Brief on Appeal.

-1-

I.   REAL PARTY IN INTEREST

The real party in interest is Genentech, Inc., South San Francisco, California, by an assignment of the application, U.S. Patent Application Serial No. 09/941,992 recorded November 16, 2001, at Reel 012176 and Frame 0450.

II.   RELATED APPEALS AND INTERFERENCES

The claims pending in the current application are directed to a polypeptide referred to herein as "PRO341". There exist two related patent applications, (1) U.S. Patent Application Serial No. 09/991,150, filed November 16, 2001, now abandoned (containing claims directed to nucleic acids encoding PRO341 polypeptides), and (2) U.S. Patent Application Serial No. 09/990,711, filed November 14, 2001 (containing claims directed to antibodies to PRO341 polypeptides). Related U.S. Patent Application Serial No. 09/990,711 is also under final rejection by the same Examiner and based upon the same outstanding rejections, an appeal is being pursued independently and concurrently herewith.

III.   STATUS OF CLAIMS

Claims 124-126 and 129-131 are in this application.

Claims 1-123 and 127-128 have been canceled.

Claims 124-126 and 129-131 stand rejected and Appellants appeal the rejection of these claims.

A copy of the rejected claims in the present Appeal is provided as Claims Appendix (Section VIII).

IV.   STATUS OF AMENDMENTS

A summary of the prosecution history for this case is as follows:

Previously, in response to a Final Office Action mailed on April 19, 2006, a Notice of Appeal was filed October 20, 2006 and an Appeal Brief was filed May 21, 2007. This was followed by another Final Office action mailed September 4, 2007, wherein the finality of the previous Office Action was withdrawn by the Examiner. A Notice of Appeal was filed on December 10, 2007 in this case.

No claim amendments have been submitted after the last final rejection of September 4, 2007. A copy of the rejected claims in the present Appeal is provided as Appendix A.

V. SUMMARY OF CLAIMED SUBJECT MATTER

The invention claimed in the present application is related to an isolated polypeptide comprising the amino acid sequence of the polypeptide of SEQ ID NO:20, referred to in the present application as "PRO341." The PRO341 gene was shown for the first time in the present application to be significantly amplified in human lung cancers as compared to normal, non-cancerous human tissue controls (Example 170). This feature is specifically recited in Claim 124, and carried by all claims dependent from Claim 124. In addition, the invention also claims the amino acid sequence of the polypeptide of SEQ ID NO:20, lacking its associated signal-peptide; or the amino acid sequence of the polypeptide encoded by the full-length coding sequence of the cDNA deposited under ATCC accession number 209792 (Claims 124-126 and 129). The invention is further directed to a chimeric polypeptide comprising one of the above polypeptides fused to a heterologous polypeptide (Claim 130), and to a chimeric polypeptide wherein the heterologous polypeptide is an epitope tag or an Fc region of an immunoglobulin (Claim 131). The preparation of chimeric PRO polypeptides (Claims 130 and 131), including those wherein the heterologous polypeptide is an epitope tag or an Fc region of an immunoglobulin, is set forth in the specification at page 374, lines 24 to page 375, line 9. Examples 140-143 and page 376, line 12 onwards describe the expression of PRO polypeptides in various host cells, including *E. coli*, mammalian cells, yeast and Baculovirus-infected insect cells.

The amino acid sequence of the native "PRO341" polypeptide and the nucleic acid sequence encoding this polypeptide (referred to in the present application as "DNA26288-1239") are shown in the present specification as SEQ ID NOs:20 and 19, respectively, and in Figures 12 and 11, described on pages 288, lines 14-17. The cDNA for PRO341 was deposited under ATCC accession number 209792.

Finally, Example 170, in the specification at page 539, line 19, to page 555, line 5, sets forth a 'Gene Amplification assay' which shows that the PRO341 gene is amplified in the genome of certain human lung cancers (see Table 9A, page 550, third column). The profiles of various primary lung tumors used for screening the PRO polypeptide compounds of the invention in the gene amplification assay are summarized on Table 8, page 546 of the specification.

VI. GROUNDS OF REJECTION TO BE REVIEWED ON APPEAL

1. Whether Claims 124-126 and 129-131 satisfy the utility/ enablement requirement under 35 U.S.C. §§101/112, first paragraph.

VII. ARGUMENTS

Summary of the Arguments

Issue 1: Utility/ Enablement

Appellants rely upon the gene amplification data of the PRO341 gene for patentable utility of the PRO341 polypeptides. This data is clearly disclosed in the instant specification in Example 170 which discloses that the gene encoding PRO341 showed <u>significant</u> amplification, ranging from **2.173 fold to 2.514-fold** in **three** different <u>lung primary tumors</u>.

Appellants have submitted, in their Response filed October 24, 2003, a Declaration by Dr. Audrey Goddard, which explains that a gene identified as being amplified <u>at least 2-fold</u> by the disclosed gene amplification assay in a tumor sample relative to a normal sample is <u>useful as a marker for the diagnosis of cancer</u>, and for monitoring cancer development and/or for measuring the efficacy of cancer therapy. Therefore, such a gene is <u>useful as a marker for the diagnosis of lung cancer</u>, and for monitoring cancer development and/or for measuring the efficacy of cancer therapy.

Appellants have also submitted throughout prosecution history ample evidence to show that, in general, if a gene is amplified in cancer, it is more likely than not that the encoded protein will be expressed at an elevated level. First, the articles by Orntoft *et al.*, Hyman *et al.*, and Pollack *et al.* collectively teach that <u>in general, gene amplification increases mRNA expression</u>.

Appellants further submit that even if there were no correlation between gene amplification and increased mRNA/protein expression, (which Appellants expressly do <u>not</u> concede), a polypeptide encoded by a gene that is amplified in cancer would <u>still</u> have a specific, substantial, and credible utility. Appellants submit that, as evidenced by the Ashkenazi Declaration and the teachings of Hanna and Mornin (both made of record in Appellants' Response filed June 18, 2004), simultaneous testing of gene amplification and gene product over-expression enables <u>more accurate tumor classification</u>, even if the gene-product, the protein, is not over-expressed. This leads to better determination of a suitable therapy for the tumor, as demonstrated by a <u>real-world example</u> of the breast cancer marker HER-2/neu.

Appellants further note that the sale of gene expression chips to measure mRNA levels is a highly successful business, with a company such as Affymetrix recording 168.3 million dollars in sales of their GeneChip arrays in 2004. Clearly, the research community believes that the information obtained from these chips is useful (*i.e.*, that it is more likely than not informative of the protein level). Therefore, as a general rule, one skilled in the art would find it <u>more likely than not</u> that PRO341 is useful as a diagnostic tool for detecting lung tumors.

As the Examiner no longer questions whether mRNA levels are not predictive of polypeptide levels, the evidence presented by Appellants support that gene amplification correlates with the increased protein expression. Based on the from **2.173 fold to 2.514-fold** in **three** different <u>lung primary tumors</u>, one of ordinary skill would find it credible that the claimed PRO341 polypeptides would have utility <u>as markers for the diagnosis of lung tumors</u>, and for monitoring cancer development and/or for measuring the efficacy of cancer therapy.

Further, Appellants submit that one of ordinary skill in the art would know how to make and use the recited polypeptides for the diagnosis of lung cancer without any undue experimentation, based on the detailed teachings in the specification.

Accordingly, this enablement rejection under 35 U.S.C. §§101 and 112, first paragraph should be withdrawn.

Response to Rejections

Issue 1. Claims 124-126 and 129-131 are Supported by a Credible, Specific and Substantial Asserted Utility, and Thus, Meet the Utility Requirement of 35 U.S.C. §§101/112, First Paragraph

The sole basis for the Examiner's rejection of Claims 124-126 and 129-131 under this section is that the data presented in Example 170 of the present specification is allegedly insufficient under the present legal standards to establish a patentable utility under 35 U.S.C. §101 for the presently claimed subject matter.

Claims 124-126 and 129-131 stand further rejected under 35 U.S.C. §112, first paragraph, allegedly "since the claimed invention is not supported by either a specific and substantial asserted utility or a well established utility for the reasons set forth above, one skilled in the art clearly would not know how to use the claimed invention."

Appellants strongly disagree and, therefore, respectfully traverse the rejection.

-5-
On Appeal to the Board of Patent Appeals and Interferences
Appellants' Brief
Application Serial No. 09/941,992
Attorney's Docket No. 123851-181895 P1C1 (formerly 39780-2730 P1C1)

A.   The Legal Standard For Utility Under 35 U.S.C. §101

According to 35 U.S.C. §101:

> Whoever invents or discovers any new and *useful* process, machine, manufacture,
> or composition of matter, or any new and *useful* improvement thereof, may obtain
> a patent therefor, subject to the conditions and requirements of this title.
> (Emphasis added).

In interpreting the utility requirement, in *Brenner v. Manson,*[1] the Supreme Court held

that the *quid pro quo* contemplated by the U.S. Constitution between the public interest and the

interest of the inventors required that a patent Applicant disclose a "substantial utility" for his or

her invention, *i.e.*, a utility "where specific benefit exists in currently available form."[2] The

Court concluded that "a patent is not a hunting license. It is not a reward for the search, but

compensation for its successful conclusion. A patent system must be related to the world of

commerce rather than the realm of philosophy."[3]

Later, in *Nelson v. Bowler,*[4] the C.C.P.A. acknowledged that tests evidencing

pharmacological activity of a compound may establish practical utility, even though they may

not establish a specific therapeutic use. The Court held that "since it is crucial to provide

researchers with an incentive to disclose pharmaceutical activities in as many compounds as

possible, we conclude adequate proof of any such activity constitutes a showing of practical

utility."[5]

In *Cross v. Iizuka,*[6] the C.A.F.C. reaffirmed *Nelson*, and added that *in vitro* results might

be sufficient to support practical utility, explaining that "*in vitro* testing, in general, is relatively

less complex, less time consuming, and less expensive than *in vivo* testing. Moreover, *in vitro*

---

[1] *Brenner v. Manson,* 383 U.S. 519, 148 U.S.P.Q. (BNA) 689 (1966).

[2] *Id.* at 534, 148 U.S.P.Q. (BNA) at 695.

[3] *Id.* at 536, 148 U.S.P.Q. (BNA) at 696.

[4] *Nelson v. Bowler,* 626 F.2d 853, 206 U.S.P.Q. (BNA) 881 (C.C.P.A. 1980).

[5] *Id.* at 856, 206 U.S.P.Q. (BNA) at 883.

[6] *Cross v. Iizuka,* 753 F.2d 1047, 224 U.S.P.Q. (BNA) 739 (Fed. Cir. 1985).

results with the particular pharmacological activity are generally predictive of *in vivo* test results, i.e. there is a reasonable correlation there between."[7] The Court perceived, "No insurmountable difficulty" in finding that, under appropriate circumstances, "*in vitro* testing, may establish a practical utility."[8]

The case law has also clearly established that Appellants' statements of utility are usually sufficient, unless such statement of utility is unbelievable on its face.[9] The PTO has the initial burden to prove that Appellants' claims of usefulness are not believable on their face.[10] In general, an Appellant's assertion of utility creates a presumption of utility that will be sufficient to satisfy the utility requirement of 35 U.S.C. §101, "unless there is a reason for one skilled in the art to question the objective truth of the statement of utility or its scope."[11,12]

Compliance with 35 U.S.C. §101 is a question of fact.[13] The evidentiary standard to be used throughout *ex parte* examination in setting forth a rejection is a preponderance of the totality of the evidence under consideration.[14] Thus, to overcome the presumption of truth that an assertion of utility by the Appellant enjoys, the Examiner must establish that it is more likely than not that one of ordinary skill in the art would doubt the truth of the statement of utility.

---

[7] *Id.* at 1050, 224 U.S.P.Q. (BNA) at 747.

[8] *Id.*

[9] *In re Gazave*, 379 F.2d 973, 154 U.S.P.Q. (BNA) 92 (C.C.P.A. 1967).

[10] *Ibid.*

[11] *In re Langer*, 503 F.2d 1380,1391, 183 U.S.P.Q. (BNA) 288, 297 (C.C.P.A. 1974).

[12] *See also In re Jolles*, 628 F.2d 1322, 206 U.S.P.Q. 885 (C.C.P.A. 1980); *In re Irons*, 340 F.2d 974, 144 U.S.P.Q. 351 (1965); *In re Sichert*, 566 F.2d 1154, 1159, 196 U.S.P.Q. 209, 212-13 (C.C.P.A. 1977).

[13] *Raytheon v. Roper*, 724 F.2d 951, 956, 220 U.S.P.Q. (BNA) 592, 596 (Fed. Cir. 1983) *cert. denied*, 469 US 835 (1984).

[14] *In re Oetiker*, 977 F.2d 1443, 1445, 24 U.S.P.Q.2d (BNA) 1443, 1444 (Fed. Cir. 1992).

Only after the Examiner made a proper *prima facie* showing of lack of utility, does the burden of rebuttal shift to the Appellant. The issue will then be decided on the totality of evidence.

The well established case law is clearly reflected in the Utility Examination Guidelines ("Utility Guidelines"),[15] which acknowledge that an invention complies with the utility requirement of 35 U.S.C. §101, if it has at least one asserted "specific, substantial, and credible utility" or a "well-established utility." Under the Utility Guidelines, a utility is "specific" when it is particular to the subject matter claimed. For example, it is generally not enough to state that a nucleic acid is useful as a diagnostic without also identifying the conditions that are to be diagnosed.

In explaining the "substantial utility" standard, M.P.E.P. §2107.01 cautions, however, that Office personnel must be careful not to interpret the phrase "immediate benefit to the public" or similar formulations used in certain court decisions to mean that products or services based on the claimed invention must be "currently available" to the public in order to satisfy the utility requirement. "Rather, any reasonable use that an applicant has identified for the invention that can be viewed as providing a public benefit should be accepted as sufficient, at least with regard to defining a 'substantial' utility."[16] Indeed, the Guidelines for Examination of Applications for Compliance With the Utility Requirement,[17] gives the following instruction to patent examiners: "If the Applicant has asserted that the claimed invention is useful for any particular practical purpose . . . and the assertion would be considered credible by a person of ordinary skill in the art, do not impose a rejection based on lack of utility."

B.   Proper Application of the Legal Standard

Appellants submit that the evidentiary standard to be used throughout *ex parte* examination of a patent application is a preponderance of the totality of the evidence under consideration. Thus, to overcome the presumption of truth that an assertion of utility by the Appellant enjoys, the Examiner must establish that it is <u>more likely than not</u> that one of ordinary

---

[15] 66 Fed. Reg. 1092 (2001).

[16] M.P.E.P. §2107.01.

[17] M.P.E.P. §2107 II(B)(1).

skill in the art would doubt the truth of the statement of utility. Only after the Examiner has made a proper *prima facie* showing of lack of utility, does the burden of rebuttal shift to the Appellant.

Appellants respectfully submit that the data presented in Example 170 starting on page 539 of the specification of the specification and the cumulative evidence of record, which underlies the current dispute, indeed support a "specific, substantial and credible" asserted utility for the presently claimed invention.

Patentable utility for the PRO341 polypeptides is based upon the gene amplification data for the gene encoding the PRO341 polypeptide. Example 170 describes the results obtained using a very well-known and routinely employed polymerase chain reaction (PCR)-based assay, the TaqMan^{TM} PCR assay, also referred to herein as the gene amplification assay. This assay allows one to <u>quantitatively</u> measure the level of gene amplification in a given sample, say, a tumor extract, or a cell line. It was well known in the art at the time the invention was made that gene amplification is an essential mechanism for oncogene activation. Appellants isolated genomic DNA from a variety of primary cancers and cancer cell lines that are listed in Table 9 (pages 539 onwards of the specification), including primary lung cancers of the type and stage indicated in Table 8 (page 546). The tumor samples were tested in triplicates with Taqman^{TM} primers and with internal controls, beta-actin and GADPH in order to quantitatively compare DNA levels between samples (page 548, lines 33-34). As a negative control, DNA was isolated from the cells of ten normal healthy individuals, which was pooled and used as a control (page 539, lines 27-29) and also, no-template controls (page 548, lines 33-34). The results of TaqMan™ PCR are reported in ΔCt units, as explained in the passage on page 539, lines 37-39. One unit corresponds to one PCR cycle or approximately a 2-fold amplification, relative to control, two units correspond to 4-fold, 3 units to 8-fold amplification and so on. Using this PCR-based assay, Appellants showed that the gene encoding for PRO341 was amplified, that is, it showed approximately 1.12-1.33 ΔCt units which corresponds to $2^{1.12} - 2^{1.33}$- fold amplification or **2.173 fold to 2.514 -fold** in three different <u>lung primary tumors</u>.

In support of their showing that these gene amplification values are significant, Appellants submitted, in the Response filed October 24, 2003, a Declaration by Dr. Audrey Goddard. Appellants particularly draw the Board's attention to page 3 of the Goddard Declaration which clearly states that:

-9-

On Appeal to the Board of Patent Appeals and Interferences
Appellants' Brief
Application Serial No. 09/941,992
Attorney's Docket No. 123851-181895 P1C1 (formerly 39780-2730 P1C1)

It is further my considered scientific opinion that an at least **2-fold increase** in gene copy number in a tumor tissue sample relative to a normal (*i.e.,* non-tumor) sample is significant and useful in that the detected increase in gene copy number in the tumor sample relative to the normal sample serves as a basis for using relative gene copy number as quantitated by the TaqMan PCR technique as a diagnostic marker for the presence or absence of tumor in a tissue sample of unknown pathology. Accordingly, a gene identified as being amplified at least 2-fold by the quantitative TaqMan PCR assay in a tumor sample relative to a normal sample is **useful as a marker for the diagnosis of cancer**, for monitoring cancer development and/or for measuring the efficacy of cancer therapy. (Emphasis added).

Appellants point out that the Declaration by Dr. Audrey Goddard provides a statement by an expert in the relevant art that "fold amplification" values of <u>at least 2-fold are considered significant</u> in the TaqMan™ PCR gene amplification assay. Appellants particularly draw the Board's attention to page 3 of the Goddard Declaration which clearly states that:

It is further my considered scientific opinion that an at least **2-fold increase** in gene copy number in a tumor tissue sample relative to a normal (*i.e.,* non-tumor) sample is significant and useful in that the detected increase in gene copy number in the tumor sample relative to the normal sample serves as a basis for using relative gene copy number as quantitated by the TaqMan PCR technique as a diagnostic marker for the presence or absence of tumor in a tissue sample of unknown pathology. Accordingly, a gene identified as being amplified at least 2-fold by the quantitative TaqMan PCR assay in a tumor sample relative to a normal sample is **useful as a marker for the diagnosis of cancer**, for monitoring cancer development and/or for measuring the efficacy of cancer therapy. (Emphasis added).

Accordingly, the **2.173 fold to 2.514-fold** in <u>three</u> different <u>lung primary tumors</u> would be considered <u>significant and credible</u> by one skilled in the art, based upon the facts disclosed in the Goddard Declaration. As any skilled artisan in the field of oncology would easily appreciate that this gene is a good candidate marker for diagnosing lung tumors and would clearly find utility for the PRO341 gene as a diagnostic for lung cancer or for diagnosing individuals at risk for developing lung cancer.

The Examiner has asserted that only three out of the fourteen lung cancer samples tested positive for the claimed polypeptide, thus, if a sample was taken from an individual with lung cancer for diagnosis, it is more likely than not that this assay would yield a false negative result. (Page 4 of the Office Action mailed September 10, 2007)

Appellants point out that, as any skilled artisan in the field of oncology would easily appreciate, not all tumor markers are generally associated with every tumor, or even, with most tumors. In fact, some tumor markers are useful for identifying rare malignancies. That is, the association of the tumor marker with a particular type of tumor lesion may be rare, or, the occurrence of that particular kind of tumor lesion itself may be rare. In either event, even these rare tumor markers, which may not give a positive hit with most common tumors, have great value in tumor diagnosis, and consequently, in tumor prognosis. The skilled artisan would know that such tumor markers are very useful for better classification of tumors. Therefore, whether the PRO341 gene is amplified in most of the lung tumors is not relevant to its identification as a tumor marker, or its patentable utility. Rather, whether the amplification data for PRO341 is significant is what lends support to its usefulness as a tumor marker. It was well known in the art at the time of filing of the application that gene amplification, which occurs in most solid tumors like lung cancers, is generally associated with poor prognosis. Therefore, the PRO341 gene becomes an important diagnostic marker to identify such malignant lung cancers, even if the malignancy associated with PRO341 molecule is a rare occurrence and the present specification clearly discloses enough evidence such that, one skilled in the art would know that PRO341 is useful as a valuable diagnostic marker for identifying certain types of lung cancers.

The Examiner has also alleged, based on Sen *et al.* and Hittelman *et al.* that the observed gene amplification was not corrected for aneuploidy. The Examiner has also asserted it is not clear whether PRO341 is amplified in cancerous lung tissue more than in damaged lung tissue. (Page 5 of the Office Action mailed September 10, 2007)

Appellants respectfully disagree and submit that their gene amplification data was not due to aneuploidy. Appellants had submitted the Ashkenazi Declaration to show that "detection of gene amplification can be used for cancer diagnosis even if the determination includes measurement of chromosomal aneuploidy." Regarding Hittelman *et al.*, Appellants agree that while aneuploidy can be a feature of damaged tissue as well, besides cancerous or pre-cancerous tissue, and may not invariably lead to cancer, Hittelman *et al.*. in fact support the Appellants' position that PRO341 is still useful in diagnosing pre-cancerous lesions or cancer itself. For instance, the art in lung cancer at the time of filing of the instant application clearly described that "epithelial tumors develop through a multistep process driven by genetic instability" in damaged lung lesions which may eventually lead to lung cancer. Many articles published around

-11-

On Appeal to the Board of Patent Appeals and Interferences
Appellants' Brief
Application Serial No. 09/941,992
Attorney's Docket No. 123851-181895 P1C1 (formerly 39780-2730 P1C1)

June 23, 1999 (the effective filing date of this application) studied such damaged or premalignant lesions and suggested that identification of such pre-cancerous lesions were very important in preventive diagnosis and treatment of lung cancer. Based on the well-known art, Appellants submit that there is utility in identifying genetic biomarkers in epithelial tissues at cancer risk.

C. A *prima facie* case of lack of utility has not been established

The Examiner has asserted, based on Pennica *et al.*, Konopka *et al.*, Godbout *et al.*, and Li *et al.* that there is a general lack of correlation between gene amplification and mRNA expression, and, thus, the data in Table 9, while may provide a basis for utility and enablement of PRO341 nucleic acid, does not provide a basis for utility or enablement of the claimed polypeptides (Pages 5-8 of the Final Office Action mailed September 10, 2007).

As a preliminary matter, Appellants respectfully submit that it is not a legal requirement to establish that gene amplification "necessarily" results in increased expression at the mRNA and polypeptide levels or that polypeptide levels can be "accurately predicted." As discussed above, the evidentiary standard to be used throughout *ex parte* examination of a patent application is a preponderance of the totality of the evidence under consideration. Accordingly, Appellants submit that in order to overcome the presumption of truth that an assertion of utility by the applicant enjoys, the Examiner must establish that **it is more likely than not** that one of ordinary skill in the art would doubt the truth of the statement of utility. Therefore, it is not legally required that there be a "necessary" correlation between the data presented and the claimed subject matter. The law requires only that one skilled in the art should accept that such a correlation is **more likely than not to exist**. Appellants respectfully submit that when the proper evidentiary standard is applied, a correlation must be acknowledged.

Appellants submit that Pennica *et al.* does not show a lack of correlation between gene (DNA) amplification and mRNA levels. According to the quoted statement from Pennica *et al.*, "WISP-1 gene amplification in human lung tumors showed a correlation between DNA amplification and over-expression, whereas overexpression of WISP-3 RNA was seen in the absence of DNA amplification. In contrast, WISP-2 DNA was amplified in lung tumors, but its mRNA expression was significantly reduced in the majority of tumors compared with expression in normal lungic mucosa from the same patient." From this, the Examiner correctly concludes that increased copy number does not *necessarily* result in increased polypeptide expression. The

standard, however, is not absolute certainty. The fact that in the case of a specific class of closely related molecules there seemed to be no correlation with gene amplification and the level of mRNA/protein expression, does not establish that it is more likely than not, in general, that such correlation does not exist. The Examiner has not shown whether the lack or correlation observed for the family of WISP polypeptides is typical, or is merely a discrepancy, <u>an exception to the rule of correlation</u>. Indeed, the working hypothesis among those skilled in the art is that, if a gene is amplified in cancer, the encoded protein is likely to be expressed at an elevated level. In fact, as noted even in Pennica *et al.*, "[a]n analysis of *WISP*-1 gene amplification and expression in human lung tumors *showed a correlation between DNA amplification and over-expression . . . ."* (Pennica *et al.*, page14722, left column, first full paragraph, emphasis added).

Accordingly, Appellants respectfully submit that Pennica *et al.* teaches nothing conclusive regarding the absence of correlation between amplification of a gene and over-expression of the encoded WISP polypeptide. More importantly, the teaching of Pennica *et al.* is specific to *WISP* genes. Pennica *et al.* has no teaching whatsoever about the correlation of gene amplification and protein expression <u>in general</u>.

Similarly, in Konopka *et al.*, Appellants submit that the Examiner has generalized a very specific result disclosed by Konopka *et al.* to cover all genes. Konopka *et al.* actually state that "[p]rotein expression is not related to amplification of the ***abl*** gene but to variation in the level of *bcr-abl* mRNA produced from a single Ph[1] template." (See Konopka *et al* ., Abstract, emphasis added). The paper does not teach anything whatsoever about the correlation of protein expression and gene amplification <u>in general</u>, and provides no basis for the generalization that apparently underlies the present rejection. The statement of Konopka *et al.* that "[p]rotein expression is not related to amplification of the *abl* gene . . . " is <u>not</u> sufficient to establish a *prima facie* case of lack of utility. Therefore, the combined teachings of Pennica *et al.* and Konopka *et al.* are not directed towards genes in general but to <u>a single gene or genes within a single family</u> and thus, their teachings cannot support a <u>general</u> conclusion regarding correlation between gene amplification and mRNA or protein levels.

The Examiner has asserted that unlike Godbout *et al.*, the instant specification does not teach structure/ function analysis and the Examiner questions whether the level of genomic amplification of DDX1 gene is comparable to that disclosed by PRO341. The Examiner has

further asserted that, there is no evidence in the present application that PRO341 confers growth advantage to the cells. (Page 7 of the Office Action mailed in September 10, 2007)

Regarding the Godbout reference, Appellants respectfully submit that it was never claimed that PRO341 is similar in any way to the DDX1 gene of Godbout *et al.,* they never claimed PRO341 was an RNA helicase or that it confers selective advantage to cell survival; on the other hand, the Godbout reference was submitted to show good correlation between protein levels based upon genomic DNA amplification, which the Examiner clearly agrees with. Moreover, selective advantage to cell survival is not the only mechanism by which genes impact cancer. Structure/function data, which the Examiner requests, is not a requirement for the utility requirement. Hence this rejection is improper.

The Examiner has cited Li *et al.* as teaching that "68.8% of the genes showing over-representation in the genome did not show elevated transcript levels." (Page 7 of the Office Action mailed in September 10, 2007)

Appellants respectfully point out that Li *et al.* acknowledge that their results differed from those obtained by Hyman *et al.* and Pollack *et al.* (of record), who found a substantially higher level of correlation between gene amplification and increased gene expression. The authors note that "[t]his discordance may reflect methodologic differences between studies or biological differences between breast cancer and lung adenocarcinoma" (page 2629, col. 1). For instance, as explained in the Supplemental Information accompanying the Li article, genes were considered to be amplified if they had a copy number ratio of at least 1.40. In the case of PRO341, as discussed in previously filed responses and in the Goddard Declaration (of record), an appropriate threshold for considering gene amplification to be significant is a copy number of at least 2.0 (which is a higher threshold). The PRO341 gene showed significant amplification of **2.173 fold to 2.514-fold** in three different lung primary tumors, and thus fully meets this standard. It is not surprising that in the Li *et al.* reference, by using a lower threshold of 1.4 for considering gene amplification, a higher number of genes not showing corresponding increases in mRNA expression were found. Moreover, Appellants add that the results of Li *et al.* do not conclusively disprove that a gene with a substantially higher level of gene amplification, such as PRO341, would be expected to show a corresponding increase in transcript expression.

In response to Applicants' argument that the discordance may reflect methodologic differences, the Examiner asserts that "Li et al. did not limit their studies to genes that were

-14-

On Appeal to the Board of Patent Appeals and Interferences
Appellants' Brief
Application Serial No. 09/941,992
Attorney's Docket No. 123851-181895 P1C1 (formerly 39780-2730 P1C1)

amplified at less than 2-fold." In support of this assertion, the Examiner cites the first paragraph of the Supplemental Material. (Page 18 of the Final Office Action mailed September 7, 2007).

Applicants respectfully point out that the Examiner has misinterpreted the methodology disclosed in the supplemental material. The evidence cited by the Examiner pertains to the inclusion criteria of the probes used for defining amplicons. In the second paragraph entitled "Relationship between genomic copy number and gene transcript level", the authors state that "[f]or each gene, the CGH data were represented by a vector that was labeled '1' for genomic overrepresentation (including amplification) ratio greater than 1.40 and '0' for no genomic overrepresentation." Nevertheless, the Examiner acknowledges that the alleged 2-fold amplification criteria would only apply to some of the samples. The Examiner has not established that a correlation does not exist in samples based solely on this threshold.

It is "more likely than not" for amplified genes to have increased mRNA

On the contrary, Appellants submit that Example 170 of the specification further discloses that, "(a)mplification is associated with overexpression of the gene product, indicating that the polypeptides are useful targets for therapeutic intervention in certain cancers such as lung, lung, breast and other cancers and diagnostic determination of the presence of those cancers" (Emphasis added). Besides, Appellants have submitted ample evidence to show that, in general, if a gene is amplified in cancer, it is "more likely than not" that the corresponding mRNA will also be expressed at an elevated level.

For instance, Appellants presented the articles by Orntoft *et al.*, Hyman *et al.*, and Pollack *et al.* (made of record in Appellants' Response filed July 7, 2004), who collectively teach that in general, for most genes, DNA amplification increases mRNA expression. The results presented by Orntoft *et al.*, Hyman *et al.*, and Pollack *et al.* are based upon wide ranging analyses of a large number of tumor associated genes. Orntoft *et al.* studied transcript levels of 5600 genes in malignant bladder cancers, many of which were linked to the gain or loss of chromosomal material, and found that in general (18 of 23 cases) chromosomal areas with more than 2-fold gain of DNA showed a corresponding increase in mRNA transcripts. Hyman *et al.* compared DNA copy numbers and mRNA expression of over 12,000 genes in breast cancer tumors and cell lines, and found that there was evidence of a prominent global influence of copy number changes on gene expression levels. In Pollack *et al.*, the authors profiled DNA copy

-15-
On Appeal to the Board of Patent Appeals and Interferences
Appellants' Brief
Application Serial No. 09/941,992
Attorney's Docket No. 123851-181895 P1C1 (formerly 39780-2730 P1C1)

number alteration across 6,691 mapped human genes in 44 predominantly advanced primary breast tumors and 10 breast cancer cell lines, and found that on average, a 2-fold change in DNA copy number was associated with a corresponding 1.5-fold change in mRNA levels. In summary, the evidence supports the Appellants' position that gene amplification is more likely than not predictive of increased mRNA and polypeptide levels.

Appellants further note that the sale of gene expression chips to measure mRNA levels is a highly successful business, with a company such as Affymetrix recording 168.3 million dollars in sales of their GeneChip® arrays in 2004. Clearly, the research community believe that the information obtained from these chips is useful (*i.e.*, that it is more likely than not that the results are informative of protein levels).

Thus, the Examiner appears to disregard the ample evidence provided in the above referenced articles based on misinterpretations of their teachings. Appellants submit that in fact, these articles lend significant support that for an amplified gene, it is more likely than not that the protein will also be overexpressed and would be viewed as reasonable and credible by one of ordinary skill in the art. The "more likely than not" standard is a much lower standard than a "necessary" correlation or "accurate" prediction, and is clearly met in the claimed invention. Moreover, the Examiner has not cited any evidence or advanced any arguments as to why Appellants' statement of overexpression of protein would not be credible. Accordingly, this point is believed to be moot.

The Examiner has stated that Appellants have not indicated whether PRO341 is in a gene cluster region of a chromosome. (Page 7 of the Office Action mailed September 10, 2007). Appellants fail to see how this is relevant to the analysis. Orntoft *et al.* did not limit their findings to only those regions of amplified gene clusters. Further, as discussed below, Hyman *et al.* and Pollack *et al.* did gene-by-gene analysis across all chromosomes.

Appellants respectfully submit that the Examiner has mischaracterized the methods used by Hyman *et al.* and Pollack *et al.* in their analysis. These papers did not use traditional CGH analysis to identify amplified genes. In Hyman *et al.*, 13,824 cDNA clones were placed on glass slides in a microarray and genomic DNA from breast cancer cell lines and normal human WBCs was hybridized to the cDNA sequences. For expression analysis, RNA from tumor cell lines was hybridized on the same microarrays. The 13,824 arrayed cDNA clones were analyzed for gene expression and gene copy number in 14 breast cancer cell lines. Hyman *et al.* state, "The results

-16-

On Appeal to the Board of Patent Appeals and Interferences
Appellants' Brief
Application Serial No. 09/941,992
Attorney's Docket No. 123851-181895 P1C1 (formerly 39780-2730 P1C1)

illustrate a considerable influence of copy number on gene expression patterns." For example, Hyman *et al.* teach that "[u]p to 44% of the highly amplified transcripts (CGH ratio, >2.5) were overexpressed (*i.e.*, belonged to the global upper 7% of expression ratios) compared with only 6% for genes with normal copy number." (See page 6242, column 1). Further, Hyman *et al.* state that "[t]he cDNA/CGH microarray technique enables the direct correlation of copy number and expression data on a gene-by-gene basis throughout the genome." (See page 6242, column 2). Therefore, the analysis performed by Hyman *et al.* was on a gene-by gene basis, and clearly shows that "it is more likely than not" that a gene which is amplified in tumor cells will have increased gene expression.

In Pollack *et al.*, DNA copy number alteration across 6,691 mapped human genes in 44 predominantly advanced primary breast tumors and 10 breast cancer cell lines was profiled. Pollack *et al.* further state, "Parallel microarray measurements of mRNA levels reveal the remarkable degree to which variation in gene copy number contributes to variation in gene expression in tumor cells." (See Abstract). "Genome-wide, of 117 high-level DNA amplifications (fluorescence ratios >4, and representing 91 different genes), 62% (representing 54 different genes; ...) are found associated with at least moderately elevated mRNA levels (mean-centered fluorescence ratios >2), and 42% (representing 36 different genes) are found associated with comparably highly elevated mRNA levels (mean-centered fluorescence ratios >4)." (See page 12966, column 1). Therefore, the analysis performed by Pollack *et al.* was also on a gene-by gene basis, and clearly shows that "it is more likely than not" that a gene which is amplified in tumor cells will have increased gene expression.

The Examiner has further asserted that "none of the three papers reported that the research was relevant to identifying probes that can be used as cancer diagnostics" (Page 13 of the Office Action mailed September 10, 2007).

Appellants respectfully point out that Hyman *et al.* conducted additional studies of one of the genes found to be amplified, HOXB7, and found "a clinical association between HOXB7 amplification and poor patient prognosis." (Page 6244, col.1 to col.2). Thus the results of Hyman *et al.* confirm that genes which are amplified in tumors have prognostic utility. The Board's attention is also respectfully directed to the final paragraph of Pollack *et al.*, wherein the authors conclude that "a substantial portion of the phenotypic uniqueness (and, by extension, the heterogeneity in clinical behavior) among patients' tumors may be traceable to underlying variation in DNA copy number." (Page 12698, col. 2). Accordingly,

Pollack *et al.* confirm that genes that are amplified in at least one type of tumor are useful as markers for that type of tumor, and for prognostic uses directed to that type of tumor.

Even if a *prima facie* case of lack of utility has been established, it should be withdrawn on consideration of the totality of evidence

Even if one assumes *arguendo* that it is more likely than not that there is no correlation between gene amplification and increased mRNA/protein expression, which Appellants submit is **not** true, a polypeptide encoded by a gene that is amplified in cancer would **still** have a specific, substantial, and credible utility. In support, Appellants respectfully draw the Board's attention to page 2 of the Declaration of Dr. Avi Ashkenazi (submitted with the Response filed October 24, 2003) which explains that,

> even when amplification of a cancer marker gene does not result in significant over-expression of the corresponding gene product, this very absence of gene product over-expression still provides significant information for cancer diagnosis and treatment. Thus, if over-expression of the gene product does not parallel gene amplification in certain tumor types but does so in others, then parallel monitoring of gene amplification and gene product over-expression enables more accurate tumor classification and hence better determination of suitable therapy. In addition, absence of over-expression is crucial information for the practicing clinician. If a gene is amplified but the corresponding gene product is not over-expressed, the clinician accordingly will decide not to treat a patient with agents that target that gene product.

Appellants thus submit that simultaneous testing of gene amplification and gene product over-expression enables more accurate tumor classification, even if the gene-product, the protein, is not over-expressed. This leads to better determination of a suitable therapy. Further, as explained in Dr. Ashkenazi's Declaration, absence of over-expression of the protein itself is crucial information for the practicing clinician. If a gene is amplified in a tumor, but the corresponding gene product is not over-expressed, the clinician will decide not to treat a patient with agents that target that gene product. This not only saves money, but also has the benefit that the patient can avoid exposure to the side effects associated with such agents.

This utility is further supported by the teachings of the article by Hanna and Mornin. (Pathology Associates Medical Laboratories, August (1999), submitted with the Response filed June 4, 2004). The article teaches that the HER-2/neu gene has been shown to be amplified and/or over-expressed in 10%-30% of invasive breast cancers and in 40%-60% of intraductal breast carcinomas. Further, the article teaches that diagnosis of breast cancer includes testing

-18-

On Appeal to the Board of Patent Appeals and Interferences
Appellants' Brief
Application Serial No. 09/941,992
Attorney's Docket No. 123851-181895 P1C1 (formerly 39780-2730 P1C1)

both the amplification of the HER-2/neu gene (by FISH) as well as the over-expression of the HER-2/neu gene product (by IHC). Even when the protein is not over-expressed, the assay relying on both tests leads to a more accurate classification of the cancer and a more effective treatment of it.

The Examiner has asserted that "Hanna et al. supports the rejection, in that Hanna et al. show that gene amplification does not reliably correlate with protein over-expression, and thus the level of polypeptide expression must be tested empirically." (Page 15 of the Office Action mailed September 10, 2007). Appellants respectfully point out that the Examiner appears to have misread Hanna et al. Hanna et al. clearly state that gene amplification (as measured by FISH) and polypeptide expression (as measured by immunohistochemistry, IHC) are well correlated ("in general, FISH and IHC results correlate well" (Hanna et al. p. 1, col. 2)). It is only a subset of tumors which show discordant results. Thus Hanna et al. support Appellants' position that it is more likely than not that gene amplification correlates with increased polypeptide expression.

Appellants have clearly shown that the gene encoding the PRO341 polypeptide is amplified in at least three lung tumors. Therefore, the PRO341 gene, similar to the HER-2/neu gene disclosed in Hanna et al., is a tumor associated gene. Furthermore, as discussed above, in the majority of amplified genes, the teachings in the art overwhelmingly show that gene amplification influences gene expression at the mRNA and protein levels. Therefore, one of skill in the art would reasonably expect in this instance, based on the amplification data for the PRO341 gene, that the PRO341 polypeptide is concomitantly overexpressed.

The Examiner appears to view the testing described in the Ashkenazi Declaration and the Hanna article as experiments involving further characterization of the PRO341 polypeptide itself. In fact, such testing is for the purpose of characterizing not the PRO341 polypeptide, but the tumors in which the gene encoding PRO341 is amplified. The PRO341 polypeptide and the claimed antibodies which bind it are therefore useful in tumor categorization, the results of which become an important tool in the hands of a physician enabling the selection of a treatment modality that holds the most promise for the successful treatment of a patient.

Thus, based on the asserted utility for PRO341 in the diagnosis of selected lung tumors, the reduction to practice of the instantly claimed protein sequence of SEQ ID NO:20 in the present application, the disclosure of the step-by-step protocols for making chimeric PRO

-19-

On Appeal to the Board of Patent Appeals and Interferences
Appellants' Brief
Application Serial No. 09/941,992
Attorney's Docket No. 123851-181895 P1C1 (formerly 39780-2730 P1C1)

polypeptides, including those wherein the heterologous polypeptide is an epitope tag or an Fc region of an immunoglobulin in the specification (at page 374, lines 24 to page 375, line 9), the disclosure of a step-by-step protocol for making and expressing PRO341 in appropriate host cells (in Examples 140-143 and page 376, line 12), the step-by-step protocol for the preparation, isolation and detection of monoclonal, polyclonal and other types of antibodies against the PRO341 protein in the specification (at pages 390-395) and the disclosure of the gene amplification assay in Example 170, the skilled artisan would know exactly how to make and use the claimed polypeptide for the diagnosis of lung cancers. Appellants submit that based on the detailed information presented in the specification and the advanced state of the art in oncology, the skilled artisan would have found such testing routine and not 'undue'.

Therefore, Appellants respectfully request reconsideration and reversal of this outstanding rejections under 35 U.S.C. §101 and §112, First Paragraph to Claims 124-126 and 129-131.

CONCLUSION

For the reasons given above, Appellants submit that present specification clearly describes, details and provides a patentable utility for the claimed invention. Moreover, it is respectfully submitted that based upon this disclosed patentable utility, the present specification clearly teaches "how to use" the presently claimed polypeptide. As such, Appellants respectfully request reconsideration and reversal of the outstanding rejection of Claims 124-126 and 129-131.

The Commissioner is authorized to charge any fees which may be required, including extension fees, or credit any overpayment to Deposit Account No. **17-1700** (referencing Attorney's Docket No. **123851-181895 P1C1**; formerly 39780-2730 P1C1).

Respectfully submitted,

Date: APRIL 10, 2008

By:_____
Panpan Gao (Reg. No. 43,626)

Goodwin Procter LLP
Customer No. 77485
135 Commonwealth Drive
Menlo Park, CA 94025
T: 650.752.3100
F: 650.853.1038

-21-
On Appeal to the Board of Patent Appeals and Interferences
Appellants' Brief
Application Serial No. 09/941,992
Attorney's Docket No. 123851-181895 P1C1 (formerly 39780-2730 P1C1)

VIII. CLAIMS APPENDIX

Claims on Appeal

124. An isolated polypeptide comprising:

(a)   the amino acid sequence of the polypeptide of SEQ ID NO:20;

(b)   the amino acid sequence of the polypeptide of SEQ ID NO:20, lacking its associated   signal peptide,

(c)   the amino acid sequence of the polypeptide encoded by the full-length coding sequence of the cDNA deposited under ATCC accession number 209792,

wherein, the nucleic acid encoding said polypeptide is amplified in lung tumors.

125.   The isolated polypeptide of Claim 124 comprising the amino acid sequence of the polypeptide of SEQ ID NO:20.

126.   The isolated polypeptide of Claim 124 comprising the amino acid sequence of the polypeptide of SEQ ID NO:20, lacking its associated signal peptide.

129.   The isolated polypeptide of Claim 124 comprising the amino acid sequence of the polypeptide encoded by the full-length coding sequence of the cDNA deposited under ATCC accession number 209792.

130.   A chimeric polypeptide comprising a polypeptide according to Claim 124 fused to a heterologous polypeptide.

131.   The chimeric polypeptide of Claim 130, wherein said heterologous polypeptide is an epitope tag or an Fc region of an immunoglobulin.

IX. EVIDENCE APPENDIX

1. Declaration of Audrey Goddard, Ph.D. under 35 C.F.R. §1.132, with attached Exhibits A-G:

    A.   Curriculum Vitae of Audrey D. Goddard, Ph.D.

    B.   Higuchi, R. *et al.*, "Simultaneous amplification and detection of specific DNA sequences," *Biotechnology* 10:413-417 (1992).

    C.   Livak, K.J., *et al.*, "Oligonucleotides with fluorescent dyes at opposite ends provide a quenched probe system useful for detecting PCR product and nucleic acid hybridization," *PCR Methods Appl.* 4:357-362 (1995).

    D.   Heid, C.A. *et al.*, "Real time quantitative PCR," *Genome Res.* 6:986-994 (1996).

    E.   Pennica, D. *et al.*, "WISP genes are members of the connective tissue growth factor family that are up-regulated in Wnt-1-transformed cells and aberrantly expressed in human lung tumors," *Proc. Natl. Acad. Sci. USA* 95:14717-14722 (1998).

    F.   Pitti, R.M. *et al.*, "Genomic amplification of a decoy receptor for Fas ligand in lung and lung cancer," *Nature* 396:699-703 (1998).

    G.   Bieche, I. *et al.*, "Novel approach to quantitative polymerase chain reaction using real-time detection: Application to the detection of gene amplification in breast cancer," *Int. J. Cancer* 78:661-666 (1998).

2. Declaration of Avi Ashkenazi, Ph.D. under 35 C.F.R. §1.132, with attached Exhibit A (Curriculum Vitae).

3. Hyman, E., *et al.*, "Impact of DNA Amplification on Gene Expression Patterns in Breast Cancer," *Cancer Research* 62:6240-6245 (2002).

4. Pollack, J.R., *et al.*, "Microarray Analysis Reveals a Major Direct Role of DNA Copy Number Alteration in the Transcriptional Program of Human Breast Tumors," *Proc. Natl. Acad. Sci. USA* 99:12963-12968 (2002).

5. Hanna *et al.*, "HER-2/neu Breast Cancer Predictive Testing," Pathology Associates Medical Laboratories (1999).

6. Konopka *et al.*, "Variable Expression of the Translocated c-abl oncogene in Philadelphia-chromosome-positive B-lymphoid cell lines from chronic myelogenous leukemia patients" *Proc. Natl. Acad. Sci. USA* 83: 4049-52, (1986).

7. Orntoft, T.F., *et al.* Molecular & Cellular Proteomics – 1:37-45 (2002).

8. Godbout, R., *et al.*, J. Biol. Chem. - 273(33):21161-8 (1998).

9. Li *et al.*, 2006, Oncogene 25: 2628-2635.

Items 1 and 2 were submitted with Appellants' Response filed October 24, 2003, and were considered by the Examiner as indicated in the Final Office Action mailed January 21, 2004.

-23-
On Appeal to the Board of Patent Appeals and Interferences
Appellants' Brief
Application Serial No. 09/941,992
Attorney's Docket No. 123851-181895 P1C1 (formerly 39780-2730 P1C1)

Items 2-3 and 5-7 were submitted with Appellants' Response filed June 18, 2004, and were considered by the Examiner as indicated in the Final Office Action mailed September 16, 2004.

Item 4 was submitted with Appellants' Response filed June 29, 2006, and was considered by the Examiner as indicated in the Final Office Action mailed September 27, 2006.

Items 8-9 were made of record by the Examiner in the Office Action mailed March 19, 2004.

X.   RELATED PROCEEDINGS APPENDIX

None.

LIBC/3255921.1

-25-
On Appeal to the Board of Patent Appeals and Interferences
Appellants' Brief
Application Serial No. 09/941,992
Attorney's Docket No. 123851-181895 P1C1 (formerly 39780-2730 P1C1)

IN THE UNITED STATES PATENT AND TRADEMARK OFFICE

In re Application of: Ashkenazi et al.	Group Art Unit: 1647
Serial No.: 09/903,925	Examiner: Fozia Hamid
Filed: July 11, 2001	CERTIFICATE OF MAILING I hereby certify that this correspondence is being deposited with the United States Postal Service with sufficient postage as first class mail in an envelope addressed to: Assistant Commissioner of Patents, Washington, D.C. 20231 on
For: SECRETED AND TRANSMEMBRANE POLYPEPTIDES AND NUCLEIC ACIDS	Date

DECLARATION OF AUDREY D. GODDARD, Ph.D UNDER 37 C.F.R. § 1.132

Assistant Commissioner of Patents
Washington, D.C. 20231

Sir:

I, Audrey D. Goddard, Ph.D. do hereby declare and say as follows:

1.   I am a Senior Clinical Scientist at the Experimental Medicine/BioOncology, Medical Affairs Department of Genentech, Inc., South San Francisco, California 94080.

2.   Between 1993 and 2001, I headed the DNA Sequencing Laboratory at the Molecular Biology Department of Genentech, Inc. During this time, my responsibilities included the identification and characterization of genes contributing to the oncogenic process, and determination of the chromosomal localization of novel genes.

3.   My scientific Curriculum Vitae, including my list of publications, is attached to and forms part of this Declaration (Exhibit A).

4.   I am familiar with a variety of techniques known in the art for detecting and quantifying the amplification of oncogenes in cancer, including the quantitative TaqMan PCR (i.e., "gene amplification") assay described in the above captioned patent application.

5.   The TaqMan PCR assay is described, for example, in the following scientific publications: Higuchi *et al.*, Biotechnology 10:413-417 (1992) (Exhibit B); Livak *et al.*, PCR Methods Appl., 4:357-362 (1995) (Exhibit C) and Heid *et al.*, Genome Res. 6:986-994 (1996) (Exhibit D). Briefly, the assay is based on the principle that successful PCR yields a fluorescent signal due to Taq DNA polymerase-mediated exonuclease digestion of a fluorescently labeled oligonucleotide that is homologous to a sequence between two PCR primers. The extent of digestion depends directly on the amount of PCR, and can be quantified accurately by measuring the increment in fluorescence that results from decreased energy transfer. This is an extremely sensitive technique, which allows detection in the exponential phase of the PCR reaction and, as a result, leads to accurate determination of gene copy number.

6.   The quantitative fluorescent TaqMan PCR assay has been extensively and successfully used to characterize genes involved in cancer development and progression. Amplification of protooncogenes has been studied in a variety of human tumors, and is widely considered as having etiological, diagnostic and prognostic significance. This use of the quantitative TaqMan PCR assay is exemplified by the following scientific publications: Pennica *et al.*, Proc. Natl. Acad. Sci. USA 95(25):14717-14722 (1998) (Exhibit E); Pitti *et al.*, Nature 396(6712):699-703 (1998) (Exhibit F) and Bieche *et al.*, Int. J. Cancer 78:661-666 (1998) (Exhibit G), the first two of which I am co-author. In particular, Pennica *et al.* have used the quantitative TaqMan PCR assay to study relative gene amplification of WISP and c-myc in various cell lines, colorectal tumors and normal mucosa. Pitti *et al.* studied the genomic amplification of a decoy receptor for Fas ligand in lung and colon cancer, using the quantitative TaqMan PCR assay. Bieche *et al.* used the assay to study gene amplification in breast cancer.

7.   It is my personal experience that the quantitative TaqMan PCR technique is technically sensitive enough to detect at least a 2-fold increase in gene copy number relative to control. It is further my considered scientific opinion that an at least 2-fold increase in gene copy number in a tumor tissue sample relative to a normal (i.e., non-tumor) sample is significant and useful in that the detected increase in gene copy number in the tumor sample relative to the normal sample serves as a basis for using relative gene copy number as quantitated by the TaqMan PCR technique as a diagnostic marker for the presence or absence of tumor in a tissue sample of unknown pathology. Accordingly, a gene identified as being amplified at least 2-fold by the quantitative TaqMan PCR assay in a tumor sample relative to a normal sample is useful as a marker for the diagnosis of cancer, for monitoring cancer development and/or for measuring the efficacy of cancer therapy.

8.   I declare further that all statements made herein of my own knowledge are true and that all statements made on information and belief are believed to be true. I declare that these statements were made with the knowledge that willful false statements and the like so made are punishable by fine or imprisonment, or both, under Section 1001 of Title 18 of the United States Code, and that such willful false statements may jeopardize the validity of the application or any patent issuing thereon.

Jan. 16, 2003

Date

Audrey Goddard

Audrey D. Goddard, Ph.D.

AUDREY D. GODDARD, Ph.D.

Genentech, Inc.
1 DNA Way
South San Francisco, CA, 94080
650.225.6429
goddarda@gene.com

110 Congo St.
San Francisco, CA, 94131
415.841.9154
415.819.2247 (mobile)
agoddard@pacbell.net

PROFESSIONAL EXPERIENCE

Genentech, Inc.   **1993-present**
South San Francisco, CA

2001 - present   Senior Clinical Scientist
Experimental Medicine / BioOncology, Medical Affairs

Responsibilities:
- *Companion diagnostic oncology products*
- *Acquisition of clinical samples from Genentech's clinical trials for translational research*
- *Translational research using clinical specimen and data for drug development and diagnostics*
- *Member of Development Science Review Committee, Diagnostic Oversight Team, 21 CFR Part 11 Subteam*

Interests:
- *Ethical and legal implications of experiments with clinical specimens and data*
- *Application of pharmacogenomics in clinical trials*

1998 - 2001   Senior Scientist
Head of the DNA Sequencing Laboratory, Molecular Biology Department, Research

Responsibilities:
- *Management of a laboratory of up to nineteen –including postdoctoral fellow, associate scientist, senior research associate and research assistants/associate levels*
- *Management of a $750K budget*
- *DNA sequencing core facility supporting a 350+ person research facility.*
- *DNA sequencing for high throughput gene discovery, - ESTs, cDNAs, and constructs*
- *Genomic sequence analysis and gene identification*
- *DNA sequence and primary protein analysis*

Research:
- *Chromosomal localization of novel genes*
- *Identification and characterization of genes contributing to the oncogenic process*
- *Identification and characterization of genes contributing to inflammatory diseases*
- *Design and development of schemes for high throughput genomic DNA sequence analysis*
- *Candidate gene prediction and evaluation*

1993 - 1998   Scientist
Head of the DNA Sequencing Laboratory, Molecular Biology Department, Research

Responsibilities
- *DNA sequencing core facility supporting a 350+ person research facility*
- *Assumed responsibility for a pre-existing team of five technicians and expanded the group into fifteen, introducing a level of middle management and additional areas of research*
- *Participated in the development of the basic plan for high throughput secreted protein discovery program – sequencing strategies, data analysis and tracking, database design*
- *High throughput EST and cDNA sequencing for new gene identification.*
- *Design and implementation of analysis tools required for high throughput gene identification.*
- *Chromosomal localization of genes encoding novel secreted proteins.*

Research:
- *Genomic sequence scanning for new gene discovery.*
- *Development of signal peptide selection methods.*
- *Evaluation of candidate disease genes.*
- *Growth hormone receptor gene SNPs in children with Idiopathic short stature*

Imperial Cancer Research Fund   **1989-1992**
London, UK with Dr. Ellen Solomon

6/89 –12/92 Postdoctoral Fellow
- Cloning and characterization of the genes fused at the acute promyelocytic leukemia translocation breakpoints on chromosomes 17 and 15.
- Prepared a successfully funded European Union multi-center grant application

McMaster University   **1983**
Hamilton, Ontario, Canada with Dr. G. D. Sweeney

5/83 – 8/83: NSERC Summer Student
- *In vitro* metabolism of β-naphthoflavone in C57Bl/6J and DBA mice

EDUCATION

Ph.D.
"Phenotypic and genotypic effects of mutations in the human retinoblastoma gene."
Supervisor: Dr. R. A. Phillips

University of Toronto
Toronto, Ontario, Canada.   1989
Department of Medical
Biophysics.

Honours B.Sc
"The *in vitro* metabolism of the cytochrome P-448 inducer β-naphthoflavone in C57BL/6J mice."
Supervisor: Dr. G. D. Sweeney

McMaster University,
Hamilton, Ontario, Canada.   1983
Department of Biochemistry

ACADEMIC AWARDS

Imperial Cancer Research Fund Postdoctoral Fellowship	1989-1992
Medical Research Council Studentship	1983-1988
NSERC Undergraduate Summer Research Award	1983
Society of Chemical Industry Merit Award (Hons. Biochem.)	1983
Dr. Harry Lyman Hooker Scholarship	1981-1983
J.L.W. Gill Scholarship	1981-1982
Business and Professional Women's Club Scholarship	1980-1981
Wyerhauser Foundation Scholarship	1979-1980

INVITED PRESENTATIONS

Genentech's gene discovery pipeline: High throughput identification, cloning and characterization of novel genes. Functional Genomics: From Genome to Function, Litchfield Park, AZ, USA. October 2000

High throughput identification, cloning and characterization of novel genes. G2K:Back to Science, Advances in Genome Biology and Technology I. Marco Island, FL, USA. February 2000

Quality control in DNA Sequencing: The use of Phred and Phrap. Bay Area Sequencing Users Meeting, Berkeley, CA, USA. April 1999

High throughput secreted protein identification and cloning. Tenth International Genome Sequencing and Analysis Conference, Miami, FL, USA. September 1998

The evolution of DNA sequencing: The Genentech perspective. Bay Area Sequencing Users Meeting, Berkeley, CA, USA. May 1998

Partial Growth Hormone Insensitivity: The role of GH-receptor mutations in Idiopathic Short Stature. Tenth Annual National Cooperative Growth Study Investigators Meeting, San Francisco, CA, USA. October, 1996

Growth hormone (GH) receptor defects are present in selected children with non-GH-deficient short stature: A molecular basis for partial GH-insensitivity. 76th Annual Meeting of The Endocrine Society, Anaheim, CA, USA. June 1994

A previously uncharacterized gene, myl, is fused to the retinoic acid receptor alpha gene in acute promyelocytic leukemia. XV International Association for Comparative Research on Leukemia and Related Disease, Padua, Italy. October 1991

PATENTS

Goddard A, Godowski PJ, Gurney AL. NL2 Tie ligand homologue polypeptide. Patent Number: 6,455,496. Date of Patent: Sept. 24, 2002.

Goddard A, Godowski PJ and Gurney AL. NL3 Tie ligand homologue nucleic acids. Patent Number: 6,426,218. Date of Patent: July 30, 2002.

Godowski P, Gurney A, Hillan KJ, Botstein D, **Goddard A**, Roy M, Ferrara N, Tumas D, Schwall R. NL4 Tie ligand homologue nucleic acid. Patent Number: 6,4137,770. Date of Patent: July 2, 2002.

Ashkenazi A, Fong S, **Goddard A**, Gurney AL, Napier MA, Tumas D, Wood WI. Nucleic acid encoding A-33 related antigen poly peptides. Patent Number: 6,410,708. Date of Patent:: Jun. 25, 2002.

Botstein DA, Cohen RL, **Goddard AD**, Gurney AL, Hillan KJ, Lawrence DA, Levine AJ, Pennica D, Roy MA and Wood WI. WISP polypeptides and nucleic acids encoding same. Patent Number: 6,387,657. Date of Patent: May 14, 2002.

Goddard A, Godowski PJ and Gurney AL. Tie ligands. Patent Number: 6,372,491. Date of Patent: April 16, 2002.

Godowski PJ, Gurney AL, **Goddard A** and Hillan K. TIE ligand homologue antibody. Patent Number: 6,350,450. Date of Patent: Feb. 26, 2002.

Fong S, Ferrara N, **Goddard A**, Godowski PJ, Gurney AL, Hillan K and Williams PM. Tie receptor tyrosine kinase ligand homologues. Patent Number: 6,348,351. Date of Patent: Feb. 19, 2002.

Goddard A, Godowski PJ and Gurney AL. Ligand homologues. Patent Number: 6,348,350. Date of Patent: Feb. 19, 2002.

Attie KM, Carlsson LMS, Gesundheit N and **Goddard A**. Treatment of partial growth hormone insensitivity syndrome. Patent Number: 6,207,640. Date of Patent: March 27, 2001.

Fong S, Ferrara N, **Goddard A**, Godowski PJ, Gurney AL, Hillan K and Williams PM. Nucleic acids encoding NL-3. Patent Number: 6,074,873. Date of Patent: June 13, 2000

Attie K, Carlsson LMS, Gesunheit N and **Goddard A**. Treatment of partial growth hormone insensitivity syndrome. Patent Number: 5,824,642. Date of Patent: October 20, 1998

Attie K, Carlsson LMS, Gesunheit N and **Goddard A**. Treatment of partial growth hormone insensitivity syndrome. Patent Number: 5,646,113. Date of Patent: July 8, 1997

Multiple additional provisional applications filed

PUBLICATIONS

Seshasayee D, Dowd P, Gu Q, Erickson S, **Goddard AD** Comparative sequence analysis of the *HER2* locus in mouse and man. Manuscript in preparation.

Abuzzahab MJ, **Goddard A**, Grigorescu F, Lautier C, Smith RJ and Chernausek SD. Human IGF-1 receptor mutations resulting in pre- and post-natal growth retardation. Manuscript in preparation.

Aggarwal S, Xie, M-H, Foster J, Frantz G, Stinson J, Corpuz RT, Simmons L, Hillan K, Yansura DG, Vandlen RL, **Goddard AD** and Gurney AL. FHFR, a novel receptor for the fibroblast growth factors. Manuscript submitted.

Adams SH, Chui C, Schilbach SL, Yu XX, **Goddard AD**, Grimaldi JC, Lee J, Dowd P, Colman S., Lewin DA. (2001) BFIT, a unique acyl-CoA thioesterase induced in thermogenic brown adipose tissue: Cloning, organization of the human gene, and assessment of a potential link to obesity. *Biochemical Journal* **360**: 135-142.

Lee J. Ho WH. Maruoka M. Corpuz RT. Baldwin DT. Foster JS. **Goddard AD**. Yansura DG. Vandlen RL. Wood WI. Gurney AL. (2001) IL-17E, a novel proinflammatory ligand for the IL-17 receptor homolog IL-17Rh1. *Journal of Biological Chemistry* **276**(2): 1660-1664.

Xie M-H, Aggarwal S, Ho W-H, Foster J, Zhang Z, Stinson J, Wood WI, **Goddard AD** and Gurney AL. (2000) Interleukin (IL)-22, a novel human cytokine that signals through the interferon-receptor related proteins CRF2-4 and IL-22R. *Journal of Biological Chemistry* **275**: 31335-31339.

Weiss GA, Watanabe CK, Zhong A, **Goddard A** and Sidhu SS. (2000) Rapid mapping of protein functional epitopes by combinatorial alanine scanning. *Proc. Natl. Acad. Sci. USA* **97**: 8950-8954.

Guo S, Yamaguchi Y, Schilbach S, Wada T.;Lee J, **Goddard A**, French D , Handa H, Rosenthal A. (2000) A regulator of transcriptional elongation controls vertebrate neuronal development. *Nature* **408**: 366-369.

Yan M, Wang L-C, Hymowitz SG, Schilbach S, Lee J, **Goddard A**, de Vos AM, Gao WQ, Dixit VM. (2000) Two-amino acid molecular switch in an epithelial morphogen that regulates binding to two distinct receptors. *Science* **290**: 523-527.

Sehl PD, Tai JTN, Hillan KJ, Brown LA, **Goddard A**, Yang R, Jin H and Lowe DG. (2000) Application of cDNA microarrays in determining molecular phenotype in cardiac growth, development, and response to injury. *Circulation* **101**: 1990-1999.

Guo S, Brush J, Teraoka H, **Goddard A**, Wilson SW, Mullins MC and Rosenthal A. (1999) Development of noradrenergic neurons in the zebrafish hindbrain requires BMP, FGF8, and the homeodomain protein soulless/Phox2A. *Neuron* **24**: 555-566.

Stone D, Murone, M, Luoh, S, Ye W, Armanini P, Gurney A, Phillips HS, Brush, J, **Goddard A**, de Sauvage FJ and Rosenthal A. (1999) Characterization of the human suppressor of fused; a negative regulator of the zinc-finger transcription factor Gli. *J. Cell Sci.* **112**: 4437-4448.

Xie M-H, Holcomb I, Deuel B, Dowd P, Huang A, Vagts A, Foster J, Liang J, Brush J, Gu Q, Hillan K, **Goddard A** and Gurney, A.L. (1999) FGF-19, a novel fibroblast growth factor with unique specificity for FGFR4. *Cytokine* **11**: 729-735.

Yan M, Lee J, Schilbach S, **Goddard A** and Dixit V. (1999) mE10, a novel caspase recruitment domain-containing proapoptotic molecule. *J. Biol. Chem.* **274**(15): 10287-10292.

Gurney AL, Marsters SA, Huang RM, Pitti RM, Mark DT, Baldwin DT, Gray AM, Dowd P, Brush J, Heldens S, Schow P, **Goddard AD**, Wood WI, Baker KP, Godowski PJ and Ashkenazi A. (1999) Identification of a new member of the tumor necrosis factor family and its receptor, a human ortholog of mouse GITR. *Current Biology* 9(4): 215-218.

Ridgway JBB, Ng E, Kern JA ,Lee J, Brush J, **Goddard A** and Carter P. (1999) Identification of a human anti-CD55 single-chain Fv by subtractive panning of a phage library using tumor and nontumor cell lines. *Cancer Research* 59: 2718-2723.

Pitti RM, Marsters SA, Lawrence DA, Roy M, Kischkel FC, Dowd P, Huang A, Donahue CJ, Sherwood SW, Baldwin DT, Godowski PJ, Wood WI, Gurney AL, Hillan KJ, Cohen RL, **Goddard AD**, Botstein D and Ashkenazi A. (1998) Genomic amplification of a decoy receptor for Fas ligand in lung and colon cancer. *Nature* **396**(6712): 699-703.

Pennica D, Swanson TA, Welsh JW, Roy MA, Lawrence DA, Lee J, Brush J, Taneyhill LA, Deuel B, Lew M, Watanabe C, Cohen RL, Melhem MF, Finley GG, Quirke P, **Goddard AD**, Hillan KJ, Gurney AL, Botstein D and Levine AJ. (1998) WISP genes are members of the connective tissue growth factor family that are up-regulated in wnt-1-transformed cells and aberrantly expressed in human colon tumors. *Proc. Natl. Acad. Sci. USA.* **95**(25): 14717-14722.

Yang RB, Mark MR, Gray A, Huang A, Xie MH, Zhang M, **Goddard A**, Wood WI, Gurney AL and Godowski PJ. (1998) Toll-like receptor-2 mediates lipopolysaccharide-induced cellular signalling. *Nature* **395**(6699): 284-288.

Merchant AM, Zhu Z, Yuan JQ, **Goddard A**, Adams CW, Presta LG and Carter P. (1998) An efficient route to human bispecific IgG. *Nature Biotechnology* **16**(7): 677-681.

Marsters SA, Sheridan JP, Pitti RM, Brush J, **Goddard A** and Ashkenazi A. (1998) Identification of a ligand for the death-domain-containing receptor Apo3. *Current Biology* **8**(9): 525-528.

Xie J, Murone M, Luoh SM, Ryan A, Gu Q, Zhang C, Bonifas JM, Lam CW, Hynes M, **Goddard A,** Rosenthal A, Epstein EH Jr. and de Sauvage FJ. (1998) Activating Smoothened mutations in sporadic basal-cell carcinoma. *Nature.* **391**(6662): 90-92.

Marsters SA, Sheridan JP, Pitti RM, Huang A, Skubatch M, Baldwin D, Yuan J, Gurney A, **Goddard AD**, Godowski P and Ashkenazi A. (1997) A novel receptor for Apo2L/TRAIL contains a truncated death domain. *Current Biology.* 7(12): 1003-1006.

Hynes M, Stone DM, Dowd M, Pitts-Meek S, **Goddard A**, Gurney A and Rosenthal A. (1997) Control of cell pattern in the neural tube by the zinc finger transcription factor *Gli-1. Neuron* **19**: 15–26.

Sheridan JP, Marsters SA, Pitti RM, Gurney A., Skubatch M, Baldwin D, Ramakrishnan L, Gray CL, Baker K, Wood WI, **Goddard AD**, Godowski P, and Ashkenazi A. (1997) Control of TRAIL-Induced Apoptosis by a Family of Signaling and Decoy Receptors. *Science* 277 (5327): 818-821.

Goddard AD, Dowd P, Chernausek S, Geffner M, Gertner J, Hintz R, Hopwood N, Kaplan S, Plotnick L, Rogol A, Rosenfield R, Saenger P, Mauras N, Hershkopf R, Angulo M and Attie, K. (1997) Partial growth hormone insensitivity: The role of growth hormone receptor mutations in idiopathic short stature. *J. Pediatr.* **131**: S51-55.

Klein RD, Sherman D, Ho WH, Stone D, Bennett GL, Moffat B, Vandlen R, Simmons L, Gu Q, Hongo JA, Devaux B, Poulsen K, Armanini M, Nozaki C, Asai N, **Goddard A**, Phillips H, Henderson CE, Takahashi M and Rosenthal A. (1997) A GPI-linked protein that interacts with Ret to form a candidate neurturin receptor. *Nature.* **387**(6634): 717-21.

Stone DM, Hynes M, Armanini M, Swanson TA, Gu Q, Johnson RL, Scott MP, Pennica D, **Goddard A**, Phillips H, Noll M, Hooper JE, de Sauvage F and Rosenthal A. (1996) The tumour-suppressor gene patched encodes a candidate receptor for Sonic hedgehog. *Nature* **384**(6605): 129-34.

Marsters SA, Sheridan JP, Donahue CJ, Pitti RM, Gray CL, **Goddard AD**, Bauer KD and Ashkenazi A. (1996) Apo-3, a new member of the tumor necrosis factor receptor family, contains a death domain and activates apoptosis and NF-kappa β. *Current Biology* **6**(12): 1669-76.

Rothe M, Xiong J, Shu HB, Williamson K, **Goddard A** and Goeddel DV. (1996) I-TRAF is a novel TRAF-interacting protein that regulates TRAF-mediated signal transduction. *Proc. Natl. Acad. Sci. USA* **93**: 8241-8246.

Yang M, Luoh SM, **Goddard A**, Reilly D, Henzel W and Bass S. (1996) The bglX gene located at 47.8 min on the Escherichia coli chromosome encodes a periplasmic beta-glucosidase. *Microbiology* **142**: 1659-65.

Goddard AD and Black DM. (1996) Familial Cancer in <u>Molecular Endocrinology of Cancer.</u> Waxman, J. Ed. Cambridge University Press, Cambridge UK, pp.187-215.

Treanor JJS, Goodman L, de Sauvage F, Stone DM, Poulson KT, Beck CD, Gray C, Armanini MP, Pollocks RA, Hefti F, Phillips HS, **Goddard A**, Moore MW, Buj-Bello A, Davis AM, Asai N, Takahashi M, Vandlen R, Henderson CE and Rosenthal A. (1996) Characterization of a receptor for GDNF. *Nature* **382**: 80-83.

Klein RD, Gu Q, **Goddard A** and Rosenthal A. (1996) Selection for genes encoding secreted proteins and receptors. *Proc. Natl. Acad. Sci. USA* **93**: 7108-7113.

Winslow JW, Moran P, Valverde J, Shih A, Yuan JQ, Wong SC, Tsai SP, **Goddard A**, Henzel WJ, Hefti F and Caras I. (1995) Cloning of AL-1, a ligand for an Eph-related tyrosine kinase receptor involved in axon bundle formation. *Neuron* **14**: 973-981.

Bennett BD, Zeigler FC, Gu Q, Fendly B, **Goddard AD**, Gillett N and Matthews W. (1995) Molecular cloning of a ligand for the EPH-related receptor protein-tyrosine kinase Htk. *Proc. Natl. Acad. Sci. USA* **92**: 1866-1870.

Huang X, Yuang J, **Goddard A**, Foulis A, James RF, Lernmark A, Pujol-Borrell R, Rabinovitch A, Somoza N and Stewart TA. (1995) Interferon expression in the pancreases of patients with type I diabetes. *Diabetes* **44**: 658-664.

Goddard AD, Yuan JQ, Fairbairn L, Dexter M, Borrow J, Kozak C and Solomon E. (1995) Cloning of the murine homolog of the leukemia-associated PML gene. *Mammalian Genome* **6**: 732-737.

Goddard AD, Covello R, Luoh SM, Clackson T, Attie KM, Gesundheit N, Rundle AC, Wells JA, Carlsson LMTI and The Growth Hormone Insensitivity Study Group. (1995) Mutations of the growth hormone receptor in children with idiopathic short stature. *N. Engl. J. Med.* **333**: 1093-1098.

Kuo SS, Moran P, Gripp J, Armanini M, Phillips HS, **Goddard A** and Caras IW. (1994) Identification and characterization of Batk, a predominantly brain-specific non-receptor protein tyrosine kinase related to Csk. *J. Neurosci. Res.* **38**: 705-715.

Mark MR, Scadden DT, Wang Z, Gu Q, **Goddard A** and Godowski PJ. (1994) Rse, a novel receptor-type tyrosine kinase with homology to Axl/Ufo, is expressed at high levels in the brain. *Journal of Biological Chemistry* **269**: 10720-10728.

Borrow J, Shipley J, Howe K, Kiely F, **Goddard A**, Sheer D, Srivastava A, Antony AC, Fioretos T, Mitelman F and Solomon E. (1994) Molecular analysis of simple variant translocations in acute promyelocytic leukemia. *Genes Chromosomes Cancer* **9**: 234-243.

Goddard AD and Solomon E. (1993) Genetics of Cancer. *Adv. Hum. Genet.* **21**: 321-376.

Borrow J, **Goddard AD**, Gibbons B, Katz F, Swirsky D, Fioretos T, Dube I, Winfield DA, Kingston J, Hagemeijer A, Rees JKH, Lister AT and Solomon E. (1992) Diagnosis of acute promyelocytic leukemia by RT-PCR: Detection of *PML-RARA* and *RARA-PML* fusion transcripts. *Br. J. Haematol.* **82**: 529-540.

Goddard AD, Borrow J and Solomon E. (1992) A previously uncharacterized gene, PML, is fused to the retinoic acid receptor alpha gene in acute promyelocytic leukemia. *Leukemia* **6 Suppl 3**: 117S–119S.

Zhu X, Dunn JM, **Goddard AD**, Squire JA, Becker A, Phillips RA and Gallie BL. (1992) Mechanisms of loss of heterozygosity in retinoblastoma. *Cytogenet. Cell. Genet.* **59**: 248-252.

Foulkes W, **Goddard A.** and Patel K. (1991) Retinoblastoma linked with Seascale [letter]. *British Med. J.* **302**: 409.

Goddard AD, Borrow J, Freemont PS and Solomon E. (1991) Characterization of a novel zinc finger gene disrupted by the t(15;17) in acute promyelocytic leukemia. *Science* **254**: 1371-1374.

Solomon E, Borrow J and **Goddard AD.** (1991) Chromosomal aberrations in cancer. *Science* **254**: 1153-1160.

Pajunen L, Jones TA, **Goddard A**, Sheer D, Solomon E, Pihlajaniemi T and Kivirikko KI. (1991) Regional assignment of the human gene coding for a multifunctional peptide (P4HB) acting as the β–subunit of prolyl-4-hydroxylase and the enzyme protein disulfide isomerase to 17q25. *Cytogenet. Cell. Genet.* **56**: 165-168.

Borrow J, Black DM, **Goddard AD**, Yagle MK, Frischauf A.-M and Solomon E. (1991) Construction and regional localization of a *Not*I linking library from human chromosome 17q. *Genomics* **10**: 477–480.

Borrow J, **Goddard AD**, Sheer D and Solomon E. (1990) Molecular analysis of acute promyelocytic leukemia breakpoint cluster region on chromosome 17. *Science* **249**: 1577-1580.

Myers JC, Jones TA, Pohjolainen E-R, Kadri AS, **Goddard AD**, Sheer D, Solomon E and Pihlajaniemi T. (1990) Molecular cloning of 5(IV) collagen and assignment of the gene to the region of the region of the X-chromosome containing the Alport Syndrome locus. *Am. J. Hum. Genet.* **46**: 1024-1033.

Gallie BL, Squire JA, **Goddard A**, Dunn JM, Canton M, Hinton D, Zhu X and Phillips RA. (1990) Mechanisms of oncogenesis in retinoblastoma. *Lab. Invest.* **62**: 394-408.

Goddard AD, Phillips RA, Greger V, Passarge E, Hopping W, Gallie BL and Horsthemke B. (1990) Use of the RB1 cDNA as a diagnostic probe in retinoblastoma families. *Clinical Genetics* **37**: 117-126.

Zhu XP, Dunn JM, Phillips RA, **Goddard AD**, Paton KE, Becker A and Gallie BL. (1989) Germline, but not somatic, mutations of the RB1 gene preferentially involve the paternal allele. *Nature* **340**: 312-314.

Gallie BL, Dunn JM, **Goddard A**, Becker A and Phillips RA. (1988) Identification of mutations in the putative retinoblastoma gene. In <u>Molecular Biology of The Eye: Genes, Vision and Ocular Disease</u>. UCLA Symposia on Molecular and Cellular Biology, New Series, Volume 88. J. Piatigorsky, T. Shinohara and P.S. Zelenka, Eds. Alan R. Liss, Inc., New York, 1988, pp. 427-436.

Goddard AD, Balakier H, Canton M, Dunn J, Squire J, Reyes E, Becker A, Phillips RA and Gallie BL. (1988) Infrequent genomic rearrangement and normal expression of the putative RB1 gene in retinoblastoma tumors. *Mol. Cell. Biol.* **8**: 2082-2088.

Squire J, Dunn J, **Goddard A**, Hoffman T, Musarella M, Willard HF, Becker AJ, Gallie BL and Phillips RA. (1986) Cloning of the esterase D gene: A polymorphic gene probe closely linked to the retinoblastoma locus on chromosome 13. *Proc. Natl. Acad. Sci.* USA **83**: 6573-6577.

Squire J, **Goddard AD**, Canton M, Becker A, Phillips RA and Gallie BL (1986) Tumour induction by the retinoblastoma mutation is independent of N-*myc* expression. *Nature* **322**: 555-557.

Goddard AD, Heddle JA, Gallie BL and Phillips RA. (1985) Radiation sensitivity of fibroblasts of bilateral retinoblastoma patients as determined by micronucleus induction *in vitro*. *Mutation Research* **152**: 31-38.

RESEARCH /

SIMULTANEOUS AMPLIFICATION AND DETECTION OF SPECIFIC DNA SEQUENCES

Russell Higuchi*, Gavin Dollinger[1], P. Sean Walsh and Robert Griffith

Roche Molecular Systems, Inc., 1400 53rd St., Emeryville, CA 94608. [1]Chiron Corporation, 1400 53rd St., Emeryville, CA 94608. *Corresponding author.

We have enhanced the polymerase chain reaction (PCR) such that specific DNA sequences can be detected without opening the reaction tube. This enhancement requires the addition of ethidium bromide (EtBr) to a PCR. Since the fluorescence of EtBr increases in the presence of double-stranded (ds) DNA an increase in fluorescence in such a PCR indicates a positive amplification, which can be easily monitored externally. In fact, amplification can be continuously monitored in order to follow its progress. The ability to simultaneously amplify specific DNA sequences and detect the product of the amplification both simplifies and improves PCR and may facilitate its automation and more widespread use in the clinic or in other situations requiring high sample throughput.

Although the potential benefits of PCR[1] to clinical diagnostics are well known[2,3], it is still not widely used in this setting, even though it is four years since thermostable DNA polymerases[4] made PCR practical. Some of the reasons for its slow acceptance are high cost, lack of automation of pre- and post-PCR processing steps, and false positive results from carryover-contamination. The first two points are related in that labor is the largest contributor to cost at the present stage of PCR development. Most current assays require some form of "downstream" processing once thermocycling is done in order to determine whether the target DNA sequence was present and has amplified. These include DNA hybridization[5,6], gel electrophoresis with or without use of restriction digestion[7,8], HPLC[9], or capillary electrophoresis[10]. These methods are labor-intense, have low throughput, and are difficult to automate. The third point is also closely related to downstream processing. The handling of the PCR product in these downstream processes increases the chances that amplified DNA will spread through the typing lab, resulting in a risk of

"carryover" false positives in subsequent testing[11].

These downstream processing steps would be eliminated if specific amplification and detection of amplified DNA took place simultaneously within an unopened reaction vessel. Assays in which such different processes take place without the need to separate reaction components have been termed "homogeneous". No truly homogeneous PCR assay has been demonstrated to date, although progress towards this end has been reported. Chehab, et al.[12], developed a PCR product detection scheme using fluorescent primers that resulted in a fluorescent PCR product. Allele-specific primers, each with different fluorescent tags, were used to indicate the genotype of the DNA. However, the unincorporated primers must still be removed in a downstream process in order to visualize the result. Recently, Holland, et al.[13], developed an assay in which the endogenous 5' exonuclease assay of *Taq* DNA polymerase was exploited to cleave a labeled oligonucleotide probe. The probe would only cleave if PCR amplification had produced its complementary sequence. In order to detect the cleavage products, however, a subsequent process is again needed.

We have developed a truly homogeneous assay for PCR and PCR product detection based upon the greatly increased fluorescence that ethidium bromide and other DNA binding dyes exhibit when they are bound to ds-DNA[14–16]. As outlined in Figure 1, a prototypic PCR
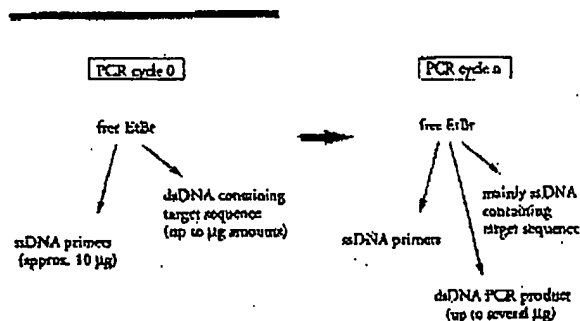

FIGURE 1 Principle of simultaneous amplification and detection of PCR product. The components of a PCR containing EtBr that are fluorescent are listed—EtBr itself, EtBr bound to either ssDNA or dsDNA. There is a large fluorescence enhancement when EtBr is bound to DNA and binding is greatly enhanced when DNA is double-stranded. After sufficient (n) cycles of PCR, the net increase in dsDNA results in additional EtBr binding, and a net increase in total fluorescence.

0 1/16 1/8 1/4 1/2 1 2 4 8 µg/ml EtBr
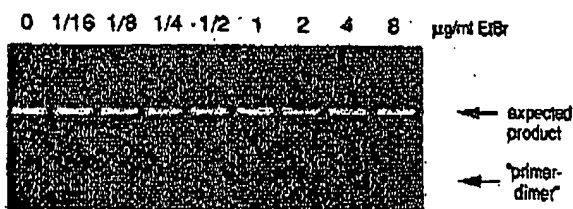
← expected product

← "primer-dimer"

FIGURE 2 Gel electrophoresis of PCR amplification products of the human, nuclear gene, HLA DQα, made in the presence of increasing amounts of EtBr (up to 8 µg/ml). The presence of EtBr has no obvious effect on the yield or specificity of amplification.
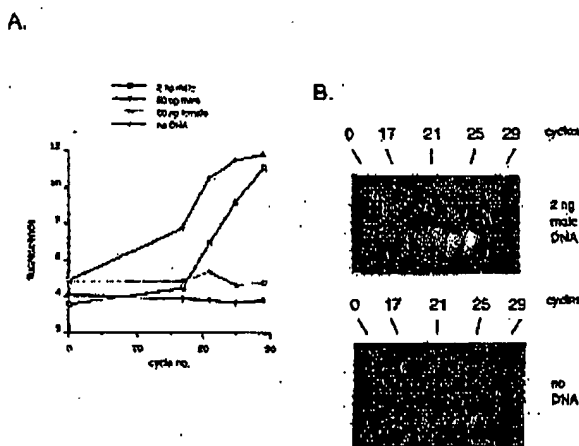
A.

B.

0 17 21 25 29 cycles

2 ng male DNA

0 17 21 25 29 cycles

no DNA

FIGURE 3 (A) Fluorescence measurements from PCRs that contain 0.5 µg/ml EtBr and that are specific for Y-chromosome repeat sequences. Five replicate PCRs were begun containing each of the DNAs specified. At each indicated cycle, one of the five replicate PCRs for each DNA was removed from thermocycling and its fluorescence measured. Units of fluorescence are arbitrary. (B) UV photography of PCR tubes (0.5 ml Eppendorf-style, polypropylene micro-centrifuge tubes) containing reactions, those starting from 2 ng male DNA and control reactions without any DNA, from (A).

begins with primers that are single-stranded DNA (ssDNA), dNTPs, and DNA polymerase. An amount of dsDNA containing the target sequence (target DNA) is also typically present. This amount can vary, depending on the application, from single-cell amounts of DNA[17] to micrograms per PCR[18]. If EtBr is present, the reagents that will fluoresce, in order of increasing fluorescence, are free EtBr itself, and EtBr bound to the single-stranded DNA primers and to the double-stranded target DNA (by its intercalation between the stacked bases of the DNA double-helix). After the first denaturation cycle, target DNA will be largely single-stranded. After a PCR is completed, the most significant change is the increase in the amount of dsDNA (the PCR product itself) of up to several micrograms. Formerly free EtBr is bound to the additional dsDNA, resulting in an increase in fluorescence. There is also some decrease in the amount of ssDNA primer, but because the binding of EtBr to ssDNA is much less than to dsDNA, the effect of this change on the total fluorescence of the sample is small. The fluorescence increase can be measured by directing excitation illumination through the walls of the amplification vessel

before and after, or even continuously during, thermocycling.

RESULTS

PCR in the presence of EtBr. In order to assess the affect of EtBr in PCR, amplifications of the human HLA DQα gene[19] were performed with the dye present at concentrations from 0.06 to 8.0 µg/ml (a typical concentration of EtBr used in staining of nucleic acids following gel electrophoresis is 0.5 µg/ml). As shown in Figure 2, gel electrophoresis revealed little or no difference in the yield or quality of the amplification product whether EtBr was absent or present at any of these concentrations, indicating that EtBr does not inhibit PCR.

Detection of human Y-chromosome specific sequences. Sequence-specific, fluorescence enhancement of EtBr as a result of PCR was demonstrated in a series of amplifications containing 0.5 µg/ml EtBr and primers specific to repeat DNA sequences found on the human Y-chromosome[20]. These PCRs initially contained either 60 ng male, 60 ng female, 2 ng male human or no DNA. Five replicate PCRs were begun for each DNA. After 0, 17, 21, 24 and 29 cycles of thermocycling, a PCR for each DNA was removed from the thermocycler, and its fluorescence measured in a spectrofluorometer and plotted vs. amplification cycle number (Fig. 3A). The shape of this curve reflects the fact that by the time an increase in fluorescence can be detected, the increase in DNA is becoming linear and not exponential with cycle number. As shown, the fluorescence increased about three-fold over the background fluorescence for the PCRs containing human male DNA, but did not significantly increase for negative control PCRs, which contained either no DNA or human female DNA. The more male DNA present to begin with—60 ng versus 2 ng—the fewer cycles were needed to give a detectable increase in fluorescence. Gel electrophoresis on the products of these amplifications showed that DNA fragments of the expected size were made in the male DNA containing reactions and that little DNA synthesis took place in the control samples.

In addition, the increase in fluorescence was visualized by simply laying the completed, unopened PCRs on a UV transilluminator and photographing them through a red filter. This is shown in figure 3B for the reactions that began with 2 ng male DNA and those with no DNA.

Detection of specific alleles of the human β-globin gene. In order to demonstrate that this approach has adequate specificity to allow genetic screening, a detection of the sickle-cell anemia mutation was performed. Figure 4 shows the fluorescence from completed amplifications containing EtBr (0.5 µg/ml) as detected by photography of the reaction tubes on a UV transilluminator. These reactions were performed using primers specific for either the wild-type or sickle-cell mutation of the human β-globin gene[21]. The specificity for each allele is imparted by placing the sickle-mutation site at the terminal 3' nucleotide of one primer. By using an appropriate primer annealing temperature, primer extension—and thus amplification—can take place only if the 3' nucleotide of the primer is complementary to the β-globin allele present[21,22].

Each pair of amplifications shown in Figure 4 consists of a reaction with either the wild-type allele specific (left tube) or sickle-allele specific (right tube) primers. Three different DNAs were typed: DNA from a homozygous, wild-type β-globin individual (AA); from a heterozygous sickle β-globin individual (AS); and from a homozygous sickle β-globin individual (SS). Each DNA (50 ng genomic DNA to start each PCR) was analyzed in triplicate (3 pairs

of reactions each). The DNA type was reflected in the relative fluorescence intensities in each pair of completed amplifications. There was a significant increase in fluorescence only where a β-globin allele DNA matched the primer set. When measured on a spectrofluorometer (data not shown), this fluorescence was about three times that present in a PCR where both β-globin alleles were mismatched to the primer set. Gel electrophoresis (not shown) established that this increase in fluorescence was due to the synthesis of nearly a microgram of a DNA fragment of the expected size for β-globin. There was little synthesis of dsDNA in reactions in which the allele-specific primer was mismatched to both alleles.

Continuous monitoring of a PCR. Using a fiber optic device, it is possible to direct excitation illumination from a spectrofluorometer to a PCR undergoing thermocycling and to return its fluorescence to the spectrofluorometer. The fluorescence readout of such an arrangement, directed at an EtBr-containing amplification of Y-chromosome specific sequences from 25 ng of human male DNA, is shown in Figure 5. The readout from a control PCR with no target DNA is also shown. Thirty cycles of PCR were monitored for each.

The fluorescence trace as a function of time clearly shows the effect of the thermocycling. Fluorescence intensity rises and falls inversely with temperature. The fluorescence intensity is minimum at the denaturation temperature (94°C) and maximum at the annealing/extension temperature (50°C). In the negative-control PCR, these fluorescence maxima and minima do not change significantly over the thirty thermocycles, indicating that there is little dsDNA synthesis without the appropriate target DNA, and there is little if any bleaching of EtBr during the continuous illumination of the sample.

In the PCR containing male DNA, the fluorescence maxima at the annealing/extension temperature begin to increase at about 4000 seconds of thermocycling, and continue to increase with time, indicating that dsDNA is being produced at a detectable level. Note that the fluorescence minima at the denaturation temperature do not significantly increase, presumably because at this temperature there is no dsDNA for EtBr to bind. Thus the course of the amplification is followed by tracking the fluorescence increase at the annealing temperature. Analysis of the products of these two amplifications by gel electrophoresis showed a DNA fragment of the expected size for the male DNA containing sample and no detectable DNA synthesis for the control sample.

DISCUSSION

Downstream processes such as hybridization to a sequence-specific probe can enhance the specificity of DNA detection by PCR. The elimination of these processes means that the specificity of this homogeneous assay depends solely on that of PCR. In the case of sickle-cell disease, we have shown that PCR alone has sufficient DNA sequence specificity to permit genetic screening. Using appropriate amplification conditions, there is little nonspecific production of dsDNA in the absence of the appropriate target allele.

The specificity required to detect pathogens can be more or less than that required to do genetic screening, depending on the number of pathogens in the sample and the amount of other DNA that must be taken with the sample. A difficult target is HIV, which requires detection of a viral genome that can be at the level of a few copies per thousands of host cells[6]. Compared with genetic screening, which is performed on cells containing at least one copy of the target sequence, HIV detection requires both more specificity and the input of more total
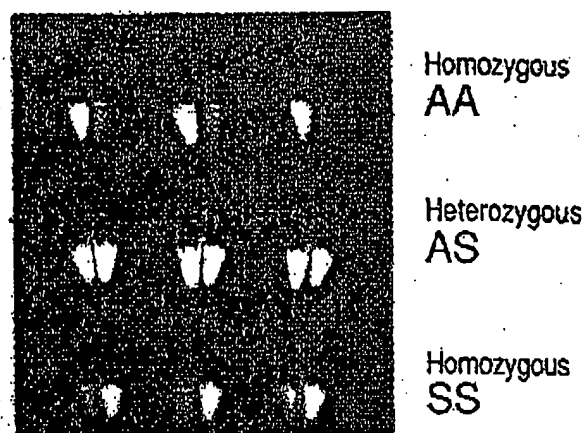

FIGURE 4 UV photography of PCR tubes containing amplifications using EtBr that are specific to wild-type (A) or sickle (S) alleles of the human β-globin gene. The left of each pair of tubes contains allele-specific primers to the wild-type alleles, the right tube primers to the sickle allele. The photograph was taken after 30 cycles of PCR, and the input DNAs and the alleles they contain are indicated. Fifty ng of DNA was used to begin PCR. Typing was done in triplicate (3 pairs of PCRs) for each input DNA.
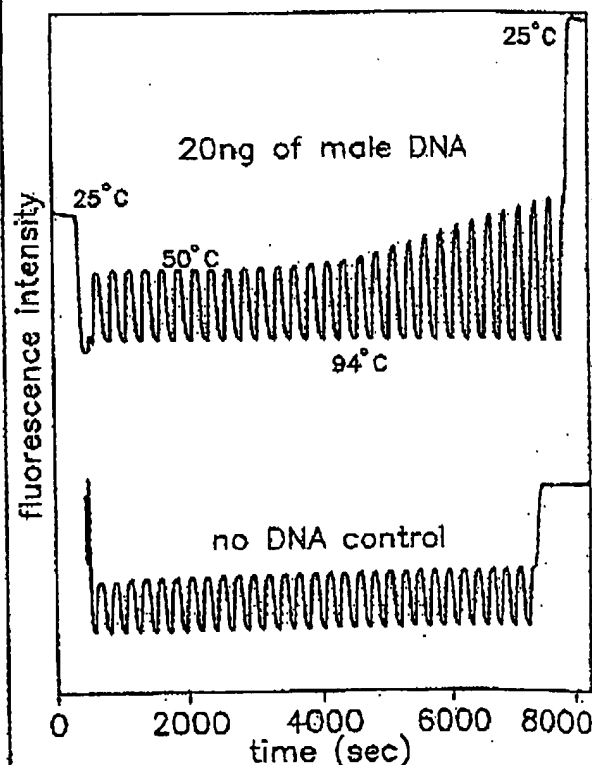
Homozygous **AA**

Heterozygous **AS**

Homozygous **SS**

FIGURE 5 Continuous, real-time monitoring of a PCR. A fiber optic was used to carry excitation light to a PCR in progress and also emitted light back to a fluorometer (see Experimental Protocol). Amplification using human male-DNA specific primers in a PCR starting with 20 ng of human male DNA (top), or in a control PCR without DNA (bottom), were monitored. Thirty cycles of PCR were followed for each. The temperature cycled between 94°C (denaturation) and 50°C (annealing and extension). Note in the male DNA PCR, the cycle (time) dependent increase in fluorescence at the annealing/extension temperature.

DNA—up to microgram amounts—in order to have sufficient numbers of target sequences. This large amount of starting DNA in an amplification significantly increases the background fluorescence over which any additional fluorescence produced by PCR must be detected. An additional complication that occurs with targets in low copy-number is the formation of the "primer-dimer" artifact. This is the result of the extension of one primer using the other primer as a template. Although this occurs infrequently, once it occurs the extension product is a substrate for PCR amplification, and can compete with true PCR targets if those targets are rare. The primer-dimer product is of course dsDNA and thus is a potential source of false signal in this homogeneous assay.

To increase PCR specificity and reduce the effect of primer-dimer amplification, we are investigating a number of approaches, including the use of nested-primer amplifications that take place in a single tube[5], and the "hot-start", in which nonspecific amplification is reduced by raising the temperature of the reaction before DNA synthesis begins[23]. Preliminary results using these approaches suggest that primer-dimer is effectively reduced and it is possible to detect the increase in EtBr fluorescence in a PCR instigated by a single HIV genome in a background of 10^5 cells. With larger numbers of cells, the background fluorescence contributed by genomic DNA becomes problematic. To reduce this background, it may be possible to use sequence-specific DNA-binding dyes that can be made to preferentially bind PCR product over genomic DNA by incorporating the dye-binding DNA sequence into the PCR product through a 5' "add-on" to the oligonucleotide primer[24].

We have shown that the detection of fluorescence generated by an EtBr-containing PCR is straightforward, both once PCR is completed and continuously during thermocycling. The ease with which automation of specific DNA detection can be accomplished is the most promising aspect of this assay. The fluorescence analysis of completed PCRs is already possible with existing instrumentation in 96-well format[25]. In this format, the fluorescence in each PCR can be quantitated before, after, and even at selected points during thermocycling by moving the rack of PCRs to a 96-microwell plate fluorescence reader[26].

The instrumentation necessary to continuously monitor multiple PCRs simultaneously is also simple in principle. A direct extension of the apparatus used here is to have multiple fiberoptics transmit the excitation light and fluorescent emissions to and from multiple PCRs. The ability to monitor multiple PCRs continuously may allow quantitation of target DNA copy number. Figure 3 shows that the larger the amount of starting target DNA, the sooner during PCR a fluorescence increase is detected. Preliminary experiments (Higuchi and Dollinger, manuscript in preparation) with continuous monitoring have shown a sensitivity to two-fold differences in initial target DNA concentration.

Conversely, if the number of target molecules is known—as it can be in genetic screening—continuous monitoring may provide a means of detecting false positive and false negative results. With a known number of target molecules, a true positive would exhibit detectable fluorescence by a predictable number of cycles of PCR. Increases in fluorescence detected before or after that cycle would indicate potential artifacts. False negative results due to, for example, inhibition of DNA polymerase, may be detected by including within each PCR an inefficiently amplifying marker. This marker results in a fluorescence increase only after a large number of cycles—many more than are necessary to detect a true

positive. If a sample fails to have a fluorescence increase after this many cycles, inhibition may be suspected. Since, in this assay, conclusions are drawn based on the presence or absence of fluorescence signal alone, such controls may be important. In any event, before any test based on this principle is ready for the clinic, an assessment of its false positive/false negative rates will need to be obtained using a large number of known samples.

In summary, the inclusion in PCR of dyes whose fluorescence is enhanced upon binding dsDNA makes it possible to detect specific DNA amplification from outside the PCR tube. In the future, instruments based upon this principle may facilitate the more widespread use of PCR in applications that demand the high throughput of samples.

EXPERIMENTAL PROTOCOL

Human HLA-DQα gene amplifications containing EtBr. PCRs were set up in 100 μl volumes containing 10 mM Tris-HCl, pH 8.3; 50 mM KCl; 4 mM MgCl$_2$; 2.5 units of *Taq* DNA polymerase (Perkin-Elmer Cetus, Norwalk, CT); 20 pmole each of human HLA-DQα gene specific oligonucleotide primers (GH26 and GH27[19] and approximately 10^7 copies of DQα PCR product diluted from a previous reaction. Ethidium bromide (EtBr; Sigma) was used at the concentrations indicated in Figure 2. Thermocycling proceeded for 20 cycles in a model 480 thermocycler (Perkin-Elmer Cetus, Norwalk, CT) using a "step-cycle" program of 94°C for 1 min. denaturation and 60°C for 30 sec. annealing and 72°C for 30 sec. extension.

Y-chromosome specific PCR. PCRs (100 μl total reaction volume) containing 0.5 μg/ml EtBr were prepared as described for HLA-DQα, except with different primers and target DNAs. These PCRs contained 15 pmole each male DNA-specific primers Y1.1 and Y1.2[20], and either 60 ng male, 60 ng female, 2 ng male, or no human DNA. Thermocycling was 94°C for 1 min. and 60°C for 1 min using a "step-cycle" program. The number of cycles for a sample were as indicated in Figure 3. Fluorescence measurement is described below.

Allele-specific, human β-globin gene PCR. Amplifications of 100 μl volume using 0.5 μg/ml of EtBr were prepared as described for HLA-DQα above except with different primers and target DNAs. These PCRs contained either primer pair HGP2/Hβ14A (wild-type globin specific primers) or HGP2/Hβ14S (sickle-globin specific primers) at 10 pmole each primer per PCR. These primers were developed by Wu et al.[21]. Three different target DNAs were used in separate amplifications—50 ng each of human DNA that was homozygous for the sickle trait (SS), DNA that was heterozygous for the sickle trait (AS), or DNA that was homozygous for the w.t. globin (AA). Thermocycling was for 30 cycles at 94°C for 1 min. and 55°C for 1 min. using a "step-cycle" program. An annealing temperature of 55°C had been shown by Wu et al.[21] to provide allele-specific amplification. Completed PCRs were photographed through a red filter (Wratten 23A) after placing the reaction tubes atop a model TM-36 transilluminator (UV-products San Gabriel, CA).

Fluorescence measurement. Fluorescence measurements were made on PCRs containing EtBr in a Fluorolog-2 fluorometer (SPEX, Edison, NJ). Excitation was at the 500 nm band with about 2 nm bandwidth with a GG 435 nm cut-off filter (Melles Griot, Inc., Irvine, CA) to exclude second-order light. Emitted light was detected at 570 nm with a bandwidth of about 7 nm. An OG 530 nm cut-off filter was used to remove the excitation light.

Continuous fluorescence monitoring of PCR. Continuous monitoring of a PCR in progress was accomplished using the spectrofluorometer and settings described above as well as a fiberoptic accessory (SPEX cat. no. 1950) to both send excitation light to, and receive emitted light from, a PCR placed in a well of a model 480 thermocycler (Perkin-Elmer Cetus). The probe end of the fiberoptic cable was attached with "5 minute-epoxy" to the open top of a PCR tube (a 0.5 ml polypropylene centrifuge tube with its cap removed) effectively sealing it. The exposed top of the PCR tube and the end of the fiberoptic cable were shielded from room light and the room lights were kept dimmed during each run. The monitored PCR was an amplification of Y-chromosome-specific repeat sequences as described above, except using an annealing/extension temperature of 50°C. The reaction was covered with mineral oil (2 drops) to prevent evaporation. Thermocycling and fluorescence measurement were started simultaneously. A time-base scan with a 10 second integration time

was used and the emission signal was ratioed to the excitation signal to control for changes in light-source intensity. Data were collected using the dm3000f, version 2.5 (SPEX) data system.

Acknowledgments

We thank Bob Jones for help with the spectrofluormetric measurements and Heatherbell Fong for editing this manuscript.

References

1. Mullis, K., Faloona, F., Scharf, S., Saiki, R., Horn, G. and Erlich, H. 1986. Specific enzymatic amplification of DNA in vitro: The polymerase chain reaction. CSHSQB 51:263-273.
2. White, T. J., Arnheim, N. and Erlich, H. A. 1989. The polymerase chain reaction. Trends Genet. 5:185-189.
3. Erlich, H. A., Gelfand, D. and Sninsky, J. J. 1991. Recent advances in the polymerase chain reaction. Science 252:1643-1651.
4. Saiki, R. K., Gelfand, D. H., Stoffel, S., Scharf, S. J., Higuchi, R., Horn, G. T., Mullis, K. B. and Erlich, H. A. 1988. Primer-directed enzymatic amplification of DNA with a thermostable DNA polymerase. Science 239:487-491.
5. Saiki, R. K., Walsh, P. S., Levenson, C. H. and Erlich, H. A. 1989. Genetic analysis of amplified DNA with immobilized sequence-specific oligonucleotide probes. Proc. Natl. Acad. Sci. USA 86:6230-6234.
6. Kwok, S. Y., Mack, D. H., Mullis, K. B., Poiesz, B. J., Ehrlich, G. D., Blair, D. and Friedman-Kien, A. S. 1987. Identification of human immunodeficiency virus sequences by using in vitro enzymatic amplification and oligomer cleavage detection. J. Virol. 61:1690-1694.
7. Chehab, F. F., Doherty, M., Cai, S. P., Kan, Y. W., Cooper, S. and Rubin, E. M. 1987. Detection of sickle cell anemia and thalassemia. Nature 329:293-294.
8. Horn, G. T., Richards, B. and Klinger, K. W. 1989. Amplification of a highly polymorphic VNTR segment by the polymerase chain reaction. Nuc. Acids Res. 16:2140.
9. Katz, E. D. and Dong, M. W. 1990. Rapid analysis and purification of polymerase chain reaction products by high-performance liquid chromatography. Biotechniques 8:546-555.
10. Heiger, D. N., Cohen, A. S. and Karger, B. L. 1990. Separation of DNA restriction fragments by high performance capillary electrophoresis with low and zero crosslinked polyacrylamide using continuous and pulsed electric fields. J. Chromatogr. 516:33-48.
11. Kwok, S. Y. and Higuchi, R. G. 1989. Avoiding false positives with PCR. Nature 339:237-238.
12. Chehab, F. F. and Kan, Y. W. 1989. Detection of specific DNA sequences by fluorescence amplification: a color complementation assay. Proc. Natl. Acad. Sci. USA 86:9178-9182.
13. Holland, P. M., Abramson, R. D., Watson, R. and Gelfand, D. H.

14. Markovits, J., Roques, B. P. and Le Pecq, J. B. 1979. Ethidium dimer: a new reagent for the fluorimetric determination of nucleic acids. Anal. Biochem. 94:259-264.
15. Kapuscinski, J. and Szer, W. 1979. Interactions of 4',6-diamidine-2-phenylindole with synthetic polynucleotides. Nuc. Acids Res. 6:3519-3534.
16. Searle, M. S. and Embrey, K. J. 1990. Sequence-specific interaction of Hoechst 33258 with the minor groove of an adenine-tract DNA duplex studied in solution by ¹H NMR spectroscopy. Nuc. Acids Res. 18:3753-3762.
17. Li, H. H., Gyllensten, U. B., Cui, X. F., Saiki, R. K., Erlich, H. A. and Arnheim, N. 1988. Amplification and analysis of DNA sequences in single human sperm and diploid cells. Nature 335:414-417.
18. Abbott, M. A., Poiesz, B. J., Byrne, B. C., Kwok, S. Y., Sninsky, J. J. and Erlich, H. A. 1988. Enzymatic gene amplification: qualitative and quantitative methods for detecting proviral DNA amplified in vitro. J. Infect. Dis. 158:1158.
19. Saiki, R. K., Bugawan, T. L., Horn, G. T., Mullis, K. B. and Erlich, H. A. 1986. Analysis of enzymatically amplified β-globin and HLA-DQα DNA with allele-specific oligonucleotide probes. Nature 324:163-166.
20. Kogan, S. C., Doherty, M. and Gitschier, J. 1987. An improved method for prenatal diagnosis of genetic diseases by analysis of amplified DNA sequences. N. Engl. J. Med. 317:985-990.
21. Wu, D. Y., Ugozzoli, L., Pal, B. K. and Wallace, R. B. 1989. Allele-specific enzymatic amplification of β-globin genomic DNA for diagnosis of sickle cell anemia. Proc. Natl. Acad. Sci. USA 86:2757-2760.
22. Kwok, S., Kellogg, D. E., McKinney, N., Spasic, D., Goda, L., Levenson, C. and Sninsky, J. J. 1990. Effects of primer-template mismatches on the polymerase chain reaction: Human immunodeficiency virus type 1 model studies. Nuc. Acids Res. 18:999-1005.
23. Chou, Q., Russell, M., Birch, D., Raymond, J. and Bloch, W. 1992. Prevention of pre-PCR mis-priming and primer dimerization improves low-copy-number amplifications. Submitted.
24. Higuchi, R. 1989. Using PCR to engineer DNA, p. 61-70. In: PCR Technology. H. A. Erlich (Ed.). Stockton Press, New York, N.Y.
25. Haff, L., Atwood, J. G., DiCesare, J., Katz, E., Picozza, E., Williams, J. F. and Woudenberg, T. 1991. A high-performance system for automation of the polymerase chain reaction. Biotechniques 10:102-109, 106-112.
26. Tumosa, N. and Kahan, L. 1989. Fluorescent EIA screening of monoclonal antibodies to cell surface antigens. J. Immun. Meth. 116:59-63.

BIOTECHNOLOGY VOL 10 APRIL 1992 417

GENENTECH, INC.
1 DNA Way
South San Francisco, CA 94080 USA
Phone: (650) 225-1000

FAX: (650) 952-9881

FACSIMILE TRANSMITTAL

Date: 19 July 2004

To: Anna Barry
                 Heller Ehrman

Re: Higuchi reference

Fax No: 324 - 6638

From: Patty Tobin, Assistant to Elizabeth M. Barnes, Ph.D.
                 Genentech, Inc. Legal Department

Number of Pages including this cover sheet: 6

RESEARCH /

SIMULTANEOUS AMPLIFICATION AND DETECTION OF SPECIFIC DNA SEQUENCES

Russell Higuchi*, Gavin Dollinger[1], P. Sean Walsh and Robert Griffith

Roche Molecular Systems, Inc., 1400 53rd St., Emeryville, CA 94608. [1]Chiron Corporation, 1400 53rd St., Emeryville, CA 94608. *Corresponding author.

We have enhanced the polymerase chain reaction (PCR) such that specific DNA sequences can be detected without opening the reaction tube. This enhancement requires the addition of ethidium bromide (EtBr) to a PCR. Since the fluorescence of EtBr increases in the presence of double-stranded (ds) DNA an increase in fluorescence in such a PCR indicates a positive amplification, which can be easily monitored externally. In fact, amplification can be continuously monitored in order to follow its progress. The ability to simultaneously amplify specific DNA sequences and detect the product of the amplification both simplifies and improves PCR and may facilitate its automation and more widespread use in the clinic or in other situations requiring high sample throughput.

Although the potential benefits of PCR[1] to clinical diagnostics are well known[2,3], it is still not widely used in this setting, even though it is four years since thermostable DNA polymerases[4] made PCR practical. Some of the reasons for its slow acceptance are high cost, lack of automation of pre- and post-PCR processing steps, and false positive results from carryover contamination. The first two points are related in that labor is the largest contributor to cost at the present stage of PCR development. Most current assays require some form of "downstream" processing once thermocycling is done in order to determine whether the target DNA sequence was present and has amplified. These include DNA hybridization[5,6], gel electrophoresis with or without use of restriction digestion[7,8], HPLC[9], or capillary electrophoresis[10]. These methods are labor-intense, have low throughput, and are difficult to automate. The third point is also closely related to downstream processing. The handling of the PCR product in these downstream processes increases the chances that amplified DNA will spread through the typing lab, resulting in a risk of "carryover" false positives in subsequent testing[11].

These downstream processing steps would be eliminated if specific amplification and detection of amplified DNA took place simultaneously within an unopened reaction vessel. Assays in which such different processes take place without the need to separate reaction components have been termed "homogeneous". No truly homogeneous PCR assay has been demonstrated to date, although progress towards this end has been reported. Chehab, et al.[12], developed a PCR product detection scheme using fluorescent primers that resulted in a fluorescent PCR product. Allele-specific primers, each with different fluorescent tags, were used to indicate the genotype of the DNA. However, the unincorporated primers must still be removed in a downstream process in order to visualize the result. Recently, Holland, et al.[13], developed an assay in which the endogenous 5' exonuclease assay of *Taq* DNA polymerase was exploited to cleave a labeled oligonucleotide probe. The probe would only cleave if PCR amplification had produced its complementary sequence. In order to detect the cleavage products, however, a subsequent process is again needed.

We have developed a truly homogeneous assay for PCR and PCR product detection based upon the greatly increased fluorescence that ethidium bromide and other DNA binding dyes exhibit when they are bound to ds-DNA[14-16]. As outlined in Figure 1, a prototypic PCR
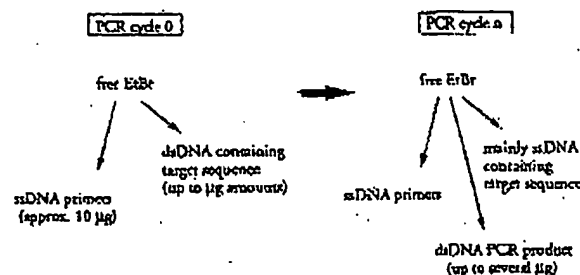

FIGURE 1 Principle of simultaneous amplification and detection of PCR product. The components of a PCR containing EtBr that are fluorescent are listed—EtBr itself, EtBr bound to either ssDNA or dsDNA. There is a large fluorescence enhancement when EtBr is bound to DNA and binding is greatly enhanced when DNA is double-stranded. After sufficient (n) cycles of PCR, the net increase in dsDNA results in additional EtBr binding, and a net increase in total fluorescence.
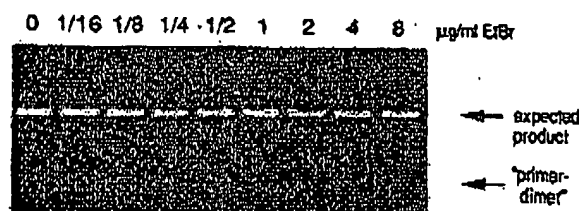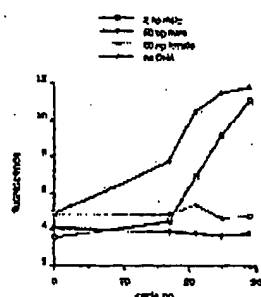
0 1/16 1/8 1/4 1/2 1 2 4 8 µg/ml EtBr

→ expected product

→ primer-dimer

FIGURE 2 Gel electrophoresis of PCR amplification products of the human, nuclear gene, HLA DQα, made in the presence of increasing amounts of EtBr (up to 8 µg/ml). The presence of EtBr has no obvious effect on the yield or specificity of amplification.
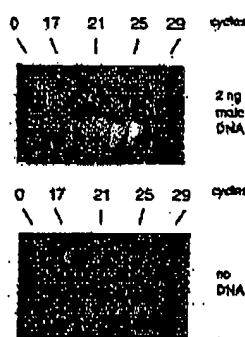
A.

B.

0 17 21 25 29 cycles

2 ng male DNA

0 17 21 25 29 cycles

no DNA

FIGURE 3 (A) Fluorescence measurements from PCRs that contain 0.5 µg/ml EtBr and that are specific for Y-chromosome repeat sequences. Five replicate PCRs were begun containing each of the DNAs specified. At each indicated cycle, one of the five replicate PCRs for each DNA was removed from thermocycling and its fluorescence measured. Units of fluorescence are arbitrary. (B) UV photography of PCR tubes (0.5 ml Eppendorf-style, polypropylene micro-centrifuge tubes) containing reactions, those starting from 2 ng male DNA and control reactions without any DNA, from (A).

begins with primers that are single-stranded DNA (ssDNA), dNTPs, and DNA polymerase. An amount of dsDNA containing the target sequence (target DNA) is also typically present. This amount can vary, depending on the application, from single-cell amounts of DNA[17] to micrograms per PCR[18]. If EtBr is present, the reagents that will fluoresce, in order of increasing fluorescence, are free EtBr itself, and EtBr bound to the single-stranded DNA primers and to the double-stranded target DNA (by its intercalation between the stacked bases of the DNA double-helix). After the first denaturation cycle, target DNA will be largely single-stranded. After a PCR is completed, the most significant change is the increase in the amount of dsDNA (the PCR product itself) of up to several micrograms. Formerly free EtBr is bound to the additional dsDNA, resulting in an increase in fluorescence. There is also some decrease in the amount of ssDNA primer, but because the binding of EtBr to ssDNA is much less than to dsDNA, the effect of this change on the total fluorescence of the sample is small. The fluorescence increase can be measured by directing excitation illumination through the walls of the amplification vessel

before and after, or even continuously during, thermocycling.

RESULTS

PCR in the presence of EtBr. In order to assess the affect of EtBr in PCR, amplifications of the human HLA DQα gene[19] were performed with the dye present at concentrations from 0.06 to 8.0 µg/ml (a typical concentration of EtBr used in staining of nucleic acids following gel electrophoresis is 0.5 µg/ml). As shown in Figure 2, gel electrophoresis revealed little or no difference in the yield or quality of the amplification product whether EtBr was absent or present at any of these concentrations, indicating that EtBr does not inhibit PCR.

Detection of human Y-chromosome specific sequences. Sequence-specific, fluorescence enhancement of EtBr as a result of PCR was demonstrated in a series of amplifications containing 0.5 µg/ml EtBr and primers specific to repeat DNA sequences found on the human Y-chromosome[20]. These PCRs initially contained either 60 ng male, 60 ng female, 2 ng male human or no DNA. Five replicate PCRs were begun for each DNA. After 0, 17, 21, 24 and 29 cycles of thermocycling, a PCR for each DNA was removed from the thermocycler, and its fluorescence measured in a spectrofluorometer and plotted vs. amplification cycle number (Fig. 3A). The shape of this curve reflects the fact that by the time an increase in fluorescence can be detected, the increase in DNA is becoming linear and not exponential with cycle number. As shown, the fluorescence increased about three-fold over the background fluorescence for the PCRs containing human male DNA, but did not significantly increase for negative control PCRs, which contained either no DNA or human female DNA. The more male DNA present to begin with—60 ng versus 2 ng—the fewer cycles were needed to give a detectable increase in fluorescence. Gel electrophoresis on the products of these amplifications showed that DNA fragments of the expected size were made in the male DNA containing reactions and that little DNA synthesis took place in the control samples.

In addition, the increase in fluorescence was visualized by simply laying the completed, unopened PCRs on a UV transilluminator and photographing them through a red filter. This is shown in figure 3B for the reactions that began with 2 ng male DNA and those with no DNA.

Detection of specific alleles of the human β-globin gene. In order to demonstrate that this approach has adequate specificity to allow genetic screening, a detection of the sickle-cell anemia mutation was performed. Figure 4 shows the fluorescence from completed amplifications containing EtBr (0.5 µg/ml) as detected by photography of the reaction tubes on a UV transilluminator. These reactions were performed using primers specific for either the wild-type or sickle-cell mutation of the human β-globin gene[21]. The specificity for each allele is imparted by placing the sickle-mutation site at the terminal 3' nucleotide of one primer. By using an appropriate primer annealing temperature, primer extension—and thus amplification—can take place only if the 3' nucleotide of the primer is complementary to the β-globin allele present[21,22].

Each pair of amplifications shown in Figure 4 consists of a reaction with either the wild-type allele specific (left tube) or sickle-allele specific (right tube) primers. Three different DNAs were typed: DNA from a homozygous, wild-type β-globin individual (AA); from a heterozygous sickle β-globin individual (AS); and from a homozygous sickle β-globin individual (SS). Each DNA (50 ng genomic DNA to start each PCR) was analyzed in triplicate (3 pairs

of reactions each). The DNA type was reflected in the relative fluorescence intensities in each pair of completed amplifications. There was a significant increase in fluorescence only where a β-globin allele DNA matched the primer set. When measured on a spectrofluorometer (data not shown), this fluorescence was about three times that present in a PCR where both β-globin alleles were mismatched to the primer set. Gel electrophoresis (not shown) established that this increase in fluorescence was due to the synthesis of nearly a microgram of a DNA fragment of the expected size for β-globin. There was little synthesis of dsDNA in reactions in which the allele-specific primer was mismatched to both alleles.

Continuous monitoring of a PCR. Using a fiber optic device, it is possible to direct excitation illumination from a spectrofluorometer to a PCR undergoing thermocycling and to return its fluorescence to the spectrofluorometer. The fluorescence readout of such an arrangement, directed at an EtBr-containing amplification of Y-chromosome specific sequences from 25 ng of human male DNA, is shown in Figure 5. The readout from a control PCR with no target DNA is also shown. Thirty cycles of PCR were monitored for each.

The fluorescence trace as a function of time clearly shows the effect of the thermocycling. Fluorescence intensity rises and falls inversely with temperature. The fluorescence intensity is minimum at the denaturation temperature (94°C) and maximum at the annealing/extension temperature (50°C). In the negative-control PCR, these fluorescence maxima and minima do not change significantly over the thirty thermocycles, indicating that there is little dsDNA synthesis without the appropriate target DNA, and there is little if any bleaching of EtBr during the continuous illumination of the sample.

In the PCR containing male DNA, the fluorescence maxima at the annealing/extension temperature begin to increase at about 4000 seconds of thermocycling, and continue to increase with time, indicating that dsDNA is being produced at a detectable level. Note that the fluorescence minima at the denaturation temperature do not significantly increase, presumably because at this temperature there is no dsDNA for EtBr to bind. Thus the course of the amplification is followed by tracking the fluorescence increase at the annealing temperature. Analysis of the products of these two amplifications by gel electrophoresis showed a DNA fragment of the expected size for the male DNA containing sample and no detectable DNA synthesis for the control sample.

DISCUSSION

Downstream processes such as hybridization to a sequence-specific probe can enhance the specificity of DNA detection by PCR. The elimination of these processes means that the specificity of this homogeneous assay depends solely on that of PCR. In the case of sickle-cell disease, we have shown that PCR alone has sufficient DNA sequence specificity to permit genetic screening. Using appropriate amplification conditions, there is little nonspecific production of dsDNA in the absence of the appropriate target allele.

The specificity required to detect pathogens can be more or less than that required to do genetic screening, depending on the number of pathogens in the sample and the amount of other DNA that must be taken with the sample. A difficult target is HIV, which requires detection of a viral genome that can be at the level of a few copies per thousands of host cells[6]. Compared with genetic screening, which is performed on cells containing at least one copy of the target sequence, HIV detection requires both more specificity and the input of more total
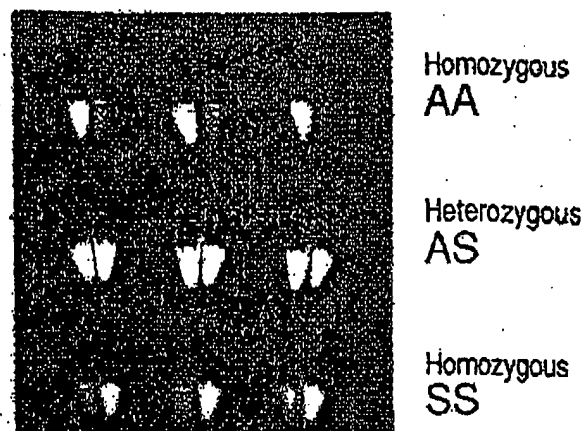

FIGURE 4 UV photography of PCR tubes containing amplifications using EtBr that are specific to wild-type (A) or sickle (S) alleles of the human β-globin gene. The left of each pair of tubes contains allele-specific primers to the wild-type alleles, the right tube primers to the sickle allele. The photograph was taken after 30 cycles of PCR, and the input DNAs and the alleles they contain are indicated. Fifty ng of DNA was used to begin PCR. Typing was done in triplicate (3 pairs of PCRs) for each input DNA.
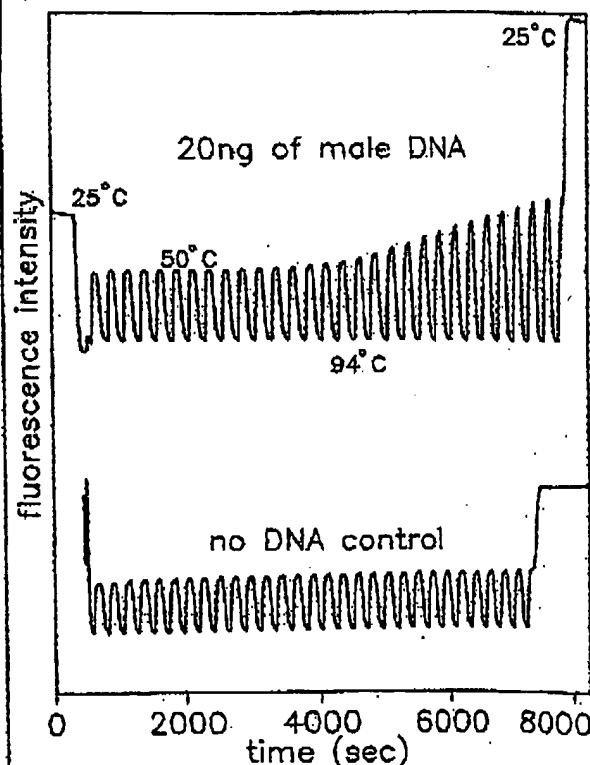

FIGURE 5 Continuous, real-time monitoring of a PCR. A fiber optic was used to carry excitation light to a PCR in progress and also emitted light back to a fluorometer (see Experimental Protocol). Amplification using human male DNA specific primers in a PCR starting with 20 ng of human male DNA (top), or in a control PCR without DNA (bottom), were monitored. Thirty cycles of PCR were followed for each. The temperature cycled between 94°C (denaturation) and 50°C (annealing and extension). Note in the male DNA PCR, the cycle (time) dependent increase in fluorescence at the annealing/extension temperature.

DNA—up to microgram amounts—in order to have sufficient numbers of target sequences. This large amount of starting DNA in an amplification significantly increases the background fluorescence over which any additional fluorescence produced by PCR must be detected. An additional complication that occurs with targets in low copy-number is the formation of the "primer-dimer" artifact. This is the result of the extension of one primer using the other primer as a template. Although this occurs infrequently, once it occurs the extension product is a substrate for PCR amplification, and can compete with true PCR targets if those targets are rare. The primer-dimer product is of course dsDNA and thus is a potential source of false signal in this homogeneous assay.

To increase PCR specificity and reduce the effect of primer-dimer amplification, we are investigating a number of approaches, including the use of nested-primer amplifications that take place in a single tube[5], and the "hot-start", in which nonspecific amplification is reduced by raising the temperature of the reaction before DNA synthesis begins[23]. Preliminary results using these approaches suggest that primer-dimer is effectively reduced and it is possible to detect the increase in EtBr fluorescence in a PCR instigated by a single HIV genome in a background of 10^5 cells. With larger numbers of cells, the background fluorescence contributed by genomic DNA becomes problematic. To reduce this background, it may be possible to use sequence-specific DNA-binding dyes that can be made to preferentially bind PCR product over genomic DNA by incorporating the dye-binding DNA sequence into the PCR product through a 5' "add-on" to the oligonucleotide primer[24].

We have shown that the detection of fluorescence generated by an EtBr-containing PCR is straightforward, both once PCR is completed and continuously during thermocycling. The ease with which automation of specific DNA detection can be accomplished is the most promising aspect of this assay. The fluorescence analysis of completed PCRs is already possible with existing instrumentation in 96-well format[25]. In this format, the fluorescence in each PCR can be quantitated before, after, and even at selected points during thermocycling by moving the rack of PCRs to a 96-microwell plate fluorescence reader[26].

The instrumentation necessary to continuously monitor multiple PCRs simultaneously is also simple in principle. A direct extension of the apparatus used here is to have multiple fiberoptics transmit the excitation light and fluorescent emissions to and from multiple PCRs. The ability to monitor multiple PCRs continuously may allow quantitation of target DNA copy number. Figure 3 shows that the larger the amount of starting target DNA, the sooner during PCR a fluorescence increase is detected. Preliminary experiments (Higuchi and Dollinger, manuscript in preparation) with continuous monitoring have shown a sensitivity to two-fold differences in initial target DNA concentration.

Conversely, if the number of target molecules is known—as it can be in genetic screening—continuous monitoring may provide a means of detecting false positive and false negative results. With a known number of target molecules, a true positive would exhibit detectable fluorescence by a predictable number of cycles of PCR. Increases in fluorescence detected before or after that cycle would indicate potential artifacts. False negative results due to, for example, inhibition of DNA polymerase, may be detected by including within each PCR an inefficiently amplifying marker. This marker results in a fluorescence increase only after a large number of cycles—many more than are necessary to detect a true

positive. If a sample fails to have a fluorescence increase after this many cycles, inhibition may be suspected. Since, in this assay, conclusions are drawn based on the presence or absence of fluorescence signal alone, such controls may be important. In any event, before any test based on this principle is ready for the clinic, an assessment of its false positive/false negative rates will need to be obtained using a large number of known samples.

In summary, the inclusion in PCR of dyes whose fluorescence is enhanced upon binding dsDNA makes it possible to detect specific DNA amplification from outside the PCR tube. In the future, instruments based upon this principle may facilitate the more widespread use of PCR in applications that demand the high throughput of samples.

EXPERIMENTAL PROTOCOL

Human HLA-DQα gene amplifications containing EtBr. PCRs were set up in 100 µl volumes containing 10 mM Tris-HCl, pH 8.3; 50 mM KCl; 4 mM MgCl$_2$; 2.5 units of Taq DNA polymerase (Perkin-Elmer Cetus, Norwalk, CT); 20 pmole each of human HLA-DQα gene specific oligonucleotide primers (GH26 and GH27[19] and approximately 10^7 copies of DQα PCR product diluted from a previous reaction. Ethidium bromide (EtBr; Sigma) was used at the concentrations indicated in Figure 2. Thermocycling proceeded for 20 cycles in a model 480 thermocycler (Perkin-Elmer Cetus, Norwalk, CT) using a "step-cycle" program of 94°C for 1 min. denaturation and 60°C for 30 sec. annealing and 72°C for 30 sec. extension.

Y-chromosome specific PCR. PCRs (100 µl total reaction volume) containing 0.5 µg/ml EtBr were prepared as described for HLA-DQα, except with different primers and target DNAs. These PCRs contained 15 pmole each male DNA-specific primers YI.1 and YI.2[20], and either 60 ng male, 60 ng female, 2 ng male, or no human DNA. Thermocycling was 94°C for 1 min. and 60°C for 1 min using a "step-cycle" program. The number of cycles for a sample were as indicated in Figure 3. Fluorescence measurement is described below.

Allele-specific, human β-globin gene PCR. Amplifications of 100 µl volume using 0.5 µg/ml of EtBr were prepared as described for HLA-DQα above except with different primers and target DNAs. These PCRs contained either primer pair HGP2/Hβ14A (wild-type globin specific primers) or HGP2/Hβ14S (sickle-globin specific primers) at 10 pmole each primer per PCR. These primers were developed by Wu et al.[21]. Three different target DNAs were used in separate amplifications—50 ng each of human DNA that was homozygous for the sickle trait (SS), DNA that was heterozygous for the sickle trait (AS), or DNA that was homozygous for the w.t. globin (AA). Thermocycling was for 30 cycles at 94°C for 1 min. and 55°C for 1 min. using a "step-cycle" program. An annealing temperature of 55°C had been shown by Wu et al.[21] to provide allele-specific amplification. Completed PCRs were photographed through a red filter (Wratten 23A) after placing the reaction tubes atop a model TM-36 transilluminator (UV-products San Gabriel, CA).

Fluorescence measurement. Fluorescence measurements were made on PCRs containing EtBr in a Fluorolog-2 fluorometer (SPEX, Edison, NJ). Excitation was at the 500 nm band with about 2 nm bandwidth with a GG 435 nm cut-off filter (Melles Griot, Inc., Irvine, CA) to exclude second-order light. Emitted light was detected at 570 nm with a bandwidth of about 7 nm. An OG 530 nm cut-off filter was used to remove the excitation light.

Continuous fluorescence monitoring of PCR. Continuous monitoring of a PCR in progress was accomplished using the spectrofluorometer and settings described above as well as a fiberoptic accessory (SPEX cat. no. 1950) to both send excitation light to, and receive emitted light from, a PCR placed in a well of a model 480 thermocycler (Perkin-Elmer Cetus). The probe end of the fiberoptic cable was attached with "5 minute-epoxy" to the open top of a PCR tube (a 0.5 ml polypropylene centrifuge tube with its cap removed) effectively sealing it. The exposed top of the PCR tube and the end of the fiberoptic cable were shielded from room light and the room lights were kept dimmed during each run. The monitored PCR was an amplification of Y-chromosome-specific repeat sequences as described above, except using an annealing/extension temperature of 50°C. The reaction was covered with mineral oil (2 drops) to prevent evaporation. Thermocycling and fluorescence measurement were started simultaneously. A time-base scan with a 10 second integration time

was used and the emission signal was ratioed to the excitation signal to control for changes in light-source intensity. Data were collected using the dm3000f, version 2.5 (SPEX) data system.

Acknowledgments

We thank Bob Jones for help with the spectrofluormetric measurements and Heatherbell Fong for editing this manuscript.

References
1. Mullis, K., Faloona, F., Scharf, S., Saiki, R., Horn, G. and Erlich, H. 1986. Specific enzymatic amplification of DNA in vitro: The polymerase chain reaction. CSHSQB 51:263–273.
2. White, T. J., Arnheim, N. and Erlich, H. A. 1989. The polymerase chain reaction. Trends Genet. 5:185–189.
3. Erlich, H. A., Gelfand, D. and Sninsky, J. J. 1991. Recent advances in the polymerase chain reaction. Science 252:1643–1651.
4. Saiki, R. K., Gelfand, D. H., Stoffel, S., Scharf, S. J., Higuchi, R., Horn, G. T., Mullis, K. B. and Erlich, H. A. 1988. Primer-directed enzymatic amplification of DNA with a thermostable DNA polymerase. Science 239:487–491.
5. Saiki, R. K., Walsh, P. S., Levenson, C. H. and Erlich, H. A. 1989. Genetic analysis of amplified DNA with immobilized sequence-specific oligonucleotide probes. Proc. Natl. Acad. Sci. USA 86:6230–6234.
6. Kwok, S. Y., Mack, D. H., Mullis, K. B., Poiesz, B. J., Ehrlich, G. D., Blair, D. and Friedman-Kien, A. S. 1987. Identification of human immunodeficiency virus sequences by using in vitro enzymatic amplification and oligomer cleavage detection. J. Virol. 61:1690–1694.
7. Chehab, F. F., Doherty, M., Cai, S. P., Kan, Y. W., Cooper, S. and Rubin, E. M. 1987. Detection of sickle cell anemia and thalassemia. Nature 329:293–294.
8. Horn, G. T., Richards, B. and Klinger, K. W. 1989. Amplification of a highly polymorphic VNTR segment by the polymerase chain reaction. Nuc. Acids Res. 16:2140.
9. Katz, E. D. and Dong, M. W. 1990. Rapid analysis and purification of polymerase chain reaction products by high-performance liquid chromatography. Biotechniques 8:546–555.
10. Heiger, D. N., Cohen, A. S. and Karger, B. L. 1990. Separation of DNA restriction fragments by high performance capillary electrophoresis with low and zero crosslinked polyacrylamide using continuous and pulsed electric fields. J. Chromatogr. 516:33–48.
11. Kwok, S. Y. and Higuchi, R. G. 1989. Avoiding false positives with PCR. Nature 339:237–238.
12. Chehab, F. F. and Kan, Y. W. 1989. Detection of specific DNA sequences by fluorescence amplification: a color complementation assay. Proc. Natl. Acad. Sci. USA 86:9178–9182.
13. Holland, P. M., Abramson, R. D., Watson, R. and Gelfand, D. H.

1991. Detection of specific polymerase chain reaction product by utilizing the 5' to 3' exonuclease activity of Thermus aquaticus DNA polymerase. Proc. Natl. Acad. Sci. USA 88:7276–7280.
14. Markovits, J., Roques, B. P. and Le Pecq, J. B. 1979. Ethidium dimer: a new reagent for the fluorimetric determination of nucleic acids. Anal. Biochem. 94:259–264.
15. Kapuscinski, J. and Szer, W. 1979. Interactions of 4',6-diamidine-2-phenylindole with synthetic polynucleotides. Nuc. Acids Res. 6:3519–3534.
16. Searle, M. S. and Embrey, K. J. 1990. Sequence-specific interaction of Hoechst 33258 with the minor groove of an adenine-tract DNA duplex studied in solution by ¹H NMR spectroscopy. Nuc. Acids Res. 18:3753–3762.
17. Li, H. H., Gyllensten, U. B., Cui, X. F., Saiki, R. K., Erlich, H. A. and Arnheim, N. 1988. Amplification and analysis of DNA sequences in single human sperm and diploid cells. Nature 335:414–417.
18. Abbott, M. A., Poiesz, B. J., Byrne, B. C., Kwok, S. Y., Sninsky, J. J. and Erlich, H. A. 1988. Enzymatic gene amplification: qualitative and quantitative methods for detecting proviral DNA amplified in vitro. J. Infect. Dis. 158:1158.
19. Saiki, R. K., Bugawan, T. L., Horn, G. T., Mullis, K. B. and Erlich, H. A. 1986. Analysis of enzymatically amplified β-globin and HLA-DQα DNA with allele-specific oligonucleotide probes. Nature 324:163–166.
20. Kogan, S. C., Doherty, M. and Gitschier, J. 1987. An improved method for prenatal diagnosis of genetic disease by analysis of amplified DNA sequences. N. Engl. J. Med. 317:985–990.
21. Wu, D. Y., Ugozzoli, L., Pal, B. K. and Wallace, R. B. 1989. Allele-specific enzymatic amplification of β-globin genomic DNA for diagnosis of sickle cell anemia. Proc. Natl. Acad. Sci. USA 86:2757–2760.
22. Kwok, S., Kellogg, D. E., McKinney, N., Spasic, D., Goda, L., Levenson, C. and Sninsky, J. J. 1990. Effects of primer-template mismatches on the polymerase chain reaction: Human immunodeficiency virus type 1 model studies. Nuc. Acids Res. 18:999–1005.
23. Chou, Q., Russell, M., Birch, D., Raymond, J. and Bloch, W. 1992. Prevention of pre-PCR mis-priming and primer dimerization improves low-copy-number amplifications. Submitted.
24. Higuchi, R. 1989. Using PCR to engineer DNA, p. 61–70. In: PCR Technology. H. A. Erlich (Ed.), Stockton Press, New York, N.Y.
25. Haff, L., Atwood, J. G., DiCesare, J., Katz, E., Picozza, E., Williams, J. F. and Woudenberg, T. 1991. A high-performance system for automation of the polymerase chain reaction. Biotechniques 10:102–103, 106–112.
26. Tumosa, N. and Kahan, L. 1989. Fluorescent EIA screening of monoclonal antibodies to cell surface antigens. J. Immun. Meth. 116:59–63.

▇▇▇▇IIIIIResearch

Oligonucleotides with Fluorescent Dyes at Opposite Ends Provide a Quenched Probe System Useful for Detecting PCR Product and Nucleic Acid Hybridization

Kenneth J. Livak, Susan J.A. Flood, Jeffrey Marmaro, William Giusti, and Karin Deetz

Perkin-Elmer, Applied Biosystems Division, Foster City, California 94404

The 5' nuclease PCR assay detects the accumulation of specific PCR product by hybridization and cleavage of a double-labeled fluorogenic probe during the amplification reaction. The probe is an oligonucleotide with both a reporter fluorescent dye and a quencher dye attached. An increase in reporter fluorescence intensity indicates that the probe has hybridized to the target PCR product and has been cleaved by the 5'→3' nucleolytic activity of *Taq* DNA polymerase. In this study, probes with the quencher dye attached to an internal nucleotide were compared with probes with the quencher dye attached to the 3'-end nucleotide. In all cases, the reporter dye was attached to the 5' end. All intact probes showed quenching of the reporter fluorescence. In general, probes with the quencher dye attached to the 3'-end nucleotide exhibited a larger signal in the 5' nuclease PCR assay than the internally labeled probes. It is proposed that the larger signal is caused by increased likelihood of cleavage by *Taq* DNA polymerase when the probe is hybridized to a template strand during PCR. Probes with the quencher dye attached to the 3'-end nucleotide also exhibited an increase in reporter fluorescence intensity when hybridized to a complementary strand. Thus, oligonucleotides with reporter and quencher dyes attached at opposite ends can be used as homogeneous hybridization probes.

A homogeneous assay for detecting the accumulation of specific PCR product that uses a double-labeled fluorogenic probe was described by Lee et al.[1] The assay exploits the 5'→3' nucleolytic activity of *Taq* DNA polymerase[2,3] and is diagramed in Figure 1. The fluorogenic probe consists of an oligonucleotide with a reporter fluorescent dye, such as a fluorescein, attached to the 5' end; and a quencher dye, such as a rhodamine, attached internally. When the fluorescein is excited by irradiation, its fluorescent emission will be quenched if the rhodamine is close enough to be excited through the process of fluorescence energy transfer (FET).[4,5] During PCR, if the probe is hybridized to a template strand, *Taq* DNA polymerase will cleave the probe because of its inherent 5'→3' nucleolytic activity. If the cleavage occurs between the fluorescein and rhodamine dyes, it causes an increase in fluorescein fluorescence intensity because the fluorescein is no longer quenched. The increase in fluorescein fluorescence intensity indicates that the probe-specific PCR product has been generated. Thus, FET between a reporter dye and a quencher dye is critical to the performance of the probe in the 5' nuclease PCR assay.

Quenching is completely dependent on the physical proximity of the two dyes.[6] Because of this, it has been assumed that the quencher dye must be attached near the 5' end. Surprisingly, we have found that attaching a rhodamine dye at the 3' end of a probe still provides adequate quenching for the probe to perform in the 5' nuclease

PCR assay. Furthermore, cleavage of this type of probe is not required to achieve some reduction in quenching. Oligonucleotides with a reporter dye on the 5' end and a quencher dye on the 3' end exhibit a much higher reporter fluorescence when double-stranded as compared with single-stranded. This should make it possible to use this type of double-labeled probe for homogeneous detection of nucleic acid hybridization.

MATERIALS AND METHODS

Oligonucleotides

Table 1 shows the nucleotide sequence of the oligonucleotides used in this study. Linker arm nucleotide (LAN) phosphoramidite was obtained from Glen Research. The standard DNA phosphoramidites, 6-carboxyfluorescein (6-FAM) phosphoramidite, 6-carboxytetramethylrhodamine succinimidyl ester (TAMRA NHS ester), and Phosphalink for attaching a 3'-blocking phosphate, were obtained from Perkin-Elmer, Applied Biosystems Division. Oligonucleotide synthesis was performed using an ABI model 394 DNA synthesizer (Applied Biosystems). Primer and complement oligonucleotides were purified using Oligo Purification Cartridges (Applied Biosystems). Double-labeled probes were synthesized with 6-FAM-labeled phosphoramidite at the 5' end, LAN replacing one of the T's in the sequence, and Phosphalink at the 3' end. Following deprotection and ethanol precipitation, TAMRA NHS ester was coupled to the LAN-containing oligonucleotide in 250

Research

Polymerization
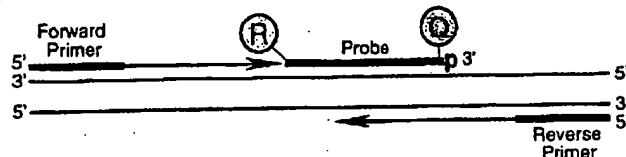
Strand displacement
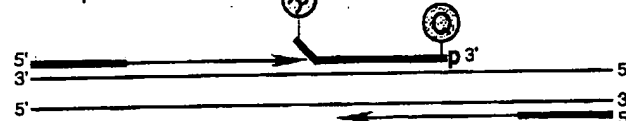
Cleavage
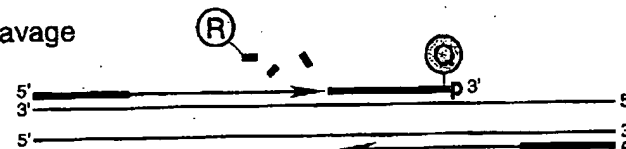
Polymerization completed
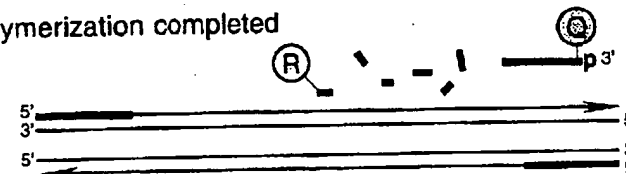
FIGURE 1 Diagram of 5' nuclease assay. Stepwise representation of the $5' \to 3'$ nucleolytic activity of *Taq* DNA polymerase acting on a fluorogenic probe during one extension phase of PCR.

mM Na-bicarbonate buffer (pH 9.0) at room temperature. Unreacted dye was removed by passage over a PD-10 Sephadex column. Finally, the double-labeled probe was purified by preparative high-performance liquid chromatography (HPLC) using an Aquapore C_8 220×4.6-mm column with 7-μm particle size. The column was developed with a 24-min linear gradient of 8–20% acetonitrile in 0.1 M TEAA (triethylamine acetate). Probes are named by designating the sequence from Table 1 and the position of the LAN–TAMRA moiety. For example, probe A1-7 has sequence A1 with LAN-TAMRA at nucleotide position 7 from the 5' end.

PCR Systems

All PCR amplifications were performed in the Perkin-Elmer GeneAmp PCR System 9600 using 50-μl reactions that contained 10 mM Tris-HCl (pH 8.3), 50 mM KCl, 200 μM dATP, 200 μM dCTP, 200 μM dGTP, 400 μM dUTP, 0.5 unit of AmpErase uracil N-glycosylase (Perkin-Elmer), and 1.25 unit of AmpliTaq DNA polymerase (Perkin-Elmer). A 295-bp segment from exon 3 of the human β-actin

gene (nucleotides 2141–2435 in the sequence of Nakajima-Iijima et al.)[7] was amplified using primers AFP and ARP (Table 1), which are modified slightly from those of du Breuil et al.[8] Actin amplification reactions contained 4 mM $MgCl_2$, 20 ng of human genomic DNA, 50 nM A1 or A3 probe, and 300 nM each

primer. The thermal regimen was 50°C (2 min), 95°C (10 min), 40 cycles of 95°C (20 sec), 60°C (1 min), and hold at 72°C. A 515-bp segment was amplified from a plasmid that consists of a segment of λ DNA (nucleotides 32,220–32,747) inserted in the *Sma*I site of vector pUC119. These reactions contained 3.5 mM $MgCl_2$, 1 ng of plasmid DNA, 50 nM P2 or P5 probe, 200 nM primer F119, and 200 nM primer R119. The thermal regimen was 50°C (2 min), 95°C (10 min), 25 cycles of 95°C (20 sec), 57°C (1 min), and hold at 72°C.

Fluorescence Detection

For each amplification reaction, a 40-μl aliquot of a sample was transferred to an individual well of a white, 96-well microtiter plate (Perkin-Elmer). Fluorescence was measured on the Perkin-Elmer TaqMan LS-50B System, which consists of a luminescence spectrometer with plate reader assembly, a 485-nm excitation filter, and a 515-nm emission filter. Excitation was at 488 nm using a 5-nm slit width. Emission was measured at 518 nm for 6-FAM (the reporter or R value) and 582 nm for TAMRA (the quencher or Q value) using a 10-nm slit width. To determine the increase in reporter emission that is caused by cleavage of the probe during PCR, three normalizations are applied to the raw emission data. First, emission intensity of a buffer blank is subtracted for each wavelength. Second, emission intensity of the reporter is

TABLE 1 Sequences of Oligonucleotides

Name	Type	Sequence
F119	primer	ACCCACAGGAACTGATCACCACTC
R119	primer	ATGTCGCGTTCCGGCTGACGTTCTGC
P2	probe	TCGCATTACTGATCGTTGCCAACCAG*Tp*
P2C	complement	GTACTGGTTGGCAACGATCAGTAATGCGATG
P5	probe	CGGATTTGCTGGTATCTATGACAAGGA*Tp*
P5C	complement	TTCATCCTTGTCATAGATACCAGCAAATCCG
AFP	primer	TCACCCACACTGTGCCCATCTACGA
ARP	primer	CAGCGGAACCGCTCATTGCCAATGG
A1	probe	ATGCCCTCCCCCATGCCATCCTGCCG*Tp*
A1C	complement	AGACGCAGGATGGCATGGGGGAGGGCATAC
A3	probe	CGCCCTGGACTTCGAGCAAGAGA*Tp*
A3C	complement	CCATCTCTTGCTCGAAGTCCAGGGCGAC

For each oligonucleotide used in this study, the nucleic acid sequence is given, written in the $5' \to 3'$ direction. There are three types of oligonucleotides: PCR primer, fluorogenic probe used in the 5' nuclease assay, and complement used to hybridize to the corresponding probe. For the probes, the underlined base indicates a position where LAN with TAMRA attached was substituted for a T. (p) The presence of a 3' phosphate on each probe.

358 *PCR Methods and Applications*

PAGE 3/7 * RCVD AT 10/24/2005 5:55:20 PM [Pacific Daylight Time] * SVR:SVCS01/0 * DNIS:6034 * CSID:(613) 991-5695 * DURATION (mm-ss):05-46

IIIIIResearch

A1-2	RAQGCCCTCCCCCATGCCATCCTGCGTp
A1-7	RATGCCCQCCCCCATGCCATCCTGCGTp
A1-14	RATGCCCTCCCCCAQGCCATCCTGCGTp
A1-19	RATGCCCTCCCCCATGCCAQCCTGCGTp
A1-22	RATGCCCTCCCCCATGCCATCCQGCGTp
A1-26	RATGCCCTCCCCCATGCCATCCTGCGQp

Probe	518 nm		582 nm		RQ⁻	RQ⁺	ΔRQ
	no temp.	+ temp.	no temp.	+ temp.			
A1-2	25.5 ± 2.1	32.7 ± 1.9	38.2 ± 3.0	38.2 ± 2.0	0.67 ± 0.01	0.86 ± 0.06	0.19 ± 0.06
A1-7	53.5 ± 4.3	395.1 ± 21.4	108.5 ± 6.3	110.3 ± 5.3	0.49 ± 0.03	3.58 ± 0.17	3.09 ± 0.18
A1-14	127.0 ± 4.9	403.5 ± 19.1	109.7 ± 5.3	93.1 ± 6.3	1.16 ± 0.02	4.34 ± 0.15	3.18 ± 0.15
A1-19	187.5 ± 17.9	422.7 ± 7.7	70.3 ± 7.4	73.0 ± 2.8	2.67 ± 0.05	5.80 ± 0.15	3.13 ± 0.16
A1-22	224.6 ± 9.4	482.2 ± 43.6	100.0 ± 4.0	96.2 ± 9.6	2.25 ± 0.03	5.02 ± 0.11	2.77 ± 0.12
A1-26	160.2 ± 8.9	454.1 ± 18.4	93.1 ± 5.4	90.7 ± 3.2	1.72 ± 0.02	5.01 ± 0.08	3.29 ± 0.08

FIGURE 2 Results of 5' nuclease assay comparing β-actin probes with TAMRA at different nucleotide positions. As described in Materials and Methods, PCR amplifications containing the indicated probes were performed, and the fluorescence emission was measured at 518 and 582 nm. Reported values are the average ± 1 s.d. for six reactions run without added template (no temp.) and six reactions run with template (+temp.). The RQ ratio was calculated for each individual reaction and averaged to give the reported RQ⁻ and RQ⁺ values.

divided by the emission intensity of the quencher to give an RQ ratio for each reaction tube. This normalizes for well-to-well variations in probe concentration and fluorescence measurement. Finally, ΔRQ is calculated by subtracting the RQ value of the no-template control (RQ⁻) from the RQ value for the complete reaction including template (RQ⁺).

RESULTS

A series of probes with increasing distances between the fluorescein reporter and rhodamine quencher were tested to investigate the minimum and maximum spacing that would give an acceptable performance in the 5' nuclease PCR assay. These probes hybridize to a target

sequence in the human β-actin gene. Figure 2 shows the results of an experiment in which these probes were included in PCR that amplified a segment of the β-actin gene containing the target sequence. Performance in the 5' nuclease PCR assay is monitored by the magnitude of ΔRQ, which is a measure of the increase in reporter fluorescence caused by PCR amplification of the probe target. Probe A1-2 has a ΔRQ value that is close to zero, indicating that the probe was not cleaved appreciably during the amplification reaction. This suggests that with the quencher dye on the second nucleotide from the 5' end, there is insufficient room for Taq polymerase to cleave efficiently between the reporter and quencher. The other five probes exhibited comparable ΔRQ values that are

clearly different from zero. Thus, all five probes are being cleaved during PCR amplification resulting in a similar increase in reporter fluorescence. It should be noted that complete digestion of a probe produces a much larger increase in reporter fluorescence than that observed in Figure 2 (data not shown). Thus, even in reactions where amplification occurs, the majority of probe molecules remain uncleaved. It is mainly for this reason that the fluorescence intensity of the quencher dye TAMRA changes little with amplification of the target. This is what allows us to use the 582-nm fluorescence reading as a normalization factor.

The magnitude of RQ⁻ depends mainly on the quenching efficiency inherent in the specific structure of the probe and the purity of the oligonucleotide. Thus, the larger RQ⁻ values indicate that probes A1-14, A1-19, A1-22, and A1-26 probably have reduced quenching as compared with A1-7. Still, the degree of quenching is sufficient to detect a highly significant increase in reporter fluorescence when each of these probes is cleaved during PCR.

To further investigate the ability of TAMRA on the 3' end to quench 6-FAM on the 5' end, three additional pairs of probes were tested in the 5' nuclease PCR assay. For each pair, one probe has TAMRA attached to an internal nucleotide and the other has TAMRA attached to the 3' end nucleotide. The results are shown in Table 2. For all three sets, the probe with the 3' quencher exhibits a ΔRQ value that is considerably higher than for the probe with the internal quencher. The RQ⁻ values suggest that differences in quenching are not as great as those observed with some of the A1 probes. These results demonstrate that a quencher dye on the 3' end of an oligonucleotide can quench efficiently the

TABLE 2 Results of 5' Nuclease Assay Comparing Probes with TAMRA Attached to an Internal or 3'-terminal Nucleotide

Probe	518 nm		582 nm		RQ⁻	RQ⁺	ΔRQ
	no temp.	+ temp.	no temp.	+ temp.			
A3-6	54.6 ± 3.2	84.8 ± 3.7	116.2 ± 6.4	115.6 ± 2.5	0.47 ± 0.02	0.73 ± 0.03	0.26 ± 0.04
A3-24	72.1 ± 2.9	236.5 ± 11.1	84.2 ± 4.0	90.2 ± 3.8	0.86 ± 0.02	2.62 ± 0.05	1.76 ± 0.05
P2-7	82.8 ± 4.4	384.0 ± 34.1	105.1 ± 6.4	120.4 ± 10.2	0.79 ± 0.02	3.19 ± 0.16	2.40 ± 0.16
P2-27	113.4 ± 6.6	555.4 ± 14.1	140.7 ± 8.5	118.7 ± 4.8	0.81 ± 0.01	4.68 ± 0.10	3.88 ± 0.10
P5-10	77.5 ± 6.5	244.4 ± 15.9	86.7 ± 4.3	95.8 ± 6.7	0.89 ± 0.05	2.55 ± 0.06	1.66 ± 0.08
P5-28	64.0 ± 5.2	333.6 ± 12.1	100.6 ± 6.1	94.7 ± 6.3	0.63 ± 0.02	3.53 ± 0.12	2.89 ± 0.13

Reactions containing the indicated probes and calculations were performed as described in Material and Methods and in the legend to Fig. 2.

Research▮▮▮▮ ▮ ▮ ▮

fluorescence of a reporter dye on the 5' end. The degree of quenching is sufficient for this type of oligonucleotide to be used as a probe in the 5' nuclease PCR assay.

To test the hypothesis that quenching by a 3' TAMRA depends on the flexibility of the oligonucleotide, fluorescence was measured for probes in the single-stranded and double-stranded states. Table 3 reports the fluorescence observed at 518 and 582 nm. The relative degree of quenching is assessed by calculating the RQ ratio. For probes with TAMRA 6–10 nucleotides from the 5' end, there is little difference in the RQ values when comparing single-stranded with double-stranded oligonucleotides. The results for probes with TAMRA at the 3' end are much different. For these probes, hybridization to a complementary strand causes a dramatic increase in RQ. We propose that this loss of quenching is caused by the rigid structure of double-stranded DNA, which prevents the 5' and 3' ends from being in proximity.

When TAMRA is placed toward the 3' end, there is a marked Mg^{2+} effect on quenching. Figure 3 shows a plot of observed RQ values for the A1 series of probes as a function of Mg^{2+} concentration. With TAMRA attached near the 5' end (probe A1-2 or A1-7), the RQ value at 0 mM Mg^{2+} is only slightly higher than RQ at 10 mM Mg^{2+}. For probes A1-19, A1-22, and A1-26, the RQ values at 0 mM Mg^{2+} are very high, indicating a much

reduced quenching efficiency. For each of these probes, there is a marked decrease in RQ at 1 mM Mg^{2+} followed by a gradual decline as the Mg^{2+} concentration increases to 10 mM. Probe A1-14 shows an intermediate RQ value at 0 mM Mg^{2+} with a gradual decline at higher Mg^{2+} concentrations. In a low-salt environment with no Mg^{2+} present, a single-stranded oligonucleotide would be expected to adopt an extended conformation because of electrostatic repulsion. The binding of Mg^{2+} ions acts to shield the negative charge of the phosphate backbone so that the oligonucleotide can adopt conformations where the 3' end is close to the 5' end. Therefore, the observed Mg^{2+} effects support the notion that quenching of a 5' reporter dye by TAMRA at or near the 3' end depends on the flexibility of the oligonucleotide.

DISCUSSION

The striking finding of this study is that it seems the rhodamine dye TAMRA, placed at any position in an oligonucleotide, can quench the fluorescent emission of a fluorescein (6-FAM) placed at the 5' end. This implies that a single-stranded, double-labeled oligonucleotide must be able to adopt conformations where the TAMRA is close to the 5' end. It should be noted that the decay of 6-FAM in the excited state requires a certain amount of time. Therefore, what

matters for quenching is not the average distance between 6-FAM and TAMRA but, rather, how close TAMRA can get to 6-FAM during the lifetime of the 6-FAM excited state. As long as the decay time of the excited state is relatively long compared with the molecular motions of the oligonucleotide, quenching can occur. Thus, we propose that TAMRA at the 3' end, or any other position, can quench 6-FAM at the 5' end because TAMRA is in proximity to 6-FAM often enough to be able to accept energy transfer from an excited 6-FAM.

Details of the fluorescence measurements remain puzzling. For example, Table 3 shows that hybridization of probes A1-26, A3-24, and P5-28 to their complementary strands not only causes a large increase in 6-FAM fluorescence at 518 nm but also causes a modest increase in TAMRA fluorescence at 582 nm. If TAMRA is being excited by energy transfer from quenched 6-FAM, then loss of quenching attributable to hybridization should cause a decrease in the fluorescence emission of TAMRA. The fact that the fluorescence emission of TAMRA increases indicates that the situation is more complex. For example, we have anecdotal evidence that the bases of the oligonucleotide, especially G, quench the fluorescence of both 6-FAM and TAMRA to some degree. When double-stranded, base-pairing may reduce the ability of the bases to quench. The primary factor causing the quenching of 6-FAM in an intact probe is the TAMRA dye. Evidence for the importance of TAMRA is that 6-FAM fluorescence remains relatively unchanged when probes labeled only with 6-FAM are used in the 5' nuclease PCR assay (data not shown). Secondary effectors of fluorescence, both before and after cleavage of the probe, need to be explored further.

Regardless of the physical mechanism, the relative independence of position and quenching greatly simplifies the design of probes for the 5' nuclease PCR assay. There are three main factors that determine the performance of a double-labeled fluorescent probe in the 5' nuclease PCR assay. The first factor is the degree of quenching observed in the intact probe. This is characterized by the value of RQ⁻, which is the ratio of reporter to quencher fluorescent emissions for a no template control PCR. Influences on the value of RQ⁻ include the particular reporter and quencher

TABLE 3 Comparison of Fluorescence Emissions of Single-stranded and Double-stranded Fluorogenic Probes

Probe	518 nm		582 nm		RQ	
	ss	ds	ss	ds	ss	ds
A1-7	27.75	68.53	61.08	138.18	0.45	0.50
A1-26	43.31	509.38	53.50	93.86	0.81	5.43
A3-6	16.75	62.88	39.33	165.57	0.43	0.38
A3-24	30.05	578.64	67.72	140.25	0.45	3.21
P2-7	35.02	70.13	54.63	121.09	0.64	0.58
P2-27	39.89	320.47	65.10	61.13	0.61	5.25
P5-10	27.34	144.85	61.95	165.54	0.44	0.87
P5-28	33.65	462.29	72.39	104.61	0.46	4.43

(ss) Single-stranded. The fluorescence emissions at 518 or 582 nm for solutions containing a final concentration of 50 nM indicated probe, 10 mM Tris-HCl (pH 8.3), 50 mM KCl, and 10 mM $MgCl_2$. (ds) Double-stranded. The solutions contained, in addition, 100 nM A1C for probes A1-7 and A1-26, 100 nM A3C for probes A3-6 and A3-24, 100 nM P2C for probes P2-7 and P2-27, or 100 nM P5C for probes P5-10 and P5-28. Before the addition of $MgCl_2$, 120 μl of each sample was heated at 95°C for 5 min. Following the addition of 80 μl of 25 mM $MgCl_2$, each sample was allowed to cool to room temperature and the fluorescence emissions were measured. Reported values are the average of three determinations.
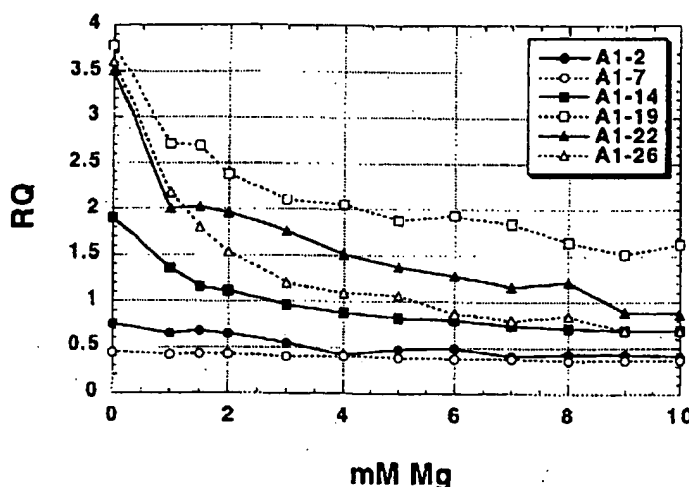
IIIIResearch

FIGURE 3 Effect of Mg^{2+} concentration on RQ ratio for the A1 series of probes. The fluorescence emission intensity at 518 and 582 nm was measured for solutions containing 50 nM probe, 10 mM Tris-HCl (pH 8.3), 50 mM KCl, and varying amounts (0-10 mM) of $MgCl_2$. The calculated RQ ratios (518 nm intensity divided by 582 nm intensity) are plotted vs. $MgCl_2$ concentration (mM Mg). The key (*upper right*) shows the probes examined.

dyes used, spacing between reporter and quencher dyes, nucleotide sequence context effects, presence of structure or other factors that reduce flexibility of the oligonucleotide, and purity of the probe. The second factor is the efficiency of hybridization, which depends on probe T_m, presence of secondary structure in probe or template, annealing temperature, and other reaction conditions. The third factor is the efficiency at which *Taq* DNA polymerase cleaves the bound probe between the reporter and quencher dyes. This cleavage is dependent on sequence complementarity between probe and template as shown by the observation that mismatches in the segment between reporter and quencher dyes drastically reduce the cleavage of probe.[1]

The rise in RQ⁻ values for the A1 series of probes seems to indicate that the degree of quenching is reduced somewhat as the quencher is placed toward the 3' end. The lowest apparent quenching is observed for probe A1-19 (see Fig. 3) rather than for the probe where the TAMRA is at the 3' end (A1-26). This is understandable, as the conformation of the 3' end position would be expected to be less restricted than the conformation of an internal position. In effect, a quencher at the 3' end is freer to adopt conformations close to the 5' reporter dye than is an internally placed quencher. For the other three sets of

probes, the interpretation of RQ⁻ values is less clear-cut. The A3 probes show the same trend as A1, with the 3' TAMRA probe having a larger RQ⁻ than the internal TAMRA probe. For the P2 pair, both probes have about the same RQ⁻ value. For the P5 probes, the RQ⁻ for the 3' probe is less than for the internally labeled probe. Another factor that may explain some of the observed variation is that purity affects the RQ⁻ value. Although all probes are HPLC purified, a small amount of contamination with unquenched reporter can have a large effect on RQ⁻.

Although there may be a modest effect on degree of quenching, the position of the quencher apparently can have a large effect on the efficiency of probe cleavage. The most drastic effect is observed with probe A1-2, where placement of the TAMRA on the second nucleotide reduces the efficiency of cleavage to almost zero. For the A3, P2, and P5 probes, ΔRQ is much greater for the 3' TAMRA probes as compared with the internal TAMRA probes. This is explained most easily by assuming that probes with TAMRA at the 3' end are more likely to be cleaved between reporter and quencher than are probes with TAMRA attached internally. For the A1 probes, the cleavage efficiency of probe A1-7 must already be quite high, as ΔRQ does not increase when the quencher is placed closer to the 3' end. This illus-

trates the importance of being able to use probes with a quencher on the 3' end in the 5' nuclease PCR assay. In this assay, an increase in the intensity of reporter fluorescence is observed only when the probe is cleaved between the reporter and quencher dyes. By placing the reporter and quencher dyes on the opposite ends of an oligonucleotide probe, any cleavage that occurs will be detected. When the quencher is attached to an internal nucleotide, sometimes the probe works well (A1-7) and other times not so well (A3-6). The relatively poor performance of probe A3-6 presumably means the probe is being cleaved 3' to the quencher rather than between the reporter and quencher. Therefore, the best chance of having a probe that reliably detects accumulation of PCR product in the 5' nuclease PCR assay is to use a probe with the reporter and quencher dyes on opposite ends.

Placing the quencher dye on the 3' end may also provide a slight benefit in terms of hybridization efficiency. The presence of a quencher attached to an internal nucleotide might be expected to disrupt base-pairing and reduce the T_m of a probe. In fact, a 2°C-3°C reduction in T_m has been observed for two probes with internally attached TAMRAs.[9] This disruptive effect would be minimized by placing the quencher at the 3' end. Thus, probes with 3' quenchers might exhibit slightly higher hybridization efficiencies than probes with internal quenchers.

The combination of increased cleavage and hybridization efficiencies means that probes with 3' quenchers probably will be more tolerant of mismatches between probe and target as compared with internally labeled probes. This tolerance of mismatches can be advantageous, as when trying to use a single probe to detect PCR-amplified products from samples of different species. Also, it means that cleavage of probe during PCR is less sensitive to alterations in annealing temperature or other reaction conditions. The one application where tolerance of mismatches may be a disadvantage is for allelic discrimination. Lee et al.[1] demonstrated that allele-specific probes were cleaved between reporter and quencher only when hybridized to a perfectly complementary target. This allowed them to distinguish the normal human cystic fibrosis allele from the *ΔF508* mutant. Their probes had TAMRA attached to the seventh nucleotide from

Research||||■ ■■■■   ■

the 5' end and were designed so that any mismatches were between the reporter and quencher. Increasing the distance between reporter and quencher would lessen the disruptive effect of mismatches and allow cleavage of the probe on the incorrect target. Thus, probes with a quencher attached to an internal nucleotide may still be useful for allelic discrimination.

In this study loss of quenching upon hybridization was used to show that quenching by a 3' TAMRA is dependent on the flexibility of a single-stranded oligonucleotide. The increase in reporter fluorescence intensity, though, could also be used to determine whether hybridization has occurred or not. Thus, oligonucleotides with reporter and quencher dyes attached at opposite ends should also be useful as hybridization probes. The ability to detect hybridization in real time means that these probes could be used to measure hybridization kinetics. Also, this type of probe could be used to develop homogeneous hybridization assays for diagnostics or other applications. Bagwell et al.[10] describe just this type of homogeneous assay where hybridization of a probe causes an increase in fluorescence caused by a loss of quenching. However, they utilized a complex probe design that requires adding nucleotides to both ends of the probe sequence to form two imperfect hairpins. The results presented here demonstrate that the simple addition of a reporter dye to one end of an oligonucleotide and a quencher dye to the other end generates a fluorogenic probe that can detect hybridization or PCR amplification.

ACKNOWLEDGMENTS

REFERENCES

1. Lee, L.G., C.R. Connell, and W. Bloch. 1993. Allelic discrimination by nick-translation PCR with fluorogenic probes. *Nucleic Acids Res.* **21**: 3761–3766.
2. Holland, P.M., R.D. Abramson, R. Watson, and D.H. Gelfand. 1991. Detection of specific polymerase chain reaction prod-uct by utilizing the 5' to 3' exonuclease activity of *Thermus aquaticus* DNA poly-merase. *Proc. Natl. Acad. Sci.* **88**: 7276–7280.
3. Lyamichev, V., M.A.D. Brow, and J.E. Dahlberg. 1993. Structure-specific endo-nucleolytic cleavage of nucleic acids by eubacterial DNA polymerases. *Science* **260**: 778–783.
4. Förster, V.Th. 1948. Zwischenmolekulare Energiewanderung und Fluoreszenz. *Ann. Phys. (Leipzig)* **2**: 55–75.
5. Lakowicz, J.R. 1983. Energy transfer. In *Principles of fluorescent spectroscopy*, pp. 303–339. Plenum Press, New York, NY.
6. Stryer, L. and R.P. Haugland. 1967. Energy transfer: A spectroscopic ruler. *Proc. Natl. Acad. Sci.* **58**: 719–726.
7. Nakajima-Iijima, S., H. Hamada, P. Reddy, and T. Kakunaga. 1985. Molecular structure of the human cytoplasmic beta-actin gene: Inter-species homology of sequences in the introns. *Proc. Natl. Acad. Sci.* **82**: 6133–6137.
8. du Breuil, R.M., J.M. Patel, and B.V. Mendelow. 1993. Quantitation of β-actin-specific mRNA transcripts using xeno-competitive PCR. *PCR Methods Applic.* **3**: 57–59.
9. Livak, K.J. (unpubl.).
10. Bagwell, C.B., M.E. Munson, R.L. Christensen, and E.J. Lovett. 1994. A new homogeneous assay system for specific nucleic acid sequences: Poly-dA and poly-A detection. *Nucleic Acids Res.* **22**: 2424–2425.

GENOME METHODS

Real Time Quantitative PCR

Christian A. Heid,[1] Junko Stevens,[2] Kenneth J. Livak,[2] and P. Mickey Williams[1,3]

[1]BioAnalytical Technology Department, Genentech, Inc., South San Francisco, California 94080;
[2]Applied BioSystems Division of Perkin Elmer Corp., Foster City, California 94404

We have developed a novel "real time" quantitative PCR method. The method measures PCR product accumulation through a dual-labeled fluorogenic probe (i.e., TaqMan Probe). This method provides very accurate and reproducible quantitation of gene copies. Unlike other quantitative PCR methods, real-time PCR does not require post-PCR sample handling, preventing potential PCR product carry-over contamination and resulting in much faster and higher throughput assays. The real-time PCR method has a very large dynamic range of starting target molecule determination (at least five orders of magnitude). Real-time quantitative PCR is extremely accurate and less labor-intensive than current quantitative PCR methods.

Quantitative nucleic acid sequence analysis has had an important role in many fields of biological research. Measurement of gene expression (RNA) has been used extensively in monitoring biological responses to various stimuli (Tan et al. 1994; Huang et al. 1995a,b; Prud'homme et al. 1995). Quantitative gene analysis (DNA) has been used to determine the genomic quantity of a particular gene, as in the case of the human *HER2* gene, which is amplified in ~30% of breast tumors (Slamon et al. 1987). Gene and genome quantitation (DNA and RNA) also have been used for analysis of human immunodeficiency virus (HIV) burden demonstrating changes in the levels of virus throughout the different phases of the disease (Connor et al. 1993; Piatak et al. 1993b; Furtado et al. 1995).

Many methods have been described for the quantitative analysis of nucleic acid sequences (both for RNA and DNA; Southern 1975; Sharp et al. 1980; Thomas 1980). Recently, PCR has proven to be a powerful tool for quantitative nucleic acid analysis. PCR and reverse transcriptase (RT)-PCR have permitted the analysis of minimal starting quantities of nucleic acid (as little as one cell equivalent). This has made possible many experiments that could not have been performed with traditional methods. Although PCR has provided a powerful tool, it is imperative

that it be used properly for quantitation (Raeymaekers 1995). Many early reports of quantitative PCR and RT-PCR described quantitation of the PCR product but did not measure the initial target sequence quantity. It is essential to design proper controls for the quantitation of the initial target sequences (Ferre 1992; Clementi et al. 1993).

Researchers have developed several methods of quantitative PCR and RT-PCR. One approach measures PCR product quantity in the log phase of the reaction before the plateau (Kellogg et al. 1990; Pang et al. 1990). This method requires that each sample has equal input amounts of nucleic acid and that each sample under analysis amplifies with identical efficiency up to the point of quantitative analysis. A gene sequence (contained in all samples at relatively constant quantities, such as β-actin) can be used for sample amplification efficiency normalization. Using conventional methods of PCR detection and quantitation (gel electrophoresis or plate capture hybridization), it is extremely laborious to assure that all samples are analyzed during the log phase of the reaction (for both the target gene and the normalization gene). Another method, quantitative competitive (QC)-PCR, has been developed and is used widely for PCR quantitation. QC-PCR relies on the inclusion of an internal control competitor in each reaction (Becker-Andre 1991; Piatak et al. 1993a,b). The efficiency of each reaction is normalized to the internal competitor. A known amount of internal competitor can be

[3]Corresponding author.

added to each sample. To obtain relative quantitation, the unknown target PCR product is compared with the known competitor PCR product. Success of a quantitative competitive PCR assay relies on developing an internal control that amplifies with the same efficiency as the target molecule. The design of the competitor and the validation of amplification efficiencies require a dedicated effort. However, because QC-PCR does not require that PCR products be analyzed during the log phase of the amplification, it is the easier of the two methods to use.

Several detection systems are used for quantitative PCR and RT-PCR analysis: (1) agarose gels, (2) fluorescent labelling of PCR products and detection with laser-induced fluorescence using capillary electrophoresis (Fasco et al. 1995; Williams et al. 1996) or acrylamide gels, and (3) plate capture and sandwich probe hybridization (Mulder et al. 1994). Although these methods proved successful, each method requires post-PCR manipulations that add time to the analysis and may lead to laboratory contamination. The sample throughput of these methods is limited (with the exception of the plate capture approach), and, therefore, these methods are not well suited for uses demanding high sample throughput (i.e., screening of large numbers of biomolecules or analyzing samples for diagnostics or clinical trials).

Here we report the development of a novel assay for quantitative DNA analysis. The assay is based on the use of the 5' nuclease assay first described by Holland et al. (1991). The method uses the 5' nuclease activity of Taq polymerase to cleave a nonextendible hybridization probe during the extension phase of PCR. The approach uses dual-labeled fluorogenic hybridization probes (Lee et al. 1993; Bassler et al. 1995; Livak et al. 1995a,b). One fluorescent dye serves as a reporter [FAM (i.e., 6-carboxyfluorescein)] and its emission spectra is quenched by the second fluorescent dye, TAMRA (i.e., 6-carboxy-tetramethyl-rhodamine). The nuclease degradation of the hybridization probe releases the quenching of the FAM fluorescent emission, resulting in an increase in peak fluorescent emission at 518 nm. The use of a sequence detector (ABI Prism) allows measurement of fluorescent spectra of all 96 wells of the thermal cycler continuously during the PCR amplification. Therefore, the reactions are monitored in real time. The output data is described and quantitative analysis of input target DNA sequences is discussed below.

RESULTS

PCR Product Detection in Real Time

The goal was to develop a high-throughput, sensitive, and accurate gene quantitation assay for use in monitoring lipid mediated therapeutic gene delivery. A plasmid encoding human factor VIII gene sequence, pF8TM (see Methods), was used as a model therapeutic gene. The assay uses fluorescent Taqman methodology and an instrument capable of measuring fluorescence in real time (ABI Prism 7700 Sequence Detector). The Taqman reaction requires a hybridization probe labeled with two different fluorescent dyes. One dye is a reporter dye (FAM), the other is a quenching dye (TAMRA). When the probe is intact, fluorescent energy transfer occurs and the reporter dye fluorescent emission is absorbed by the quenching dye (TAMRA). During the extension phase of the PCR cycle, the fluorescent hybridization probe is cleaved by the 5'-3' nucleolytic activity of the DNA polymerase. On cleavage of the probe, the reporter dye emission is no longer transferred efficiently to the quenching dye, resulting in an increase of the reporter dye fluorescent emission spectra. PCR primers and probes were designed for the human factor VIII sequence and human β-actin gene (as described in Methods). Optimization reactions were performed to choose the appropriate probe and magnesium concentrations yielding the highest intensity of reporter fluorescent signal without sacrificing specificity. The instrument uses a charge-coupled device (i.e., CCD camera) for measuring the fluorescent emission spectra from 500 to 650 nm. Each PCR tube was monitored sequentially for 25 msec with continuous monitoring throughout the amplification. Each tube was re-examined every 8.5 sec. Computer software was designed to examine the fluorescent intensity of both the reporter dye (FAM) and the quenching dye (TAMRA). The fluorescent intensity of the quenching dye, TAMRA, changes very little over the course of the PCR amplification (data not shown). Therefore, the intensity of TAMRA dye emission serves as an internal standard with which to normalize the reporter dye (FAM) emission variations. The software calculates a value termed ΔRn (or ΔRQ) using the following equation: $\Delta Rn = (Rn^+) - (Rn^-)$, where Rn^+ = emission intensity of reporter/emission intensity of quencher at any given time in a reaction tube, and Rn^- = emission intensity of re-

HUD ET AL.

porter/emission intensity of quencher measured prior to PCR amplification in that same reaction tube. For the purpose of quantitation, the last three data points (ΔRns) collected during the extension step for each PCR cycle were analyzed. The nucleolytic degradation of the hybridization probe occurs during the extension phase of PCR, and, therefore, reporter fluorescent emission increases during this time. The three data points were averaged for each PCR cycle and the mean value for each was plotted in an "amplification plot" shown in Figure 1A. The ΔRn mean value is plotted on the y-axis, and time, represented by cycle number, is plotted on the x-axis. During the early cycles of the PCR amplification, the ΔRn

value remains at base line When sufficient hybridization probe has been cleaved by the Taq polymerase nuclease activity, the intensity of reporter fluorescent emission increases. Most PCR amplifications reach a plateau phase of reporter fluorescent emission if the reaction is carried out to high cycle numbers. The amplification plot is examined early in the reaction, at a point that represents the log phase of product accumulation. This is done by assigning an arbitrary threshold that is based on the variability of the base-line data. In Figure 1A, the threshold was set at 10 standard deviations above the mean of base line emission calculated from cycles 1 to 15. Once the threshold is chosen, the point at which
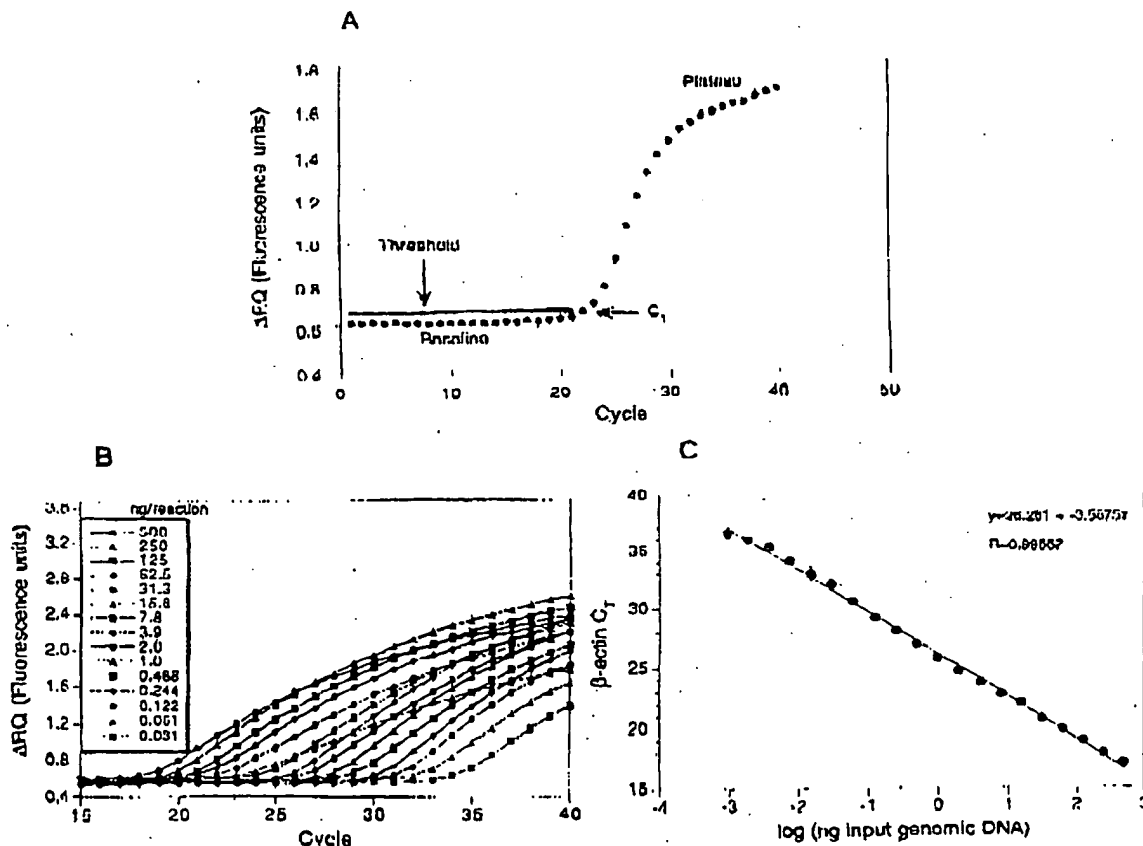
Figure 1   PCR product detection in real time. (A) The Model 7700 software will construct amplification plots from the extension phase fluorescent emission data collected during the PCR amplification. The standard deviation is determined from the data points collected from the base line of the amplification plot. C_T values are calculated by determining the point at which the fluorescence exceeds a threshold limit (usually 10 times the standard deviation of the base line). (B) Overlay of amplification plots of serially (1:2) diluted human genomic DNA samples amplified with β-actin primers. (C) Input DNA concentration of the samples plotted versus C_T. All

the amplification plot crosses the threshold is defined as C_T. C_T is reported as the cycle number at this point. As will be demonstrated, the C_T value is predictive of the quantity of input target.

C_T Values Provide a Quantitative Measurement of Input Target Sequences

Figure 1B shows amplification plots of 15 different PCR amplifications overlaid. The amplifications were performed on a 1:2 serial dilution of human genomic DNA. The amplified target was human β actin. The amplification plots shift to the right (to higher threshold cycles) as the input target quantity is reduced. This is expected because reactions with fewer starting copies of the target molecule require greater amplification to degrade enough probe to attain the threshold fluorescence. An arbitrary threshold of 10 standard deviations above the base line was used to determine the C_T values. Figure 1C represents the C_T values plotted versus the sample dilution value. Each dilution was amplified in triplicate PCR amplifications and plotted as mean values with error bars representing one standard deviation. The C_T values decrease linearly with increasing target quantity. Thus, C_T values can be used as a quantitative measurement of the input target number. It should be noted that the amplification plot for the 15.6-ng sample shown in Figure 1B does not reflect the same fluorescent rate of increase exhibited by most of the other samples. The 15.6-ng sample also achieves endpoint plateau at a lower fluorescent value than would be expected based on the input DNA. This phenomenon has been observed occasionally with other samples (data not shown) and may be attributable to late cycle inhibition; this hypothesis is still under investigation. It is important to note that the flattened slope and early plateau do not impact significantly the calculated C_T value as demonstrated by the fit on the line shown in Figure 1C. All triplicate amplifications resulted in very similar C_T values—the standard deviation did not exceed 0.5 for any dilution. This experiment contains a >100,000-fold range of input target molecules. Using C_T values for quantitation permits a much larger assay range than directly using total fluorescent emission intensity for quantitation. The linear range of fluorescent intensity measurement of the ABI Prism 7700 Sequence

ments over a very large range of relative starting target quantities.

Sample Preparation Validation

Several parameters influence the efficiency of PCR amplification: magnesium and salt concentrations, reaction conditions (i.e., time and temperature), PCR target size and composition, primer sequences, and sample purity. All of the above factors are common to a single PCR assay except sample to sample purity. In an effort to validate the method of sample preparation for the factor VIII assay, PCR amplification reproducibility and efficiency of 10 replicate sample preparations were examined. After genomic DNA was prepared from the 10 replicate samples, the DNA was quantitated by ultraviolet spectroscopy. Amplifications were performed analyzing β-actin gene content in 100 and 25 ng of total genomic DNA. Each PCR amplification was performed in triplicate. Comparison of C_T values for each triplicate sample show minimal variation based on standard deviation and coefficient of variance (Table 1). Therefore, each of the triplicate PCR amplifications was highly reproducible, demonstrating that real time PCR using this instrumentation introduces minimal variation into the quantitative PCR analysis. Comparison of the mean C_T values of the 10 replicate sample preparations also showed minimal variability, indicating that each sample preparation yielded similar results for β-actin gene quantity. The highest C_T difference between any of the samples was 0.85 and 0.71 for the 100 and 25 ng samples, respectively. Additionally, the amplification of each sample exhibited an equivalent rate of fluorescent emission intensity change per amount of DNA target analyzed as indicated by similar slopes derived from the sample dilutions (Fig. 2). Any sample containing an excess of a PCR inhibitor would exhibit a greater measured β-actin C_T value for a given quantity of DNA. In addition, the inhibitor would be diluted along with the sample in the dilution analysis (Fig. 2), altering the expected C_T value change. Each sample amplification yielded a similar result in the analysis, demonstrating that this method of sample preparation is highly reproducible with regard to sample purity.

Quantitative Analysis of a Plasmid After

HI ID I-I AL

Table 1.	Reproducibility of Sample Preparation Method							
	100 ng				**25 ng**			
Sample no.	C_T	mean	standard deviation	CV	C_T	mean	standard deviation	CV
1	18.24				20.48			
	18.23				20.55			
	18.33	18.27	0.06	0.32	20.5	20.51	0.03	0.17
2	18.33				20.61			
	18.35				20.59			
	18.44	18.37	0.06	0.32	20.41	20.54	0.11	0.54
3	18.3				20.54			
	18.3				20.6			
	18.42	18.34	0.07	0.36	20.49	20.54	0.06	0.28
4	18.15				20.48			
	18.23				20.44			
	18.32	18.23	0.08	0.46	20.38	20.43	0.05	0.26
5	18.4				20.68			
	18.38				20.87			
	18.46	18.42	0.04	0.23	20.63	20.73	0.13	0.61
6	18.54				21.09			
	18.67				21.04			
	19	18.74	0.24	1.26	21.04	21.06	0.03	0.15
7	18.28				20.67			
	18.36				20.73			
	18.52	18.39	0.12	0.66	20.65	20.68	0.04	0.2
8	18.45				20.98			
	18.7				20.84			
	18.73	18.63	0.16	0.83	20.75	20.86	0.12	0.57
9	18.18				20.46			
	18.34				20.54			
	18.36	18.29	0.1	0.55	20.48	20.51	0.07	0.32
10	18.42				20.79			
	18.57				20.78			
	18.66	18.55	0.12	0.65	20.62	20.73	0.1	0.16
Mean	(1 10)	18.42	0.17	0.90		20.66	0.19	0.94

tor containing a partial cDNA for human factor VIII, pF8TM. A series of transfections was set up using a decreasing amount of the plasmid (40, 4, 0.5, and 0.1 µg). Twenty-four hours post-transfection, total DNA was purified from each flask of cells. β-Actin gene quantity was chosen as a value for normalization of genomic DNA concentration from each sample. In this experiment, β-actin gene content should remain constant relative to total genomic DNA. Figure 3 shows the result of the β-actin DNA measurement (100 ng total DNA determined by ultraviolet spectroscopy) of each sample. Each sample was analyzed in triplicate and the mean β-actin C_T values of the triplicates were plotted (error bars represent one standard deviation). The highest difference

between any two sample means was 0.95 C_T. Ten nanograms of total DNA of each sample were also examined for β-actin. The results again showed that very similar amounts of genomic DNA were present: the maximum mean β-actin C_T value difference was 1.0. As Figure 3 shows, the rate of β-actin C_T change between the 100 and 10-ng samples was similar (slope values range between 3.56 and 3.45). This verifies again that the method of sample preparation yields samples of identical PCR integrity (i.e., no sample contained an excessive amount of a PCR inhibitor). However, these results indicate that each sample contained slight differences in the actual amount of genomic DNA analyzed. Determination of actual genomic DNA concentration was accomplished
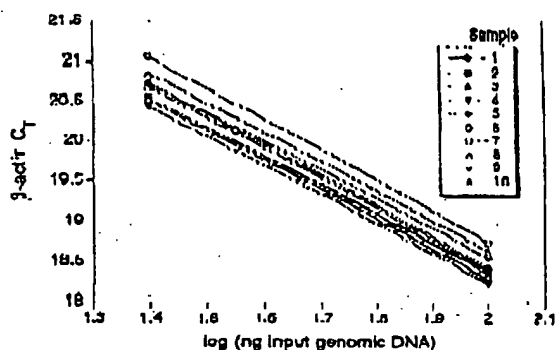
Figure 2 Sample preparation purity. The replicate samples shown in Table 1 were also amplified in triplicate using 25 ng of each DNA sample. The figure shows the input DNA concentration (100 and 25 ng) vs. C_t. In the figure, the 100 and 25 ng points for each sample are connected by a line.

by plotting the mean β-actin C_t value obtained for each 100-ng sample on a β-actin standard curve (shown in Fig. 4C). The actual genomic DNA concentration of each sample, a, was obtained by extrapolation to the x-axis.

Figure 4A shows the measured (i.e., non-normalized) quantities of factor VIII plasmid DNA (pF8TM) from each of the four transient cell transfections. Each reaction contained 100 ng of total sample DNA (as determined by UV spectroscopy). Each sample was analyzed in triplicate
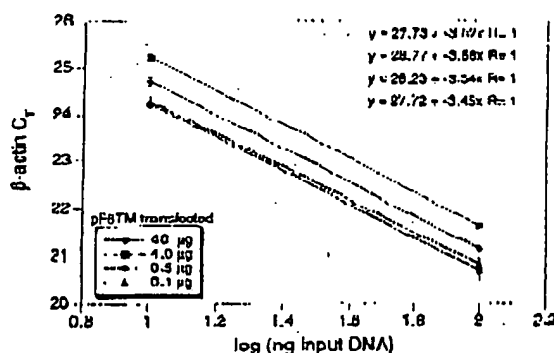
Figure 3 Analysis of transfected cell DNA quantity and purity. The DNA preparations of the four 293 cell transfections (40, 4, 0.5, and 0.1 μg of pF8TM) were analyzed for the β-actin gene. 100 and 10 ng (determined by ultraviolet spectroscopy) of each sample were amplified in triplicate. For each amount of pF8TM that was transfected, the β-actin C_T values are plotted versus the total input DNA concentration.

PCR amplifications. As shown, pF8TM purified from the 293 cells decreases (mean C_t values increase) with decreasing amounts of plasmid transfected. The mean C_t values obtained for pF8TM in Figure 4A were plotted on a standard curve comprised of serially diluted pF8TM, shown in Figure 4B. The quantity of pF8TM, b, found in each of the four transfections was determined by extrapolation to the x-axis of the standard curve in Figure 4B. These uncorrected values, b, for pF8TM were normalized to determine the actual amount of pF8TM found per 100 ng of genomic DNA by using the equation:

$$\frac{b \times 100 \text{ ng}}{a} = \text{actual pF8TM copies per 100 ng of genomic DNA}$$

where a = actual genomic DNA in a sample and b = pF8TM copies from the standard curve. The normalized quantity of pF8TM per 100 ng of genomic DNA for each of the four transfections is shown in Figure 4D. These results show that the quantity of factor VIII plasmid associated with the 293 cells, 24 hr after transfection, decreases with decreasing plasmid concentration used in the transfection. The quantity of pF8TM associated with 293 cells, after transfection with 40 μg of plasmid, was 35 pg per 100 ng genomic DNA. This results in ~520 plasmid copies per cell.

DISCUSSION

We have described a new method for quantitating gene copy numbers using real-time analysis of PCR amplifications. Real-time PCR is compatible with either of the two PCR (RT-PCR) approaches: (1) quantitative competitive where an internal competitor for each target sequence is used for normalization (data not shown) or (2) quantitative comparative PCR using a normalization gene contained within the sample (i.e., β-actin) or a "housekeeping" gene for RT-PCR. If equal amounts of nucleic acid are analyzed for each sample and if the amplification efficiency before quantitative analysis is identical for each sample, the internal control (normalization gene or competitor) should give equal signals for all samples.

The real-time PCR method offers several advantages over the other two methods currently employed (see the introduction). First, the real-time PCR method is performed in a closed-tube system and requires no post-PCR manipulation
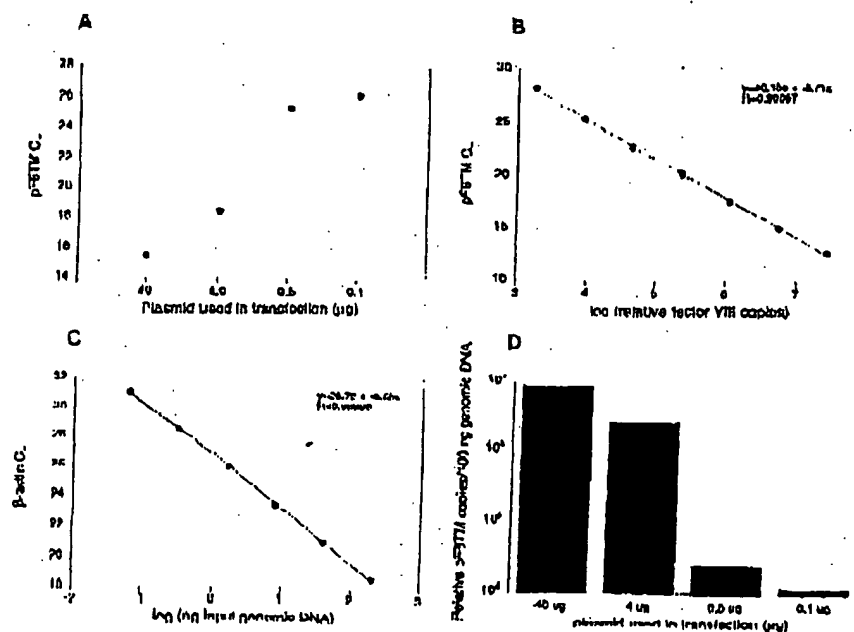
HUO ET AL.

Figure 4 Quantitative analysis of pF8TM in transfected cells. (A) Amount of plasmid DNA used for the transfection plotted against the mean C_t value determined for pF8TM remaining 24 hr after transfection. (B,C) Standard curves of pF8TM and β-actin, respectively. pF8TM DNA (B) and genomic DNA (C) were diluted serially 1:5 before amplification with the appropriate primers. The β-actin standard curve was used to normalize the results of A to 100 ng of genomic DNA. (D) The amount of pF8TM present per 100 ng of genomic DNA.

of sample. Therefore, the potential for PCR contamination in the laboratory is reduced because amplified products can be analyzed and disposed of without opening the reaction tubes. Second, this method supports the use of a normalization gene (i.e., β-actin) for quantitative PCR or housekeeping genes for quantitative RT-PCR controls. Analysis is performed in real time during the log phase of product accumulation. Analysis during log phase permits many different genes (over a wide input target range) to be analyzed simultaneously, without concern of reaching reaction plateau at different cycles. This will make multigene analysis assays much easier to develop, because individual internal competitors will not be needed for each gene under analysis. Third, sample throughput will increase dramatically with the new method because there is no post-PCR processing time. Additionally, working in a 96-well format is highly compatible with automation technology.

The real-time PCR method is highly reproducible. Replicate amplifications can be analyzed

for each sample minimizing potential error. The system allows for a very large assay dynamic range (approaching 1,000,000-fold starting target). Using a standard curve for the target of interest, relative copy number values can be determined for any unknown sample. Fluorescent threshold values, C_t, correlate linearly with relative DNA copy numbers. Real time quantitative RT-PCR methodology (Gibson et al., this issue) has also been developed. Finally, real time quantitative PCR methodology can be used to develop high-throughput screening assays for a variety of applications [quantitative gene expression (RT-PCR), gene copy assays (Her2, HIV, etc.), genotyping (knockout mouse analysis), and immuno-PCR].

Real-time PCR may also be performed using intercalating dyes (Higuchi et al. 1992) such as ethidium bromide. The fluorogenic probe method offers a major advantage over intercalating dyes—greater specificity (i.e., primer dimers and nonspecific PCR products are not detected).

METHODS

Generation of a Plasmid Containing a Partial cDNA for Human Factor VIII

Total RNA was harvested (RNAzol B from Tel Test, Inc., Friendswood, TX) from cells transfected with a factor VIII expression vector, pCIS2.8c251) (Eaton et al. 1986; Gorman et al. 1990). A factor VIII partial cDNA sequence was generated by RT-PCR (GeneAmp RNA PCR Kit (part N808-0179, PE Applied Biosystems, Foster City, CA)] using the PCR primers F8for and F8rev (primer sequences are shown below). The amplicon was reamplified using modified F8for and F8rev primers (appended with HamdIII and HindIII restriction site sequences at the 5' end) and cloned into pGEM-3Z (Promega Corp., Madison, WI). The resulting clone, pF8TM, was used for transient transfection of 293 cells.

Amplification of Target DNA and Detection of Amplicon Factor VIII Plasmid DNA

(pF8TM) was amplified with the primers F8for 5'-CCC-GTCCCAAGAGTGACGTTGTC-3' and F8rev 5'-AAACCT-CACCCTGGATCGTACG-3'. The reaction produced a 422-bp PCR product. The forward primer was designed to recognize a unique sequence found in the 5' untranslated region of the parent pCIS2.8c251) plasmid and therefore does not recognize and amplify the human factor VIII gene. Primers were chosen with the assistance of the computer program Oligo 4.0 (National Biosciences, Inc., Plymouth, MN). The human β-actin gene was amplified with the primers β-actin forward primer 5'-TCACCCACACTGT GCCCATCTACGA-3' and β-actin reverse primer 5'-CAG-CGGAACCGCTCATTGCCAATGG-3'. The reaction produced a 295-bp PCR product.

Amplification reactions (50 µl) contained a DNA sample, 10× PCR Buffer II (5 µl), 200 µM dATP, dCTP, dGTP, and 400 µM dUTP, 4 mM MgCl₂, 1.25 Units AmpliTaq DNA polymerase, 0.5 unit AmpErase uracil N-glycosylase (UNG), 50 pmole of each factor VIII primer, and 15 pmole of each β-actin primer. The reactions also contained one of the following detection probes (100 nM each): F8probe 5'-(FAM)ACCCTGTCCCACCTGCTTCTTTCTGT-GCCTT(TAMRA)p 3' and β-actin probe 5' (FAM)ATGCCC-X(TAMRA)CCCCCATGCCATCp-3' where p indicates phosphorylation and X indicates a linker arm nucleotide. Reaction tubes were MicroAmp Optical Tubes (part number N801 0933, Perkin Elmer) that were frosted (at Perkin Elmer) to prevent light from reflecting. Tube caps were similar to MicroAmp Caps but specially designed to prevent light scattering. All of the PCR consumables were supplied by PE Applied Biosystems (Foster City, CA) except the factor VIII primers, which were synthesized at Genentech, Inc. (South San Francisco, CA). Probes were designed using the Oligo 4.0 software, following guidelines suggested in the Model 7700 Sequence Detector Instrument manual. Briefly, probe T_m should be at least 5°C higher than the annealing temperature used during thermal cycling; primers should not form stable duplexes with the probe.

The thermal cycling conditions included 2 min at 50°C and 10 min at 95°C. Thermal cycling proceeded with

reactions were performed in the Model 7700 Sequence Detector (PE Applied Biosystems), which contains a Gene-Amp PCR System 9600. Reaction conditions were programmed on a Power Macintosh 7100 (Apple Computer, Santa Clara, CA) linked directly to the Model 7700 Sequence Detector. Analysis of data was also performed on the Macintosh computer. Collection and analysis software was developed at PE Applied Biosystems.

Transfection of Cells with Factor VIII Construct

Four T175 flasks of 293 cells (ATCC CRL 1573), a human fetal kidney suspension cell line, were grown to 80% confluency and transfected pF8TM. Cells were grown in the following media: 50% HAM'S F12 without GHT, 50% low glucose Dulbecco's modified Eagle medium (DMEM) without glycine with sodium bicarbonate, 10% fetal bovine serum, 2 mM L-glutamine, and 1% penicillin-streptomycin. The media was changed 30 min before the transfection. pF8TM DNA amounts of 40, 4, 0.5, and 0.1 µg were added to 1.5 ml of a solution containing 0.125 M CaCl₂ and 1× HEPES. The four mixtures were left at room temperature for 10 min and then added dropwise to the cells. The flasks were incubated at 37°C and 5% CO₂ for 24 hr, washed with PBS, and resuspended in PBS. The resuspended cells were divided into aliquots and DNA was extracted immediately using the QIAamp Blood Kit (Qiagen, Chatsworth, CA). DNA was eluted into 200 µl of 30 mM Tris-HCl at pH 8.0.

ACKNOWLEDGMENTS

REFERENCES

Bassler, H.A., S.J. Flood, K.J. Livak, J. Marmaro, R. Knom, and C.A. Batt. 1995. Use of a fluorogenic probe in a PCR-based assay for the detection of Listeria monocytogenes. App. Environ. Microbiol. 61: 3724–3728.

Becker-Andre, M. 1991. Quantitative evaluation of mRNA levels. Meth. Mol. Cell. Biol. 2: 189 201.

Clementi, M., S. Menzo, P. Bagnarelli, A. Manzin, A. Valenza, and P.E. Varaldo. 1993. Quantitative PCR and RT-PCR in virology. [Review]. PCR Methods Applic. 2: 191–196.

Connor, R.I., H. Mohri, Y. Cao, and D.D. Ho. 1993. Increased viral burden and cytopathicity correlate temporally with CD4+ T-lymphocyte decline and clinical progression in human immunodeficiency virus type 1-infected individuals. J. Virol. 67: 1772–1777.

Eaton, D.L., W.I. Wood, D. Eaton, P.E. Hass, P.

HFID LT AL.

Venar, and C. Gorman. 1986. Construction and characterization of an active factor VIII variant lacking the central one third of the molecule. *Biochemistry* 25: 8343-8347.

Basco, M.J., C.P. Treanor, S. Spivack, H.L. Bigge, and L.S. Kaminsky. 1995. Quantitative RNA-polymerase chain reaction-DNA analysis by capillary electrophoresis and laser-induced fluorescence. *Anal. Biochem.* 224: 140-147.

Ferre, F. 1992. Quantitative or semi-quantitative PCR: Reality versus myth. *PCR Methods Applic.* 2: 1-9.

Furtado, M.R., L.A. Kingsley, and S.M. Wolinsky. 1995. Changes in the viral mRNA expression pattern correlate with a rapid rate of CD4 + T-cell number decline in human immunodeficiency virus type 1-infected individuals. *J. Virol.* 69: 2092-2100.

Gibson, U.E.M., C.A. Heid, and P.M. Williams. 1996 A novel method for real time quantitative competitive RT-PCR. *Genome Res.* (this issue).

Gorman, C.M., D.R. Gies, and G. McCray. 1990. Transient production of proteins using an adenovirus transformed cell line. *DNA Prot. Engin. Tech.* 2: 3 10.

Higuchi, R., G. Dollinger, P.S. Walsh, and R. Griffith. 1992. Simultaneous amplification and detection of specific DNA sequences. *Biotechnology* 10: 413 417.

Holland, P.M., R.D. Abramson, R. Watson, and D.H. Gelfand. 1991. Detection of specific polymerase chain reaction product by utilizing the 5'—3' exonuclease activity of Thermus aquaticus DNA polymerase. *Proc. Natl. Acad. Sci.* 88: 7276-7280.

Huang, S.K., H.Q. Xiao, T.J. Kleine, G. Paciotti, D.G. Marsh, L.M. Lichtenstein, and M.C. Liu. 1995a. IL-13 expression at the sites of allergen challenge in patients with asthma. *J. Immun.* 155: 2688-2694.

Huang, S.K., M. Yi, E. Palmer, and D.G. Marsh. 1995b. A dominant T cell receptor beta-chain in response to a short ragweed allergen. *Amb a 5. J. Immun.* 154: 6157-6162.

Kellogg, D.E., J.J. Sninsky, and S. Kwok. 1990. Quantitation of HIV-1 proviral DNA relative to cellular DNA by the polymerase chain reaction. *Anal. Biochem.* 189: 202-208.

Lee, L.G., C.R. Connell, and W. Bloch. 1993. Allelic discrimination by nick-translation PCR with fluorogenic probes. *Nucleic Acids Res.* 21: 3761-3766.

Livak, K.J., S.J. Flood, J. Marmaro, W. Giusti, and K. Deetz. 1995a. Oligonucleotides with fluorescent dyes at opposite ends provide a quenched probe system useful for detecting PCR product and nucleic acid hybridization. *PCR Methods Applic.* 4: 357 362.

Livak, K.J., J. Marmaro, and J.A. Todd. 1996b. Towards

fully automated genome-wide polymorphism screening [Letter] *Nature Genet.* 9: 341-342.

Mulder, J., N. McKinney, C. Christopherson, J. Sninsky, L. Greenfield, and S. Kwok. 1994. Rapid and simple PCR assay for quantitation of human immunodeficiency virus type 1 RNA in plasma: Application to acute retroviral infection. *J. Clin. Microbiol.* 32: 292 300.

Pang, S., Y. Koyanagi, S. Miles, C. Wiley, H.V. Vinters, and I.S. Chen. 1990. High levels of unintegrated HIV-1 DNA in brain tissue of AIDS dementia patients. *Nature* 343: 85-89.

Piatak, M.J., K.C. Luk, B. Williams, and J.D. Lifson. 1993a. Quantitative competitive polymerase chain reaction for accurate quantitation of HIV DNA and RNA species. *BioTechniques* 14: 70-81.

Piatak, M.J., M S Saag, L.C. Yang, S.J. Clark, J.C. Kappes, K.C. Luk, B.H. Hahn, G.M. Shaw, and J.D. Lifson. 1993b. High levels of HIV-1 in plasma during all stages of infection determined by competitive PCR [see Comments]. *Science* 259: 1749-1754.

Prud'homme, G.J., D.H. Kono, and A.N. Theofilopoulos. 1995. Quantitative polymerase chain reaction analysis reveals marked overexpression of interleukin-1 beta, interleukin-1 and interferon-gamma mRNA in the lymph nodes of lupus-prone mice. *Mol. Immunol.* 32: 495-503.

Raeymaekers, L. 1995. A commentary on the practical applications of competitive PCR. *Genome Res.* 5: 91 94.

Sharp, P.A., A.J. Berk, and S.M. Berget. 1980. Transcription maps of adenovirus. *Methods Enzymol.* 65: 750-768.

Slamon, D.J., G.M. Clark, S.C. Wong, W.J. Levin, A. Ullrich, and W.L. McGuire. 1987. Human breast cancer: Correlation of relapse and survival with amplification of the HER-2/neu oncogene. *Science* 235: 177-182.

Southern, E.M. 1975. Detection of specific sequences among DNA fragments separated by gel electrophoresis. *J. Mol. Biol.* 98: 503-517.

Tan, X., X. Sun, C.F. Gonzalez, and W. Hsueh. 1994. PAF and TNF increase the precursor of NF-kappa B p50 mRNA in mouse intestine: Quantitative analysis by competitive PCR. *Biochim. Biophys. Acta* 1215: 157 162.

Thomas, P.S. 1980. Hybridization of denatured RNA and small DNA fragments transferred to nitrocellulose. *Proc. Natl. Acad. Sci.* 77: 5201-5205.

Williams, S., C. Schwer, A. Krishnarao, C. Heid, B. Karger, and P.M. Williams. 1996. Quantitative competitive PCR: Analysis of amplified products of the HIV-1 gag gene by capillary electrophoresis with laser induced fluorescence detection. *Anal. Biochem.* (in press).

WISP genes are members of the connective tissue growth factor family that are up-regulated in Wnt-1-transformed cells and aberrantly expressed in human colon tumors

Diane Pennica*†, Todd A. Swanson*, James W. Welsh*, Margaret A. Roy‡, David A. Lawrence*,
James Lee‡, Jennifer Brush‡, Lisa A. Taneyhill§, Bethanne Deuel‡, Michael Lew¶, Colin Watanabe‖,
Robert L. Cohen*, Mona F. Melhem**, Gene G. Finley**, Phil Quirke††, Audrey D. Goddard‡,
Kenneth J. Hillan¶, Austin L. Gurney‡, David Botstein‡,‡‡, and Arnold J. Levine§

Departments of *Molecular Oncology, ‡Molecular Biology, ‖Scientific Computing, and ¶Pathology, Genentech Inc., 1 DNA Way, South San Francisco, CA 94080;
**University of Pittsburgh School of Medicine, Veterans Administration Medical Center, Pittsburgh, PA 15240; ††University of Leeds, Leeds, LS29JT United
Kingdom; ‡‡Department of Genetics, Stanford University, Palo Alto, CA 94305; and §Department of Molecular Biology, Princeton University, Princeton, NJ
08544

Contributed by David Botstein and Arnold J. Levine, October 21, 1998

ABSTRACT   Wnt family members are critical to many developmental processes, and components of the Wnt signaling pathway have been linked to tumorigenesis in familial and sporadic colon carcinomas. Here we report the identification of two genes, WISP-1 and WISP-2, that are up-regulated in the mouse mammary epithelial cell line C57MG transformed by Wnt-1, but not by Wnt-4. Together with a third related gene, WISP-3, these proteins define a subfamily of the connective tissue growth factor family. Two distinct systems demonstrated WISP induction to be associated with the expression of Wnt-1. These included (i) C57MG cells infected with a Wnt-1 retroviral vector or expressing Wnt-1 under the control of a tetracyline repressible promoter, and (ii) Wnt-1 transgenic mice. The WISP-1 gene was localized to human chromosome 8q24.1–8q24.3. WISP-1 genomic DNA was amplified in colon cancer cell lines and in human colon tumors and its RNA overexpressed (2- to >30-fold) in 84% of the tumors examined compared with patient-matched normal mucosa. WISP-3 mapped to chromosome 6q22–6q23 and also was overexpressed (4- to >40-fold) in 63% of the colon tumors analyzed. In contrast, WISP-2 mapped to human chromosome 20q12–20q13 and its DNA was amplified, but RNA expression was reduced (2- to >30-fold) in 79% of the tumors. These results suggest that the WISP genes may be downstream of Wnt-1 signaling and that aberrant levels of WISP expression in colon cancer may play a role in colon tumorigenesis.

Wnt-1 is a member of an expanding family of cysteine-rich, glycosylated signaling proteins that mediate diverse developmental processes such as the control of cell proliferation, adhesion, cell polarity, and the establishment of cell fates (1, 2). Wnt-1 originally was identified as an oncogene activated by the insertion of mouse mammary tumor virus in virus-induced mammary adenocarcinomas (3, 4). Although Wnt-1 is not expressed in the normal mammary gland, expression of Wnt-1 in transgenic mice causes mammary tumors (5).

In mammalian cells, Wnt family members initiate signaling by binding to the seven-transmembrane spanning Frizzled receptors and recruiting the cytoplasmic protein Dishevelled (Dsh) to the cell membrane (1, 2, 6). Dsh then inhibits the kinase activity of the normally constitutively active glycogen synthase kinase-3β (GSK-3β) resulting in an increase in β-catenin levels. Stabilized β-catenin interacts with the transcription factor TCF/Lef1, forming a complex that appears in

the nucleus and binds TCF/Lef1 target DNA elements to activate transcription (7, 8). Other experiments suggest that the adenomatous polyposis coli (APC) tumor suppressor gene also plays an important role in Wnt signaling by regulating β-catenin levels (9). APC is phosphorylated by GSK-3β, binds to β-catenin, and facilitates its degradation. Mutations in either APC or β-catenin have been associated with colon carcinomas and melanomas, suggesting these mutations contribute to the development of these types of cancer, implicating the Wnt pathway in tumorigenesis (1).

Although much has been learned about the Wnt signaling pathway over the past several years, only a few of the transcriptionally activated downstream components activated by Wnt have been characterized. Those that have been described cannot account for all of the diverse functions attributed to Wnt signaling. Among the candidate Wnt target genes are those encoding the nodal-related 3 gene, Xnr3, a member of the transforming growth factor (TGF)-β superfamily, and the homeobox genes, engrailed, goosecoid, twin (Xtwn), and siamois (2). A recent report also identifies c-myc as a target gene of the Wnt signaling pathway (10).

To identify additional downstream genes in the Wnt signaling pathway that are relevant to the transformed cell phenotype, we used a PCR-based cDNA subtraction strategy, suppression subtractive hybridization (SSH) (11), using RNA isolated from C57MG mouse mammary epithelial cells and C57MG cells stably transformed by a Wnt-1 retrovirus. Overexpression of Wnt-1 in this cell line is sufficient to induce a partially transformed phenotype, characterized by elongated and refractile cells that lose contact inhibition and form a multilayered array (12, 13). We reasoned that genes differentially expressed between these two cell lines might contribute to the transformed phenotype.

In this paper, we describe the cloning and characterization of two genes up-regulated in Wnt-1 transformed cells, WISP-1 and WISP-2, and a third related gene, WISP-3. The WISP genes are members of the CCN family of growth factors, which includes connective tissue growth factor (CTGF), Cyr61, and nov, a family not previously linked to Wnt signaling.

MATERIALS AND METHODS

SSH. SSH was performed by using the PCR-Select cDNA Subtraction Kit (CLONTECH). Tester double-stranded

cDNA was synthesized from 2 μg of poly(A)$^+$ RNA isolated from the C57MG/Wnt-1 cell line and driver cDNA from 2 μg of poly(A)$^+$ RNA from the parent C57MG cells. The subtracted cDNA library was subcloned into a pGEM-T vector for further analysis.

cDNA Library Screening. Clones encoding full-length mouse *WISP-1* were isolated by screening a λgt10 mouse embryo cDNA library (CLONTECH) with a 70-bp probe from the original partial clone 568 sequence corresponding to amino acids 128–169. Clones encoding full-length human *WISP-1* were isolated by screening λgt10 lung and fetal kidney cDNA libraries with the same probe at low stringency. Clones encoding full-length mouse and human *WISP-2* were isolated by screening a C57MG/Wnt-1 or human fetal lung cDNA library with a probe corresponding to nucleotides 1463–1512. Full-length cDNAs encoding *WISP-3* were cloned from human bone marrow and fetal kidney libraries.

Expression of Human *WISP* RNA. PCR amplification of first-strand cDNA was performed with human Multiple Tissue cDNA panels (CLONTECH) and 300 μM of each dNTP at 94°C for 1 sec, 62°C for 30 sec, 72°C for 1 min, for 22–32 cycles. *WISP* and glyceraldehyde-3-phosphate dehydrogenase primer sequences are available on request.

In Situ **Hybridization.** ^{33}P-labeled sense and antisense riboprobes were transcribed from an 897-bp PCR product corresponding to nucleotides 601–1440 of mouse *WISP-1* or a 294-bp PCR product corresponding to nucleotides 82–375 of mouse *WISP-2*. All tissues were processed as described (40).

Radiation Hybrid Mapping. Genomic DNA from each hybrid in the Stanford G3 and Genebridge4 Radiation Hybrid Panels (Research Genetics, Huntsville, AL) and human and hamster control DNAs were PCR-amplified, and the results were submitted to the Stanford or Massachusetts Institute of Technology web servers.

Cell Lines, Tumors, and Mucosa Specimens. Tissue specimens were obtained from the Department of Pathology (University of Pittsburgh) for patients undergoing colon resection and from the University of Leeds, United Kingdom. Genomic DNA was isolated (Qiagen) from the pooled blood of 10 normal human donors, surgical specimens, and the following ATCC human cell lines: SW480, COLO 320DM, HT-29, WiDr, and SW403 (colon adenocarcinomas), SW620 (lymph node metastasis, colon adenocarcinoma), HCT 116 (colon carcinoma), SK-CO-1 (colon adenocarcinoma, ascites), and HM7 (a variant of ATCC colon adenocarcinoma cell line LS 174T). DNA concentration was determined by using Hoechst dye 33258 intercalation fluorimetry. Total RNA was prepared by homogenization in 7 M GuSCN followed by centrifugation over CsCl cushions or prepared by using RNAzol.

Gene Amplification and RNA Expression Analysis. Relative gene amplification and RNA expression of *WISP*s and c-*myc* in the cell lines, colorectal tumors, and normal mucosa were determined by quantitative PCR. Gene-specific primers and fluorogenic probes (sequences available on request) were designed and used to amplify and quantitate the genes. The relative gene copy number was derived by using the formula $2^{(\Delta ct)}$ where ΔCt represents the difference in amplification cycles required to detect the *WISP* genes in peripheral blood lymphocyte DNA compared with colon tumor DNA or colon tumor RNA compared with normal mucosal RNA. The ∂-method was used for calculation of the SE of the gene copy number or RNA expression level. The *WISP*-specific signal was normalized to that of the glyceraldehyde-3-phosphate dehydrogenase housekeeping gene. All TaqMan assay reagents were obtained from Perkin–Elmer Applied Biosystems.

RESULTS

Isolation of *WISP-1* and *WISP-2* by SSH. To identify Wnt-1-inducible genes, we used the technique of SSH using the

mouse mammary epithelial cell line C57MG and C57MG cells that stably express Wnt-1 (11). Candidate differentially expressed cDNAs (1,384 total) were sequenced. Thirty-nine percent of the sequences matched known genes or homologues, 32% matched expressed sequence tags, and 29% had no match. To confirm that the transcript was differentially expressed, semiquantitative reverse transcription–PCR and Northern analysis were performed by using mRNA from the C57MG and C57MG/Wnt-1 cells.

Two of the cDNAs, *WISP-1* and *WISP-2*, were differentially expressed, being induced in the C57MG/Wnt-1 cell line, but not in the parent C57MG cells or C57MG cells overexpressing Wnt-4 (Fig. 1 *A* and *B*). Wnt-4, unlike Wnt-1, does not induce the morphological transformation of C57MG cells and has no effect on β-catenin levels (13, 14). Expression of *WISP-1* was up-regulated approximately 3-fold in the C57MG/Wnt-1 cell line and *WISP-2* by approximately 5-fold by both Northern analysis and reverse transcription–PCR.

An independent, but similar, system was used to examine *WISP* expression after Wnt-1 induction. C57MG cells expressing the *Wnt-1* gene under the control of a tetracycline-repressible promoter produce low amounts of Wnt-1 in the repressed state but show a strong induction of *Wnt-1* mRNA and protein within 24 hr after tetracycline removal (8). The levels of Wnt-1 and *WISP* RNA isolated from these cells at various times after tetracycline removal were assessed by quantitative PCR. Strong induction of Wnt-1 mRNA was seen as early as 10 hr after tetracycline removal. Induction of *WISP* mRNA (2- to 6-fold) was seen at 48 and 72 hr (data not shown). These data support our previous observations that show that *WISP* induction is correlated with Wnt-1 expression. Because the induction is slow, occurring after approximately 48 hr, the induction of *WISP*s may be an indirect response to Wnt-1 signaling.

cDNA clones of human *WISP-1* were isolated and the sequence compared with mouse *WISP-1*. The cDNA sequences of mouse and human *WISP-1* were 1,766 and 2,830 bp in length, respectively, and encode proteins of 367 aa, with predicted relative molecular masses of ≈40,000 (M_r 40 K). Both have hydrophobic N-terminal signal sequences, 38 conserved cysteine residues, and four potential N-linked glycosylation sites and are 84% identical (Fig. 2*A*).

Full-length cDNA clones of mouse and human *WISP-2* were 1,734 and 1,293 bp in length, respectively, and encode proteins of 251 and 250 aa, respectively, with predicted relative molecular masses of ≈27,000 (M_r 27 K) (Fig. 2*B*). Mouse and human *WISP-2* are 73% identical. Human *WISP-2* has no potential N-linked glycosylation sites, and mouse *WISP-2* has one at
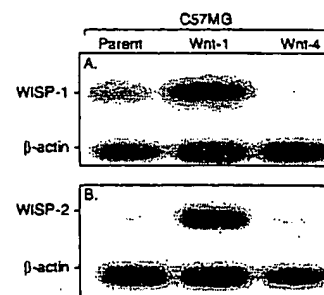

FIG. 1. *WISP-1* and *WISP-2* are induced by Wnt-1, but not Wnt-4, expression in C57MG cells. Northern analysis of *WISP-1* (*A*) and *WISP-2* (*B*) expression in C57MG, C57MG/Wnt-1, and C57MG/Wnt-4 cells. Poly(A)$^+$ RNA (2 μg) was subjected to Northern blot analysis and hybridized with a 70-bp mouse *WISP-1*-specific probe (amino acids 278–300) or a 190-bp *WISP-2*-specific probe (nucleotides 1438–1627) in the 3′ untranslated region. Blots were rehybridized with human β-actin probe.
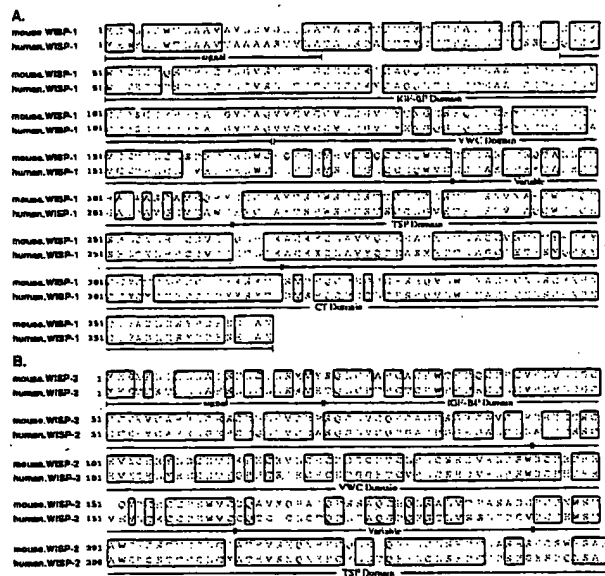
Cell Biology, Medical Sciences: Pennica *et al.*

Proc. Natl. Acad. Sci. USA 95 (1998)   14719

FIG. 2. Encoded amino acid sequence alignment of mouse and human *WISP-1* (*A*) and mouse and human *WISP-2* (*B*). The potential signal sequence, insulin-like growth factor-binding protein (IGF-BP), VWC, thrombospondin (TSP), and C-terminal (CT) domains are underlined.

FIG. 3. (*A*) Encoded amino acid sequence alignment of human WISPs. The cysteine residues of WISP-1 and WISP-2 that are not present in WISP-3 are indicated with a dot. (*B*) Schematic representation of the WISP proteins showing the domain structure and cysteine residues (vertical lines). The four cysteine residues in the VWC domain that are absent in WISP-3 are indicated with a dot. (*C*) Expression of *WISP* mRNA in human tissues. PCR was performed on human multiple-tissue cDNA panels (CLONTECH) from the indicated adult and fetal tissues.

position 197. *WISP-2* has 28 cysteine residues that are conserved among the 38 cysteines found in *WISP-1*.

Identification of *WISP-3*. To search for related proteins, we screened expressed sequence tag (EST) databases with the WISP-1 protein sequence and identified several ESTs as potentially related sequences. We identified a homologous protein that we have called WISP-3. A full-length human *WISP-3* cDNA of 1,371 bp was isolated corresponding to those ESTs that encode a 354-aa protein with a predicted molecular mass of 39,293. WISP-3 has two potential N-linked glycosylation sites and 36 cysteine residues. An alignment of the three human WISP proteins shows that WISP-1 and WISP-3 are the most similar (42% identity), whereas WISP-2 has 37% identity with WISP-1 and 32% identity with WISP-3 (Fig. 3*A*).

***WISPs* Are Homologous to the CTGF Family of Proteins.** Human *WISP-1*, *WISP-2*, and *WISP-3* are novel sequences; however, mouse *WISP-1* is the same as the recently identified *Elm1* gene. *Elm1* is expressed in low, but not high, metastatic mouse melanoma cells, and suppresses the *in vivo* growth and metastatic potential of K-1735 mouse melanoma cells (15). Human and mouse *WISP-2* are homologous to the recently described rat gene, *rCop-1* (16). Significant homology (36–44%) was seen to the CCN family of growth factors. This family includes three members, CTGF, Cyr61, and the protooncogene *nov*. CTGF is a chemotactic and mitogenic factor for fibroblasts that is implicated in wound healing and fibrotic disorders and is induced by TGF-β (17). Cyr61 is an extracellular matrix signaling molecule that promotes cell adhesion, proliferation, migration, angiogenesis, and tumor growth (18, 19). *nov* (nephroblastoma overexpressed) is an immediate early gene associated with quiescence and found altered in Wilms tumors (20). The proteins of the CCN family share functional, but not sequence, similarity to Wnt-1. All are secreted, cysteine-rich heparin binding glycoproteins that associate with the cell surface and extracellular matrix.

WISP proteins exhibit the modular architecture of the CCN family, characterized by four conserved cysteine-rich domains (Fig. 3*B*) (21). The N-terminal domain, which includes the first 12 cysteine residues, contains a consensus sequence (GCGC-CXXC) conserved in most insulin-like growth factor (IGF)-
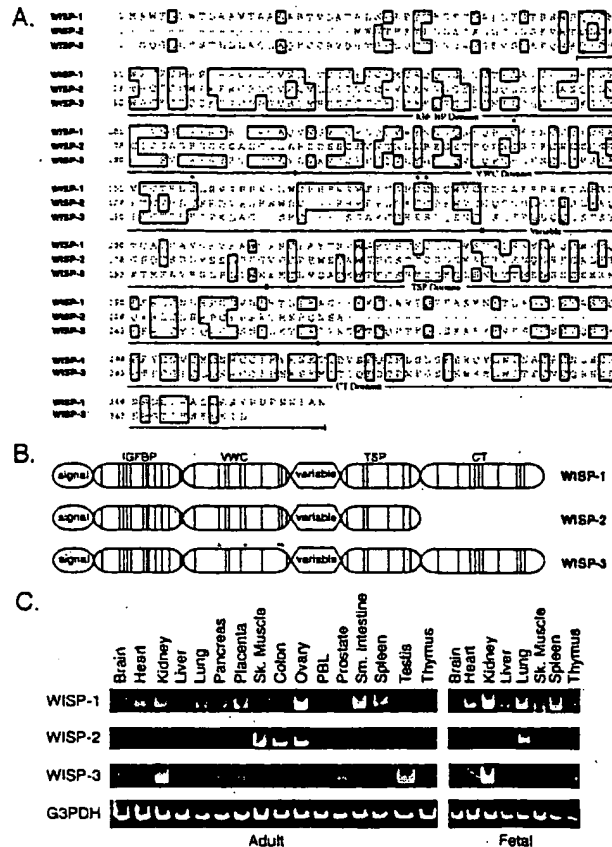
binding proteins (BP). This sequence is conserved in WISP-2 and WISP-3, whereas WISP-1 has a glutamine in the third position instead of a glycine. CTGF recently has been shown to specifically bind IGF (22) and a truncated *nov* protein lacking the IGF-BP domain is oncogenic (23). The von Willebrand factor type C module (VWC), also found in certain collagens and mucins, covers the next 10 cysteine residues, and is thought to participate in protein complex formation and oligomerization (24). The VWC domain of WISP-3 differs from all CCN family members described previously, in that it contains only six of the 10 cysteine residues (Fig. 3*A* and *B*). A short variable region follows the VWC domain. The third module, the thrombospondin (TSP) domain is involved in binding to sulfated glycoconjugates and contains six cysteine residues and a conserved WSxCSxxCG motif first identified in thrombospondin (25). The C-terminal (CT) module containing the remaining 10 cysteines is thought to be involved in dimerization and receptor binding (26). The CT domain is present in all CCN family members described to date but is absent in WISP-2 (Fig. 3*A* and *B*). The existence of a putative signal sequence and the absence of a transmembrane domain suggest that WISPs are secreted proteins, an observation supported by an analysis of their expression and secretion from mammalian cell and baculovirus cultures (data not shown).

Expression of *WISP* mRNA in Human Tissues. Tissue-specific expression of human *WISPs* was characterized by PCR

analysis on adult and fetal multiple tissue cDNA panels. *WISP-1* expression was seen in the adult heart, kidney, lung, pancreas, placenta, ovary, small intestine, and spleen (Fig. 3C). Little or no expression was detected in the brain, liver, skeletal muscle, colon, peripheral blood leukocytes, prostate, testis, or thymus. *WISP-2* had a more restricted tissue expression and was detected in adult skeletal muscle, colon, ovary, and fetal lung. Predominant expression of *WISP-3* was seen in adult kidney and testis and fetal kidney. Lower levels of *WISP-3* expression were detected in placenta, ovary, prostate, and small intestine.

In Situ **Localization of *WISP-1* and *WISP-2*.** Expression of *WISP-1* and *WISP-2* was assessed by *in situ* hybridization in mammary tumors from Wnt-1 transgenic mice. Strong expression of *WISP-1* was observed in stromal fibroblasts lying within the fibrovascular tumor stroma (Fig. 4 A–D). However, low-level *WISP-1* expression also was observed focally within tumor cells (data not shown). No expression was observed in normal breast. Like *WISP-1*, *WISP-2* expression also was seen in the tumor stroma in breast tumors from Wnt-1 transgenic animals (Fig. 4 E–H). However, *WISP-2* expression in the stroma was in spindle-shaped cells adjacent to capillary vessels, whereas

FIG. 4.   (*A*, *C*, *E*, and *G*) Representative hematoxylin/eosin-stained images from breast tumors in Wnt-1 transgenic mice. The corresponding dark-field images showing *WISP-1* expression are shown in *B* and *D*. The tumor is a moderately well-differentiated adenocarcinoma showing evidence of adenoid cystic change. At low power (*A* and *B*), expression of *WISP-1* is seen in the delicate branching fibrovascular tumor stroma (arrowhead). At higher magnification, expression is seen in the stromal(s) fibroblasts (*C* and *D*), and tumor cells are negative. Focal expression of *WISP-1*, however, was observed in tumor cells in some areas. Images of *WISP-2* expression are shown in *E–H*. At low power (*E* and *F*), expression of WISP-2 is seen in cells lying within the fibrovascular tumor stroma. At higher magnification, these cells appeared to be adjacent to capillary vessels whereas tumor cells are negative (*G* and *H*).

the predominant cell type expressing *WISP-1* was the stromal fibroblasts.

Chromosome Localization of the *WISP* Genes. The chromosomal location of the human *WISP* genes was determined by radiation hybrid mapping panels. *WISP-1* is approximately 3.48 cR from the meiotic marker AFM259xc5 [logarithm of odds (lod) score 16.31] on chromosome 8q24.1 to 8q24.3, in the same region as the human locus of the *nov*H family member (27) and roughly 4 Mbs distal to c-*myc* (28). Preliminary fine mapping indicates that *WISP-1* is located near D8S1712 STS. *WISP-2* is linked to the marker SHGC-33922 (lod = 1,000) on chromosome 20q12–20q13.1. Human *WISP-3* mapped to chromosome 6q22–6q23 and is linked to the marker AFM211ze5 (lod = 1,000). *WISP-3* is approximately 18 Mbs proximal to CTGF and 23 Mbs proximal to the human cellular oncogene *MYB* (27, 29).

Amplification and Aberrant Expression of *WISPs* in Human Colon Tumors. Amplification of protooncogenes is seen in many human tumors and has etiological and prognostic significance. For example, in a variety of tumor types, c-*myc* amplification has been associated with malignant progression and poor prognosis (30). Because *WISP-1* resides in the same general chromosomal location (8q24) as c-*myc*, we asked whether it was a target of gene amplification, and, if so, whether this amplification was independent of the c-*myc* locus. Genomic DNA from human colon cancer cell lines was assessed by quantitative PCR and Southern blot analysis. (Fig. 5 *A* and *B*). Both methods detected similar degrees of *WISP-1* amplification. Most cell lines showed significant (2- to 4-fold) amplification, with the HT-29 and WiDr cell lines demonstrating an 8-fold increase. Significantly, the pattern of amplification observed did not correlate with that observed for c-*myc*, indicating that the c-*myc* gene is not part of the amplicon that involves the *WISP-1* locus.

We next examined whether the *WISP* genes were amplified in a panel of 25 primary human colon adenocarcinomas. The relative *WISP* gene copy number in each colon tumor DNA was compared with pooled normal DNA from 10 donors by quantitative PCR (Fig. 6). The copy number of *WISP-1* and *WISP-2* was significantly greater than one, approximately 2-fold for *WISP-1* in about 60% of the tumors and 2- to 4-fold for *WISP-2* in 92% of the tumors (*P* < 0.001 for each). The copy number for *WISP-3* was indistinguishable from one (*P* = 0.166). In addition, the copy number of *WISP-2* was significantly higher than that of *WISP-1* (*P* < 0.001).

The levels of *WISP* transcripts in RNA isolated from 19 adenocarcinomas and their matched normal mucosa were
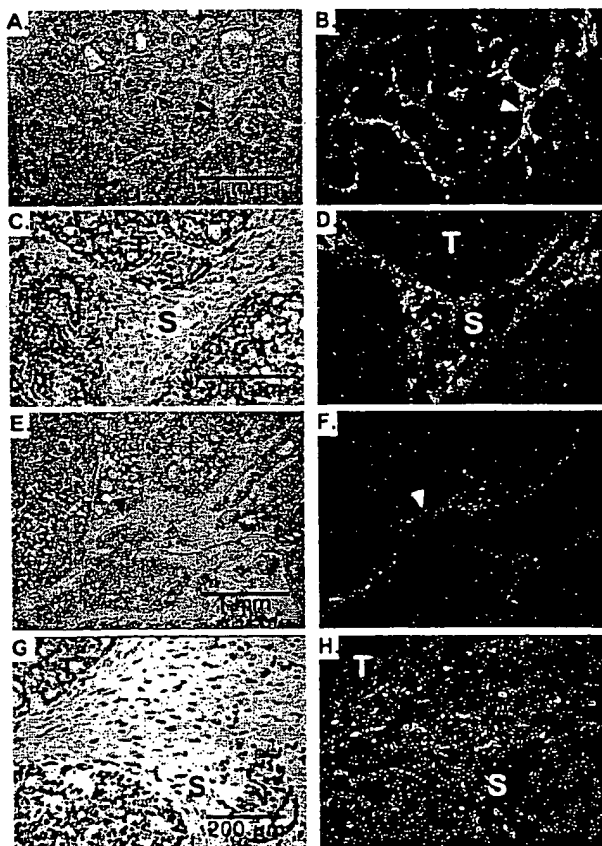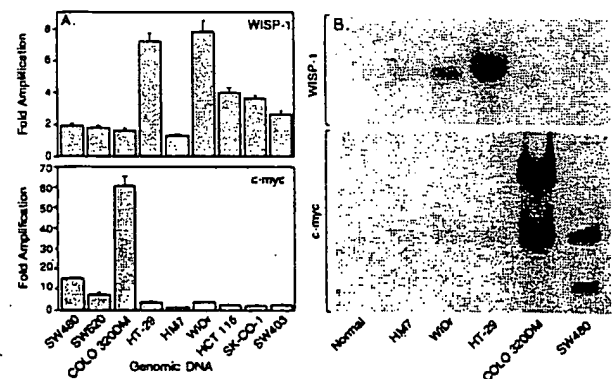

FIG. 5.   Amplification of *WISP-1* genomic DNA in colon cancer cell lines. (*A*) Amplification in cell line DNA was determined by quantitative PCR. (*B*) Southern blots containing genomic DNA (10 µg) digested with *Eco*RI (*WISP-1*) or *Xba*I (c-*myc*) were hybridized with a 100-bp human *WISP-1* probe (amino acids 186–219) or a human c-*myc* probe (located at bp 1901–2000). The *WISP* and *myc* genes are detected in normal human genomic DNA after a longer film exposure.
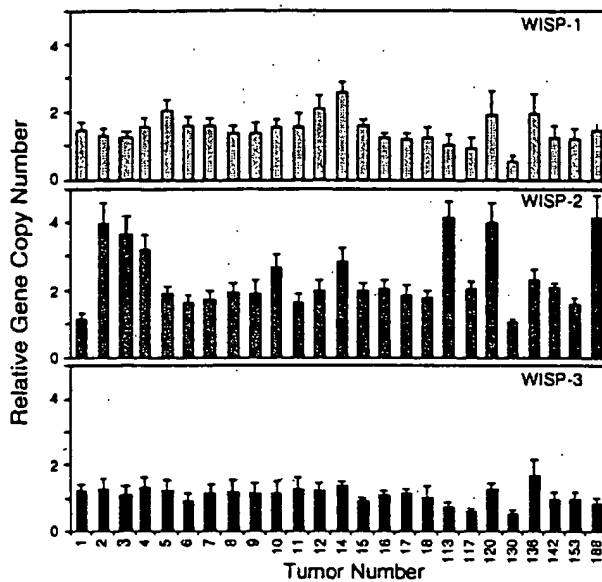
FIG. 6. Genomic amplification of *WISP* genes in human colon tumors. The relative gene copy number of the *WISP* genes in 25 adenocarcinomas was assayed by quantitative PCR, by comparing DNA from primary human tumors with pooled DNA from 10 healthy donors. The data are means ± SEM from one experiment done in triplicate. The experiment was repeated at least three times.

assessed by quantitative PCR (Fig. 7). The level of *WISP-1* RNA present in tumor tissue varied but was significantly increased (2- to >25-fold) in 84% (16/19) of the human colon tumors examined compared with normal adjacent mucosa. Four of 19 tumors showed greater than 10-fold overexpression. In contrast, in 79% (15/19) of the tumors examined, *WISP-2* RNA expression was significantly lower in the tumor than the mucosa. Similar to *WISP-1*, *WISP-3* RNA was overexpressed in 63% (12/19) of the colon tumors compared with the normal
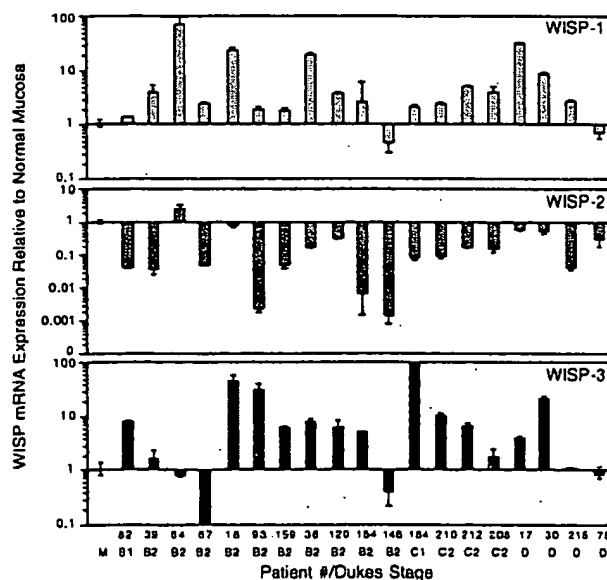

FIG. 7. *WISP* RNA expression in primary human colon tumors relative to expression in normal mucosa from the same patient. Expression of *WISP* mRNA in 19 adenocarcinomas was assayed by quantitative PCR. The Dukes stage of the tumor is listed under the sample number. The data are means ± SEM from one experiment done in triplicate. The experiment was repeated at least twice.

mucosa. The amount of overexpression of *WISP-3* ranged from 4- to >40-fold.

DISCUSSION

One approach to understanding the molecular basis of cancer is to identify differences in gene expression between cancer cells and normal cells. Strategies based on assumptions that steady-state mRNA levels will differ between normal and malignant cells have been used to clone differentially expressed genes (31). We have used a PCR-based selection strategy, SSH, to identify genes selectively expressed in C57MG mouse mammary epithelial cells transformed by Wnt-1.

Three of the genes isolated, *WISP-1*, *WISP-2*, and *WISP-3*, are members of the CCN family of growth factors, which includes CTGF, Cyr61, and *nov*, a family not previously linked to Wnt signaling.

Two independent experimental systems demonstrated that *WISP* induction was associated with the expression of Wnt-1. The first was C57MG cells infected with a Wnt-1 retroviral vector or C57MG cells expressing Wnt-1 under the control of a tetracyline-repressible promoter, and the second was in Wnt-1 transgenic mice, where breast tissue expresses Wnt-1, whereas normal breast tissue does not. No *WISP* RNA expression was detected in mammary tumors induced by polyoma virus middle T antigen (data not shown). These data suggest a link between Wnt-1 and *WISP*s in that in these two situations, *WISP* induction was correlated with Wnt-1 expression.

It is not clear whether the *WISP*s are directly or indirectly induced by the downstream components of the Wnt-1 signaling pathway (i.e., β-catenin-TCF-1/Lef1). The increased levels of *WISP* RNA were measured in Wnt-1-transformed cells, hours or days after Wnt-1 transformation. Thus, *WISP* expression could result from Wnt-1 signaling directly through β-catenin transcription factor regulation or alternatively through Wnt-1 signaling turning on a transcription factor, which in turn regulates *WISP*s.

The *WISP*s define an additional subfamily of the CCN family of growth factors. One striking difference observed in the protein sequence of WISP-2 is the absence of a CT domain, which is present in CTGF, Cyr61, *nov*, WISP-1, and WISP-3. This domain is thought to be involved in receptor binding and dimerization. Growth factors, such as TGF-β, platelet-derived growth factor, and nerve growth factor, which contain a cystine knot motif exist as dimers (32). It is tempting to speculate that WISP-1 and WISP-3 may exist as dimers, whereas WISP-2 exists as a monomer. If the CT domain is also important for receptor binding, WISP-2 may bind its receptor through a different region of the molecule than the other CCN family members. No specific receptors have been identified for CTGF or *nov*. A recent report has shown that integrin $\alpha_v\beta_3$ serves as an adhesion receptor for Cyr61 (33).

The strong expression of *WISP-1* and *WISP-2* in cells lying within the fibrovascular tumor stroma in breast tumors from Wnt-1 transgenic animals is consistent with previous observations that transcripts for the related CTGF gene are primarily expressed in the fibrous stroma of mammary tumors (34). Epithelial cells are thought to control the proliferation of connective tissue stroma in mammary tumors by a cascade of growth factor signals similar to that controlling connective tissue formation during wound repair. It has been proposed that mammary tumor cells or inflammatory cells at the tumor interstitial interface secrete TGF-β1, which is the stimulus for stromal proliferation (34). TGF-β1 is secreted by a large percentage of malignant breast tumors and may be one of the growth factors that stimulates the production of CTGF and WISPs in the stroma.

It was of interest that *WISP-1* and *WISP-2* expression was observed in the stromal cells that surrounded the tumor cells

(epithelial cells) in the Wnt-1 transgenic mouse sections of breast tissue. This finding suggests that paracrine signaling could occur in which the stromal cells could supply WISP-1 and WISP-2 to regulate tumor cell growth on the WISP extracellular matrix. Stromal cell-derived factors in the extracellular matrix have been postulated to play a role in tumor cell migration and proliferation (35). The localization of *WISP-1* and *WISP-2* in the stromal cells of breast tumors supports this paracrine model.

An analysis of *WISP-1* gene amplification and expression in human colon tumors showed a correlation between DNA amplification and overexpression, whereas overexpression of *WISP-3* RNA was seen in the absence of DNA amplification. In contrast, *WISP-2* DNA was amplified in the colon tumors, but its mRNA expression was significantly reduced in the majority of tumors compared with the expression in normal colonic mucosa from the same patient. The gene for human *WISP-2* was localized to chromosome 20q12–20q13, at a region frequently amplified and associated with poor prognosis in node negative breast cancer and many colon cancers, suggesting the existence of one or more oncogenes at this locus (36–38). Because the center of the 20q13 amplicon has not yet been identified, it is possible that the apparent amplification observed for *WISP-2* may be caused by another gene in this amplicon.

A recent manuscript on *rCop-1*, the rat orthologue of *WISP-2*, describes the loss of expression of this gene after cell transformation, suggesting it may be a negative regulator of growth in cell lines (16). Although the mechanism by which *WISP-2* RNA expression is down-regulated during malignant transformation is unknown, the reduced expression of *WISP-2* in colon tumors and cell lines suggests that it may function as a tumor suppressor. These results show that the *WISP* genes are aberrantly expressed in colon cancer and suggest that their altered expression may confer selective growth advantage to the tumor.

Members of the Wnt signaling pathway have been implicated in the pathogenesis of colon cancer, breast cancer, and melanoma, including the tumor suppressor gene adenomatous polyposis coli and β-catenin (39). Mutations in specific regions of either gene can cause the stabilization and accumulation of cytoplasmic β-catenin, which presumably contributes to human carcinogenesis through the activation of target genes such as the *WISPs*. Although the mechanism by which Wnt-1 transforms cells and induces tumorigenesis is unknown, the identification of *WISPs* as genes that may be regulated downstream of Wnt-1 in C57MG cells suggests they could be important mediators of Wnt-1 transformation. The amplification and altered expression patterns of the *WISPs* in human colon tumors may indicate an important role for these genes in tumor development.

1. Cadigan, K. M. & Nusse, R. (1997) *Genes Dev.* 11, 3286–3305.
2. Dale, T. C. (1998) *Biochem. J.* 329, 209–223.
3. Nusse, R. & Varmus, H. E. (1982) *Cell* 31, 99–109.
4. van Ooyen, A. & Nusse, R. (1984) *Cell* 39, 233–240.
5. Tsukamoto, A. S., Grosschedl, R., Guzman, R. C., Parslow, T. & Varmus, H. E. (1988) *Cell* 55, 619–625.
6. Brown, J. D. & Moon, R. T. (1998) *Curr. Opin. Cell. Biol.* 10, 182–187.
7. Molenaar, M., van de Wetering, M., Oosterwegel, M., Peterson-Maduro, J., Godsave, S., Korinek, V., Roose, J., Destree, O. & Clevers, H. (1996) *Cell* 86, 391–399.
8. Korinek, V., Barker, N., Willert, K., Molenaar, M., Roose, J., Wagenaar, G., Markman, M., Lamers, W., Destree, O. & Clevers, H. (1998) *Mol. Cell. Biol.* 18, 1248–1256.
9. Munemitsu, S., Albert, I., Souza, B., Rubinfeld, B. & Polakis, P. (1995) *Proc. Natl. Acad. Sci. USA* 92, 3046–3050.
10. He, T. C., Sparks, A. B., Rago, C., Hermeking, H., Zawel, L., da Costa, L. T., Morin, P. J., Vogelstein, B. & Kinzler, K. W. (1998) *Science* 281, 1509–1512.
11. Diatchenko, L., Lau, Y. F., Campbell, A. P., Chenchik, A., Moqadam, F., Huang, B., Lukyanov, S., Lukyanov, K., Gurskaya, N., Sverdlov, E. D. & Siebert, P. D. (1996) *Proc. Natl. Acad. Sci. USA* 93, 6025–6030.
12. Brown, A. M., Wildin, R. S., Prendergast, T. J. & Varmus, H. E. (1986) *Cell* 46, 1001–1009.
13. Wong, G. T., Gavin, B. J. & McMahon, A. P. (1994) *Mol. Cell. Biol.* 14, 6278–6286.
14. Shimizu, H., Julius, M. A., Giarre, M., Zheng, Z., Brown, A. M. & Kitajewski, J. (1997) *Cell Growth Differ.* 8, 1349–1358.
15. Hashimoto, Y., Shindo-Okada, N., Tani, M., Nagamachi, Y., Takeuchi, K., Shiroishi, T., Toma, H. & Yokota, J. (1998) *J. Exp. Med.* 187, 289–296.
16. Zhang, R., Averboukh, L., Zhu, W., Zhang, H., Jo, H., Dempsey, P. J., Coffey, R. J., Pardee, A. B. & Liang, P. (1998) *Mol. Cell. Biol.* 18, 6131–6141.
17. Grotendorst, G. R. (1997) *Cytokine Growth Factor Rev.* 8, 171–179.
18. Kireeva, M. L., Mo, F. E., Yang, G. P. & Lau, L. F. (1996) *Mol. Cell. Biol.* 16, 1326–1334.
19. Babic, A. M., Kireeva, M. L., Kolesnikova, T. V. & Lau, L. F. (1998) *Proc. Natl. Acad. Sci. USA* 95, 6355–6360.
20. Martinerie, C., Huff, V., Joubert, I., Badzioch, M., Saunders, G., Strong, L. & Perbal, B. (1994) *Oncogene* 9, 2729–2732.
21. Bork, P. (1993) *FEBS Lett.* 327, 125–130.
22. Kim, H. S., Nagalla, S. R., Oh, Y., Wilson, E., Roberts, C. T., Jr. & Rosenfeld, R. G. (1997) *Proc. Natl. Acad. Sci. USA* 94, 12981–12986.
23. Joliot, V., Martinerie, C., Dambrine, G., Plassiart, G., Brisac, M., Crochet, J. & Perbal, B. (1992) *Mol. Cell. Biol.* 12, 10–21.
24. Mancuso, D. J., Tuley, E. A., Westfield, L. A., Worrall, N. K., Shelton-Inloes, B. B., Sorace, J. M., Alevy, Y. G. & Sadler, J. E. (1989) *J. Biol. Chem.* 264, 19514–19527.
25. Holt, G. D., Pangburn, M. K. & Ginsburg, V. (1990) *J. Biol. Chem.* 265, 2852–2855.
26. Voorberg, J., Fontijn, R., Calafat, J., Janssen, H., van Mourik, J. A. & Pannekoek, H. (1991) *J. Cell. Biol.* 113, 195–205.
27. Martinerie, C., Viegas-Pequignot, E., Guenard, I., Dutrillaux, B., Nguyen, V. C., Bernheim, A. & Perbal, B. (1992) *Oncogene* 7, 2529–2534.
28. Takahashi, E., Hori, T., O'Connell, P., Leppert, M. & White, R. (1991) *Cytogenet. Cell. Genet.* 57, 109–111.
29. Meese, E., Meltzer, P. S., Witkowski, C. M. & Trent, J. M. (1989) *Genes Chromosomes Cancer* 1, 88–94.
30. Garte, S. J. (1993) *Crit. Rev. Oncog.* 4, 435–449.
31. Zhang, L., Zhou, W., Velculescu, V. E., Kern, S. E., Hruban, R. H., Hamilton, S. R., Vogelstein, B. & Kinzler, K. W. (1997) *Science* 276, 1268–1272.
32. Sun, P. D. & Davies, D. R. (1995) *Annu. Rev. Biophys. Biomol. Struct.* 24, 269–291.
33. Kireeva, M. L., Lam, S. C. T. & Lau, L. F. (1998) *J. Biol. Chem.* 273, 3090–3096.
34. Frazier, K. S. & Grotendorst, G. R. (1997) *Int. J. Biochem. Cell. Biol.* 29, 153–161.
35. Wernert, N. (1997) *Virchows Arch.* 430, 433–443.
36. Tanner, M. M., Tirkkonen, M., Kallioniemi, A., Collins, C., Stokke, T., Karhu, R., Kowbel, D., Shadravan, F., Hintz, M., Kuo, W. L., *et al.* (1994) *Cancer Res.* 54, 4257–4260.
37. Brinkmann, U., Gallo, M., Polymeropoulos, M. H. & Pastan, I. (1996) *Genome Res.* 6, 187–194.
38. Bischoff, J. R., Anderson, L., Zhu, Y., Mossie, K., Ng, L., Souza, B., Schryver, B., Flanagan, P., Clairvoyant, F., Ginther, C., *et al.* (1998) *EMBO J.* 17, 3052–3065.
39. Morin, P. J., Sparks, A. B., Korinek, V., Barker, N., Clevers, H., Vogelstein, B. & Kinzler, K. W. (1997) *Science* 275, 1787–1790.
40. Lu, L. H. & Gillett, N. (1994) *Cell Vision* 1, 169–176.

methods. Peptides AENK or AEQK were dissolved in water, made isotonic with NaCl and diluted into RPMI growth medium. T-cell-proliferation assays were done essentially as described[20,21]. Briefly, after antigen pulsing (30 μg ml⁻¹ TTCF) with tetrapeptides (1–2 mg ml⁻¹), PBMCs or EBV-B cells were washed in PBS and fixed for 45 s in 0.05% glutaraldehyde. Glycine was added to a final concentration of 0.1M and the cells were washed five times in RPMI 1640 medium containing 1% FCS before co-culture with T-cell clones in round-bottom 96-well microtitre plates. After 48 h, the cultures were pulsed with 1 μCi of ³H-thymidine and harvested for scintillation counting 16 h later. Predigestion of native TTCF was done by incubating 200 μg TTCF with 0.25 μg pig kidney legumain in 500 μl 50 mM citrate buffer, pH 5.5, for 1 h at 37 °C.

Glycopeptide digestions. The peptides HIDNEEDI, HIDN(N-glucosamine)EEDI and HIDNESDI, which are based on the TTCF sequence, and QQQHLFGSNVTDCSGNFCLFR(KKK), which is based on human transferrin, were obtained by custom synthesis. The three C-terminal lysine residues were added to the natural sequence to aid solubility. The transferrin glycopeptide QQQHLFGSNVTDCSGNFCLFR was prepared by tryptic (Promega) digestion of 5 mg reduced, carboxy-methylated human transferrin followed by concanavalin A chromatography[11]. Glycopeptides corresponding to residues 622–642 and 421–452 were isolated by reverse-phase HPLC and identified by mass spectrometry and N-terminal sequencing. The lyophilized transferrin-derived peptides were redissolved in 50 mM sodium acetate, pH 5.5, 10 mM dithiothreitol, 20% methanol. Digestions were performed for 3 h at 30 °C with 5–50 mU ml⁻¹ pig kidney legumain or B-cell AEP. Products were analysed by HPLC or MALDI-TOF mass spectrometry using a matrix of 10 mg ml⁻¹ α-cyanocinnamic acid in 50% acetonitrile/0.1% TFA and a PerSeptive Biosystems Elite STR mass spectrometer set to linear or reflector mode. Internal standardization was obtained with a matrix ion of 568.13 mass units.

1. Chen, J. M. et al. Cloning, isolation, and characterisation of mammalian legumain, an asparaginyl endopeptidase. J. Biol. Chem. 272, 8090–8098 (1997).
2. Kembhavi, A. A., Buttle, D. J., Knight, C. G. & Barrett, A. J. The two cysteine endopeptidases of legume seeds: purification and characterization by use of specific fluorometric assays. Arch. Biochem. Biophys. 303, 208–213 (1993).
3. Dalton, J. P., Hola Jamriska, L. & Bridley, P. J. Asparaginyl endopeptidase activity in adult Schistosoma mansoni. Parasitology 111, 575–580 (1995).
4. Bennett, K. et al. Antigen processing for presentation by class II major histocompatibility complex requires cleavage by cathespin E. Eur. J. Immunol. 22, 1519–1524 (1992).
5. Riese, R. J. et al. Essential role for cathepsin S in MHC class II-associated invariant chain processing and peptide loading. Immunity 4, 357–366 (1996).
6. Rodriguez, G. M. & Diment, S. Role of cathepsin D in antigen presentation of ovalbumin. J. Immunol. 149, 2894–2898 (1992).
7. Hewitt, E. W. et al. Natural processing sites for human cathepsin E and cathepsin D in tetanus toxin: implications for T cell epitope generation. J. Immunol. 159, 4693–4699 (1997).
8. Watts, C. Capture and processing of exogenous antigens for presentation on MHC molecules. Annu. Rev. Immunol. 15, 821–850 (1997).
9. Chapman, H. A. Endosomal proteases and MHC class II function. Curr. Opin. Immunol. 10, 93–102 (1998).
10. Fineschi, B. & Miller, J. Endosomal proteases and antigen processing. Trends Biochem. Sci. 22, 377–382 (1997).
11. Lu, J. & van Halbeek, H. Complete ¹H and ¹³C resonance assignments of a 21-amino acid glycopeptide prepared from human serum transferrin. Carbohydr. Res. 296, 1–21 (1996).
12. Fearon, D. T. & Locksley, R. M. The instructive role of innate immunity in the acquired immune response. Science 272, 50–54 (1996).
13. Medzhitov, R. & Janeway, C. A. J. Innate immunity: the virtues of a nonclonal system of recognition. Cell 91, 295–298 (1997).
14. Wyatt, R. et al. The antigenic structure of the HIV gp120 envelope glycoprotein. Nature 393, 705–711 (1998).
15. Botarelli, P. et al. N-glycosylation of HIV gp120 may constrain recognition by T lymphocytes. J. Immunol. 147, 3128–3132 (1991).
16. Davidson, H. W., West, M. A. & Watts, C. Endocytosis, intracellular trafficking, and processing of membrane IgG and monovalent antigen/membrane IgG complexes in B lymphocytes. J. Immunol. 144, 4101–4109 (1990).
17. Barrett, A. J. & Kirschke, H. Cathepsin B, cathepsin H and cathepsin L. Methods Enzymol. 80, 535–559 (1981).
18. Makoff, A. J., Ballantine, S. P., Smallwood, A. E. & Fairweather, N. F. Expression of tetanus toxin fragment C in E. coli: its purification and potential use as a vaccine. Biotechnology 7, 1043–1046 (1989).
19. Lane, D. P. & Harlow, E. Antibodies: A Laboratory Manual (Cold Spring Harbor Laboratory Press, 1988).
20. Lanzavecchia, A. Antigen-specific interaction between T and B cells. Nature 314, 537–539 (1985).
21. Pond, L. & Watts, C. Characterization of transport of newly assembled, T cell-stimulatory MHC class II-peptide complexes from MHC class II compartments to the cell surface. J. Immunol. 159, 543–553 (1997).

Genomic amplification of a decoy receptor for Fas ligand in lung and colon cancer

Robert M. Pitti*†, Scot A. Marsters*†, David A. Lawrence*†, Margaret Roy*, Frank C. Kischkel*, Patrick Dowd*, Arthur Huang*, Christopher J. Donahue*, Steven W. Sherwood*, Daryl T. Baldwin*, Paul J. Godowski*, William I. Wood*, Austin L. Gurney*, Kenneth J. Hillan*, Robert L. Cohen*, Audrey D. Goddard*, David Botstein‡ & Avi Ashkenazi*

* Departments of Molecular Oncology, Molecular Biology, and Immunology, Genentech Inc., 1 DNA Way, South San Francisco, California 94080, USA
‡ Department of Genetics, Stanford University, Stanford, California 94305, USA
† These authors contributed equally to this work

Fas ligand (FasL) is produced by activated T cells and natural killer cells and it induces apoptosis (programmed cell death) in target cells through the death receptor Fas/Apo1/CD95 (ref. 1). One important role of FasL and Fas is to mediate immune-cytotoxic killing of cells that are potentially harmful to the organism, such as virus-infected or tumour cells[1]. Here we report the discovery of a soluble decoy receptor, termed decoy receptor 3 (DcR3), that binds to FasL and inhibits FasL-induced apoptosis. The DcR3 gene was amplified in about half of 35 primary lung and colon tumours studied, and DcR3 messenger RNA was expressed in malignant tissue. Thus, certain tumours may escape FasL-dependent immune-cytotoxic attack by expressing a decoy receptor that blocks FasL.

By searching expressed sequence tag (EST) databases, we identified a set of related ESTs that showed homology to the tumour necrosis factor (TNF) receptor (TNFR) gene superfamily[2]. Using the overlapping sequence, we isolated a previously unknown full-length complementary DNA from human fetal lung. We named the protein encoded by this cDNA decoy receptor 3 (DcR3). The cDNA encodes a 300-amino-acid polypeptide that resembles members of the TNFR family (Fig. 1a): the amino terminus contains a leader sequence, which is followed by four tandem cysteine-rich domains (CRDs). Like one other TNFR homologue, osteoprotegerin (OPG)[3], DcR3 lacks an apparent transmembrane sequence, which indicates that it may be a secreted, rather than a membrane-asscociated, molecule. We expressed a recombinant, histidine-tagged form of DcR3 in mammalian cells; DcR3 was secreted into the cell culture medium, and migrated on polyacrylamide gels as a protein of relative molecular mass 35,000 (data not shown). DcR3 shares sequence identity in particular with OPG (31%) and TNFR2 (29%), and has relatively less homology with Fas (17%). All of the cysteines in the four CRDs of DcR3 and OPG are conserved; however, the carboxy-terminal portion of DcR3 is 101 residues shorter.

We analysed expression of DcR3 mRNA in human tissues by northern blotting (Fig. 1b). We detected a predominant 1.2-kilobase transcript in fetal lung, brain, and liver, and in adult spleen, colon and lung. In addition, we observed relatively high DcR3 mRNA expression in the human colon carcinoma cell line SW480.

To investigate potential ligand interactions of DcR3, we generated a recombinant, Fc-tagged DcR3 protein. We tested binding of DcR3–Fc to human 293 cells transfected with individual TNF-family ligands, which are expressed as type 2 transmembrane proteins (these transmembrane proteins have their N termini in the cytosol). DcR3–Fc showed a significant increase in binding to cells transfected with FasL[4] (Fig. 2a), but not to cells transfected with TNF[5], Apo2L/TRAIL[6,7], Apo3L/TWEAK[8,9], or OPGL/TRANCE/

RANKL[10-12] (data not shown). DcR3–Fc immunoprecipitated shed FasL from FasL-transfected 293 cells (Fig. 2b) and purified soluble FasL (Fig. 2c), as did the Fc-tagged ectodomain of Fas but not TNFR1. Gel-filtration chromatography showed that DcR3–Fc and soluble FasL formed a stable complex (Fig. 2d). Equilibrium analysis indicated that DcR3–Fc and Fas–Fc bound to soluble FasL with a comparable affinity ($K_d = 0.8 \pm 0.2$ and 1.1 ± 0.1 nM, respectively; Fig. 2e), and that DcR3–Fc could block nearly all of the binding of soluble FasL to Fas–Fc (Fig. 2e, inset). Thus, DcR3 competes with Fas for binding to FasL.

To determine whether binding of DcR3 inhibits FasL activity, we tested the effect of DcR3–Fc on apoptosis induction by soluble FasL in Jurkat T leukaemia cells, which express Fas (Fig. 3a). DcR3–Fc and Fas–Fc blocked soluble-FasL-induced apoptosis in a similar dose-dependent manner, with half-maximal inhibition at ~0.1 µg ml^{-1}. Time-course analysis showed that the inhibition did not merely delay cell death, but rather persisted for at least 24 hours (Fig. 3b). We also tested the effect of DcR3–Fc on activation-induced cell death (AICD) of mature T lymphocytes, a FasL-dependent process[1]. Consistent with previous results[13], activation of interleukin-2-stimulated CD4-positive T cells with anti-CD3 antibody increased the level of apoptosis twofold, and Fas–Fc blocked this effect substantially (Fig. 3c); DcR3–Fc blocked the

induction of apoptosis to a similar extent. Thus, DcR3 binding blocks apoptosis induction by FasL.

FasL-induced apoptosis is important in elimination of virus-infected cells and cancer cells by natural killer cells and cytotoxic T lymphocytes; an alternative mechanism involves perforin and granzymes[1,14-16]. Peripheral blood natural killer cells triggered marked cell death in Jurkat T leukaemia cells (Fig. 3d); DcR3–Fc and Fas–Fc each reduced killing of target cells from ~65% to ~30%, with half-maximal inhibition at ~1 µg ml^{-1}; the residual killing was probably mediated by the perforin/granzyme pathway. Thus, DcR3 binding blocks FasL-dependent natural killer cell activity. Higher DcR3–Fc and Fas–Fc concentrations were required to block natural killer cell activity compared with those required to block soluble FasL activity, which is consistent with the greater potency of membrane-associated FasL compared with soluble FasL[17].

Given the role of immune-cytotoxic cells in elimination of tumour cells and the fact that DcR3 can act as an inhibitor of FasL, we proposed that DcR3 expression might contribute to the ability of some tumours to escape immune-cytotoxic attack. As genomic amplification frequently contributes to tumorigenesis, we investigated whether the DcR3 gene is amplified in cancer. We analysed DcR3 gene-copy number by quantitative polymerase chain
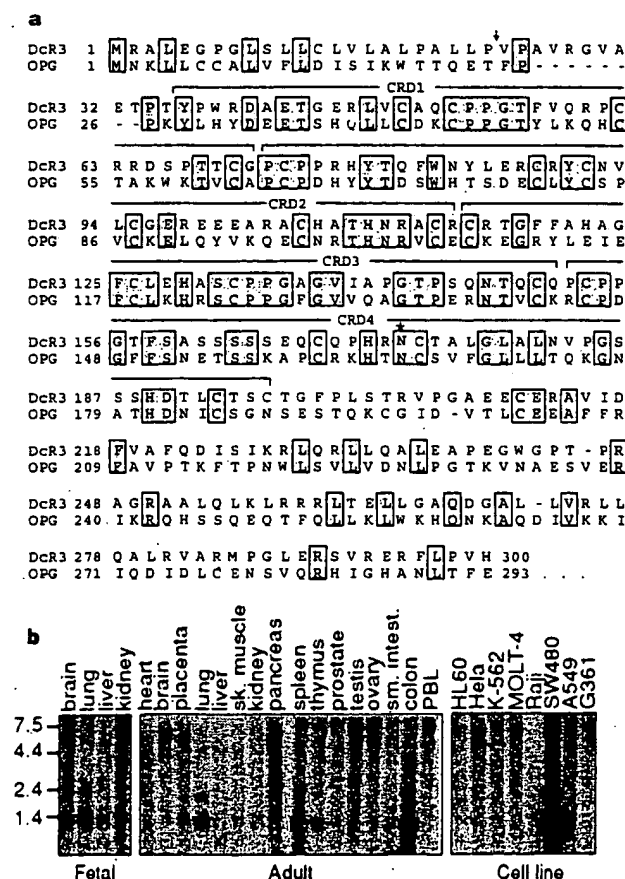

Figure 1 Primary structure and expression of human DcR3. a, Alignment of the amino-acid sequences of DcR3 and of osteoprotegerin (OPG); the C-terminal 101 residues of OPG are not shown. The putative signal cleavage site (arrow), the cysteine-rich domains (CRD 1–4), and the N-linked glycosylation site (asterisk) are shown. b, Expression of DcR3 mRNA. Northern hybridization analysis was done using the DcR3 cDNA as a probe and blots of poly(A)[+] RNA (Clontech) from human fetal and adult tissues or cancer cell lines. PBL, peripheral blood lymphocyte.
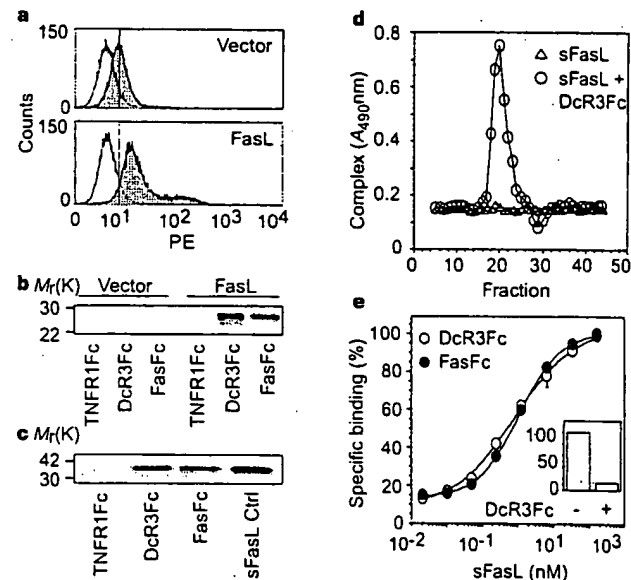

Figure 2 Interaction of DcR3 with FasL. a, 293 cells were transfected with pRK5 vector (top) or with pRK5 encoding full-length FasL (bottom), incubated with DcR3-Fc (solid line, shaded area), TNFR1-Fc (dotted line) or buffer control (dashed line) (the dashed and dotted lines overlap), and analysed for binding by FACS. Statistical analysis showed a significant difference ($P < 0.001$) between the binding of DcR3-Fc to cells transfected with FasL or pRK5. PE, phycoerythrin-labelled cells. b, 293 cells were transfected as in a and metabolically labelled, and cell supernatants were immunoprecipitated with Fc-tagged TNFR1, DcR3 or Fas. c, Purified soluble FasL (sFasL) was immunoprecipitated with TNFR1-Fc, DcR3-Fc or Fas-Fc and visualized by immunoblot with anti-FasL antibody. sFasL was loaded directly for comparison in the right-hand lane. d, Flag-tagged sFasL was incubated with DcR3-Fc or with buffer and resolved by gel filtration; column fractions were analysed in an assay that detects complexes containing DcR3-Fc and sFasL-Flag. e, Equilibrium binding of DcR3-Fc or Fas-Fc to sFasL-Flag. Inset, competition of DcR3-Fc with Fas-Fc for binding to sFasL-Flag.

reaction (PCR)[18] in genomic DNA from 35 primary lung and colon tumours, relative to pooled genomic DNA from peripheral blood leukocytes (PBLs) of 10 healthy donors. Eight of 18 lung tumours and 9 of 17 colon tumours showed DcR3 gene amplification, ranging from 2- to 18-fold (Fig. 4a, b). To confirm this result, we analysed the colon tumour DNAs with three more, independent sets of DcR3-based PCR primers and probes; we observed nearly the same amplification (data not shown).

We then analysed DcR3 mRNA expression in primary tumour tissue sections by in situ hybridization. We detected DcR3 expression in 6 out of 15 lung tumours, 2 out of 2 colon tumours, 2 out of 5 breast tumours, and 1 out of 1 gastric tumour (data not shown). A section through a squamous-cell carcinoma of the lung is shown in Fig. 4c. DcR3 mRNA was localized to infiltrating malignant epithelium, but was essentially absent from adjacent stroma, indicating tumour-specific expression. Although the individual tumour specimens that we analysed for mRNA expression and gene amplification were different, the in situ hybridization results are consistent with the finding that the DcR3 gene is amplified frequently in tumours. SW480 colon carcinoma cells, which showed abundant DcR3 mRNA expression (Fig. 1b), also had marked DcR3 gene amplification, as shown by quantitative PCR (fourfold) and by Southern blot hybridization (fivefold) (data not shown).

If DcR3 amplification in cancer is functionally relevant, then DcR3 should be amplified more than neighbouring genomic regions that are not important for tumour survival. To test this, we mapped the human DcR3 gene by radiation-hybrid analysis; DcR3 showed linkage to marker AFM218xe7 (T160), which maps to chromosome position 20q13. Next, we isolated from a bacterial artificial chromosome (BAC) library a human genomic clone that carries DcR3, and sequenced the ends of the clone's insert. We then determined, from the nine colon tumours that showed twofold or greater amplification of DcR3, the copy number of the DcR3-flanking sequences (reverse and forward) from the BAC, and of seven genomic markers that span chromosome 20 (Fig. 4d). The DcR3-linked reverse marker showed an average amplification of roughly threefold, slightly less than the approximately fourfold amplification of DcR3; the other markers showed little or no amplification. These data indicate that DcR3 may be at the 'epicentre' of a distal chromosome 20 region that is amplified in colon cancer, consistent with the possibility that DcR3 amplification promotes tumour survival.

Our results show that DcR3 binds specifically to FasL and inhibits FasL activity. We did not detect DcR3 binding to several other TNF-ligand-family members; however, this does not rule out the possibility that DcR3 interacts with other ligands, as do some other TNFR family members, including OPG[2,19].

FasL is important in regulating the immune response; however, little is known about how FasL function is controlled. One mechanism involves the molecule cFLIP, which modulates apoptosis signalling downstream of Fas[20]. A second mechanism involves proteolytic shedding of FasL from the cell surface[17]. DcR3 competes with Fas for
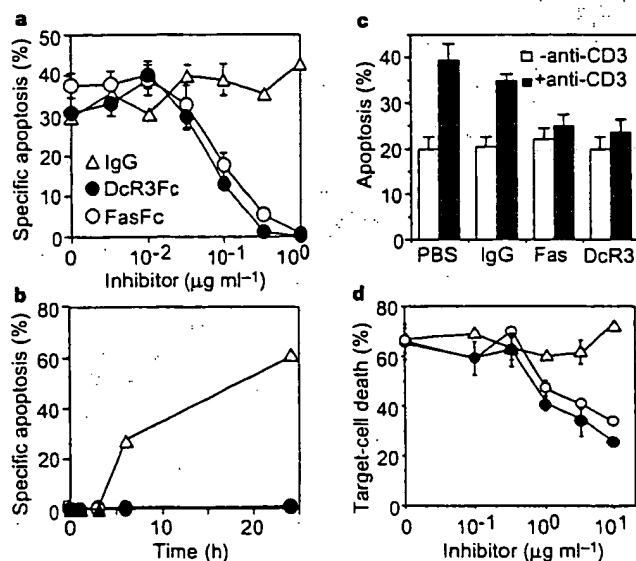

Figure 3 Inhibition of FasL activity by DcR3. a, Human Jurkat T leukaemia cells were incubated with Flag-tagged soluble FasL (sFasL; 5 ng ml^{-1}) oligomerized with anti-Flag antibody (0.1 μg ml^{-1}) in the presence of the proposed inhibitors DcR3-Fc, Fas-Fc or human IgG1 and assayed for apoptosis (mean ± s.e.m. of triplicates). b, Jurkat cells were incubated with sFasL-Flag plus anti-Flag antibody as in a, in presence of 1 μg ml^{-1} DcR3-Fc (filled circles), Fas-Fc (open circles) or human IgG1 (triangles), and apoptosis was determined at the indicated time points. c, Peripheral blood T cells were stimulated with PHA and interleukin-2, followed by control (white bars) or anti-CD3 antibody (filled bars), together with phosphate-buffered saline (PBS), human IgG1, Fas-Fc, or DcR3-Fc (10 μg ml^{-1}). After 16 h, apoptosis of CD4* cells was determined (mean ± s.e.m. of results from five donors). d, Peripheral blood natural killer cells were incubated with ^{51}Cr-labelled Jurkat cells in the presence of DcR3-Fc (filled circles), Fas-Fc (open circles) or human IgG1 (triangles), and target-cell death was determined by release of [51]Cr (mean ± s.d. for two donors, each in triplicate).
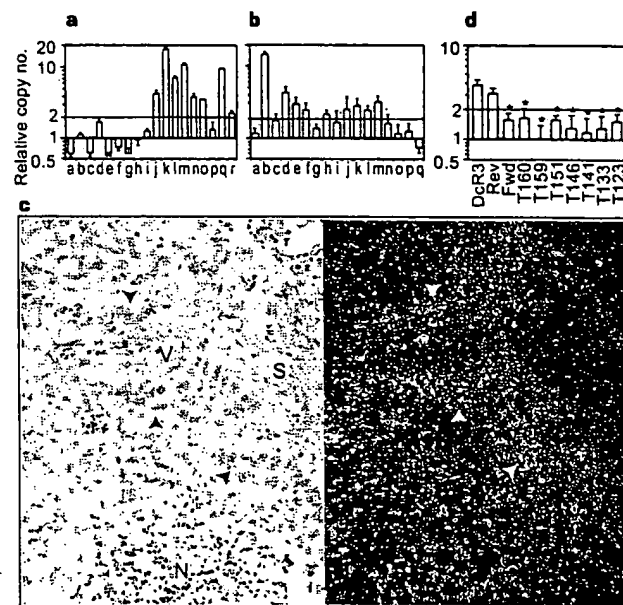
Figure 4 Genomic amplification of DcR3 in tumours. a, Lung cancers, comprising eight adenocarcinomas (c, d, f, g, h, j, k, r), seven squamous-cell carcinomas (a, e, m, n, o, p, q), one non-small-cell carcinoma (b), one small-cell carcinoma (i), and one bronchial adenocarcinoma (l). The data are means ± s.d. of 2 experiments done in duplicate. b, Colon tumours, comprising 17 adenocarcinomas. Data are means ± s.e.m. of five experiments done in duplicate. c, In situ hybridization analysis of DcR3 mRNA expression in a squamous-cell carcinoma of the lung. A representative bright-field image (left) and the corresponding dark-field image (right) show DcR3 mRNA over infiltrating malignant epithelium (arrowheads). Adjacent non-malignant stroma (S), blood vessel (V) and necrotic tumour tissue (N) are also shown. d, Average amplification of DcR3 compared with amplification of neighbouring genomic regions (reverse and forward, Rev and Fwd), the DcR3-linked marker T160, and other chromosome-20 markers, in the nine colon tumours showing DcR3 amplification of twofold or more (b). Data are from two experiments done in duplicate. Asterisk indicates P < 0.01 for a Student's t-test comparing each marker with DcR3.

FasL binding; hence, it may represent a third mechanism of extracellular regulation of FasL activity. A decoy receptor that modulates the function of the cytokine interleukin-1 has been described[21]. In addition, two decoy receptors that belong to the TNFR family, DcR1 and DcR2, regulate the FasL-related apoptosis-inducing molecule Apo2L[22]. Unlike DcR1 and DcR2, which are membrane-associated proteins, DcR3 is directly secreted into the extracellular space. One other secreted TNFR-family member is OPG[3], which shares greater sequence homology with DcR3 (31%) than do DcR1 (17%) or DcR2 (19%); OPG functions as a third decoy for Apo2L[19]. Thus, DcR3 and OPG define a new subset of TNFR-family members that function as secreted decoys to modulate ligands that induce apoptosis. Pox viruses produce soluble TNFR homologues that neutralize specific TNF-family ligands, thereby modulating the antiviral immune response[2]. Our results indicate that a similar mechanism, namely, production of a soluble decoy receptor for FasL, may contribute to immune evasion by certain tumours.   □

Methods

Isolation of DcR3 cDNA. Several overlapping ESTs in GenBank (accession numbers AA025672, AA025673 and W67560) and in Lifeseq™ (Incyte Pharmaceuticals; accession numbers 1339238, 1533571, 1533650, 1542861, 1789372 and 2207027) showed similarity to members of the TNFR family. We screened human cDNA libraries by PCR with primers based on the region of EST consensus; fetal lung was positive for a product of the expected size. By hybridization to a PCR-generated probe based on the ESTs, one positive clone (DNA30942) was identified. When searching for potential alternatively spliced forms of DcR3 that might encode a transmembrane protein, we isolated 50 more clones; the coding regions of these clones were identical in size to that of the initial clone (data not shown).

Fc-fusion proteins (immunoadhesins). The entire DcR3 sequence, or the ectodomain of Fas or TNFR1, was fused to the hinge and Fc region of human IgG1, expressed in insect SF9 cells or in human 293 cells, and purified as described[23].

Fluorescence-activated cell sorting (FACS) analysis. We transfected 293 cells using calcium phosphate or Effectene (Qiagen) with pRK5 vector or pRK5 encoding full-length human FasL[4] (2 μg), together with pRK5 encoding CrmA (2 μg) to prevent cell death. After 16 h, the cells were incubated with biotinylated DcR3–Fc or TNFR1–Fc and then with phycoerythrin-conjugated streptavidin (GibcoBRL), and were assayed by FACS. The data were analysed by Kolmogorov–Smirnov statistical analysis. There was some detectable staining of vector-transfected cells by DcR3–Fc; as these cells express little FasL (data not shown), it is possible that DcR3 recognized some other factor that is expressed constitutively on 293 cells.

Immunoprecipitation. Human 293 cells were transfected as above, and metabolically labelled with [35S]cysteine and [35S]methionine (0.5 mCi; Amersham). After 16 h of culture in the presence of z-VAD-fmk (10 μM), the medium was immunoprecipitated with DcR3–Fc, Fas–Fc or TNFR1–Fc (5 μg), followed by protein A–Sepharose (Repligen). The precipitates were resolved by SDS–PAGE and visualized on a phosphorimager (Fuji BAS2000). Alternatively, purified, Flag-tagged soluble FasL (1 μg) (Alexis) was incubated with each Fc-fusion protein (1 μg), precipitated with protein A–Sepharose, resolved by SDS–PAGE and visualized by immunoblotting with rabbit anti-FasL antibody (Oncogene Research).

Analysis of complex formation. Flag-tagged soluble FasL (25 μg) was incubated with buffer or with DcR3–Fc (40 μg) for 1.5 h at 24 °C. The reaction was loaded onto a Superdex 200 HR 10/30 column (Pharmacia) and developed with PBS; 0.6-ml fractions were collected. The presence of DcR3–Fc–FasL complex in each fraction was analysed by placing 100 μl aliquots into microtitre wells precoated with anti-human IgG (Boehringer) to capture DcR3–Fc, followed by detection with biotinylated anti-Flag antibody Bio M2 (Kodak) and streptavidin–horseradish peroxidase (Amersham). Calibration of the column indicated an apparent relative molecular mass of the complex of 420K (data not shown), which is consistent with a stoichiometry of two DcR3–Fc homodimers to two soluble FasL homotrimers.

Equilibrium binding analysis. Microtitre wells were coated with anti-human

IgG, blocked with 2% BSA in PBS. DcR3–Fc or Fas–Fc was added, followed by serially diluted Flag-tagged soluble FasL. Bound ligand was detected with anti-Flag antibody as above. In the competition assay, Fas–Fc was immobilized as above; and the wells were blocked with excess IgG1 before addition of Flag-tagged soluble FasL plus DcR3–Fc.

T-cell AICD. CD3+ lymphocytes were isolated from peripheral blood of individual donors using anti-CD3 magnetic beads (Miltenyi Biotech), stimulated with phytohaemagglutinin (PHA; 2 μg ml^{-1}) for 24 h, and cultured in the presence of interleukin-2 (100 U ml^{-1}) for 5 days. The cells were plated in wells coated with anti-CD3 antibody (Pharmingen) and analysed for apoptosis 16 h later by FACS analysis of annexin-V-binding of CD4+ cells[24].

Natural killer cell activity. Natural killer cells were isolated from peripheral blood of individual donors using anti-CD56 magnetic beads (Miltenyi Biotech), and incubated for 16 h with ^{51}Cr-loaded Jurkat cells at an effector-to-target ratio of 1:1 in the presence of DcR3–Fc, Fas–Fc or human IgG1. Target-cell death was determined by release of ^{51}Cr in effector–target co-cultures relative to release of ^{51}Cr by detergent lysis of equal numbers of Jurkat cells.

Gene-amplification analysis. Surgical specimens were provided by J. Kern (lung tumours) and P. Quirke (colon tumours). Genomic DNA was extracted (Qiagen) and the concentration was determined using Hoechst dye 33258 intercalation fluorometry. Amplification was determined by quantitative PCR[18] using a TaqMan instrument (ABI). The method was validated by comparison of PCR and Southern hybridization data for the Myc and HER-2 oncogenes (data not shown). Gene-specific primers and fluorogenic probes were designed on the basis of the sequence of DcR3 or of nearby regions identified on a BAC carrying the human DcR3 gene; alternatively, primers and probes were based on Stanford Human Genome Center marker AFM218xe7 (T160), which is linked to DcR3 (likelihood score = 5.4), SHGC-36268 (T159), the nearest available marker which maps to ~500 kilobases from T160, and five extra markers that span chromosome 20. The DcR3-specific primer sequences were 5′-CTTCTTCGCGCACGCTG-3′ and 5′-ATCACGCCGGCACCAG-3′ and the fluorogenic probe sequence was 5′-(FAM-ACACGATGCGTGCTCCAAGCAG AAp-(TAMARA), where FAM is 5′-fluorescein phosphoramidite. Relative gene-copy numbers were derived using the formula $2^{(\Delta CT)}$, where ΔCT is the difference in amplification cycles required to detect DcR3 in peripheral blood lymphocyte DNA compared to test DNA.

1. Nagata, S. Apoptosis by death factor. *Cell* 88, 355–365 (1997).
2. Smith, C. A., Farrah, T. & Goodwin, R. G. The TNF receptor superfamily of cellular and viral proteins: activation, costimulation, and death. *Cell* 76, 959–962 (1994).
3. Simonet, W. S. et al. Osteoprotegerin: a novel secreted protein involved in the regulation of bone density. *Cell* 89, 309–319 (1997).
4. Suda, T., Takahashi, T., Golstein, P. & Nagata, S. Molecular cloning and expression of Fas ligand, a novel member of the TNF family. *Cell* 75, 1169–1178 (1993).
5. Pennica, D. et al. Human tumour necrosis factor: precursor structure, expression and homology to lymphotoxin. *Nature* 312, 724–729 (1984).
6. Pitti, R. M. et al. Induction of apoptosis by Apo-2 ligand, a new member of the tumor necrosis factor receptor family. *J. Biol. Chem.* 271, 12687–12690 (1996).
7. Wiley, S. R. et al. Identification and characterization of a new member of the TNF family that induces apoptosis. *Immunity* 3, 673–682 (1995).
8. Marsters, S. A. et al. Identification of a ligand for the death-domain-containing receptor Apo3. *Curr. Biol.* 8, 525–528 (1998).
9. Chicheportiche, Y. et al. TWEAK, a new secreted ligand in the TNF family that weakly induces apoptosis. *J. Biol. Chem.* 272, 32401–32410 (1997).
10. Wong, B. R. et al. TRANCE is a novel ligand of the TNFR family that activates c-Jun-N-terminal kinase in T cells. *J. Biol. Chem.* 272, 25190–25194 (1997).
11. Anderson, D. M. et al. A homolog of the TNF receptor and its ligand enhance T-cell growth and dendritic-cell function. *Nature* 390, 175–179 (1997).
12. Lacey, D. L. et al. Osteoprotegerin ligand is a cytokine that regulates osteoclast differentiation and activation. *Cell* 93, 165–176 (1998).
13. Dhein, J., Walczak, H., Baumler, C., Debatin, K. M. & Krammer, P. H. Autocrine T-cell suicide mediated by Apo1/(Fas/CD95). *Nature* 373, 438–441 (1995).
14. Arase, H., Arase, N. & Saito, T. Fas-mediated cytotoxicity by freshly isolated natural killer cells. *J. Exp. Med.* 181, 1235–1238 (1995).
15. Medvedev, A. E. et al. Regulation of Fas and Fas ligand expression in NK cells by cytokines and the involvement of Fas ligand in NK/LAK cell-mediated cytotoxicity. *Cytokine* 9, 394–404 (1997).
16. Moretta, A. Mechanisms in cell-mediated cytotoxicity. *Cell* 90, 13–18 (1997).
17. Tanaka, M., Itai, T., Adachi, M. & Nagata, S. Downregualtion of Fas ligand by shedding. *Nature Med.* 4, 31–36 (1998).
18. Gelmini, S. et al. Quantitative PCR-based homogeneous assay with fluorogenic probes to measure c-erbB-2 oncogene amplification. *Clin. Chem.* 43, 752–758 (1997).
19. Emery, J. G. et al. Osteoprotegerin is a receptor for the cytotoxic ligand TRAIL. *J. Biol. Chem.* 273, 14363–14367 (1998).
20. Wallach, D. Placing death under control. *Nature* 388, 123–125 (1997).
21. Collota, F. et al. Interleukin-1 type II receptor: a decoy target for IL-1 that is regulated by IL-4. *Science* 261, 472–475 (1993).

22. Ashkenazi, A. & Dixit, V. M. Death receptors: signaling and modulation. *Science* 281, 1305–1308 (1998).
23. Ashkenazi, A. & Chamow, S. M. Immunoadhesins as research tools and therapeutic agents. *Curr. Opin. Immunol.* 9, 195–200 (1997).
24. Marsten, S. *et al.* Activation of apoptosis by Apo-2 ligand is independent of FADD but blocked by CrmA. *Curr. Biol.* 6, 750–752 (1996).

Crystal structure of the ATP-binding subunit of an ABC transporter

Li-Wei Hung*, Iris Xiaoyan Wang†, Kishiko Nikaido†, Pei-Qi Liu†, Giovanna Ferro-Luzzi Ames† & Sung-Hou Kim*‡

* E. O. Lawrence Berkeley National Laboratory, † Department of Molecular and Cell Biology, and ‡ Department of Chemistry, University of California at Berkeley, Berkeley, California 94720, USA

ABC transporters (also known as traffic ATPases) form a large family of proteins responsible for the translocation of a variety of compounds across membranes of both prokaryotes and eukaryotes[1]. The recently completed *Escherichia coli* genome sequence revealed that the largest family of paralogous *E. coli* proteins is composed of ABC transporters[2]. Many eukaryotic proteins of medical significance belong to this family, such as the cystic fibrosis transmembrane conductance regulator (CFTR), the P-glycoprotein (or multidrug-resistance protein) and the heterodimeric transporter associated with antigen processing (Tap1–Tap2). Here we report the crystal structure at 1.5 Å resolution of HisP, the ATP-binding subunit of the histidine permease, which is an ABC transporter from *Salmonella typhimurium*. We correlate the details of this structure with the biochemical, genetic and biophysical properties of the wild-type and several mutant HisP proteins. The structure provides a basis for understanding properties of ABC transporters and of defective CFTR proteins.

ABC transporters contain four structural domains: two nucleotide-binding domains (NBDs), which are highly conserved throughout the family, and two transmembrane domains[1]. In prokaryotes these domains are often separate subunits which are assembled into a membrane-bound complex; in eukaryotes the domains are generally fused into a single polypeptide chain. The periplasmic histidine permease of *S. typhimurium* and *E. coli*[1,3–8] is a well-characterized ABC transporter that is a good model for this superfamily. It consists of a membrane-bound complex, HisQMP$_2$, which comprises integral membrane subunits, HisQ and HisM, and two copies of HisP, the ATP-binding subunit. HisP, which has properties intermediate between those of integral and peripheral membrane proteins[9], is accessible from both sides of the membrane, presumably by its interaction with HisQ and HisM[6]. The two HisP subunits form a dimer, as shown by their cooperativity in ATP hydrolysis[5], the requirement for both subunits to be present for activity[8], and the formation of a HisP dimer upon chemical cross-linking. Soluble HisP also forms a dimer[3]. HisP has been purified and characterized in an active soluble form[3] which can be reconstituted into a fully active membrane-bound complex[8].

The overall shape of the crystal structure of the HisP monomer is that of an 'L' with two thick arms (arm I and arm II); the ATP-binding pocket is near the end of arm I (Fig. 1). A six-stranded β-sheet (β3 and β8–β12) spans both arms of the L, with a domain of a α- plus β-type structure (β1, β2, β4–β7, α1 and α2) on one side (within arm I) and a domain of mostly α-helices (α3–α9) on the
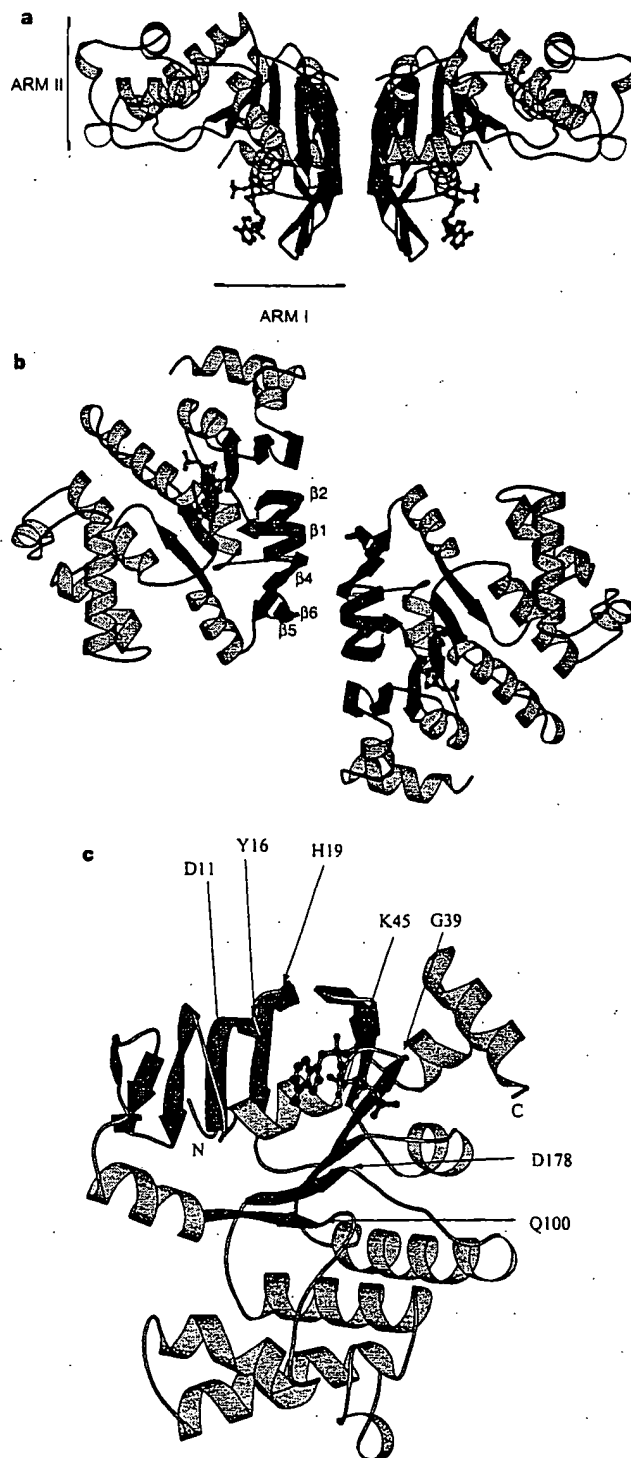
Figure 1 Crystal structure of HisP. a, View of the dimer along an axis perpendicular to its two-fold axis. The top and bottom of the dimer are suggested to face towards the periplasmic and cytoplasmic sides, respectively (see text). The thickness of arm II is about 25 Å, comparable to that of membrane. α-Helices are shown in orange and β-sheets in green. b, View along the two-fold axis of the HisP dimer, showing the relative displacement of the monomers not apparent in a. The β-strands at the dimer interface are labelled. c, View of one monomer from the bottom of arm I, as shown in a, towards arm II, showing the ATP-binding pocket. a–c, The protein and the bound ATP are in 'ribbon' and 'ball-and-stick' representations, respectively. Key residues discussed in the text are indicated in c. These figures were prepared with MOLSCRIPT[20]. N, amino terminus; C, C terminus.

NOVEL APPROACH TO QUANTITATIVE POLYMERASE CHAIN REACTION USING REAL-TIME DETECTION: APPLICATION TO THE DETECTION OF GENE AMPLIFICATION IN BREAST CANCER

Ivan Bièche[1,2], Martine Olivi[1], Marie-Hélène Champème[2], Dominique Vidaud[1], Rosette Lidereau[2] and Michel Vidaud[1]*

[1]*Laboratoire de Génétique Moléculaire, Faculté des Sciences Pharmaceutiques et Biologiques de Paris, Paris, France*
[2]*Laboratoire d'Oncogénétique, Centre René Huguenin, St-Cloud, France*

Gene amplification is a common event in the progression of human cancers, and amplified oncogenes have been shown to have diagnostic, prognostic and therapeutic relevance. A kinetic quantitative polymerase-chain-reaction (PCR) method, based on fluorescent TaqMan methodology and a new instrument (ABI Prism 7700 Sequence Detection System) capable of measuring fluorescence in real-time, was used to quantify gene amplification in tumor DNA. Reactions are characterized by the point during cycling when PCR amplification is still in the exponential phase, rather than the amount of PCR product accumulated after a fixed number of cycles. None of the reaction components is limited during the exponential phase, meaning that values are highly reproducible in reactions starting with the same copy number. This greatly improves the precision of DNA quantification. Moreover, real-time PCR does not require post-PCR sample handling, thereby preventing potential PCR-product carry-over contamination; it possesses a wide dynamic range of quantification and results in much faster and higher sample throughput. The real-time PCR method, was used to develop and validate a simple and rapid assay for the detection and quantification of the 3 most frequently amplified genes (*myc*, *ccnd1* and *erbB2*) in breast tumors. Extra copies of *myc*, *ccnd1* and *erbB2* were observed in 10, 23 and 15%, respectively, of 108 breast-tumor DNA; the largest observed numbers of gene copies were 4.6, 18.6 and 15.1, respectively. These results correlated well with those of Southern blotting. The use of this new semi-automated technique will make molecular analysis of human cancers simpler and more reliable, and should find broad applications in clinical and research settings. *Int. J. Cancer* 78:661–666, 1998.
© 1998 Wiley-Liss, Inc.

Gene amplification plays an important role in the pathogenesis of various solid tumors, including breast cancer, probably because over-expression of the amplified target genes confers a selective advantage. The first technique used to detect genomic amplification was cytogenetic analysis. Amplification of several chromosome regions, visualized either as extrachromosomal double minutes (dmins) or as integrated homogeneously staining regions (HSRs), are among the main visible cytogenetic abnormalities in breast tumors. Other techniques such as comparative genomic hybridization (CGH) (Kallioniemi *et al.*, 1994) have also been used in broad searches for regions of increased DNA copy numbers in tumor cells, and have revealed some 20 amplified chromosome regions in breast tumors. Positional cloning efforts are underway to identify the critical gene(s) in each amplified region. To date, genes known to be amplified frequently in breast cancers include *myc* (8q24), *ccnd1* (11q13), and *erbB2* (17q12-q21) (for review, see Bièche and Lidereau, 1995).

Amplification of the *myc*, *ccnd1*, and *erbB2* proto-oncogenes should have clinical relevance in breast cancer, since independent studies have shown that these alterations can be used to identify sub-populations with a worse prognosis (Berns *et al.*, 1992; Schuuring *et al.*, 1992; Slamon *et al.*, 1987). Muss *et al.* (1994) suggested that these gene alterations may also be useful for the prediction and assessment of the efficacy of adjuvant chemotherapy and hormone therapy.

However, published results diverge both in terms of the frequency of these alterations and their clinical value. For instance, over 500 studies in 10 years have failed to resolve the controversy surrounding the link suggested by Slamon *et al.* (1987) between *erbB2* amplification and disease progression. These discrepancies are partly due to the clinical, histological and ethnic heterogeneity of breast cancer, but technical considerations are also probably involved.

Specific genes (DNA) were initially quantified in tumor cells by means of blotting procedures such as Southern and slot blotting. These batch techniques require large amounts of DNA (5–10 µg/reaction) to yield reliable quantitative results. Furthermore, meticulous care is required at all stages of the procedures to generate blots of sufficient quality for reliable dosage analysis. Recently, PCR has proven to be a powerful tool for quantitative DNA analysis, especially with minimal starting quantities of tumor samples (small, early-stage tumors and formalin-fixed, paraffin-embedded tissues).

Quantitative PCR can be performed by evaluating the amount of product either after a given number of cycles (end-point quantitative PCR) or after a varying number of cycles during the exponential phase (kinetic quantitative PCR). In the first case, an internal standard distinct from the target molecule is required to ascertain PCR efficiency. The method is relatively easy but implies generating, quantifying and storing an internal standard for each gene studied. Nevertheless, it is the most frequently applied method to date.

One of the major advantages of the kinetic method is its rapidity in quantifying a new gene, since no internal standard is required (an external standard curve is sufficient). Moreover, the kinetic method has a wide dynamic range (at least 5 orders of magnitude), giving an accurate value for samples differing in their copy number. Unfortunately, the method is cumbersome and has therefore been rarely used. It involves aliquot sampling of each assay mix at regular intervals and quantifying, for each aliquot, the amplification product. Interest in the kinetic method has been stimulated by a novel approach using fluorescent TaqMan methodology and a new instrument (ABI Prism 7700 Sequence Detection System) capable of measuring fluorescence in real time (Gibson *et al.*, 1996; Heid *et al.*, 1996). The TaqMan reaction is based on the 5′ nuclease assay first described by Holland *et al.* (1991). The latter uses the 5′ nuclease activity of Taq polymerase to cleave a specific fluorogenic oligonucleotide probe during the extension phase of PCR. The approach uses dual-labeled fluorogenic hybridization probes (Lee *et al.*, 1993). One fluorescent dye, co-valently linked to the 5′ end of the oligonucleotide, serves as a reporter [FAM (*i.e.*, 6-carboxyfluorescein)] and its emission spectrum is quenched by a second fluorescent dye, TAMRA (*i.e.*, 6-carboxy-tetramethyl-rhodamine) attached to the 3′ end. During the extension phase of the PCR

*Correspondence to: Laboratoire de Génétique Moléculaire, Faculté des Sciences Pharmaceutiques et Biologiques de Paris, 4 Avenue de l'Observatoire, F-75006 Paris, France. Fax: (33)1-4407-1754. E-mail: mvidaud@teaser.fr

cycle, the fluorescent hybridization probe is hydrolyzed by the 5'-3' nucleolytic activity of DNA polymerase. Nuclease degradation of the probe releases the quenching of FAM fluorescence emission, resulting in an increase in peak fluorescence emission. The fluorescence signal is normalized by dividing the emission intensity of the reporter dye (FAM) by the emission intensity of a reference dye (*i.e.*, ROX, 6-carboxy-X-rhodamine) included in TaqMan buffer, to obtain a ratio defined as the Rn (normalized reporter) for a given reaction tube. The use of a sequence detector enables the fluorescence spectra of all 96 wells of the thermal cycler to be measured continuously during PCR amplification.

The real-time PCR method offers several advantages over other current quantitative PCR methods (Celi *et al.*, 1994): *(i)* the probe-based homogeneous assay provides a real-time method for detecting only specific amplification products, since specific hybridation of both the primers and the probe is necessary to generate a signal; *(ii)* the C_t (threshold cycle) value used for quantification is measured when PCR amplification is still in the log phase of PCR product accumulation. This is the main reason why C_t is a more reliable measure of the starting copy number than are end-point measurements, in which a slight difference in a limiting component can have a drastic effect on the amount of product; *(iii)* use of C_t values gives a wider dynamic range (at least 5 orders of magnitude), reducing the need for serial dilution; *(iv)* The real-time PCR method is run in a closed-tube system and requires no post-PCR sample handling, thus avoiding potential contamination; *(v)* the system is highly automated, since the instrument continuously measures fluorescence in all 96 wells of the thermal cycler during PCR amplification and the corresponding software processes, and analyzes the fluorescence data; *(vi)* the assay is rapid, as results are available just one minute after thermal cycling is complete; *(vii)* the sample throughput of the method is high, since 96 reactions can be analyzed in 2 hr.

Here, we applied this semi-automated procedure to determine the copy numbers of the 3 most frequently amplified genes in breast tumors (*myc, ccnd1* and *erb*B2), as well as 2 genes (*alb* and *app*) located in a chromosome region in which no genetic changes have been observed in breast tumors. The results for 108 breast tumors were compared with previous Southern-blot data for the same samples.

MATERIAL AND METHODS

Tumor and blood samples

Samples were obtained from 108 primary breast tumors removed surgically from patients at the Centre René Huguenin; none of the patients had undergone radiotherapy or chemotherapy. Immediately after surgery, the tumor samples were placed in liquid nitrogen until extraction of high-molecular-weight DNA. Patients were included in this study if the tumor sample used for DNA preparation contained more than 60% of tumor cells (histological analysis). A blood sample was also taken from 18 of the same patients.

DNA was extracted from tumor tissue and blood leukocytes according to standard methods.

Real-time PCR

Theoretical basis. Reactions are characterized by the point during cycling when amplification of the PCR product is first detected, rather than by the amount of PCR product accumulated after a fixed number of cycles. The higher the starting copy number of the genomic DNA target, the earlier a significant increase in fluorescence is observed. The parameter C_t (threshold cycle) is defined as the fractional cycle number at which the fluorescence generated by cleavage of the probe passes a fixed threshold above baseline. The target gene copy number in unknown samples is quantified by measuring C_t and by using a standard curve to determine the starting copy number. The precise amount of genomic DNA (based on optical density) and its quality (*i.e.*, lack

of extensive degradation) are both difficult to assess. We therefore also quantified a control gene *(alb)* mapping to chromosome region 4q11-q13. in which no genetic alterations have been found in breast-tumor DNA by means of CGH (Kallioniemi *et al.*, 1994).

Thus, the ratio of the copy number of the target gene to the copy number of the *alb* gene normalizes the amount and quality of genomic DNA. The ratio defining the level of amplification is termed "N", and is determined as follows:

$$N = \frac{\text{copy number of target gene } (app, myc, ccnd1, erbB2)}{\text{copy number of reference gene } (alb)}$$

Primers, probes, reference human genomic DNA and PCR consumables. Primers and probes were chosen with the assistance of the computer programs Oligo 4.0 (National Biosciences, Plymouth, MN), EuGene (Daniben Systems, Cincinnati, OH) and Primer Express (Perkin-Elmer Applied Biosystems, Foster City, CA).

Primers were purchased from DNAgency (Malvern, PA) and probes from Perkin-Elmer Applied Biosystems.

Nucleotide sequences for the oligonucleotide hybridization probes and primers are available on request.

The TaqMan PCR Core reagent kit, MicroAmp optical tubes, and MicroAmp caps were from Perkin-Elmer Applied Biosystems.

Standard-curve construction. The kinetic method requires a standard curve. The latter was constructed with serial dilutions of specific PCR products, according to Piatak *et al.* (1993). In practice, each specific PCR product was obtained by amplifying 20 ng of a standard human genomic DNA (Boehringer, Mannheim, Germany) with the same primer pairs as those used later for real-time quantitative PCR. The 5 PCR products were purified using MicroSpin S-400 HR columns (Pharmacia, Uppsala, Sweden) electrophorezed through an acrylamide gel and stained with ethidium bromide to check their quality. The PCR products were then quantified spectrophotometrically and pooled, and serially diluted 10-fold in mouse genomic DNA (Clontech, Palo Alto, CA) at a constant concentration of 2 ng/µl. The standard curve used for real-time quantitative PCR was based on serial dilutions of the pool of PCR products ranging from 10^{-7} (10^5 copies of each gene) to 10^{-10} (10^2 copies). This series of diluted PCR products was aliquoted and stored at $-80°C$ until use.

The standard curve was validated by analyzing 2 known quantities of calibrator human genomic DNA (20 ng and 50 ng).

PCR amplification. Amplification mixes (50 µl) contained the sample DNA (around 20 ng, around 6600 copies of disomic genes), $10\times$ TaqMan buffer (5 µl), 200 µM dATP, dCTP, dGTP, and 400 µM dUTP, 5 mM MgCl$_2$, 1.25 units of AmpliTaq Gold, 0.5 units of AmpErase uracil N-glycosylase (UNG), 200 nM each primer and 100 nM probe. The thermal cycling conditions comprised 2 min at 50°C and 10 min at 95°C. Thermal cycling consisted of 40 cycles at 95°C for 15 s and 65°C for 1 min. Each assay included: a standard curve (from 10^5 to 10^2 copies) in duplicate, a no-template control, 20 ng and 50 ng of calibrator human genomic DNA (Boehringer) in triplicate, and about 20 ng of unknown genomic DNA in triplicate (26 samples can thus be analyzed on a 96-well microplate). All samples with a coefficient of variation (CV) higher than 10% were retested.

All reactions were performed in the ABI Prism 7700 Sequence Detection System (Perkin-Elmer Applied Biosystems), which detects the signal from the fluorogenic probe during PCR.

Equipment for real-time detection. The 7700 system has a built-in thermal cycler and a laser directed via fiber optical cables to each of the 96 sample wells. A charge-coupled-device (CDD) camera collects the emission from each sample and the data are analyzed automatically. The software accompanying the 7700 system calculates C_t and determines the starting copy number in the samples.

Determination of gene amplification. Gene amplification was calculated as described above. Only samples with an N value higher than 2 were considered to be amplified.

RESULTS

To validate the method, real-time PCR was performed on genomic DNA extracted from 108 primary breast tumors, and 18 normal leukocyte DNA samples from some of the same patients. The target genes were the *myc, ccnd1.* and *erb*B2 proto-oncogenes, and the β-amyloid precursor protein gene (*app*), which maps to a chromosome region (21q21.2) in which no genetic alterations have been found in breast tumors (Kallioniemi *et al.,* 1994). The reference disomic gene was the albumin gene (*alb,* chromosome 4q11-q13).

Validation of the standard curve and dynamic range of real-time PCR

The standard curve was constructed from PCR products serially diluted in genomic mouse DNA at a constant concentration of 2 ng/μl. It should be noted that the 5 primer pairs chosen to analyze the 5 target genes do not amplify genomic mouse DNA (data not shown). Figure 1 shows the real-time PCR standard curve for the *alb* gene. The dynamic range was wide (at least 4 orders of magnitude), with samples containing as few as 10^2 copies or as many as 10^5 copies.

Copy-number ratio of the 2 reference genes (app and alb)

The *app* to *alb* copy-number ratio was determined in 18 normal leukocyte DNA samples and all 108 primary breast-tumor DNA
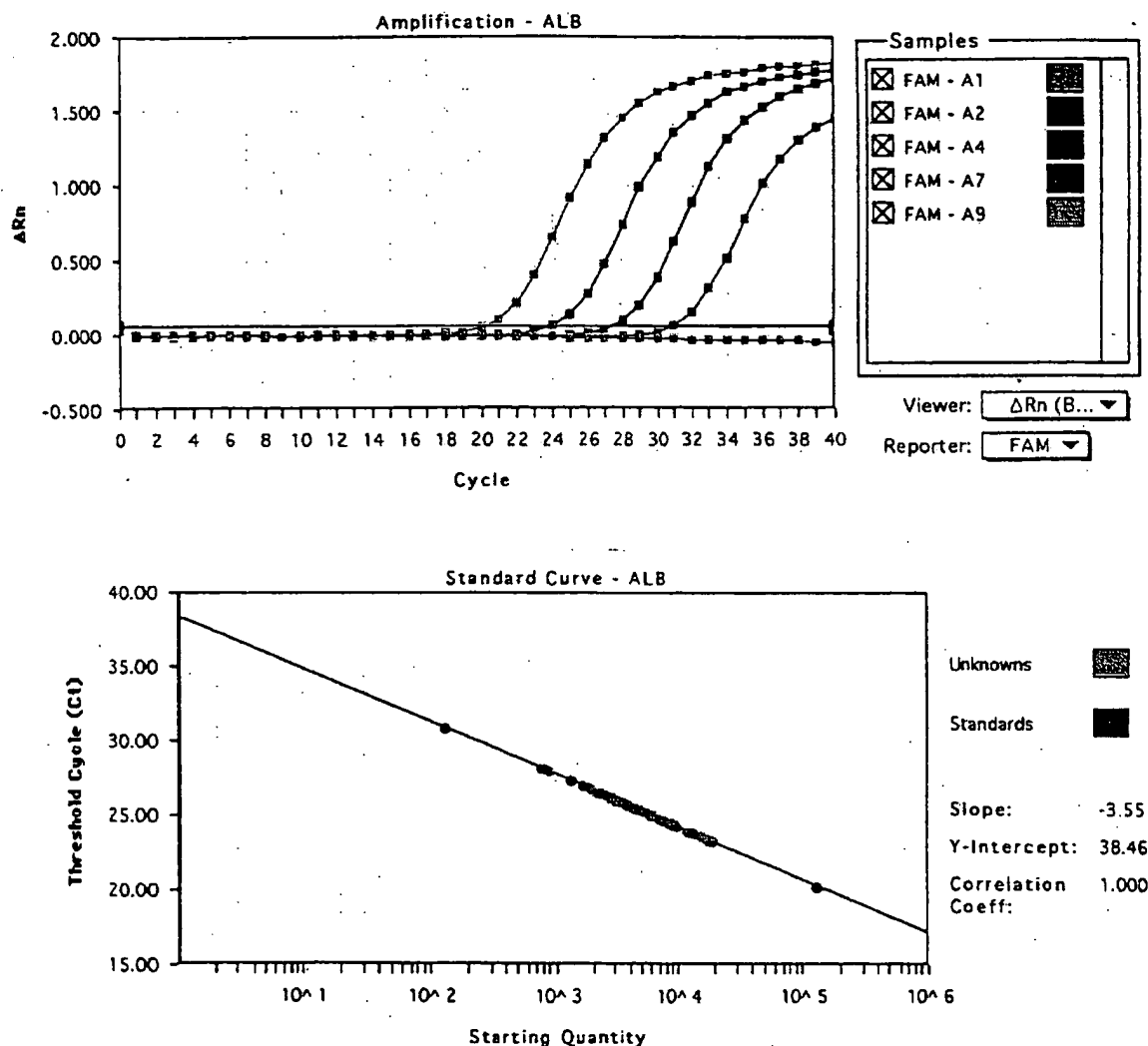

FIGURE 1 – Albumin (*alb*) gene dosage by real-time PCR. Top: Amplification plots for reactions with starting *alb* gene copy number ranging from 10^5 (A9), 10^4 (A7), 10^3 (A4) to 10^2 (A2) and a no-template control (A1). Cycle number is plotted *vs.* change in normalized reporter signal (ΔRn). For each reaction tube, the fluorescence signal of the reporter dye (FAM) is divided by the fluorescence signal of the passive reference dye (ROX), to obtain a ratio defined as the normalized reporter signal (Rn). ΔRn represents the normalized reporter signal (Rn) minus the baseline signal established in the first 15 PCR cycles. ΔRn increases during PCR as *alb* PCR product copy number increases until the reaction reaches a plateau. C_t (threshold cycle) represents the fractional cycle number at which a significant increase in Rn above a baseline signal (horizontal black line) can first be detected. Two replicate plots were performed for each standard sample, but the data for only one are shown here. Bottom: Standard curve plotting log starting copy number *vs.* C_t (threshold cycle). The black dots represent the data for standard samples plotted in duplicate and the red dots the data for unknown genomic DNA samples plotted in triplicate. The standard curve shows 4 orders of linear dynamic range.

samples. We selected these 2 genes because they are located in 2 chromosome regions (app. 21q21.2; alb, 4q11-q13) in which no obvious genetic changes (including gains or losses) have been observed in breast cancers (Kallioniemi et al., 1994). The ratio for the 18 normal leukocyte DNA samples fell between 0.7 and 1.3 (mean 1.02 ± 0.21), and was similar for the 108 primary breast-tumor DNA samples (0.6 to 1.6, mean 1.06 ± 0.25), confirming that alb and app are appropriate reference disomic genes for breast-tumor DNA. The low range of the ratios also confirmed that the nucleotide sequences chosen for the primers and probes were not polymorphic, as mismatches of their primers or probes with the subject's DNA would have resulted in differential amplification.

myc, ccnd1 and erbB2 gene dose in normal leukocyte DNA

To determine the cut-off point for gene amplification in breast-cancer tissue, 18 normal leukocyte DNA samples were tested for the gene dose (N), calculated as described in "Material and Methods". The N value of these samples ranged from 0.5 to 1.3 (mean 0.84 ± 0.22) for myc; 0.7 to 1.6 (mean 1.06 ± 0.23) for ccnd1 and 0.6 to 1.3 (mean 0.91 ± 0.19) for erbB2. Since N values for myc, ccnd1 and erbB2 in normal leukocyte DNA consistently fell between 0.5 and 1.6, values of 2 or more were considered to represent gene amplification in tumor DNA.

myc, ccnd1 and erbB2 gene dose in breast-tumor DNA

myc, ccnd1 and erbB2 gene copy numbers in the 108 primary breast tumors are reported in Table 1. Extra copies of ccnd1 were more frequent (23%, 25/108) than extra copies of erbB2 (15%, 16/108) and myc (10%, 11/108), and ranged from 2 to 18.6 for ccnd1, 2 to 15.1 for erbB2, and only 2 to 4.6 for the myc gene. Figure 2 and Table II represent tumors in which the ccnd1 gene was amplified 16-fold (T145), 6-fold (T133) and non-amplified (T118). The 3 genes were never found to be co-amplified in the same tumor. erbB2 and ccnd1 were co-amplified in only 3 cases, myc and ccnd1 in 2 cases and myc and erbB2 in 1 case. This favors the hypothesis that gene amplifications are independent events in breast cancer. Interestingly, 5 tumors showed a decrease of at least 50% in the erbB2 copy number (N < 0.5), suggesting that they bore deletions of the 17q21 region (the site of erbB2). No such decrease in copy number was observed with the other 2 proto-oncogenes.

Comparison of gene dose determined by real-time quantitative PCR and Southern-blot analysis

Southern-blot analysis of myc, ccnd1 and erbB2 amplifications had previously been done on the same 108 primary breast tumors. A perfect correlation between the results of real-time PCR and Southern blot was obtained for tumors with high copy numbers (N ≥ 5). However, there were cases (1 myc, 6 ccnd1 and 4 erbB2) in which real-time PCR showed gene amplification whereas Southern-blot did not, but these were mainly cases with low extra copy numbers (N from 2 to 2.9).

DISCUSSION

The clinical applications of gene amplification assays are currently limited, but would certainly increase if a simple, standardized and rapid method were perfected. Gene amplification status has been studied mainly by means of Southern blotting, but this method is not sensitive enough to detect low-level gene amplification nor accurate enough to quantify the full range of amplification values. Southern blotting is also time-consuming, uses radioactive

reagents and requires relatively large amounts of high-quality genomic DNA, which means it cannot be used routinely in many laboratories. An amplification step is therefore required to determine the copy number of a given target gene from minimal quantities of tumor DNA (small early-stage tumors, cytopuncture specimens or formalin-fixed, paraffin-embedded tissues).

In this study, we validated a PCR method developed for the quantification of gene over-representation in tumors. The method, based on real-time analysis of PCR amplification, has several advantages over other PCR-based quantitative assays such as competitive quantitative PCR (Celi et al., 1994). First, the real-time PCR method is performed in a closed-tube system, avoiding the risk of contamination by amplified products. Re-amplification of carryover PCR products in subsequent experiments can also be prevented by using the enzyme uracil N-glycosylase (UNG) (Longo et al., 1990). The second advantage is the simplicity and rapidity of sample analysis, since no post-PCR manipulations are required. Our results show that the automated method is reliable. We found it possible to determine, in triplicate, the number of copies of a target gene in more than 100 tumors per day. Third, the system has a linear dynamic range of at least 4 orders of magnitude, meaning that samples do not have to contain equal starting amounts of DNA. This technique should therefore be suitable for analyzing formalin-fixed, paraffin-embedded tissues. Fourth, and above all, real-time PCR makes DNA quantification much more precise and reproducible, since it is based on C_t values rather than end-point measurement of the amount of accumulated PCR product. Indeed, the ABI Prism 7700 Sequence Detection System enables C_t to be calculated when PCR amplification is still in the exponential phase and when none of the reaction components is rate-limiting. The within-run CV of the C_t value for calibrator human DNA (5 replicates) was always below 5%, and the between-assay precision in 5 different runs was always below 10% (data not shown). In addition, the use of a standard curve is not absolutely necessary, since the copy number can be determined simply by comparing the C_t ratio of the target gene with that of reference genes. The results obtained by the 2 methods (with and without a standard curve) are similar in our experiments (data not shown). Moreover, unlike competitive quantitative PCR, real-time PCR does not require an internal control (the design and storage of internal controls and the validation of their amplification efficiency is laborious).

The only potential disavantage of real-time PCR, like all other PCR-based methods and solid-matrix blotting techniques (Southern blots and dot blots) is that is cannot avoid dilution artifacts inherent in the extraction of DNA from tumor cells contained in heterogeneous tissue specimens. Only FISH and immunohistochemistry can measure alterations on a cell-by-cell basis (Pauletti et al., 1996; Slamon et al., 1989). However, FISH requires expensive equipment and trained personnel and is also time-consuming. Moreover, FISH does not assess gene expression and therefore cannot detect cases in which the gene product is over-expressed in the absence of gene amplification, which will be possible in the future by real-time quantitative RT-PCR. Immunohistochemistry is subject to considerable variations in the hands of different teams, owing to alterations of target proteins during the procedure, the different primary antibodies and fixation methods used and the criteria used to define positive staining.

The results of this study are in agreement with those reported in the literature. (i) Chromosome regions 4q11-q13 and 21q21.2 (which bear alb and app, respectively) showed no genetic alterations in the breast-cancer samples studied here, in keeping with the results of CGH (Kallioniemi et al., 1994). (ii) We found that amplifications of these 3 oncogenes were independent events, as reported by other teams (Berns et al., 1992; Borg et al., 1992). (iii) The frequency and degree of myc amplification in our breast tumor DNA series were lower than those of ccnd1 and erbB2 amplification, confirming the findings of Borg et al. (1992) and Courjal et al. (1997). (iv) The maxima of ccnd1 and erbB2 over-representation were 18-fold and 15-fold, also in keeping with earlier results (about

TABLE I – DISTRIBUTION OF AMPLIFICATION LEVEL (N) FOR myc, ccnd1 AND erbB2 GENES IN 108 HUMAN BREAST TUMORS

Gene	Amplification level (N)			
	<0.5	0.5-1.9	2-4.9	≥5
myc	0	97 (89.8%)	11 (10.2%)	0
ccnd1	0	83 (76.9%)	17 (15.7%)	8 (7.4%)
erbB2	5 (4.6%)	87 (80.6%)	8 (7.4%)	8 (7.4%)
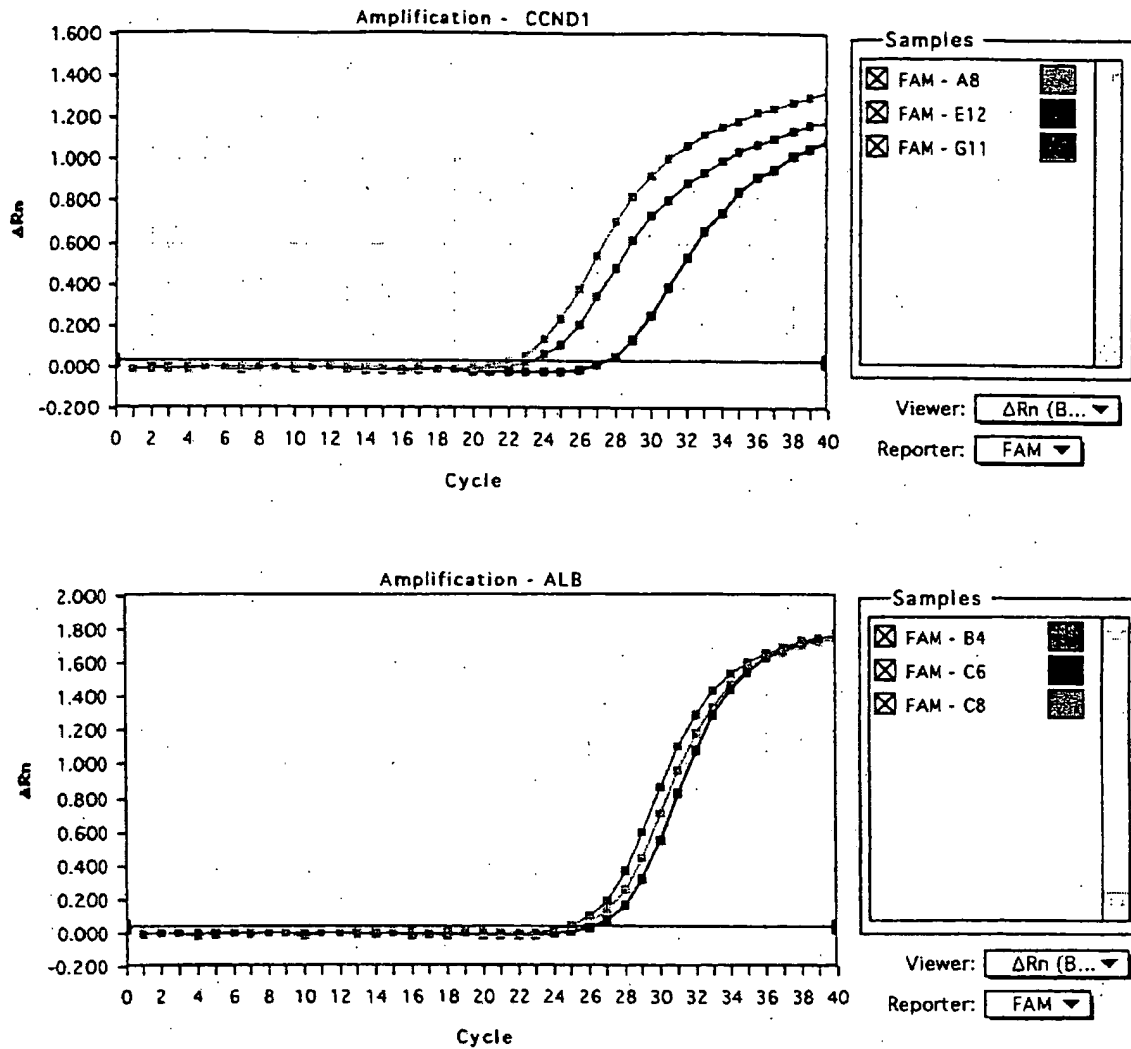
Tumor	CCND1		ALB	
	C_t	Copy number	C_t	Copy number
■ T118	27.3	4605	26.5	4365
▨ T133	23.2	61659	25.2	10092
▨ T145	22.1	125892	25.6	7762

FIGURE 2 – *ccnd1* and *alb* gene dosage by real-time PCR in 3 breast tumor samples: T118 (E12, C6, black squares), T133 (G11, B4, red squares) and T145 (A8, C8, blue squares). Given the C_t of each sample, the initial copy number is inferred from the standard curve obtained during the same experiment. Triplicate plots were performed for each tumor sample, but the data for only one are shown here. The results are shown in Table II.

30-fold maximum) (Berns *et al.*, 1992; Borg *et al.*, 1992; Courjal *et al.*, 1997). (*v*) The *erb*B2 copy numbers obtained with real-time PCR were in good agreement with data obtained with other quantitative PCR-based assays in terms of the frequency and degree of amplification (An *et al.*, 1995; Deng *et al.*, 1996; Valeron

et al., 1996). Our results also correlate well with those recently published by Gelmini *et al.* (1997), who used the TaqMan system to measure *erb*B2 amplification in a small series of breast tumors (n = 25), but with an instrument (LS-50B luminescence spectrometer, Perkin-Elmer Applied Biosystems) which only allows end-

Tumor	*ccnd1*			*alb*			N*ccnd1/alb*
	Copy number	Mean	SD	Copy number	Mean	SD	
T118	4525			4223			
	4605	4603	77	4365	4325	89	1.06
	4678			4387			
T133	59821			9787			
	61659	61100	1111	10092	10137	375	6.03
	61821			10533			
T145	128563			7321			
	125892	125392	3448	7762	7672	316	16.34
	121722			7933			

[1]For each sample, 3 replicate experiments were performed and the mean and the standard deviation (SD) was determined. The level of *ccnd1* gene amplification (N*ccnd1/alb*) is determined by dividing the average *ccnd1* copy number value by the average *alb* copy number value.

point measurement of fluorescence intensity. Here we report *myc* and *ccnd1* gene dosage in breast cancer by means of quantitative PCR. (vi) We found a high degree of concordance between real-time quantitative PCR and Southern blot analysis in terms of gene amplification, especially for samples with high copy numbers ($\geq$5-fold). The slightly higher frequency of gene amplification (especially *ccnd1* and *erb*B2) observed by means of real-time quantitative PCR as compared with Southern-blot analysis may be explained by the higher sensitivity of the former method. However, we cannot rule out the possibility that some tumors with a few extra

gene copies observed in real-time PCR had additional copies of an arm or a whole chromosome (trisomy, tetrasomy or polysomy) rather than true gene amplification. These 2 types of genetic alteration (polysomy and gene amplification) could be easily distinguished in the future by using an additional probe located on the same chromosome arm, but some distance from the target gene. It is noteworthy that high gene copy numbers have the greatest prognostic significance in breast carcinoma (Borg *et al.*, 1992; Slamon *et al.*, 1987).

Finally, this technique can be applied to the detection of gene deletion as well as gene amplification. Indeed, we found a decreased copy number of *erb*B2 (but not of the other 2 proto-oncogenes) in several tumors; *erb*B2 is located in a chromosome region (17q21) reported to contain both deletions and amplifications in breast cancer (Bièche and Lidereau, 1995).

In conclusion, gene amplification in various cancers can be used as a marker of pre-neoplasia, also for early diagnosis of cancer, staging, prognostication and choice of treatment. Southern blotting is not sufficiently sensitive, and FISH is lengthy and complex. Real-time quantitative PCR overcomes both these limitations, and is a sensitive and accurate method of analyzing large numbers of samples in a short time. It should find a place in routine clinical gene dosage.

ACKNOWLEDGEMENTS

REFERENCES

AN, H.X., NIEDERACHER, D., BECKMANN, M.W., GÖHRING, U.J., SCHARL, A., PICARD, F., VAN ROEYEN, C., SCHNÜRCH, H.G. and BENDER, H.G., *erb*B2 gene amplification detected by fluorescent differential polymerase chain reaction in paraffin-embedded breast carcinoma tissues. *Int. J. Cancer (Pred. Oncol.)*, 64, 291–297 (1995).

BERNS, E.M.J.J., KLIJN, J.G.M., VAN PUTTEN, W.L.J., VAN STAVEREN, I.L., PORTENGEN, H. and FOEKENS, J.A., *c-myc* amplification is a better prognostic factor than HER2/*neu* amplification in primary breast cancer. *Cancer Res.*, 52, 1107–1113 (1992).

BIÈCHE, I. and LIDEREAU, R., Genetic alterations in breast cancer. *Genes Chrom. Cancer*, 14, 227–251 (1995).

BORG, A., BALDETORP, B., FERNO, M., OLSSON, H. and SIGURDSSON, H., *c-myc* amplification is an independent prognostic factor in post-menopausal breast cancer. *Int. J. Cancer*, 51, 687–691 (1992).

CELI, F.S., COHEN, M.M., ANTONARAKIS, S.E., WERTHEIMER, E., ROTH, J. and SHULDINER, A.R., Determination of gene dosage by a quantitative adaptation of the polymerase chain reaction (gd-PCR): rapid detection of deletions and duplications of gene sequences. *Genomics*, 21, 304–310 (1994).

COURJAL, F., CUNY, M., SIMONY-LAFONTAINE, J., LOUASSON, G., SPEISER, P., ZEILLINGER, R., RODRIGUEZ, C. and THEILLET, C., Mapping of DNA amplifications at 15 chromosomal localizations in 1875 breast tumors: definition of phenotypic groups. *Cancer Res.*, 57, 4360–4367 (1997).

DENG, G., YU, M., CHEN, L.C., MOORE, D., KURISU, W., KALLIONIEMI, A., WALDMAN, F.M., COLLINS, C. and SMITH, H.S., Amplifications of oncogene *erb*B-2 and chromosome 20q in breast cancer determined by differentially competitive polymerase chain reaction. *Breast Cancer Res. Treat.*, 40, 271–281 (1996).

GELMINI, S., ORLANDO, C., SESTTNI, R., VONA, G., PINZANI, P., RUOCCO, L. and PAZZAGLI, M., Quantitative polymerase chain reaction-based homogeneous assay with fluorogenic probes to measure *c-erB*-2 oncogene amplification. *Clin. Chem.*, 43, 752–758 (1997).

GIBSON, U.E.M., HEID, C.A. and WILLIAMS, P.M., A novel method for real-time quantitative RT-PCR. *Genome Res.*, 6, 995–1001 (1996).

HEID, C.A., STEVENS, J., LIVAK, K.J. and WILLIAMS, P.M., Real-time quantitative PCR. *Genome Res.*, 6, 986–994 (1996).

HOLLAND, P.M., ABRAMSON, R.D., WATSON, R. and GELFAND, D.H., Detection of specific polymerase chain reaction product by utilizing the 5′ to 3′ exonuclease activity of *Thermus aquaticus* DNA polymerase. *Proc. nat. Acad. Sci. (Wash.)*, 88, 7276–7280 (1991).

KALLIONIEMI, A., KALLIONIEMI, O.P., PIPER, J., TANNER, M., STOKKES, T., CHEN, L., SMITH, H.S., PINKEL, D., GRAY, J.W. and WALDMAN, F.M., Detection and mapping of amplified DNA sequences in breast cancer by comparative genomic hybridization. *Proc. nat. Acad. Sci. (Wash.)*, 91, 2156–2160 (1994).

LEE, L.G., CONNELL, C.R. and BLOCH, W., Allelic discrimination by nick-translation PCR with fluorogenic probe. *Nucleic Acids Res.*, 21, 3761–3766 (1993).

LONGO, N., BERNINGER, N.S. and HARTLEY, J.L., Use of uracil DNA glycosylase to control carry-over contamination in polymerase chain reactions. *Gene*, 93, 125–128 (1990).

MUSS, H.B., THOR, A.D., BERRY, D.A., KUTE, T., LIU, E.T., KOERNER, F., CIRRINCIONE, C.T., BUDMAN, D.R., WOOD, W.C., BARCOS, M. and HENDERSON, I.C., *c-erb*B-2 expression and response to adjuvant therapy in women with node-positive early breast cancer. *New Engl. J. Med.*, 330, 1260–1266 (1994).

PAULETTI, G., GODOLPHIN, W., PRESS, M.F. and SALMON, D.J., Detection and quantification of HER-2/*neu* gene amplification in human breast cancer archival material using fluorescence *in situ* hybridization. *Oncogene*, 13, 63–72 (1996).

PIATAK, M., LUK, K.C., WILLIAMS, B. and LIFSON, J.D., Quantitative competitive polymerase chain reaction for accurate quantitation of HIV DNA and RNA species. *Biotechniques*, 14, 70–80 (1993).

SCHUURING, E., VERHOEVEN, E., VAN TINTEREN, H., PETERSE, J.L., NUNNIK, B., THUNNISSEN, F.B.J.M., DEVILEE, P., CORNELISSE, C.J., VAN DE VIJVER, M.J., MOOI, W.J. and MICHALIDES, R.J.A.M., Amplification of genes within the chromosome 11q13 region is indicative of poor prognosis in patients with operable breast cancer. *Cancer Res.*, 52, 5229–5234 (1992).

SLAMON, D.J., CLARK, G.M., WONG, S.G., LEVIN, W.S., ULLRICH, A. and McGUIRE, W.L., Human breast cancer: correlation of relapse and survival with amplification of the HER-2/*neu* oncogene. *Science*, 235, 177–182 (1987).

SLAMON, D.J., GODOLPHIN, W., JONES, L.A., HOLT, J.A., WONG, S.G., KEITH, D.E., LEVIN, W.J., STUART, S.G., UDOVE, J., ULLRICH, A. and PRESS, M.F., Studies of the HER-2/*neu* proto-oncogene in human breast and ovarian cancer. *Science*, 244, 707–712 (1989).

VALERON, P.F., CHIRINO, R., FERNANDEZ, L., TORRES, S., NAVARRO, D., AGUIAR, J., CABRERA, J.J., DIAZ-CHICO, B.N. and DIAZ-CHICO, J.C., Validation of a differential PCR and an ELISA procedure in studying HER-2/*neu* status in breast cancer. *Int. J. Cancer*, 65, 129–133 (1996).
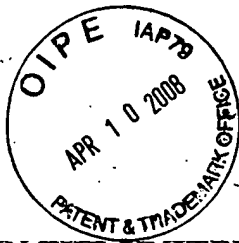
IN THE UNITED STATES PATENT AND TRADEMARK OFFICE

Applicant : Ashkenazi et al.	Group Art Unit 1647
App. No. : 09/903,925	CERTIFICATE OF EXPRESS MAILING
Filed : July 11, 2001	I hereby certify that this correspondence is being deposited with the United States Postal Service with sufficient postage as first class mail in an envelope addressed to Commissioner of Patents, Washington D.C. 20231 on:
For : SECRETED AND TRANSMEMBRANE POLYPEPTIDES AND NUCLEIC ACIDS ENCODING THE SAME	
	_____ (Date)
Examiner : Hamud, Fozia M	_____

Commissioner of Patents
P.O. Box 1450
Alexandria, VA 22313-1450

DECLARATION OF AVI ASHKENAZI, Ph.D UNDER 37 C.F.R. § 1.132

I, Avi Ashkenazi, Ph.D. declare and say as follows: -

1.   I am Director and Staff Scientist at the Molecular Oncology Department of Genentech, Inc., South San Francisco, CA 94080.

2.   I joined Genentech in 1988 as a postdoctoral fellow. Since then, I have investigated a variety of cellular signal transduction mechanisms, including apoptosis, and have developed technologies to modulate such mechanisms as a means of therapeutic intervention in cancer and autoimmune disease. I am currently involved in the investigation of a series of secreted proteins over-expressed in tumors, with the aim to identify useful targets for the development of therapeutic antibodies for cancer treatment.

3.   My scientific Curriculum Vitae, including my list of publications, is attached to and forms part of this Declaration (Exhibit A).

4.   Gene amplification is a process in which chromosomes undergo changes to contain multiple copies of certain genes that normally exist as a single copy, and is an important factor in the pathophysiology of cancer. Amplification of certain genes (e.g., Myc or Her2/Neu)

gives cancer cells a growth or survival advantage relative to normal cells, and might also provide a mechanism of tumor cell resistance to chemotherapy or radiotherapy.

5. If gene amplification results in over-expression of the mRNA and the corresponding gene product, then it identifies that gene product as a promising target for cancer therapy, for example by the therapeutic antibody approach. Even in the absence of over-expression of the gene product, amplification of a cancer marker gene - as detected, for example, by the reverse transcriptase TaqMan® PCR or the fluorescence *in situ* hybridization (FISH) assays -is useful in the diagnosis or classification of cancer, or in predicting or monitoring the efficacy of cancer therapy. An increase in gene copy number can result not only from intrachromosomal changes but also from chromosomal aneuploidy. It is important to understand that detection of gene amplification can be used for cancer diagnosis even if the determination includes measurement of chromosomal aneuploidy. Indeed, as long as a significant difference relative to normal tissue is detected, it is irrelevant if the signal originates from an increase in the number of gene copies per chromosome and/or an abnormal number of chromosomes.

6. I understand that according to the Patent Office, absent data demonstrating that the increased copy number of a gene in certain types of cancer leads to increased expression of its product, gene amplification data are insufficient to provide substantial utility or well established utility for the gene product (the encoded polypeptide), or an antibody specifically binding the encoded polypeptide. However, even when amplification of a cancer marker gene does not result in significant over-expression of the corresponding gene product, this very absence of gene product over-expression still provides significant information for cancer diagnosis and treatment. Thus, if over-expression of the gene product does not parallel gene amplification in certain tumor types but does so in others, then parallel monitoring of gene amplification and gene product over-expression enables more accurate tumor classification and hence better determination of suitable therapy. In addition, absence of over-expression is crucial information for the practicing clinician. If a gene is amplified but the corresponding gene product is not over-expressed, the clinician accordingly will decide not to treat a patient with agents that target that gene product.

7. I hereby declare that all statements made herein of my own knowledge are true and that all statements made on information or belief are believed to be true, and further that these statements were made with the knowledge that willful false statements and the like so

made are punishable by fine or imprisonment, or both, under Section 1001 of Title 18 of the United States Code and that such willful statements may jeopardize the validity of the application or any patent issued thereon.

By: _~Avi Ashkenazi~_   Date: _9/15/03_
    Avi Ashkenazi, Ph.D.

CURRICULUM VITAE
Avi Ashkenazi
July 2003

Personal:

Date of birth:	29 November, 1956
Address:	1456 Tarrytown Street, San Mateo, CA 94402
Phone:	(650) 578-9199 (home); (650) 225-1853 (office)
Fax:	(650) 225-6443 (office)
Email:	aa@gene.com

Education:

1983:	B.S. in Biochemistry, with honors, Hebrew University, Israel
1986:	Ph.D. in Biochemistry, Hebrew University, Israel

Employment:

1983-1986:	Teaching assistant, undergraduate level course in Biochemistry
1985-1986:	Teaching assistant, graduate level course on Signal Transduction
1986 - 1988:	Postdoctoral fellow, Hormone Research Dept., UCSF, and Developmental Biology Dept., Genentech, Inc., with J. Ramachandran
1988 - 1989:	Postdoctoral fellow, Molecular Biology Dept., Genentech, Inc., with D. Capon
1989 - 1993:	Scientist, Molecular Biology Dept., Genentech, Inc.
1994 -1996:	Senior Scientist, Molecular Oncology Dept., Genentech, Inc.
1996-1997:	Senior Scientist and Interim director, Molecular Oncology Dept., Genentech, Inc.
1997-1990:	Senior Scientist and preclinical project team leader, Genentech, Inc.
1999 -2002:	Staff Scientist in Molecular Oncology, Genentech, Inc.
2002-present:	Staff Scientist and Director in Molecular Oncology, Genentech, Inc.

Awards:

1988:	First prize, The Boehringer Ingelheim Award

Editorial:

Editorial Board Member: Current Biology

Associate Editor, Clinical Cancer Research.

Associate Editor, Cancer Biology and Therapy.

Refereed papers:

1. Gertler, A., Ashkenazi, A., and Madar, Z. Binding sites for human growth hormone and ovine and bovine prolactins in the mammary gland and liver of the lactating cow. *Mol. Cell. Endocrinol.* 34, 51-57 (1984).

2. Gertler, A., Shamay, A., Cohen, N., Ashkenazi, A., Friesen, H., Levanon, A., Gorecki, M., Aviv, H., Hadari, D., and Vogel, T. Inhibition of lactogenic activities of ovine prolactin and human growth hormone (hGH) by a novel form of a modified recombinant hGH. *Endocrinology* 118, 720-726 (1986).

3. Ashkenazi, A., Madar, Z., and Gertler, A. Partial purification and characterization of bovine mammary gland prolactin receptor. *Mol. Cell. Endocrinol.* 50, 79-87 (1987).

4. Ashkenazi, A., Pines, M., and Gertler, A. Down-regulation of lactogenic hormone receptors in Nb2 lymphoma cells by cholera toxin. *Biochemistry Internatl.* 14, 1065-1072 (1987).

5. Ashkenazi, A., Cohen, R., and Gertler, A. Characterization of lactogen receptors in lactogenic hormone-dependent and independent Nb2 lymphoma cell lines. *FEBS Lett.* 210, 51-55 (1987).

6. Ashkenazi, A., Vogel, T., Barash, I., Hadari, D., Levanon, A., Gorecki, M., and Gertler, A. Comparative study on in vitro and in vivo modulation of lactogenic and somatotropic receptors by native human growth hormone and its modified recombinant analog. *Endocrinology* 121, 414-419 (1987).

7. Peralta, E., Winslow, J., Peterson, G., Smith, D., Ashkenazi, A., Ramachandran, J., Schimerlik, M., and Capon, D. Primary structure and biochemical properties of an M2 muscarinic receptor. *Science* 236, 600-605 (1987).

8. Peralta, E. Ashkenazi, A., Winslow, J., Smith, D., Ramachandran, J., and Capon, D. J. Distinct primary structures, ligand-binding properties and tissue-specific expression of four human muscarinic acetylcholine receptors. *EMBO J.* 6, 3923-3929 (1987).

9. Ashkenazi, A., Winslow, J., Peralta, E., Peterson, G., Schimerlik, M., Capon, D., and Ramachandran, J. An M2 muscarinic receptor subtype coupled to both adenylyl cyclase and phosphoinositide turnover. *Science* 238, 672-675 (1987).

10. Pines, M., <u>Ashkenazi, A.</u>, Cohen-Chapnik, N., Binder, L., and Gertler, A. Inhibition of the proliferation of Nb2 lymphoma cells by femtomolar concentrations of cholera toxin and partial reversal of the effect by 12-o-tetradecanoyl-phorbol-13-acetate. *J. Cell. Biochem.* 37, 119-129 (1988).

11. Peralta, E. <u>Ashkenazi, A.</u>, Winslow, J. Ramachandran, J., and Capon, D. Differential regulation of PI hydrolysis and adenylyl cyclase by muscarinic receptor subtypes. *Nature* 334, 434-437 (1988).

12. <u>Ashkenazi., A.</u> Peralta, E., Winslow, J., Ramachandran, J., and Capon, D. Functionally distinct G proteins couple different receptors to PI hydrolysis in the same cell. *Cell* 56, 487-493 (1989).

13. <u>Ashkenazi, A.</u>, Ramachandran, J., and Capon, D. Acetylcholine analogue stimulates DNA synthesis in brain-derived cells via specific muscarinic acetylcholine receptor subtypes. *Nature* 340, 146-150 (1989).

14. Lammare, D., <u>Ashkenazi, A.</u>, Fleury, S., Smith, D., Sekaly, R., and Capon, D. The MHC-binding and gp120-binding domains of CD4 are distinct and separable. *Science* 245, 743-745 (1989).

15. <u>Ashkenazi., A.</u>, Presta, L., Marsters, S., Camerato, T., Rosenthal, K., Fendly, B., and Capon, D. Mapping the CD4 binding site for human immunodefficiency virus type 1 by alanine-scanning mutagenesis. *Proc. Natl. Acad. Sci. USA.* 87, 7150-7154 (1990).

16. Chamow, S., Peers, D., Byrn, R., Mulkerrin, M., Harris, R., Wang, W., Bjorkman, P., Capon, D., and <u>Ashkenazi, A.</u> Enzymatic cleavage of a CD4 immunoadhesin generates crystallizable, biologically active Fd-like fragments. *Biochemistry* 29, 9885-9891 (1990).

17. <u>Ashkenazi, A.</u>, Smith, D., Marsters, S., Riddle, L., Gregory, T., Ho, D., and Capon, D. Resistance of primary isolates of human immunodefficiency virus type 1 to soluble CD4 is independent of CD4-rgp120 binding affinity. *Proc. Natl. Acad. Sci. USA.* 88, 7056-7060 (1991).

18. <u>Ashkenazi, A.</u>, Marsters, S., Capon, D., Chamow, S., Figari., I., Pennica, D., Goeddel., D., Palladino, M., and Smith, D. Protection against endotoxic shock by a tumor necrosis factor receptor immunoadhesin. *Proc. Natl. Acad. Sci. USA.* 88, 10535-10539 (1991).

19. Moore, J., McKeating, J., Huang, Y., <u>Ashkenazi, A.</u>, and Ho, D. Virions of primary HIV-1 isolates resistant to sCD4 neutralization differ in sCD4 affinity and glycoprotein gp120 retention from sCD4-sensitive isolates. *J. Virol.* 66, 235-243 (1992).

20. Jin, H., Oksenberg, D., Ashkenazi, A., Peroutka, S., Duncan, A., Rozmahel., R., Yang, Y., Mengod, G., Palacios, J., and O'Dowd, B. Characterization of the human 5-hydroxytryptamine$_{1B}$ receptor. *J. Biol. Chem.* **267**, 5735-5738 (1992).

21. Marsters, A., Frutkin, A., Simpson, N., Fendly, B. and Ashkenazi, A. Identification of cysteine-rich domains of the type 1 tumor necrosis receptor involved in ligand binding. *J. Biol. Chem.* **267**, 5747-5750 (1992).

22. Chamow, S., Kogan, T., Peers, D., Hastings, R., Bym, R., and Ashkenazi, A. Conjugation of sCD4 without loss of biological activity via a novel carbohydrate-directed cross-linking reagent. *J. Biol. Chem.* **267**, 15916-15922 (1992).

23. Oksenberg, D., Marsters, A., O'Dowd, B., Jin, H., Havlik, S., Peroutka, S., and Ashkenazi, A. A single amino-acid difference confers major pharmacologic variation between human and rodent 5-HT$_{1B}$ receptors. *Nature* **360**, 161-163 (1992).

24. Haak-Frendscho, M., Marsters, S., Chamow, S., Peers, D., Simpson, N., and Ashkenazi, A. Inhibition of interferon γ by an interferon γ receptor immunoadhesin. *Immunology* **79**, 594-599 (1993).

25. Penica, D., Lam, V., Weber, R., Kohr, W., Basa, L., Spellman, M., Ashkenazi, Shire, S., and Goeddel, D. Biochemical characterization of the extracellular domain of the 75-kd tumor necrosis factor receptor. *Biochemistry* **32**, 3131-3138. (1993).

26. Barfod, L., Zheng, Y., Kuang, W., Hart, M., Evans, T., Cerione, R., and Ashkenazi, A. Cloning and expression of a human CDC42 GTPase Activating Protein reveals a functional SH3-binding domain. *J. Biol. Chem.* **268**, 26059-26062 (1993).

27. Chamow, S., Zhang, D., Tan, X., Mhtre, S., Marsters, S., Peers, D., Bym, R., Ashkenazi, A., and Yunghans, R. A humanized bispecific immunoadhesin-antibody that retargets CD3+ effectors to kill HIV-1-infected cells. *J. Immunol.* **153**, 4268-4280 (1994).

28. Means, R., Krantz, S., Luna, J., Marsters, S., and Ashkenazi, A. Inhibition of murine erythroid colony formation in vitro by iterferon γ and correction by interferon γ receptor immunoadhesin. *Blood* **83**, 911-915 (1994).

29. Haak-Frendscho, M., Marsters, S., Mordenti, J., Gillet, N., Chen, S., andAshkenazi, A. Inhibition of TNF by a TNF receptor immunoadhesin: comparison with an anti-TNF mAb. *J. Immunol.* **152**, 1347-1353 (1994).

30. Chamow, S., Kogan, T., Venuti, M., Gadek, T., Peers, D., Mordenti, J., Shak, S., and <u>Ashkenazi, A.</u> Modification of CD4 immunoadhesin with monomethoxy-PEG aldehyde via reductive alkilation. *Bioconj. Chem.* 5, 133-140 (1994).

31. Jin, H., Yang, R., Marsters, S., Bunting, S., Wurm, F., Chamow, S., and <u>Ashkenazi, A.</u> Protection against rat endotoxic shock by p55 tumor necrosis factor (TNF) receptor immunoadhesin: comparison to anti-TNF monoclonal antibody. *J. Infect. Diseases* 170, 1323-1326 (1994).

32. Beck, J., Marsters, S., Harris, R., <u>Ashkenazi, A.</u>, and Chamow, S. Generation of soluble interleukin-1 receptor from an immunoadhesin by specific cleavage. *Mol. Immunol.* 31, 1335-1344 (1994).

33. Pitti, B., Marsters, M., Haak-Frendscho, M., Osaka, G., Mordenti, J., Chamow, S., and <u>Ashkenazi, A.</u> Molecular and biological properties of an interleukin-1 receptor immunoadhesin. *Mol. Immunol.* 31, 1345-1351 (1994).

34. Oksenberg, D., Havlik, S., Peroutka, S., and <u>Ashkenazi, A.</u> The third intracellular loop of the 5-HT2 receptor specifies effector coupling. *J. Neurochem.* 64, 1440-1447 (1995).

35. Bach, E., Szabo, S., Dighe, A., <u>Ashkenazi, A.</u>, Aguet, M., Murphy, K., and Schreiber, R. Ligand-induced autoregulation of IFN-γ receptor β chain expression in T helper cell subsets. *Science* 270, 1215-1218 (1995).

36. Jin, H., Yang, R., Marsters, S., <u>Ashkenazi, A.</u>, Bunting, S., Marra, M., Scott, R., and Baker, J. Protection against endotoxic shock by bactericidal/permeability-increasing protein in rats. *J. Clin. Invest.* 95, 1947-1952 (1995).

37. Marsters, S., Penica, D., Bach, E., Schreiber, R., and <u>Ashkenazi, A.</u> Interferon γ signals via a high-affinity multisubunit receptor complex that contains two types of polypeptide chain. *Proc. Natl. Acad. Sci. USA.* 92, 5401-5405 (1995).

38. Van Zee, K., Moldawer, L., Oldenburg, H., Thompson, W., Stackpole, S., Montegut, W., Rogy, M., Meschter, C., Gallati, H., Schiller, C., Richter, W., Loetcher, H., <u>Ashkenazi, A.</u>, Chamow, S., Wurm, F., Calvano, S., Lowry, S., and Lesslauer, W. Protection against lethal E. coli bacteremia in baboons by pretreatment with a 55-kDa TNF receptor-Ig fusion protein, Ro45-2081. *J. Immunol.* 156, 2221-2230 (1996).

39. Pitti, R., Marsters, S., Ruppert, S., Donahue, C., Moore, A., and <u>Ashkenazi, A.</u> Induction of apoptosis by Apo-2 Ligand, a new member of the tumor necrosis factor cytokine family. *J. Biol. Chem.* 271, 12687-12690 (1996).

40. Marsters, S., Pitti, R., Donahue, C., Rupert, S., Bauer, K., and <u>Ashkenazi, A.</u> Activation of apoptosis by Apo-2 ligand is independent of FADD but blocked by CrmA. *Curr. Biol.* 6, 1669-1676 (1996).

41. Marsters, S., Skubatch, M., Gray, C., and <u>Ashkenazi, A.</u> Herpesvirus entry mediator, a novel member of the tumor necrosis factor receptor family, activates the NF-κB and AP-1 transcription factors. *J. Biol. Chem.* 272, 14029-14032 (1997).

42. Sheridan, J., Marsters, S., Pitti, R., Gurney, A., Skubatch, M., Baldwin, D., Ramakrishnan, L., Gray, C., Baker, K., Wood, W.I., Goddard, A., Godowski, P., and <u>Ashkenazi, A.</u> Control of TRAIL-induced apoptosis by a family of signaling and decoy receptors. *Science* 277, 818-821 (1997).

43. Marsters, S., Sheridan, J., Pitti, R., Gurney, A., Skubatch, M., Balswin, D., Huang, A., Yuan, J., Goddard, A., Godowski, P., and <u>Ashkenazi, A.</u> A novel receptor for Apo2L/TRAIL contains a truncated death domain. *Curr. Biol.* 7, 1003-1006 (1997).

44. Marsters, A., Sheridan, J., Pitti, R., Brush, J., Goddard, A., and <u>Ashkenazi, A.</u> Identification of a ligand for the death-domain-containing receptor Apo3. *Curr. Biol.* 8, 525-528 (1998).

45. Rieger, J., Naumann, U., Glaser, T., <u>Ashkenazi, A.</u>, and Weller, M. Apo2 ligand: a novel weapon against malignant glioma? *FEBS Lett.* 427, 124-128 (1998).

46. Pender, S., Fell, J., Chamow, S., <u>Ashkenazi, A.</u>, and MacDonald, T. A p55 TNF receptor immunoadhesin prevents T cell mediated intestinal injury by inhibiting matrix metalloproteinase production. *J. Immunol.* 160, 4098-4103 (1998).

47. Pitti, R., Marsters, S., Lawrence, D., Roy, Kischkel, F., M., Dowd, P., Huang, A., Donahue, C., Sherwood, S., Baldwin, D., Godowski, P., Wood, W., Gurney, A., Hillan, K., Cohen, R., Goddard, A., Botstein, D., and <u>Ashkenazi, A.</u> Genomic amplification of a decoy receptor for Fas ligand in lung and colon cancer. *Nature* 396, 699-703 (1998).

48. Mori, S., Marakami-Mori, K., Nakamura, S., <u>Ashkenazi, A.</u>, and Bonavida, B. Sensitization of AIDS Kaposi's sarcoma cells to Apo-2 ligand-induced apoptosis by actinomycin D. *J. Immunol.* 162, 5616-5623 (1999).

49. Gurney, A. Marsters, S., Huang, A., Pitti, R., Mark, M., Baldwin, D., Gray, A., Dowd, P., Brush, J., Heldens, S., Schow, P., Goddard, A., Wood, W., Baker, K., Godowski, P., and <u>Ashkenazi, A.</u> Identification of a new member of the tumor necrosis factor family and its receptor, a human ortholog of mouse GITR. *Curr. Biol.* 9, 215-218 (1999).

50.   Ashkenazi, A., Pai, R., Fong, s., Leung, S., Lawrence, D., Marsters, S., Blackie, C., Chang, L., McMurtrey, A., Hebert, A., DeForge, L., Khoumenis, I., Lewis, D., Harris, L., Bussiere, J., Koeppen, H., Shahrokh, Z., and Schwall, R. Safety and anti-tumor activity of recombinant soluble Apo2 ligand. *J. Clin. Invest.* **104**, 155-162 (1999).

51.   Chuntharapai, A., Gibbs, V., Lu, J., Ow, A., Marsters, S., Ashkenazi, A., De Vos, A., Kim, K.J. Determination of residues involved in ligand binding and signal transmissiion in the human IFN-α receptor 2. *J. Immunol.* **163**, 766-773 (1999).

52.   Johnsen, A.-C., Haux, J., Steinkjer, B., Nonstad, U., Egeberg, K., Sundan, A., Ashkenazi, A., and Espevik, T. Regulation of Apo2L/TRAIL expression in NK cells – involvement in NK cell-mediated cytotoxicity. *Cytokine* **11**, 664-672 (1999).

53.   Roth, W., Isenmann, S., Naumann, U., Kugler, S., Bahr, M., Dichgans, J., Ashkenazi, A., and Weller, M. Eradication of intracranial human malignant glioma xenografts by Apo2L/TRAIL. *Biochem. Biophys. Res. Commun.* **265**, 479-483 (1999).

54.   Hymowitz, S.G., Christinger, H.W., Fuh, G., Ultsch, M., O'Connell, M., Kelley, R.F., Ashkenazi, A. and de Vos, A.M. Triggering Cell Death: The Crystal Structure of Apo2L/TRAIL in a Complex with Death Receptor 5. *Molec. Cell* **4**, 563–571 (1999).

55.   Hymowitz, S.G., O'Connel, M.P., Utsch, M.H., Hurst, A., Totpal, K., Ashkenazi, A., de Vos, A.M., Kelley, R.F. A unique zinc-binding site revealed by a high-resolution X-ray structure of homotrimeric Apo2L/TRAIL. *Biochemistry* **39**, 633-640 (2000).

56.   Zhou, Q., Fukushima, P., DeGraff, W., Mitchell, J.B., Stetler-Stevenson, M., Ashkenazi, A., and Steeg, P.S. Radiation and the Apo2L/TRAIL apoptotic pathway preferentially inhibit the colonization of premalignant human breast cancer cells overexpressing cyclin D1. *Cancer Res.* **60**, 2611-2615 (2000).

57.   Kischkel, F.C., Lawrence, D. A., Chuntharapai, A., Schow, P., Kim, J., and Ashkenazi, A. Apo2L/TRAIL-dependent recruitment of endogenous FADD and Caspase-8 to death receptors 4 and 5. *Immunity* **12**, 611-620 (2000).

58.   Yan, M., Marsters, S.A., Grewal, I.S., Wang, H., *Ashkenazi, A., and *Dixit, V.M. Identification of a receptor for BlyS demonstrates a crucial role in humoral immunity. *Nature Immunol.* **1**, 37-41 (2000).

59. Marsters, S.A., Yan, M., Pitti, R.M., Haas, P.E., Dixit, V.M., and <u>Ashkenazi, A.</u> Interaction of the TNF homologues BLyS and APRIL with the TNF receptor homologues BCMA and TACI. *Curr. Biol.* 10, 785-788 (2000).

60. Kischkel, F.C., and <u>Ashkenazi, A.</u> Combining enhanced metabolic labeling with immunoblotting to detect interactions of endogenous cellular proteins. *Biotechniques* 29, 506-512 (2000).

61. Lawrence, D., Shahrokh, Z., Marsters, S., Achilles, K., Shih, D. Mounho, B., Hillan, K., Totpal, K. DeForge, L., Schow, P., Hooley, J., Sherwood, S., Pai, R., Leung, S., Khan, L., Gliniak, B., Bussiere, J., Smith, C., Strom, S., Kelley, S., Fox, J., Thomas, D., and <u>Ashkenazi, A.</u> Differential hepatocyte toxicity of recombinant Apo2L/TRAIL versions. *Nature Med.* 7, 383-385 (2001).

62. Chuntharapai, A., Dodge, K., Grimmer, K., Schroeder, K., Martsters, S.A., Koeppen, H., <u>Ashkenazi, A.</u>, and Kim, K.J. Isotype-dependent inhibition of tumor growth in vivo by monoclonal antibodies to death receptor 4. *J. Immunol.* 166, 4891-4898 (2001).

63. Pollack, I.F., Erff, M., and <u>Ashkenazi, A.</u> Direct stimulation of apoptotic signaling by soluble Apo2L/tumor necrosis factor-related apoptosis-inducing ligand leads to selective killing of glioma cells. *Clin. Cancer Res.* 7, 1362-1369 (2001).

64. Wang, H., Marsters, S.A., Baker, T., Chan, B., Lee, W.P., Fu, L., Tumas, D., Yan, M., Dixit, V.M., *<u>Ashkenazi, A.</u>, and *Grewal, I.S. TACI-ligand interactions are required for T cell activation and collagen-induced arthritis in mice. *Nature Immunol.* 2, 632-637 (2001).

65. Kischkel, F.C., Lawrence, D. A., Tinel, A., Virmani, A., Schow, P., Gazdar, A., Blenis, J., Arnott, D., and <u>Ashkenazi, A.</u> Death receptor recruitment of endogenous caspase-10 and apoptosis initiation in the absence of caspase-8. *J. Biol. Chem.* 276, 46639-46646 (2001).

66. LeBlanc, H., Lawrence, D.A., Varfolomeev, E., Totpal, K., Morlan, J., Schow, P., Fong, S., Schwall, R., Sinicropi, D., and <u>Ashkenazi, A</u> Tumor cell resistance to death receptor induced apoptosis through mutational inactivation of the proapoptotitc Bcl-2 homolog Bax. *Nature Med.* 8, 274-281 (2002).

67. Miller, K., Meng, G., Liu, J., Hurst, A., Hsei, V., Wong, W-L., Ekert, R., Lawrence, D., Sherwood, S., DeForge, L., Gaudreault., Keller, G., Sliwkowski, M., <u>Ashkenazi, A.</u>, and Presta, L. Design, Construction, and analyses of multivalent antibodies. *J. Immunol.* 170, 4854-4861 (2003).

68.   Varfolomeev, E., Kischkel, F., Martin, F., Wanh, H., Lawrence, D., Olsson, C., Tom, L., Erickson, S., French, D., Schow, P., Grewal, I. and <u>Ashkenazi, A.</u> Immune system development in APRIL knockout mice. Submitted.

Review articles:

1.   <u>Ashkenazi, A.,</u> Peralta, E., Winslow, J., Ramachandran, J., and Capon, D., J. Functional role of muscarinic acetylcholine receptor subtype diversity. *Cold Spring Harbor Symposium on Quantitative Biology.* LIII, 263-272 (1988).

2.   <u>Ashkenazi, A.</u>, Peralta, E., Winslow, J., Ramachandran, J., and Capon, D. Functional diversity of muscarinic receptor subtypes in cellular signal transduction and growth. *Trends Pharmacol. Sci.* Dec Supplement, 12-21 (1989).

3.   Chamow, S., Duliege, A., Ammann, A., Kahn, J.; Allen, D., Eichberg, J., Byrn, R., Capon, D., Ward, R., and <u>Ashkenazi, A.</u> CD4 immunoadhesins in anti-HIV therapy: new developments. *Int. J. Cancer* Supplement 7, 69-72 (1992).

4.   <u>Ashkenazi, A.</u>, Capon, and D. Ward, R. Immunoadhesins. *Int. Rev. Immunol.* 10, 217-225 (1993).

5.   <u>Ashkenazi, A.</u>, and Peralta, E. Muscarinic Receptors. In *Handbook of Receptors and Channels.* (S. Peroutka, ed.), CRC Press, Boca Raton, Vol. I, p. 1-27, (1994).

6.   Krantz, S. B., Means, R. T., Jr., Lina, J., Marsters, S. A., and <u>Ashkenazi, A.</u> Inhibition of erythroid colony formation in vitro by gamma interferon. In *Molecular Biology of Hematopoiesis* (N. Abraham, R. Shadduck, A. Levine F. Takaku, eds.) Intercept Ltd. Paris, Vol. 3, p. 135-147 (1994).

7.   <u>Ashkenazi, A.</u> Cytokine neutralization as a potential therapeutic approach for SIRS and shock. *J. Biotechnology in Healthcare* 1, 197-206 (1994).

8.   <u>Ashkenazi, A.</u>, and Chamow, S. M. Immunoadhesins: an alternative to human monoclonal antibodies. *Immunomethods: A companion to Methods in Enzimology* 8, 104-115 (1995).

9.   Chamow, S., and <u>Ashkenazi, A.</u> Immunoadhesins: Principles and Applications. *Trends Biotech.* 14, 52-60 (1996).

10.   <u>Ashkenazi, A.</u>, and Chamow, S. M. Immunoadhesins as research tools and therapeutic agents. *Curr. Opin. Immunol.* 9, 195-200 (1997).

11.   <u>Ashkenazi, A.</u>, and Dixit, V. Death receptors: signaling and modulation. *Science* 281, 1305-1308 (1998).

12.   <u>Ashkenazi, A.</u>, and Dixit, V. Apoptosis control by death and decoy receptors. *Curr. Opin. Cell. Biol.* 11, 255-260 (1999).

13. Ashkenazi, A. Chapters on Apo2L/TRAIL; DR4, DR5, DcR1, DcR2; and DcR3. Online Cytokine Handbook (www.apnet.com/cytokinereference/).

14. Ashkenazi, A. Targeting death and decoy receptors of the tumor necrosis factor superfamily. *Nature Rev. Cancer* 2, 420-430 (2002).

15. LeBlanc, H. and Ashkenazi, A. Apoptosis signaling by Apo2L/TRAIL. *Cell Death and Differentiation* 10, 66-75 (2003).

16. Almasan, A. and Ashkenazi, A. Apo2L/TRAIL: apoptosis signaling, biology, and potential for cancer therapy. Cytokine and Growth Factor Reviews 14, 337-348 (2003).

Book:

Antibody Fusion Proteins (Chamow, S., and Ashkenazi, A., eds., John Wiley and Sons Inc.) (1999).

Talks:

1. Resistance of primary HIV isolates to CD4 is independent of CD4-gp120 binding affinity. UCSD Symposium, HIV Disease: Pathogenesis and Therapy. Greenelefe, FL, March 1991.

2. Use of immuno-hybrids to extend the half-life of receptors. IBC conference on Biopharmaceutical Halflife Extension. New Orleans, LA, June 1992.

3. Results with TNF receptor Immunoadhesins for the Treatment of Sepsis. IBC conference on Endotoxemia and Sepsis. Philadelphia, PA, June 1992.

4. Immunoadhesins: an alternative to human antibodies. IBC conference on Antibody Engineering. San Diego, CA, December 1993.

5. Tumor necrosis factor receptor: a potential therapeutic for human septic shock. American Society for Microbiology Meeting, Atlanta, GA, May 1993.

6. Protective efficiacy of TNF receptor immunoadhesin vs anti-TNF monoclonal antibody in a rat model for endotoxic shock. 5th International Congress on TNF. Asilomar, CA, May 1994.

7. Interferon-γ signals via a multisubunit receptor complex that contains two types of polypeptide chain. American Association of Immunologists Conference. San Franciso, CA, July 1995.

8. Immunoadhesins: Principles and Applications. Gordon Research Conference on Drug Delivery in Biology and Medicine. Ventura, CA, February 1996.

9. Apo-2 Ligand, a new member of the TNF family that induces apoptosis in tumor cells. Cambridge Symposium on TNF and Related Cytokines in Treatment of Cancer. Hilton-Head, NC, March 1996.

10. Induction of apoptosis by Apo2 Ligand. American Society for Biochemistry and Molecular Biology, Symposium on Growth Factors and Cytokine Receptors. New Orleans, LA, June, 1996.

11. Apo2 ligand, an extracellular trigger of apoptosis. 2nd Clontech Symposium, Palo Alto, CA, October 1996.

12. Regulation of apoptosis by members of the TNF ligand and receptor families. Stanford University School of Medicine, Palo Alto, CA, December 1996.

13. Apo-3: a novel receptor that regulates cell death and inflammation. 4th International Congress on Immune Consequences of Trauma, Shock, and Sepsis. Munich, Germany, March 1997.

14. New members of the TNF ligand and receptor families that regulate apoptosis, inflammation, and immunity. UCLA School of Medicine, LA, CA, March 1997.

15. Immunoadhesins: an alternative to monoclonal antibodies. 5th World Conference on Bispecific Antibodies. Volendam, Holland, June 1997.

16. Control of Apo2L signaling. Cold Spring Harbor Laboratory Symposium on Programmed Cell Death. Cold Spring Harbor, New York. September, 1997.

17. Chairman and speaker, Apoptosis Signaling session. IBC's 4th Annual Conference on Apoptosis. San Diego, CA., October 1997.

18. Control of Apo2L signaling by death and decoy receptors. American Association for the Advancement of Science. Philladelphia, PA, February 1998.

19. Apo2 ligand and its receptors. American Society of Immunologists. San Francisco, CA, April 1998.

20. Death receptors and ligands. 7th International TNF Congress. Cape Cod, MA, May 1998.

21. Apo2L as a potential therapeutic for cancer. UCLA School of Medicine. LA, CA, June 1998.

22. Apo2L as a potential therapeutic for cancer. Gordon Research Conference on Cancer Chemotherapy. New London, NH, July 1998.

23. Control of apoptosis by Apo2L. Endocrine Society Conference, Stevenson, WA, August 1998.

24. Control of apoptosis by Apo2L. International Cytokine Society Conference, Jerusalem, Israel, October 1998.

25.   Apoptosis control by death and decoy receptors. American Association for Cancer Research Conference, Whistler, BC, Canada, March 1999.

26.   Apoptosis control by death and decoy receptors. American Society for Biochemistry and Molecular Biology Conference, San Francisco, CA, May 1999.

27.   Apoptosis control by death and decoy receptors. Gordon Research Conference on Apoptosis, New London, NH, June 1999.

28.   Apoptosis control by death and decoy receptors. Arthritis Foundation Research Conference, Alexandria GA, Aug 1999.

29.   Safety and anti-tumor activity of recombinant soluble Apo2L/TRAIL. Cold Spring Harbor Laboratory Symposium on Programmed Cell Death. . Cold Spring Harbor, NY, September 1999.

30.   The Apo2L/TRAIL system: therapeutic potential. American Association for Cancer Research, Lake Tahoe, NV, Feb 2000.

31.   Apoptosis and cancer therapy. Stanford University School of Medicine, Stanford, CA, Mar 2000.

32.   Apoptosis and cancer therapy. University of Pennsylvania School of Medicine, Philladelphia, PA, Apr 2000.

33.   Apoptosis signaling by Apo2L/TRAIL. International Congress on TNF. Trondheim, Norway, May 2000.

34.   The Apo2L/TRAIL system: therapeutic potential. Cap-CURE summit meeting. Santa Monica, CA, June 2000..

35.   The Apo2L/TRAIL system: therapeutic potential. MD Anderson Cancer Center. Houston, TX, June 2000.

36.   Apoptosis signaling by Apo2L/TRAIL. The Protein Society, 14th Symposium. San Diego, CA, August 2000.

37.   Anti-tumor activity of Apo2L/TRAIL. AAPS annual meeting. Indianapolis, IN Aug 2000.

38.   Apoptosis signaling and anti-cancer potential of Apo2L/TRAIL. Cancer Research Institute, UC San Francisco, CA, September 2000.

39.   Apoptosis signaling by Apo2L/TRAIL. Kenote address, TNF family Minisymposium, NIH. Bethesda, MD, September 2000.

40.   Death receptors: signaling and modulation. Keystone symposium on the Molecular basis of cancer. Taos, NM, Jan 2001.

41.   Preclinical studies of Apo2L/TRAIL in cancer. Symposium on Targeted therapies in the treatment of lung cancer. Aspen, CO, Jan 2001.

42. Apoptosis signaling by Apo2L/TRAIL. Wiezmann Institute of Science, Rehovot, Israel, March 2001.

43. Apo2L/TRAIL: Apoptosis signaling and potential for cancer therapy. Weizmann Institute of Science, Rehovot, Israel, March 2001.

44. Targeting death receptors in cancer with Apo2L/TRAIL. Cell Death and Disease conference, North Falmouth, MA, Jun 2001.

45. Targeting death receptors in cancer with Apo2L/TRAIL. Biotechnology Organization conference, San Diego, CA, Jun 2001.

46. Apo2L/TRAIL signaling and apoptosis resistance mechanisms. Gordon Research Conference on Apoptosis, Oxford, UK, July 2001.

47. Apo2L/TRAIL signaling and apoptosis resistance mechanisms. Cleveland Clinic Foundation, Cleveland, OH, Oct 2001.

48. Apoptosis signaling by death receptors: overview. International Society for Interferon and Cytokine Research conference, Cleveland, OH, Oct 2001.

49. Apoptosis signaling by death receptors. American Society of Nephrology Conference. San Francisco, CA, Oct 2001.

50. Targeting death receptors in cancer. Apoptosis: commercial opportunities. San Diego, CA, Apr 2002.

51. Apo2L/TRAIL signaling and apoptosis resistance mechanisms. Kimmel Cancer Research Center, Johns Hopkins University, Baltimore MD. May 2002.

52. Apoptosis control by Apo2L/TRAIL. (Keynote Address) University of Alabama Cancer Center Retreat, Birmingham, Ab. October 2002.

53. Apoptosis signaling by Apo2L/TRAIL. (Session co-chair) TNF international. conference. San Diego, CA. October 2002.

54. Apoptosis signaling by Apo2L/TRAIL. Swiss Institute for Cancer Research (ISREC). Lausanne, Swizerland. Jan 2003.

55. Apoptosis induction with Apo2L/TRAIL. Conference on New Targets and Innovative Strategies in Cancer Treatment. Monte Carlo. February 2003.

56. Apoptosis signaling by Apo2L/TRAIL. Hermelin Brain Tumor Center Symposium on Apoptosis. Detroit, MI. April 2003.

57. Targeting apoptosis through death receptors. Sixth Annual Conference on Targeted Therapies in the Treatment of Breast Cancer. Kona, Hawaii. July 2003.

58. Targeting apoptosis through death receptors. Second International Conference on Targeted Cancer Therapy. Washington, DC. Aug 2003.

Issued Patents:

1. Ashkenazi, A., Chamow, S. and Kogan, T. Carbohydrate-directed crosslinking reagents. US patent 5,329,028 (Jul 12, 1994).

2. Ashkenazi, A., Chamow, S. and Kogan, T. Carbohydrate-directed crosslinking reagents. US patent 5,605,791 (Feb 25, 1997).

3. Ashkenazi, A., Chamow, S. and Kogan, T. Carbohydrate-directed crosslinking reagents. US patent 5,889,155 (Jul 27, 1999).

4. Ashkenazi, A., APO-2 Ligand. US patent 6,030,945 (Feb 29, 2000).

5. Ashkenazi, A., Chuntharapai, A., Kim, J., APO-2 ligand antibodies. US patent 6,046, 048 (Apr 4, 2000).

6. Ashkenazi, A., Chamow, S. and Kogan, T. Carbohydrate-directed crosslinking reagents. US patent 6,124,435 (Sep 26, 2000).

7. Ashkenazi, A., Chuntharapai, A., Kim, J., Method for making monoclonal and cross-reactive antibodies. US patent 6,252,050 (Jun 26, 2001).

8. Ashkenazi, A. APO-2 Receptor. US patent 6,342,369 (Jan 29, 2002).

9. Ashkenazi, A. Fong, S., Goddard, A., Gurney, A., Napier, M., Tumas, D., Wood, W. A-33 polypeptides. US patent 6,410,708 (Jun 25, 2002).

10. Ashkenazi, A. APO-3 Receptor. US patent 6,462,176 B1 (Oct 8, 2002).

11. Ashkenazi, A. APO-2LI and APO-3 polypeptide antibodies. US patent 6,469,144 B1 (Oct 22, 2002).

12. Ashkenazi, A., Chamow, S. and Kogan, T. Carbohydrate-directed crosslinking reagents. US patent 6,582,928B1 (Jun 24, 2003).

Impact of DNA Amplification on Gene Expression Patterns in Breast Cancer[1,2]

Elizabeth Hyman,[3] Päivikki Kauraniemi,[3] Sampsa Hautaniemi, Maija Wolf, Spyro Mousses, Ester Rozenblum, Markus Ringnér, Guido Sauter, Outi Monni, Abdel Elkahloun, Olli-P. Kallioniemi, and Anne Kallioniemi[4]

Howard Hughes Medical Institute-NIH Research Scholar, Bethesda, Maryland 20892 [E. H.]; Cancer Genetics Branch, National Human Genome Research Institute, NIH, Bethesda, Maryland 20892 [E. H., P. K., S. H., M. W., S. M., E. R., M. R., A. E., O. K., A. K.]; Laboratory of Cancer Genetics, Institute of Medical Technology, University of Tampere and Tampere University Hospital, FIN-33520 Tampere, Finland [P. K., A. K.]; Signal Processing Laboratory, Tampere University of Technology, FIN-33101 Tampere, Finland [S. H.]; Institute of Pathology, University of Basel, CH-4003 Basel, Switzerland [G. S.]; and Biomedicum Biochip Center, Helsinki University Hospital, Biomedicum Helsinki, FIN-00014 Helsinki, Finland [O. M.]

ABSTRACT

Genetic changes underlie tumor progression and may lead to cancer-specific expression of critical genes. Over 1100 publications have described the use of comparative genomic hybridization (CGH) to analyze the pattern of copy number alterations in cancer, but very few of the genes affected are known. Here, we performed high-resolution CGH analysis on cDNA microarrays in breast cancer and directly compared copy number and mRNA expression levels of 13,824 genes to quantitate the impact of genomic changes on gene expression. We identified and mapped the boundaries of 24 independent amplicons, ranging in size from 0.2 to 12 Mb. Throughout the genome, both high- and low-level copy number changes had a substantial impact on gene expression, with 44% of the highly amplified genes showing overexpression and 10.5% of the highly overexpressed genes being amplified. Statistical analysis with random permutation tests identified 270 genes whose expression levels across 14 samples were systematically attributable to gene amplification. These included most previously described amplified genes in breast cancer and many novel targets for genomic alterations, including the *HOXB7* gene, the presence of which in a novel amplicon at 17q21.3 was validated in 10.2% of primary breast cancers and associated with poor patient prognosis. In conclusion, CGH on cDNA microarrays revealed hundreds of novel genes whose overexpression is attributable to gene amplification. These genes may provide insights to the clonal evolution and progression of breast cancer and highlight promising therapeutic targets.

INTRODUCTION

Gene expression patterns revealed by cDNA microarrays have facilitated classification of cancers into biologically distinct categories, some of which may explain the clinical behavior of the tumors (1–6). Despite this progress in diagnostic classification, the molecular mechanisms underlying gene expression patterns in cancer have remained elusive, and the utility of gene expression profiling in the identification of specific therapeutic targets remains limited.

Accumulation of genetic defects is thought to underlie the clonal evolution of cancer. Identification of the genes that mediate the effects of genetic changes may be important by highlighting transcripts that are actively involved in tumor progression. Such transcripts and their encoded proteins would be ideal targets for anticancer therapies, as demonstrated by the clinical success of new therapies against amplified oncogenes, such as *ERBB2* and *EGFR* (7, 8), in breast cancer and other solid tumors. Besides amplifications of known oncogenes, over
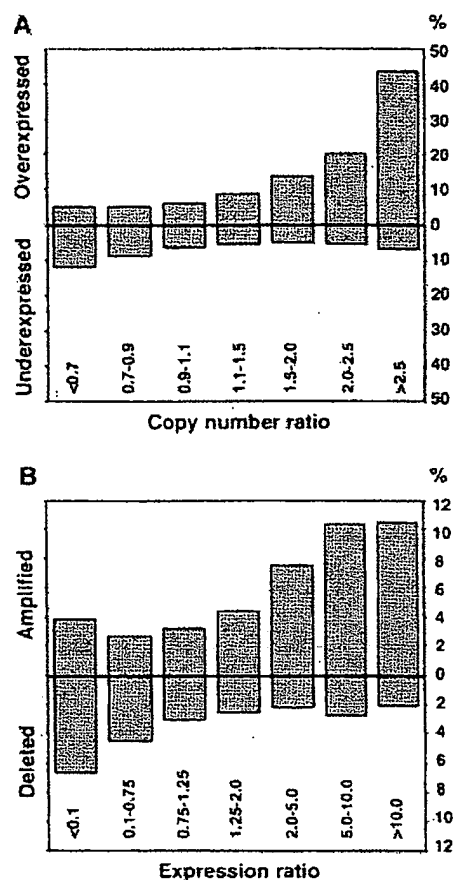

Fig. 1. Impact of gene copy number on global gene expression levels. *A*, percentage of over- and underexpressed genes (*Y axis*) according to copy number ratios (*X axis*). Threshold values used for over- and underexpression were >2.184 (global upper 7% of the cDNA ratios) and <0.4826 (global lower 7% of the expression ratios). *B*, percentage of amplified and deleted genes according to expression ratios. Threshold values for amplification and deletion were >1.5 and <0.7.

20 recurrent regions of DNA amplification have been mapped in breast cancer by CGH[5] (9, 10). However, these amplicons are often large and poorly defined, and their impact on gene expression remains unknown.

We hypothesized that genome-wide identification of those gene expression changes that are attributable to underlying gene copy number alterations would highlight transcripts that are actively involved in the causation or maintenance of the malignant phenotype. To identify such transcripts, we applied a combination of cDNA and CGH microarrays to: (*a*) determine the global impact that gene copy number variation plays in breast cancer development and progression; and (*b*) identify and characterize those genes whose mRNA expres-

[5] The abbreviations used are: CGH, comparative genomic hybridization; FISH, fluorescence *in situ* hybridization; RT-PCR, reverse transcription-PCR.
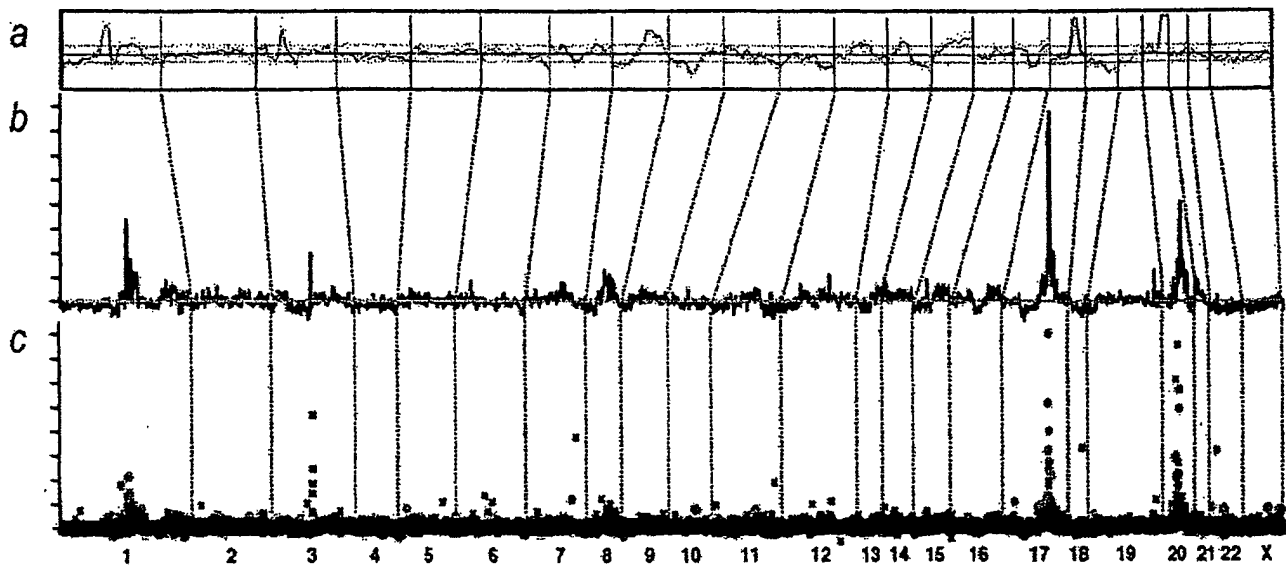
Fig. 2. Genome-wide copy number and expression analysis in the MCF-7 breast cancer cell line. *A*, chromosomal CGH analysis of MCF-7. The copy number ratio profile (*blue line*) across the entire genome from 1p telomere to Xq telomere is shown along with ±1 SD (*orange lines*). The *black horizontal line* indicates a ratio of 1.0; *red line*, a ratio of 0.8; and *green line*, a ratio of 1.2. *B–C*, genome-wide copy number analysis in MCF-7 by CGH on cDNA microarray. The copy number ratios were plotted as a function of the position of the cDNA clones along the human genome. In *B*, individual data points are connected with a line, and a moving median of 10 adjacent clones is shown. *Red horizontal line*, the copy number ratio of 1.0. In *C*, individual data points are labeled by color coding according to cDNA expression ratios. The *bright red dots* indicate the upper 2%, and *dark red dots*, the next 5% of the expression ratios in MCF-7 cells (overexpressed genes); *bright green dots* indicate the lowest 2%, and *dark green dots*, the next 5% of the expression ratios (underexpressed genes); the rest of the observations are shown with *black crosses*. The chromosome numbers are shown at the *bottom* of the figure, and chromosome boundaries are indicated with a *dashed line*.

sion is most significantly associated with amplification of the corresponding genomic template.

MATERIALS AND METHODS

Breast Cancer Cell Lines. Fourteen breast cancer cell lines (BT-20, BT-474, HCC1428, Hs578t, MCF7, MDA-361, MDA-436, MDA-453, MDA-468, SKBR-3, T-47D, UACC812, ZR-75-1, and ZR-75-30) were obtained from the American Type Culture Collection (Manassas, VA). Cells were grown under recommended culture conditions. Genomic DNA and mRNA were isolated using standard protocols.

Copy Number and Expression Analyses by cDNA Microarrays. The preparation and printing of the 13,824 cDNA clones on glass slides were performed as described (11–13). Of these clones, 244 represented uncharacterized expressed sequence tags, and the remainder corresponded to known genes. CGH experiments on cDNA microarrays were done as described (14, 15). Briefly, 20 µg of genomic DNA from breast cancer cell lines and normal human WBCs were digested for 14–18 h with *Alu*I and *Rsa*I (Life Technologies, Inc., Rockville, MD) and purified by phenol/chloroform extraction. Six µg of digested cell line DNAs were labeled with Cy3-dUTP (Amersham Pharmacia) and normal DNA with Cy5-dUTP (Amersham Pharmacia) using the Bioprime Labeling kit (Life Technologies, Inc.). Hybridization (14, 15) and posthybridization washes (13) were done as described. For the expression analyses, a standard reference (Universal Human Reference RNA; Stratagene, La Jolla, CA) was used in all experiments. Forty µg of reference RNA were labeled with Cy3-dUTP and 3.5 µg of test mRNA with Cy5-dUTP, and the labeled cDNAs were hybridized on microarrays as described (13, 15). For both microarray analyses, a laser confocal scanner (Agilent Technologies, Palo Alto, CA) was used to measure the fluorescence intensities at the target locations using the DEARRAY software (16). After background subtraction, average intensities at each clone in the test hybridization were divided by the average intensity of the corresponding clone in the control hybridization. For the copy number analysis, the ratios were normalized on the basis of the distribution of ratios of all targets on the array and for the expression analysis on the basis of 88 housekeeping genes, which were spotted four times onto the array. Low quality measurements (*i.e.*, copy number data with mean reference intensity <100 fluorescent units, and expression data with both test and reference intensity <100 fluorescent units and/or with spot size <50 units)

were excluded from the analysis and were treated as missing values. The distributions of fluorescence ratios were used to define cutpoints for increased/decreased copy number. Genes with CGH ratio >1.43 (representing the upper 5% of the CGH ratios across all experiments) were considered to be amplified, and genes with ratio <0.73 (representing the lower 5%) were considered to be deleted.

Statistical Analysis of CGH and cDNA Microarray Data. To evaluate the influence of copy number alterations on gene expression, we applied the following statistical approach. CGH and cDNA calibrated intensity ratios were log-transformed and normalized using median centering of the values in each cell line. Furthermore, cDNA ratios for each gene across all 14 cell lines were median centered. For each gene, the CGH data were represented by a vector that was labeled 1 for amplification (ratio, >1.43) and 0 for no amplification. Amplification was correlated with gene expression using the signal-to-noise statistics (1). We calculated a weight, w_g, for each gene as follows:

$$w_g = \frac{m_{g1} - m_{g0}}{\sigma_{g1} + \sigma_{g0}}$$

where m_{g1}, σ_{g1} and m_{g0}, σ_{g0} denote the means and SDs for the expression levels for amplified and nonamplified cell lines, respectively. To assess the statistical significance of each weight, we performed 10,000 random permutations of the label vector. The probability that a gene had a larger or equal weight by random permutation than the original weight was denoted by α. A low α (<0.05) indicates a strong association between gene expression and amplification.

Genomic Localization of cDNA Clones and Amplicon Mapping. Each cDNA clone on the microarray was assigned to a Unigene cluster using the Unigene Build 141.[6] A database of genomic sequence alignment information for mRNA sequences was created from the August 2001 freeze of the University of California Santa Cruz's GoldenPath database.[7] The chromosome and bp positions for each cDNA clone were then retrieved by relating these data sets. Amplicons were defined as a CGH copy number ratio >2.0 in at least two adjacent clones in two or more cell lines or a CGH ratio >2.0 in at least three adjacent clones in a single cell line. The amplicon start and end positions were

Table 1 *Summary of independent amplicons in 14 breast cancer cell lines by CGH microarray*

Location	Start (Mb)	End (Mb)	Size (Mb)
1p13	132.79	132.94	0.2
1q21	173.92	177.25	3.3
1q22	179.28	179.57	0.3
3p14	71.94	74.66	2.7
7p12.1–7p11.2	55.62	60.95	5.3
7q31	125.73	130.96	5.2
7q32	140.01	140.68	0.7
8q21.11–8q21.13	86.45	92.46	6.0
8q21.3	98.45	103.05	4.6
8q23.3–8q24.14	129.88	142.15	12.3
8q24.22	151.21	152.16	1.0
9p13	38.65	39.25	0.6
13q22–q31	77.15	81.38	4.2
16q22	86.70	87.62	0.9
17q11	29.30	30.85	1.6
17q12–q21.2	39.79	42.80	3.0
17q21.32–q21.33	52.47	55.80	3.3
17q22–q23.3	63.81	69.70	5.9
17q23.3–q24.3	69.93	74.99	5.1
19q13	40.63	41.40	0.8
20q11.22	34.59	35.85	1.3
20q13.12	44.00	45.62	1.6
20q13.12–q13.13	46.45	49.43	3.0
20q13.2–q13.32	51.32	59.12	7.8

extended to include neighboring nonamplified clones (ratio, <1.5). The amplicon size determination was partially dependent on local clone density.

FISH. Dual-color interphase FISH to breast cancer cell lines was done as described (17). Bacterial artificial chromosome clone RP11-361K8 was labeled with SpectrumOrange (Vysis, Downers Grove, IL), and Spectrum-Orange-labeled probe for *EGFR* was obtained from Vysis. SpectrumGreen-labeled chromosome 7 and 17 centromere probes (Vysis) were used as a reference. A tissue microarray containing 612 formalin-fixed, paraffin-embedded primary breast cancers (17) was applied in FISH analyses as described (18). The use of these specimens was approved by the Ethics Committee of the University of Basel and by the NIH. Specimens containing a 2-fold or higher increase in the number of test probe signals, as compared with corresponding centromere signals, in at least 10% of the tumor cells were considered to be amplified. Survival analysis was performed using the Kaplan-Meier method and the log-rank test.

RT-PCR. The *HOXB7* expression level was determined relative to *GAPDH.* Reverse transcription and PCR amplification were performed using Access RT-PCR System (Promega Corp., Madison, WI) with 10 ng of mRNA as a template. *HOXB7* primers were 5'-GAGCAGAGGGACTCGGACTT-3' and 5'-GCGTCAGGTAGCGATTGTAG-3'.

RESULTS

Global Effect of Copy Number on Gene Expression. 13,824 arrayed cDNA clones were applied for analysis of gene expression and gene copy number (CGH microarrays) in 14 breast cancer cell lines. The results illustrate a considerable influence of copy number on gene expression patterns. Up to 44% of the highly amplified transcripts (CGH ratio, >2.5) were overexpressed (*i.e.,* belonged to the global upper 7% of expression ratios), compared with only 6% for genes with normal copy number levels (Fig. 1A). Conversely, 10.5% of the transcripts with high-level expression (cDNA ratio, >10) showed increased copy number (Fig. 1B). Low-level copy number increases and decreases were also associated with similar, although less dramatic, outcomes on gene expression (Fig. 1).

Identification of Distinct Breast Cancer Amplicons. Base-pair locations obtained for 11,994 cDNAs (86.8%) were used to plot copy number changes as a function of genomic position (Fig. 2, Supplement Fig. A). The average spacing of clones throughout the genome was 267 kb. This high-resolution mapping identified 24 independent breast cancer amplicons, spanning from 0.2 to 12 Mb of DNA (Table 1). Several amplification sites detected previously by chromosomal

CGH were validated, with 1q21, 17q12–q21.2, 17q22–q23, 20q13.1, and 20q13.2 regions being most commonly amplified. Furthermore, the boundaries of these amplicons were precisely delineated. In addition, novel amplicons were identified at 9p13 (38.65–39.25 Mb), and 17q21.3 (52.47–55.80 Mb).

Direct Identification of Putative Amplification Target Genes. The cDNA/CGH microarray technique enables the direct correlation of copy number and expression data on a gene-by-gene basis throughout the genome. We directly annotated high-resolution CGH plots with gene expression data using color coding. Fig. 2C shows that most of the amplified genes in the MCF-7 breast cancer cell line at 1p13, 17q22–q23, and 20q13 were highly overexpressed. A view of chromosome 7 in the MDA-468 cell line implicates *EGFR* as the most highly overexpressed and amplified gene at 7p11–p12 (Fig. 3A). In BT-474, the two known amplicons at 17q12 and 17q22–q23 contained numerous highly overexpressed genes (Fig. 3B). In addition, several genes, including the homeobox genes *HOXB2* and *HOXB7,* were highly amplified in a previously undescribed independent amplicon at 17q21.3. *HOXB7* was systematically amplified (as validated by FISH, Fig. 3B, inset) as well as overexpressed (as verified by RT-PCR, data not shown) in BT-474, UACC812, and ZR-75-30 cells. Furthermore, this novel
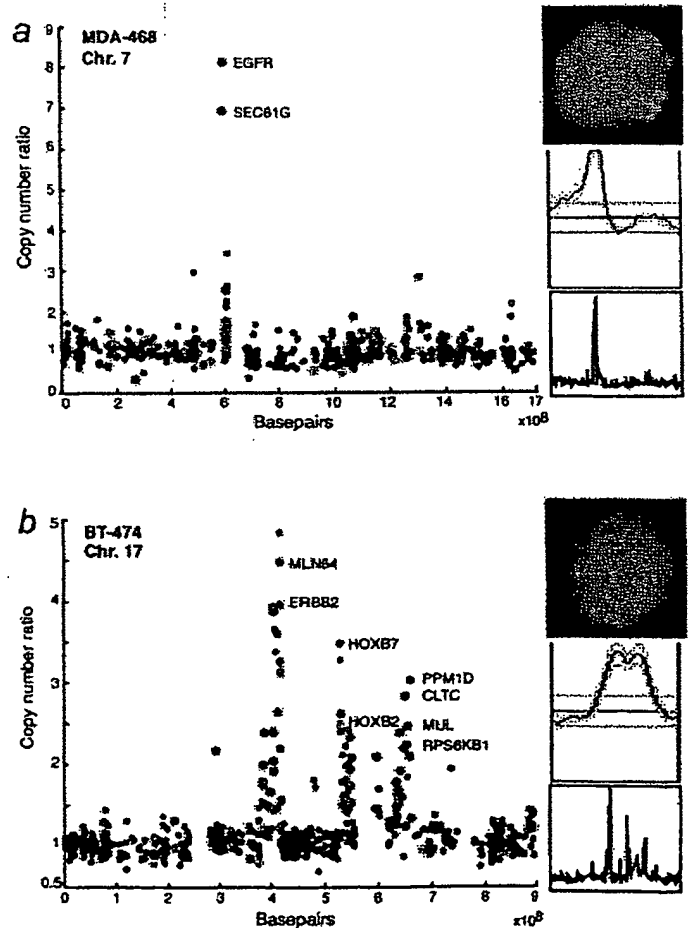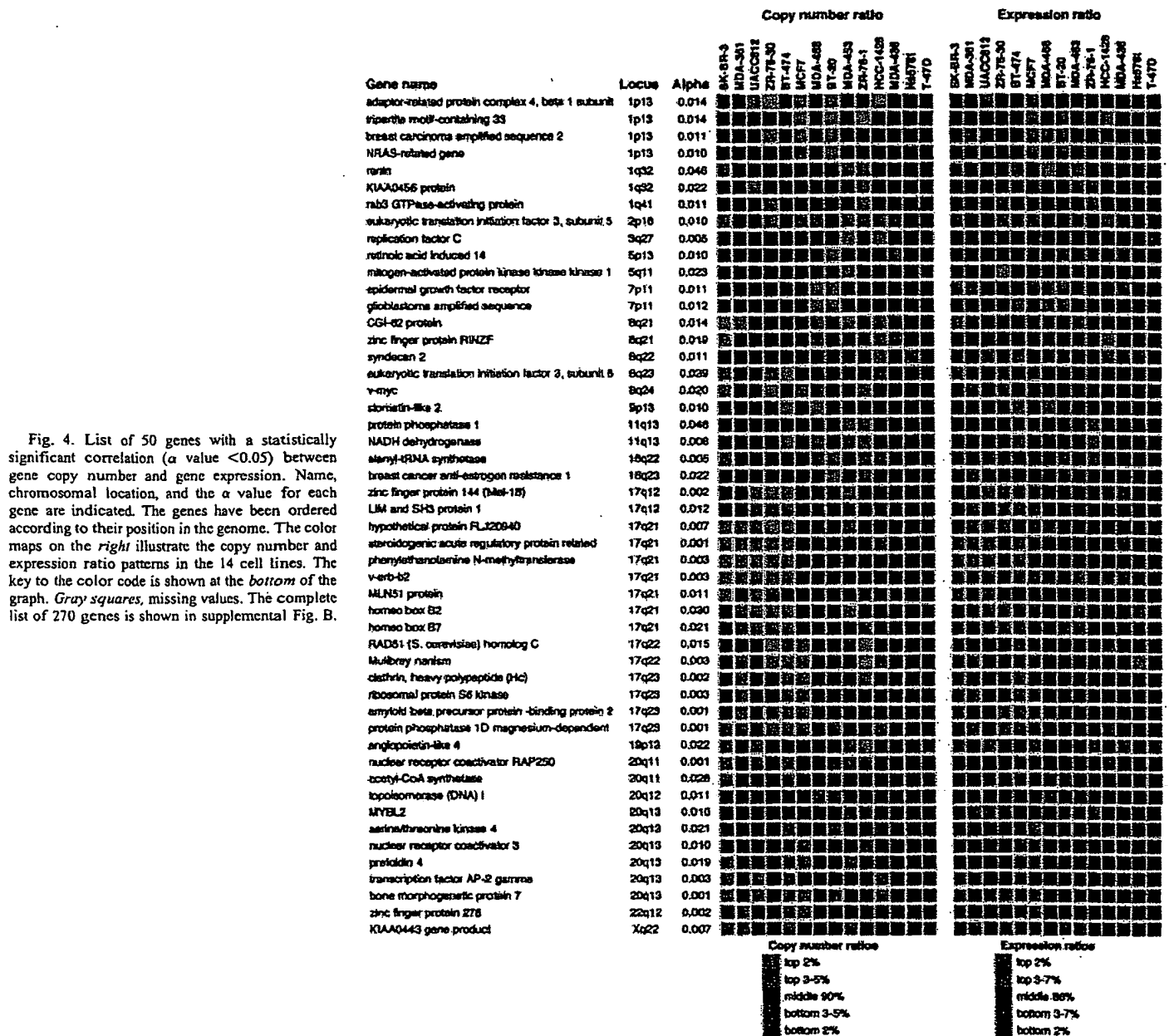

Fig. 3. Annotation of gene expression data on CGH microarray profiles. *A,* genes in the 7p11-p12 amplicon in the MDA-468 cell line are highly expressed (*red dots*) and include the *EGFR* oncogene. *B,* several genes in the 17q12, 17q21.3, and 17q23 amplicons in the BT-474 breast cancer cell line are highly overexpressed (*red*) and include the *HOXB7* gene. The data labels and color coding are as indicated for Fig. 2C. *Insets* show chromosomal CGH profiles for the corresponding chromosomes and validation of the increased copy number by interphase FISH using *EGFR* (*red*) and chromosome 7 centromere probe (*green*) to MDA-468 (*A*) and *HOXB7*-specific probe (*red*) and chromosome 17 centromere (*green*) to BT-474 cells (*B*).

Fig. 4. List of 50 genes with a statistically significant correlation (α value <0.05) between gene copy number and gene expression. Name, chromosomal location, and the α value for each gene are indicated. The genes have been ordered according to their position in the genome. The color maps on the *right* illustrate the copy number and expression ratio patterns in the 14 cell lines. The key to the color code is shown at the *bottom* of the graph. *Gray squares*, missing values. The complete list of 270 genes is shown in supplemental Fig. B.

amplification was validated to be present in 10.2% of 363 primary breast cancers by FISH to a tissue microarray and was associated with poor prognosis of the patients ($P = 0.001$).

Statistical Identification and Characterization of 270 Highly Expressed Genes in Amplicons. Statistical comparison of expression levels of all genes as a function of gene amplification identified 270 genes whose expression was significantly influenced by copy number across all 14 cell lines (Fig. 4, Supplemental Fig. B). According to the gene ontology data,[8] 91 of the 270 genes represented hypothetical proteins or genes with no functional annotation, whereas 179 had associated functional information available. Of these, 151 (84%) are implicated in apoptosis, cell proliferation, signal transduction, and transcription, whereas 28 (16%) had functional annotations that could not be directly linked with cancer.

DISCUSSION

The importance of recurrent gene and chromosome copy number changes in the development and progression of solid tumors has been characterized in >1000 publications applying CGH[9] (9, 10), as well as in a large number of other molecular cytogenetic, cytogenetic, and molecular genetic studies. The effects of these somatic genetic changes on gene expression levels have remained largely unknown, although a few studies have explored gene expression changes occurring in specific amplicons (15, 19–21). Here, we applied genome-wide cDNA microarrays to identify transcripts whose expression changes were attributable to underlying gene copy number alterations in breast cancer.

The overall impact of copy number on gene expression patterns was substantial with the most dramatic effects seen in the case of high-

---

[8] Internet address: http://www.geneontology.org/.

[9] Internet address: http://www.ncbi.nlm.nih.gov/entrez.

level copy number increase. Low-level copy number gains and losses also had a significant influence on expression levels of genes in the regions affected, but these effects were more subtle on a gene-by-gene basis than those of high-level amplifications. However, the impact of low-level gains on the dysregulation of gene expression patterns in cancer may be equally important if not more important than that of high-level amplifications. Aneuploidy and low-level gains and losses of chromosomal arms represent the most common types of genetic alterations in breast and other cancers and, therefore, have an influence on many genes. Our results in breast cancer extend the recent studies on the impact of aneuploidy on global gene expression patterns in yeast cells, acute myeloid leukemia, and a prostate cancer model system (22–24).

The CGH microarray analysis identified 24 independent breast cancer amplicons. We defined the precise boundaries for many amplicons detected previously by chromosomal CGH (9, 10, 25, 26) and also discovered novel amplicons that had not been detected previously, presumably because of their small size (only 1–2 Mb) or close proximity to other larger amplicons. One of these novel amplicons involved the homeobox gene region at 17q21.3 and led to the overexpression of the *HOXB7* and *HOXB2* genes. The homeodomain transcription factors are known to be key regulators of embryonic development and have been occasionally reported to undergo aberrant expression in cancer (27, 28). *HOXB7* transfection induced cell proliferation in melanoma, breast, and ovarian cancer cells and increased tumorigenicity and angiogenesis in breast cancer (29–32). The present results imply that gene amplification may be a prominent mechanism for overexpressing *HOXB7* in breast cancer and suggest that *HOXB7* contributes to tumor progression and confers an aggressive disease phenotype in breast cancer. This view is supported by our finding of amplification of *HOXB7* in 10% of 363 primary breast cancers, as well as an association of amplification with poor prognosis of the patients.

We carried out a systematic search to identify genes whose expression levels across all 14 cell lines were attributable to amplification status. Statistical analysis revealed 270 such genes (representing ~2% of all genes on the array), including not only previously described amplified genes, such as *HER-2, MYC, EGFR*, ribosomal protein s6 kinase, and *AIB3*, but also numerous novel genes such as *NRAS-related gene* (1p13), *syndecan-2* (8q22), and *bone morphogenic protein* (20q13.1), whose activation by amplification may similarly promote breast cancer progression. Most of the 270 genes have not been implicated previously in breast cancer development and suggest novel pathogenetic mechanisms. Although we would not expect all of them to be causally involved, it is intriguing that 84% of the genes with associated functional information were implicated in apoptosis, cell proliferation, signal transduction, transcription, or other cellular processes that could directly imply a possible role in cancer progression. Therefore, a detailed characterization of these genes may provide biological insights to breast cancer progression and might lead to the development of novel therapeutic strategies.

In summary, we demonstrate application of cDNA microarrays to the analysis of both copy number and expression levels of over 12,000 transcripts throughout the breast cancer genome, roughly once every 267 kb. This analysis provided: (a) evidence of a prominent global influence of copy number changes on gene expression levels; (b) a high-resolution map of 24 independent amplicons in breast cancer; and (c) identification of a set of 270 genes, the overexpression of which was statistically attributable to gene amplification. Characterization of a novel amplicon at 17q21.3 implicated amplification and overexpression of the *HOXB7* gene in breast cancer, including a clinical association

between *HOXB7* amplification and poor patient prognosis. Overall, our results illustrate how the identification of genes activated by gene amplification provides a powerful approach to highlight genes with an important role in cancer as well as to prioritize and validate putative targets for therapy development.

REFERENCES

1. Golub, T. R., Slonim, D. K., Tamayo, P., Huard, C., Gaasenbeek, M., Mesirov, J. P., Coller, H., Loh, M. L., Downing, J. R., Caligiuri, M. A., Bloomfield, C. D., and Lander, E. S. Molecular classification of cancer: class discovery and class prediction by gene expression monitoring. Science (Wash. DC), *286:* 531–537, 1999.
2. Alizadeh, A. A., Eisen, M. B., Davis, R. E., Ma, C., Lossos, I. S., Rosenwald, A., Boldrick, J. C., Sabet, H., Tran, T., Yu, X., *et al.* Distinct types of diffuse large B-cell lymphoma identified by gene expression profiling. Nature (Lond.), *403:* 503–511, 2000.
3. Bittner, M., Meltzer, P., Chen, Y., Jiang, Y., Seftor, E., Hendrix, M., Radmacher, M., Simon, R., Yakhini, Z., Ben-Dor, A., *et al.* Molecular classification of cutaneous malignant melanoma by gene expression profiling. Nature (Lond.), *406:* 536–540, 2000.
4. Perou, C. M., Sorlie, T., Eisen, M. B., van de Rijn, M., Jeffrey, S. S., Rees, C. A., Pollack, J. R., Ross, D. T., Johnsen, H., Akslen, L. A., *et al.* Molecular portraits of human breast tumours. Nature (Lond.), *406:* 747–752, 2000.
5. Dhanasekaran, S. M., Barrette, T. R., Ghosh, D., Shah, R., Varambally, S., Kurachi, K., Pienta, K. J., Rubin, M. A., and Chinnaiyan, A. M. Delineation of prognostic biomarkers in prostate cancer. Nature (Lond.), *412:* 822–826, 2001.
6. Sorlie, T., Perou, C. M., Tibshirani, R., Aas, T., Geisler, S., Johnsen, H., Hastie, T., Eisen, M. B., van de Rijn, M., Jeffrey, S. S., *et al.* Gene expression patterns of breast carcinomas distinguish tumor subclasses with clinical implications. Proc. Natl. Acad. Sci. USA, *98:* 10869–10874, 2001.
7. Ross, J. S., and Fletcher, J. A. The *HER-2/neu* oncogene: prognostic factor, predictive factor and target for therapy. Semin. Cancer Biol., *9:* 125–138, 1999.
8. Arteaga, C. L. The epidermal growth factor receptor: from mutant oncogene in nonhuman cancers to therapeutic target in human neoplasia. J. Clin. Oncol., *19:* 32–40, 2001.
9. Knuutila, S., Bjorkqvist, A. M., Autio, K., Tarkkanen, M., Wolf, M., Monni, O., Szymanska, J., Larramendy, M. L., Tapper, J., Pere, H., El-Rifai, W., *et al.* DNA copy number amplifications in human neoplasms: review of comparative genomic hybridization studies. Am. J. Pathol., *152:* 1107–1123, 1998.
10. Knuutila S., Autio K., and Aalto Y. Online access to CGH data of DNA sequence copy number changes. Am. J. Pathol., *157:* 689, 2000.
11. DeRisi, J., Penland, L., Brown, P. O., Bittner, M. L., Meltzer, P. S., Ray, M., Chen, Y., Su, Y. A., and Trent, J. M. Use of a cDNA microarray to analyse gene expression patterns in human cancer. Nat. Genet., *14:* 457–460, 1996.
12. Shalon, D., Smith, S. J., and Brown, P. O. A DNA microarray system for analyzing complex DNA samples using two-color fluorescent probe hybridization. Genome Res., *6:* 639–645, 1996.
13. Mousses, S., Bittner, M. L., Chen, Y., Dougherty, E. R., Baxevanis, A., Meltzer, P. S., and Trent, J. M. Gene expression analysis by cDNA microarrays. *In:* F. J. Livesey and S. P. Hunt (eds.), Functional Genomics, pp. 113–137. Oxford: Oxford University Press, 2000.
14. Pollack, J. R., Perou, C. M., Alizadeh, A. A., Eisen, M. B., Pergamenschikov, A., Williams, C. F., Jeffrey, S. S., Botstein, D., and Brown, P. O. Genome-wide analysis of DNA copy-number changes using cDNA microarrays. Nat. Genet., *23:* 41–46, 1999.
15. Monni, O., Bärlund, M., Mousses, S., Kononen, J., Sauter, G., Heiskanen, M., Paavola, P., Avela, K., Chen, Y., Bittner, M. L., and Kallioniemi, A. Comprehensive copy number and gene expression profiling of the 17q23 amplicon in human breast cancer. Proc. Natl. Acad. Sci. USA, *98:* 5711–5716, 2001.
16. Chen, Y., Dougherty, E. R., and Bittner, M. L. Ratio-based decisions and the quantitative analysis of cDNA microarray images. J. Biomed. Optics, *2:* 364–374, 1997.
17. Bärlund, M., Forozan, F., Kononen, J., Bubendorf, L., Chen, Y., Bittner, M. L., Torhorst, J., Haas, P., Bucher, C., Sauter, G., *et al.* Detecting activation of ribosomal protein S6 kinase by complementary DNA and tissue microarray analysis. J. Natl. Cancer Inst., *92:* 1252–1259, 2000.
18. Andersen, C. L., Hostetter, G., Grigoryan, A., Sauter, G., and Kallioniemi, A. Improved procedure for fluorescence *in situ* hybridization on tissue microarrays. Cytometry, *45:* 83–86, 2001.
19. Kauraniemi, P., Bärlund, M., Monni, O., and Kallioniemi, A. New amplified and highly expressed genes discovered in the ERBB2 amplicon in breast cancer by cDNA microarrays. Cancer Res., *61:* 8235–8240, 2001.
20. Clark, J., Edwards, S., John, M., Flohr, P., Gordon, T., Maillard, K., Giddings, I., Brown, C., Bagherzadeh, A., Campbell, C., Shipley, J., Wooster, R., and Cooper, C. S. Identification of amplified and expressed genes in breast cancer by comparative hybridization onto microarrays of randomly selected cDNA clones. Genes Chromosomes Cancer, *34:* 104–114, 2002.
21. Varis, A., Wolf, M., Monni, O., Vakkari, M. L., Kokkola, A., Moskaluk, C., Frierson, H., Powell, S. M., Knuutila, S., Kallioniemi, A., and El-Rifai, W. Targets of gene amplification and overexpression at 17q in gastric cancer. Cancer Res., *62:* 2625–2629, 2002.
22. Hughes, T. R., Roberts, C. J., Dai, H., Jones, A. R., Meyer, M. R., Slade, D., Burchard, J., Dow, S., Ward, T. R., Kidd, M. J., Friend, S. H., and Marton M. J.

Widespread aneuploidy revealed by DNA microarray expression profiling. Nat. Genet., *25:* 333–337, 2000.

23. Virtaneva, K., Wright, F. A., Tanner, S. M., Yuan, B., Lemon, W. J., Caligiuri, M. A., Bloomfield, C. D., de La Chapelle, A., and Krahe, R. Expression profiling reveals fundamental biological differences in acute myeloid leukemia with isolated trisomy 8 and normal cytogenetics. Proc. Natl. Acad. Sci. USA, *98:* 1124–1129, 2001.

24. Phillips, J. L., Hayward, S. W., Wang, Y., Vasselli, J., Pavlovich, C., Padilla-Nash, H., Pezullo, J. R., Ghadimi, B. M., Grossfeld, G. D., Rivera, A., Linehan, W. M., Cunha, G. R., and Ried, T. The consequences of chromosomal aneuploidy on gene expression profiles in a cell line model for prostate carcinogenesis. Cancer Res., *61:* 8143–8149, 2001.

25. Bärlund, M., Tirkkonen, M., Forozan, F., Tanner, M. M., Kallioniemi, O. P., and Kallioniemi, A. Increased copy number at 17q22–q24 by CGH in breast cancer is due to high-level amplification of two separate regions. Genes Chromosomes Cancer, *20:* 372–376, 1997.

26. Tanner, M. M., Tirkkonen, M., Kallioniemi, A., Isola, J., Kuukasjärvi, T., Collins, C., Kowbel, D., Guan, X. Y., Trent, J., Gray, J. W., Meltzer, P., and Kallioniemi O. P. Independent amplification and frequent co-amplification of three nonsyntenic regions on the long arm of chromosome 20 in human breast cancer. Cancer Res., *56:* 3441–3445, 1996.

27. Cillo, C., Faiella, A., Cantile, M., and Boncinelli, E. Homeobox genes and cancer. Exp. Cell Res., *248:* 1–9, 1999.

28. Cillo, C., Cantile, M., Faiella, A., and Boncinelli, E. Homeobox genes in normal and malignant cells. J. Cell. Physiol., *188:* 161–169, 2001.

29. Care, A., Silvani, A., Meccia, E., Mattia, G., Stoppacciaro, A., Parmiani, G., Peschle, C., and Colombo, M. P. HOXB7 constitutively activates basic fibroblast growth factor in melanomas. Mol. Cell. Biol., *16:* 4842–4851, 1996.

30. Care, A., Silvani, A., Meccia, E., Mattia, G., Peschle, C., and Colombo, M. P. Transduction of the SkBr3 breast carcinoma cell line with the *HOXB7* gene induces bFGF expression, increases cell proliferation and reduces growth factor dependence. Oncogene, *16:* 3285–3289, 1998.

31. Care, A., Felicetti, F., Meccia, E., Bottero, L., Parenza, M., Stoppacciaro, A., Peschle, C., and Colombo, M. P. HOXB7: a key factor for tumor-associated angiogenic switch. Cancer Res., *61:* 6532–6539, 2001.

32. Naora, H., Yang, Y. Q., Montz, F. J., Seidman, J. D., Kurman, R. J., and Roden, R. B. A serologically identified tumor antigen encoded by a homeobox gene promotes growth of ovarian epithelial cells. Proc. Natl. Acad. Sci. USA, *98:* 4060–4065, 2001.

Microarray analysis reveals a major direct role of DNA copy number alteration in the transcriptional program of human breast tumors

Jonathan R. Pollack[*†‡], Therese Sørlie[§], Charles M. Perou[¶], Christian A. Rees[‖**], Stefanie S. Jeffrey[††], Per E. Lonning[‡‡], Robert Tibshirani[§§], David Botstein[‖], Anne-Lise Børresen-Dale[§], and Patrick O. Brown[†¶¶]

Departments of *Pathology, ‖Genetics, ††Surgery, §§Health Research and Policy, and ¶¶Biochemistry, and †Howard Hughes Medical Institute, Stanford University School of Medicine, Stanford, CA 94305; §Department of Genetics, Norwegian Radium Hospital, Montebello, N-0310 Oslo, Norway; ‡‡Department of Medicine (Oncology), Haukeland University Hospital, N-5021 Bergen, Norway; and ¶Department of Genetics and Lineberger Comprehensive Cancer Center, University of North Carolina, Chapel Hill, NC 27599

Genomic DNA copy number alterations are key genetic events in the development and progression of human cancers. Here we report a genome-wide microarray comparative genomic hybridization (array CGH) analysis of DNA copy number variation in a series of primary human breast tumors. We have profiled DNA copy number alteration across 6,691 mapped human genes, in 44 predominantly advanced, primary breast tumors and 10 breast cancer cell lines. While the overall patterns of DNA amplification and deletion corroborate previous cytogenetic studies, the high-resolution (gene-by-gene) mapping of amplicon boundaries and the quantitative analysis of amplicon shape provide significant improvement in the localization of candidate oncogenes. Parallel microarray measurements of mRNA levels reveal the remarkable degree to which variation in gene copy number contributes to variation in gene expression in tumor cells. Specifically, we find that 62% of highly amplified genes show moderately or highly elevated expression, that DNA copy number influences gene expression across a wide range of DNA copy number alterations (deletion, low-, mid- and high-level amplification), that on average, a 2-fold change in DNA copy number is associated with a corresponding 1.5-fold change in mRNA levels, and that overall, at least 12% of all the variation in gene expression among the breast tumors is directly attributable to underlying variation in gene copy number. These findings provide evidence that widespread DNA copy number alteration can lead directly to global deregulation of gene expression, which may contribute to the development or progression of cancer.

Conventional cytogenetic techniques, including comparative genomic hybridization (CGH) (1), have led to the identification of a number of recurrent regions of DNA copy number alteration in breast cancer cell lines and tumors (2–4). While some of these regions contain known or candidate oncogenes [e.g., FGFR1 (8p11), MYC (8q24), CCND1 (11q13), ERBB2 (17q12), and ZNF217 (20q13)] and tumor suppressor genes [RB1 (13q14) and TP53 (17p13)], the relevant gene(s) within other regions (e.g., gain of 1q, 8q22, and 17q22–24, and loss of 8p) remain to be identified. A high-resolution genome-wide map, delineating the boundaries of DNA copy number alterations in tumors, should facilitate the localization and identification of oncogenes and tumor suppressor genes in breast cancer. In this study, we have created such a map, using array-based CGH (5–7) to profile DNA copy number alteration in a series of breast cancer cell lines and primary tumors.

An unresolved question is the extent to which the widespread DNA copy number changes that we and others have identified in breast tumors alter expression of genes within involved regions. Because we had measured mRNA levels in parallel in the same samples (8), using the same DNA microarrays, we had an opportunity to explore on a genomic scale the relationship between DNA copy number changes and gene expression. From

this analysis, we have identified a significant impact of widespread DNA copy number alteration on the transcriptional programs of breast tumors.

Materials and Methods

Tumors and Cell Lines. Primary breast tumors were predominantly large (>3 cm), intermediate-grade, infiltrating ductal carcinomas, with more than 50% being lymph node positive. The fraction of tumor cells within specimens averaged at least 50%. Details of individual tumors have been published (8, 9), and are summarized in Table 1, which is published as supporting information on the PNAS web site, www.pnas.org. Breast cancer cell lines were obtained from the American Type Culture Collection. Genomic DNA was isolated either using Qiagen genomic DNA columns, or by phenol/chloroform extraction followed by ethanol precipitation.

DNA Labeling and Microarray Hybridizations. Genomic DNA labeling and hybridizations were performed essentially as described in Pollack et al. (7), with slight modifications. Two micrograms of DNA was labeled in a total volume of 50 microliters and the volumes of all reagents were adjusted accordingly. "Test" DNA (from tumors and cell lines) was fluorescently labeled (Cy5) and hybridized to a human cDNA microarray containing 6,691 different mapped human genes (i.e., UniGene clusters). The "reference" (labeled with Cy3) for each hybridization was normal female leukocyte DNA from a single donor. The fabrication of cDNA microarrays and the labeling and hybridization of mRNA samples have been described (8).

Data Analysis and Map Positions. Hybridized arrays were scanned on a GenePix scanner (Axon Instruments, Foster City, CA), and fluorescence ratios (test/reference) calculated using SCANALYZE software (available at http://rana.lbl.gov). Fluorescence ratios were normalized for each array by setting the average log fluorescence ratio for all array elements equal to 0. Measurements with fluorescence intensities more than 20% above background were considered reliable. DNA copy number profiles that deviated significantly from background ratios measured in normal genomic DNA control hybridizations were interpreted as evidence of real DNA copy number alteration (see *Estimating Significance of Altered Fluorescence Ratios* in the supporting information). When indicated, DNA copy number profiles are displayed as a moving average (symmetric 5-nearest neighbors). Map positions for arrayed human cDNAs were assigned by
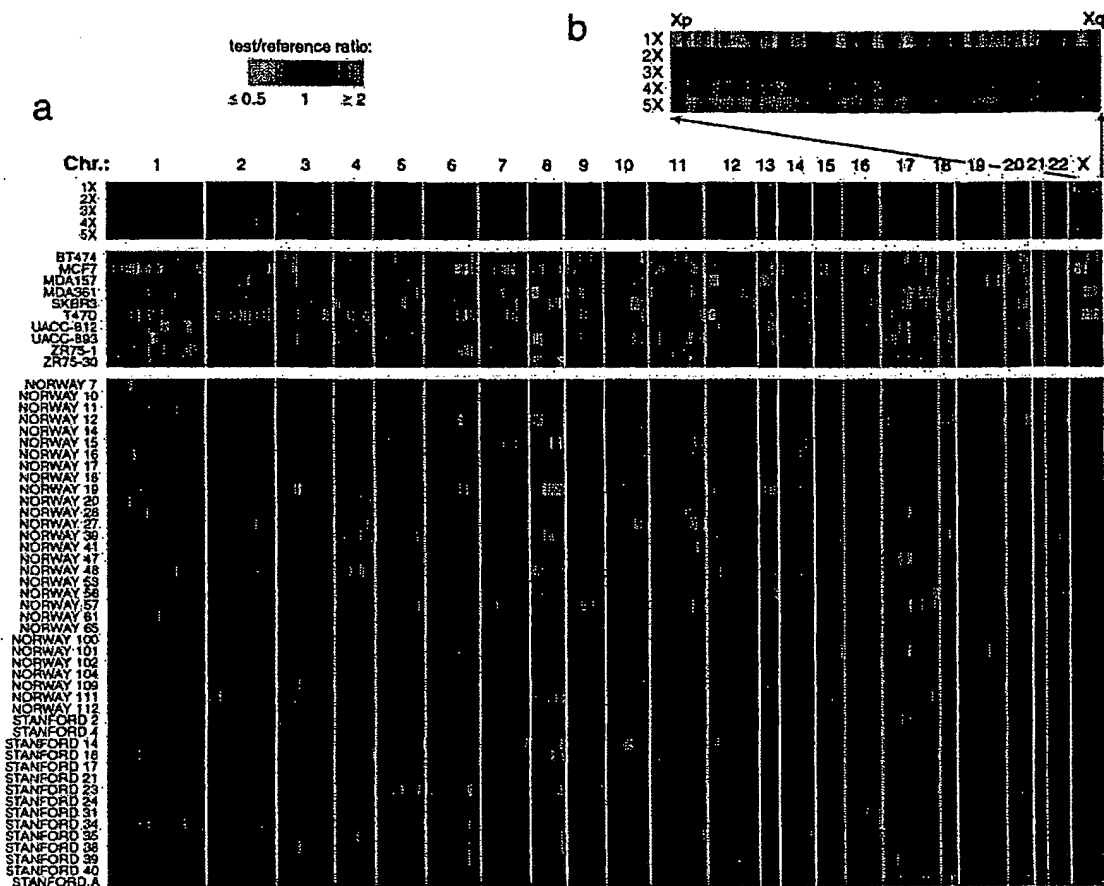
Fig. 1. Genome-wide measurement of DNA copy number alteration by array CGH. (a) DNA copy number profiles are illustrated for cell lines containing different numbers of X chromosomes, for breast cancer cell lines, and for breast tumors. Each row represents a different cell line or tumor, and each column represents one of 6,691 different mapped human genes present on the microarray, ordered by genome map position from 1pter through Xqter. Moving average (symmetric 5-nearest neighbors) fluorescence ratios (test/reference) are depicted using a log₂-based pseudocolor scale (indicated), such that red luminescence reflects fold-amplification, green luminescence reflects fold-deletion, and black indicates no change (gray indicates poorly measured data). (b) Enlarged view of DNA copy number profiles across the X chromosome, shown for cell lines containing different numbers of X chromosomes.

identifying the starting position of the best and longest match of any DNA sequence represented in the corresponding UniGene cluster (10) against the "Golden Path" genome assembly (http://genome.ucsc.edu/; Oct 7, 2000 Freeze). For UniGene clusters represented by multiple arrayed elements, mean fluorescence ratios (for all elements representing the same UniGene cluster) are reported. For mRNA measurements, fluorescence ratios are "mean-centered" (i.e., reported relative to the mean ratio across the 44 tumor samples). The data set described here can be accessed in its entirety in the supporting information.

Results

We performed CGH on 44 predominantly locally advanced, primary breast tumors and 10 breast cancer cell lines, using cDNA microarrays containing 6,691 different mapped human genes (Fig. 1a; also see *Materials and Methods* for details of microarray hybridizations). To take full advantage of the improved spatial resolution of array CGH, we ordered (fluorescence ratios for) the 6,691 cDNAs according to the "Golden Path" (http://genome.ucsc.edu/) genome assembly of the draft human genome sequences (11). In so doing, arrayed cDNAs not only themselves represent genes of potential interest (e.g., candidate oncogenes within amplicons), but also provide precise genetic landmarks for chromosomal regions of amplification and

deletion. Parallel analysis of DNA from cell lines containing different numbers of X chromosomes (Fig. 1b), as we did before (7), demonstrated the sensitivity of our method to detect single-copy loss (45, XO), and 1.5- (47,XXX), 2- (48,XXXX), or 2.5-fold (49,XXXXX) gains (also see Fig. 5, which is published as supporting information on the PNAS web site). Fluorescence ratios were linearly proportional to copy number ratios, which were slightly underestimated, in agreement with previous observations (7). Numerous DNA copy number alterations were evident in both the breast cancer cell lines and primary tumors (Fig. 1a), detected in the tumors despite the presence of euploid non-tumor cell types; the magnitudes of the observed changes were generally lower in the tumor samples. DNA copy-number alterations were found in every cancer cell line and tumor, and on every human chromosome in at least one sample. Recurrent regions of DNA copy number gain and loss were readily identifiable. For example, gains within 1q, 8q, 17q, and 20q were observed in a high proportion of breast cancer cell lines/tumors (90%/69%, 100%/47%, 100%/60%, and 90%/44%, respectively), as were losses within 1p, 3p, 8p, and 13q (80%/24%, 80%/22%, 80%/22%, and 70%/18%, respectively), consistent with published cytogenetic studies (refs. 2–4; a complete listing of gains/losses is provided in Tables 2 and 3, which are published as supporting information on the PNAS web site). The total
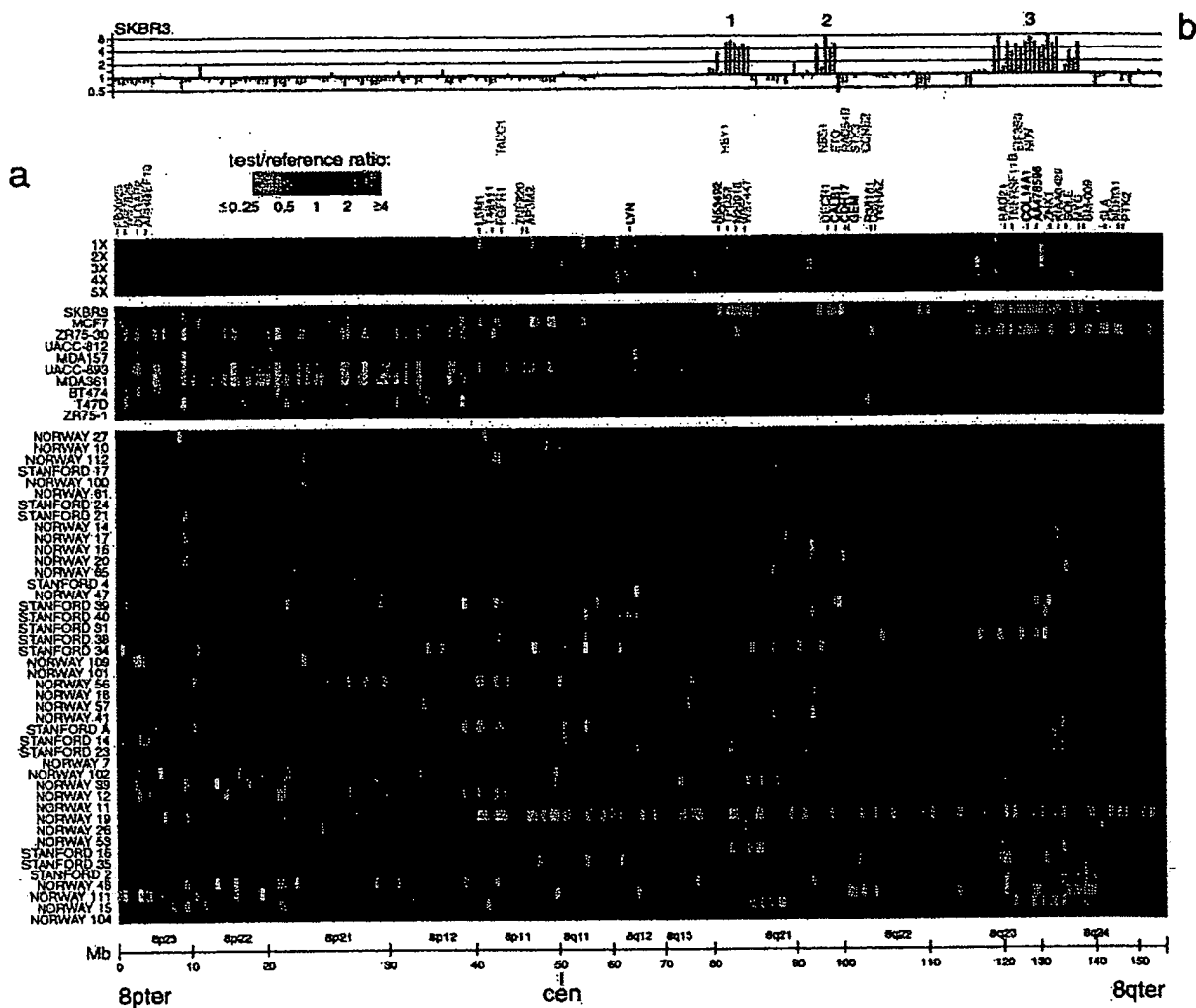
Fig. 2. DNA copy number alteration across chromosome 8 by array CGH. (a) DNA copy number profiles are illustrated for cell lines containing different numbers of X chromosomes, for breast cancer cell lines, and for breast tumors. Breast cancer cell lines and tumors are separately ordered by hierarchical clustering to highlight recurrent copy number changes. The 241 genes present on the microarrays and mapping to chromosome 8 are ordered by position along the chromosome. Fluorescence ratios (test/reference) are depicted by a log$_2$ pseudocolor scale (indicated). Selected genes are indicated with color-coded text (red, increased; green, decreased; black, no change; gray, not well measured) to reflect correspondingly altered mRNA levels (observed in the majority of the subset of samples displaying the DNA copy number change). The map positions for genes of interest that are not represented on the microarray are indicated in the row above those genes represented on the array. (b) Graphical display of DNA copy number profile for breast cancer cell line SKBR3. Fluorescence ratios (tumor/normal) are plotted on a log$_2$ scale for chromosome 8 genes, ordered along the chromosome.

number of genomic alterations (gains and losses) was found to be significantly higher in breast tumors that were high grade ($P = 0.008$), consistent with published CGH data (3), estrogen receptor negative ($P = 0.04$), and harboring TP53 mutations ($P = 0.0006$) (see Table 4, which is published as supporting information on the PNAS web site).

The improved spatial resolution of our array CGH analysis is illustrated for chromosome 8, which displayed extensive DNA copy number alteration in our series. A detailed view of the variation in the copy number of 241 genes mapping to chromosome 8 revealed multiple regions of recurrent amplification; each of these potentially harbors a different known or previously uncharacterized oncogene (Fig. 2a). The complexity of amplicon structure is most easily appreciated in the breast cancer cell line SKBR3. Although a conventional CGH analysis of 8q in SKBR3 identified only two distinct regions of amplification (12), we observed three distinct regions of high-level amplification (labeled 1–3 in Fig. 2b). For each of these regions we can define the

boundaries of the interval recurrently amplified in the tumors we examined; in each case, known or plausible candidate oncogenes can be identified (a description of these regions, as well as the recurrently amplified regions on chromosomes 17 and 20, can be found in Figs. 6 and 7, which are published as supporting information on the PNAS web site).

For a subset of breast cancer cell lines and tumors (4 and 37, respectively), and a subset of arrayed genes (6,095), mRNA levels were quantitatively measured in parallel by using cDNA microarrays (8). The parallel assessment of mRNA levels is useful in the interpretation of DNA copy number changes. For example, the highly amplified genes that are also highly expressed are the strongest candidate oncogenes within an amplicon. Perhaps more significantly, our parallel analysis of DNA copy number changes and mRNA levels provides us the opportunity to assess the global impact of widespread DNA copy number alteration on gene expression in tumor cells.

A strong influence of DNA copy number on gene expression is evident in an examination of the pseudocolor representations
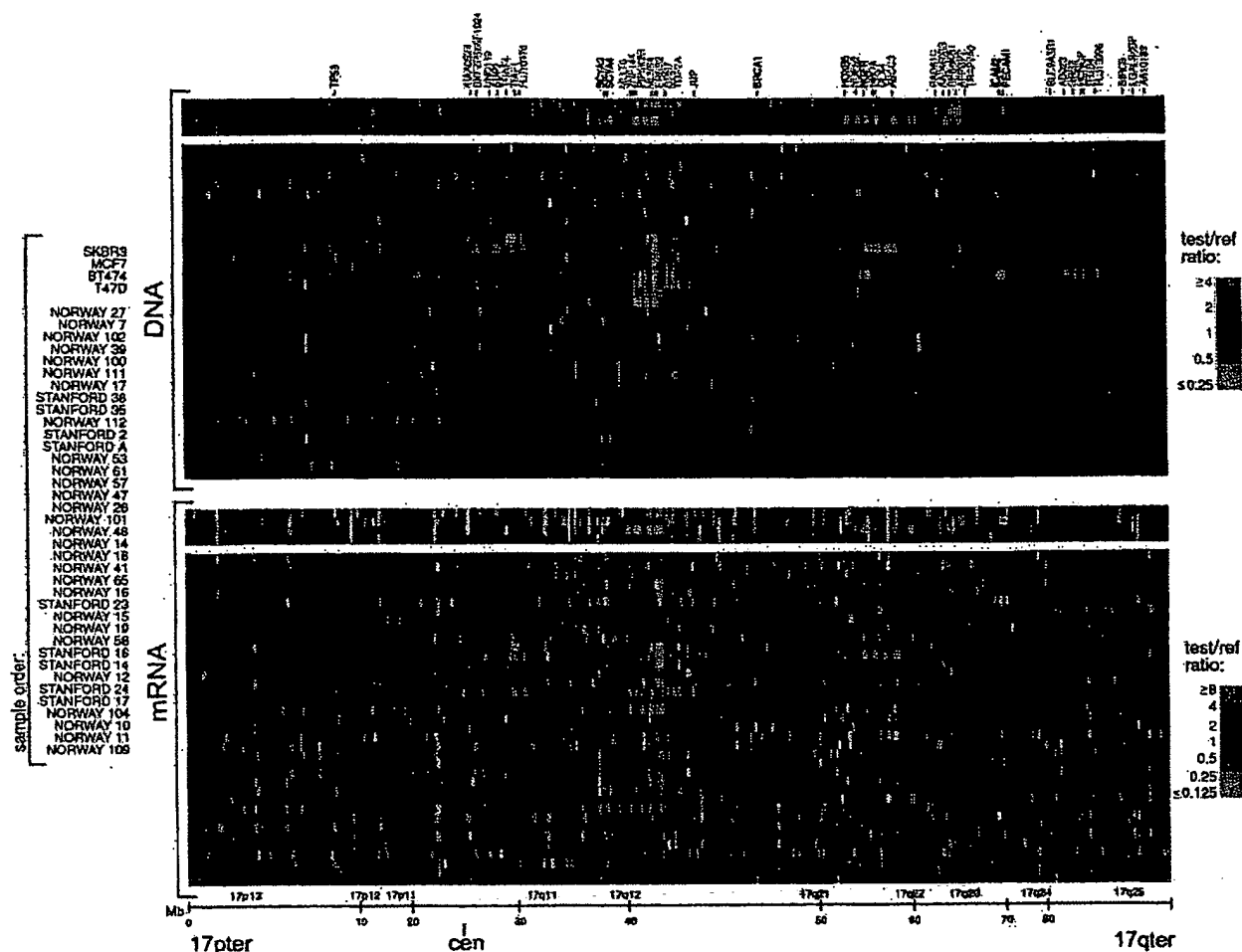
Fig. 3. Concordance between DNA copy number and gene expression across chromosome 17. DNA copy number alteration (*Upper*) and mRNA levels (*Lower*) are illustrated for breast cancer cell lines and tumors. Breast cancer cell lines and tumors are separately ordered by hierarchical clustering (*Upper*), and the identical sample order is maintained (*Lower*). The 354 genes present on the microarrays and mapping to chromosome 17, and for which both DNA copy number and mRNA levels were determined, are ordered by position along the chromosome; selected genes are indicated in color-coded text (see Fig. 2 legend). Fluorescence ratios (test/reference) are depicted by separate $\log_2$ pseudocolor scales (indicated).

of DNA copy number and mRNA levels for genes on chromosome 17 (Fig. 3). The overall patterns of gene amplification and elevated gene expression are quite concordant; i.e., a significant fraction of highly amplified genes appear to be correspondingly highly expressed. The concordance between high-level amplification and increased gene expression is not restricted to chromosome 17. Genome-wide, of 117 high-level DNA amplifications (fluorescence ratios >4, and representing 91 different genes), 62% (representing 54 different genes; see Table 5, which is published as supporting information on the PNAS web site) are found associated with at least moderately elevated mRNA levels (mean-centered fluorescence ratios >2), and 42% (representing 36 different genes) are found associated with comparably highly elevated mRNA levels (mean-centered fluorescence ratios >4).

To determine the extent to which DNA deletion and lower-level amplification (in addition to high-level amplification) are also associated with corresponding alterations in mRNA levels, we performed three separate analyses on the complete data set (4 cell lines and 37 tumors, across 6,095 genes). First, we determined the average mRNA levels for each of five classes of genes, representing DNA deletion, no change, and low-, medium-, and high-level amplification (Fig. 4a). For both the

breast cancer cell lines and tumors, average mRNA levels tracked with DNA copy number across all five classes, in a statistically significant fashion (*P* values for pair-wise Student's *t* tests comparing adjacent classes: cell lines, 4×10^{-49}, 1×10^{-49}, 5×10^{-5}, 1×10^{-2}; tumors, 1×10^{-43}, 1×10^{-214}, 5×10^{-41}, 1×10^{-4}). A linear regression of the average log(DNA copy number), for each class, against average log(mRNA level) demonstrated that on average, a 2-fold change in DNA copy number was accompanied by 1.4- and 1.5-fold changes in mRNA level for the breast cancer cell lines and tumors, respectively (Fig. 4a, regression line not shown). Second, we characterized the distribution of the 6,095 correlations between DNA copy number and mRNA level, each across the 37 tumor samples (Fig. 4b). The distribution of correlations forms a normal-shaped curve, but with the peak markedly shifted in the positive direction from zero. This shift is statistically significant, as evidenced in a plot of observed vs. expected correlations (Fig. 4c), and reflects a pervasive global influence of DNA copy number alterations on gene expression. Notably, the highest correlations between DNA copy number and mRNA level (the right tail of the distribution in Fig. 4b) comprise both amplified and deleted genes (data not shown). Third, we used a linear regression model to estimate the fraction of all variation measured in mRNA levels among the 37
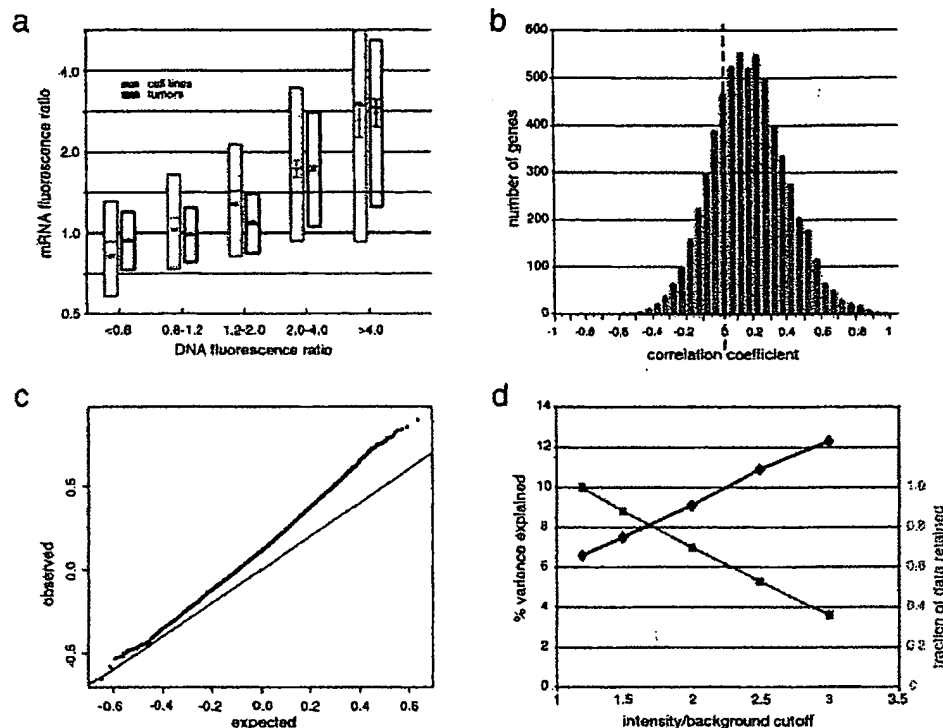
Fig. 4. Genome-wide influence of DNA copy number alterations on mRNA levels. (a) For breast cancer cell lines (gray) and tumor samples (black), both mean-centered mRNA fluorescence ratio ($\log_2$ scale) quartiles (box plots indicate 25th, 50th, and 75th percentile) and averages (diamonds; Y-value error bars indicate standard errors of the mean) are plotted for each of five classes of genes, representing DNA deletion (tumor/normal ratio < 0.8), no change (0.8–1.2), low- (1.2–2), medium- (2–4), and high-level (>4) amplification. P values for pair-wise Student's t tests, comparing averages between adjacent classes (moving left to right), are 4×10^{-49}, 1×10^{-49}, 5×10^{-5}, 1×10^{-2} (cell lines), and 1×10^{-43}, 1×10^{-214}, 5×10^{-41}, 1×10^{-4} (tumors). (b) Distribution of correlations between DNA copy number and mRNA levels, for 6,095 different human genes across 37 breast tumor samples. (c) Plot of observed versus expected correlation coefficients. The expected values were obtained by randomization of the sample labels in the DNA copy number data set. The line of unity is indicated. (d) Percent variance in gene expression (among tumors) directly explained by variation in gene copy number. Percent variance explained (black line) and fraction of data retained (gray line) are plotted for different fluorescence intensity/background (a rough surrogate for signal/noise) cutoff values. Fraction of data retained is relative to the 1.2 intensity/background cutoff. Details of the linear regression model used to estimate the fraction of variation in gene expression attributable to underlying DNA copy number alteration can be found in the supporting information (see *Estimating the Fraction of Variation in Gene Expression Attributable to Underlying DNA Copy Number Alteration*).

tumors that could be attributed to underlying variation in DNA copy number. From this analysis, we estimate that, overall, about 7% of all of the observed variation in mRNA levels can be explained directly by variation in copy number of the altered genes (Fig. 4d). We can reduce the effects of experimental measurement error on this estimate by using only that fraction of the data most reliably measured (fluorescence intensity/background >3); using that data, our estimate of the percent variation in mRNA levels directly attributable to variation in gene copy number increases to 12% (Fig. 4d). This still undoubtedly represents a significant underestimate, as the observed variation in global gene expression is affected not only by true variation in the expression programs of the tumor cells themselves, but also by the variable presence of non-tumor cell types within clinical samples.

Discussion

This genome-wide, array CGH analysis of DNA copy number alteration in a series of human breast tumors demonstrates the usefulness of defining amplicon boundaries at high resolution (gene-by-gene), and quantitatively measuring amplicon shape, to assist in locating and identifying candidate oncogenes. By analyzing mRNA levels in parallel, we have also discovered that changes in DNA copy number have a large, pervasive, direct effect on global gene expression patterns in both breast cancer

cell lines and tumors. Although the DNA microarrays used in our analysis may display a bias toward characterized and/or highly expressed genes, because we are examining such a large fraction of the genome (approximately 20% of all human genes), and because, as detailed above, we are likely underestimating the contribution of DNA copy number changes to altered gene expression, we believe our findings are likely to be generalizable (but would nevertheless still be remarkable if only applicable to this set of ~6,100 genes).

In budding yeast, aneuploidy has been shown to result in chromosome-wide gene expression biases (13). Two recent studies have begun to examine the global relationship between DNA copy number and gene expression in cancer cells. In agreement with our findings, Phillips et al. (14) have shown that with the acquisition of tumorigenicity in an immortalized prostate epithelial cell line, new chromosomal gains and losses resulted in a statistically significant respective increase and decrease in the average expression level of involved genes. In contrast, Platzer et al. (15) recently reported that in metastatic colon tumors only ~4% of genes within amplified regions were found more highly (>2-fold) expressed, when compared with normal colonic epithelium. This report differs substantially from our finding that 62% of highly amplified genes in breast cancer exhibit at least 2-fold increased expression. These contrasting findings may reflect methodological differences between the

studies. For example, the study of Platzer *et al.* (15) may have systematically under-measured gene expression changes. In this regard it is remarkable that only 14 transcripts of many thousand residing within unamplified chromosomal regions were found to exhibit at least 4-fold altered expression in metastatic colon cancer. Additionally, their reliance on lower-resolution chromosomal CGH may have resulted in poorly delimiting the boundaries of high-complexity amplicons, effectively overcalling regions with amplification. Alternatively, the contrasting findings for amplified genes may represent real biological differences between breast and metastatic colon tumors; resolution of this issue will require further studies.

Our finding that widespread DNA copy number alteration has a large, pervasive and direct effect on global gene expression patterns in breast cancer has several important implications. First, this finding supports a high degree of copy number-dependent gene expression in tumors. Second, it suggests that most genes are not subject to specific autoregulation or dosage compensation. Third, this finding cautions that elevated expression of an amplified gene cannot alone be considered strong independent evidence of a candidate oncogene's role in tumorigenesis. In our study, fully 62% of highly amplified genes demonstrated moderately or highly elevated expression. This highlights the importance of high-resolution mapping of amplicon boundaries and shape [to identify the "driving" gene(s) within amplicons (16)], on a large number of samples, in addition to functional studies. Fourth, this finding suggests that analyzing

the genomic distribution of expressed genes, even within existing microarray gene expression data sets, may permit the inference of DNA copy number aberration, particularly aneuploidy (where gene expression can be averaged across large chromosomal regions; see Fig. 3 and supporting information). Fifth, this finding implies that a substantial portion of the phenotypic uniqueness (and by extension, the heterogeneity in clinical behavior) among patients' tumors may be traceable to underlying variation in DNA copy number. Sixth, this finding supports a possible role for widespread DNA copy number alteration in tumorigenesis (17, 18), beyond the amplification of specific oncogenes and deletion of specific tumor suppressor genes. Widespread DNA copy number alteration, and the concomitant widespread imbalance in gene expression, might disrupt critical stochiometric relationships in cell metabolism and physiology (e.g., proteosome, mitotic spindle), possibly promoting further chromosomal instability and directly contributing to tumor development or progression. Finally, our findings suggest the possibility of cancer therapies that exploit specific or global imbalances in gene expression in cancer.

1. Kallioniemi, A., Kallioniemi, O. P., Sudar, D., Rutovitz, D., Gray, J. W., Waldman, F. & Pinkel, D. (1992) *Science* 258, 818–821.
2. Kallioniemi, A., Kallioniemi, O. P., Piper, J., Tanner, M., Stokke, T., Chen, L., Smith, H. S., Pinkel, D., Gray, J. W. & Waldman, F. M. (1994) *Proc. Natl. Acad. Sci. USA* 91, 2156–2160.
3. Tirkkonen, M., Tanner, M., Karhu, R., Kallioniemi, A., Isola, J. & Kallioniemi, O. P. (1998) *Genes Chromosomes Cancer* 21, 177–184.
4. Forozan, F., Mahlamaki, E. H., Monni, O., Chen, Y., Veldman, R., Jiang, Y., Gooden, G. C., Ethier, S. P., Kallioniemi, A. & Kallioniemi, O. P. (2000) *Cancer Res.* 60, 4519–4525.
5. Solinas-Toldo, S., Lampel, S., Stilgenbauer, S., Nickolenko, J., Benner, A., Dohner, H., Cremer, T. & Lichter, P. (1997) *Genes Chromosomes Cancer* 20, 399–407.
6. Pinkel, D., Segraves, R., Sudar, D., Clark, S., Poole, I., Kowbel, D., Collins, C., Kuo, W. L., Chen, C., Zhai, Y., *et al.* (1998) *Nat. Genet.* 20, 207–211.
7. Pollack, J. R., Perou, C. M., Alizadeh, A. A., Eisen, M. B., Pergamenschikov, A., Williams, C. F., Jeffrey, S. S., Botstein, D. & Brown, P. O. (1999) *Nat. Genet.* 23, 41–46.
8. Perou, C. M., Sorlie, T., Eisen, M. B., van de Rijn, M., Jeffrey, S. S., Rees, C. A., Pollack, J. R., Ross, D. T., Johnsen, H., Akslen, L. A., *et al.* (2000) *Nature (London)* 406, 747–752.
9. Sorlie, T., Perou, C. M., Tibshirani, R., Aas, T., Geisler, S., Johnsen, H., Hastie,

T., Eisen, M. B., van de Rijn, M., Jeffrey, S. S., *et al.* (2001) *Proc. Natl. Acad. Sci. USA* 98, 10869–10874.
10. Schuler, G. D. (1997) *J. Mol. Med.* 75, 694–698.
11. Lander, E. S., Linton, L. M., Birren, B., Nusbaum, C., Zody, M. C., Baldwin, J., Devon, K., Dewar, K., Doyle, M., FitzHugh, W., *et al.* (2001) *Nature (London)* 409, 860–921.
12. Fejzo, M. S., Godfrey, T., Chen, C., Waldman, F. & Gray, J. W. (1998) *Genes Chromosomes Cancer* 22, 105–113.
13. Hughes, T. R., Roberts, C. J., Dai, H., Jones, A. R., Meyer, M. R., Slade, D., Burchard, J., Dow, S., Ward, T. R., Kidd, M. J., *et al.* (2000) *Nat. Genet.* 25, 333–337.
14. Phillips, J. L., Hayward, S. W., Wang, Y., Vasselli, J., Pavlovich, C., Padilla-Nash, H., Pezullo, J. R., Ghadimi, B. M., Grossfeld, G. D., Rivera, A., *et al.* (2001) *Cancer Res.* 61, 8143–8149.
15. Platzer, P., Upender, M. B., Wilson, K., Willis, J., Lutterbaugh, J., Nosrati, A., Willson, J. K., Mack, D., Ried, T. & Markowitz, S. (2002) *Cancer Res.* 62, 1134–1138.
16. Albertson, D. G., Ylstra, B., Segraves, R., Collins, C., Dairkee, S. H., Kowbel, D., Kuo, W. L., Gray, J. W. & Pinkel, D. (2000) *Nat. Genet.* 25, 144–146.
17. Li, R., Yerganian, G., Duesberg, P., Kraemer, A., Willer, A., Rausch, C. & Hehlmann, R. (1997) *Proc. Natl. Acad. Sci. USA* 94, 14506–14511.
18. Rasnick, D. & Duesberg, P. H. (1999) *Biochem. J.* 340, 621–630.

HER-2/neu Breast Cancer Predictive Testing

Julie Sanford Hanna, Ph.D. and Dan Mornin, M.D.

EACH YEAR, OVER 182,000 WOMEN in the United States are diagnosed with breast cancer, and approximately 45,000 die of the disease.[1] Incidence appears to be increasing in the United States at a rate of roughly 2% per year. The reasons for the increase are unclear, but non-genetic risk factors appear to play a large role.[2]

Five-year survival rates range from approximately 65%-85%, depending on demographic group, with a significant percentage of women experiencing recurrence of their cancer within 10 years of diagnosis. One of the factors most predictive for recurrence once a diagnosis of breast cancer has been made is the number of axillary lymph nodes to which tumor has metastasized. Most node-positive women are given adjuvant therapy, which increases their survival. However, 20%-30% of patients without axillary node involvement also develop recurrent disease, and the difficulty lies in how to identify this high-risk subset of patients. These patients could benefit from increased surveillance, early intervention, and treatment.

Prognostic markers currently used in breast cancer recurrence prediction include tumor size, histological grade, steroid hormone receptor status, DNA ploidy, proliferative index, and cathepsin D status. Expression of growth factor receptors and over-expression of the HER-2/neu oncogene have also been identified as having value regarding treatment regimen and prognosis.

HER-2/neu (also known as c-erbB2) is an oncogene that encodes a transmembrane glycoprotein that is homologous to, but distinct from, the epidermal growth factor receptor. Numerous studies have indicated that high levels of expression of this protein are associated with rapid tumor growth, certain forms of therapy resistance, and shorter disease-free survival. The gene has been shown to be amplified and/or overexpressed in 10%-30% of invasive breast cancers and in 40%-60% of intraductal breast carcinoma.[3]

There are two distinct FDA-approved methods by which HER-2/neu status can be evaluated: immunohistochemistry (IHC, HercepTest™) and FISH (fluorescent in situ hybridization, PathVysion™ Kit). Both methods can be performed on archived and current specimens. The first method allows visual assessment of the amount of HER-2/neu protein present on the cell membrane. The latter method allows direct quantification of the level of gene amplification present in the tumor, enabling differentiation between low- versus high-amplification. At least one study has demonstrated a difference in

recurrence risk in women younger than 40 years of age for low- versus high-amplified tumors (54.5% compared to 85.7%); this is compared to a recurrence rate of 16.7% for patients with no HER-2/neu gene amplification.[4] HER-2/neu status may be particularly important to establish in women with small (≤1 cm) tumor size.

The choice of methodology for determination of HER-2/neu status depends in part on the clinical setting. FDA approval for the Vysis FISH test was granted based on clinical trials involving 1549 node-positive patients. Patients received one of three different treatments consisting of different doses of cyclophosphamide, Adriamycin, and 5-fluorouracil (CAF). The study showed that patients with amplified HER-2/neu benefited from treatment with higher doses of adriamycin-based therapy, while those with normal HER-2/neu levels did not. The study therefore identified a sub-set of women, who because they did not benefit from more aggressive treatment, did not need to be exposed to the associated side effects. In addition, other evidence indicates that HER-2/neu amplification in node-negative patients can be used as an independent prognostic indicator for early recurrence, recurrent disease at any time and disease-related death.[5] Demonstration of HER-2/neu gene amplification by FISH has also been shown to be of value in predicting response to chemotherapy in stage-2 breast cancer patients.

Selection of patients for Herceptin© (Trastuzumab) monoclonal antibody therapy, however, is based upon demonstration of HER-2/neu protein overexpression using HercepTest™. Studies using Herceptin© in patients with metastatic breast cancer show an increase in time to disease progression, increased response rate to chemotherapeutic agents and a small increase in overall survival rate. The FISH assays have not yet been approved for this purpose, and studies looking at response to Herceptin© in patients with or without gene amplification status determined by FISH are in progress.

In general, FISH and IHC results correlate well. However, subsets of tumors are found which show discordant results; i.e., protein overexpression without gene amplification or lack of protein overexpression with gene amplification. The clinical significance of such results is unclear. Based on the above considerations, HER-2/neu testing at SHMC/PAML will utilize immunohistochemistry (HercepTest©) as a screen, followed by FISH in IHC-negative cases. Alternatively, either method may be ordered individually depending on the clinical setting or clinician preference.

CPT code information

HER-2/neu via IHC

88342 (including interpretive report)

HER-2/neu via FISH

88271×2 Molecular cytogenetics, DNA probe, each

88274 Molecular cytogenetics, interphase in situ hybrid-ization, analyze 25-99 cells

88291 Cytogenetics and molecular cytogenetics, interpre-tation and report

Procedural Information

Immunohistochemistry is performed using the FDA-approved DAKO antibody kit, Herceptest©. The DAKO kit contains reagents required to complete a two-step immunohisto-chemical staining procedure for routinely processed, paraffin-embedded specimens. Following incubation with the primary rabbit antibody to human HER-2/neu protein, the kit employs a ready-to-use dextran-based visualization reagent. This re-agent consists of both secondary goat anti-rabbit antibody molecules with horseradish peroxidase molecules linked to a common dextran polymer backbone, thus eliminating the need for sequential application of link antibody and peroxidase conjugated antibody. Enzymatic conversion of the subse-quently added chromogen results in formation of visible reaction product at the antigen site. The specimen is then coun-terstained; a pathologist using light-microscopy interprets results.

FISH analysis at SHMC/PAML is performed using the FDA-approved PathVysion™ HER-2/neu DNA probe kit, pro-duced by Vysis, Inc. Formalin fixed, paraffin-embedded breast tissue is processed using routine histological methods, and then slides are treated to allow hybridization of DNA probes to the nuclei present in the tissue section. The Pathvysion™ kit con-tains two direct-labeled DNA probes, one specific for the alphoid repetitive DNA (CEP 17, spectrum orange) present at the chromosome 17 centromere and the second for the HER-2/neu oncogene located at 17q11.2-12 (spectrum green). Enu-meration of the probes allows a ratio of the number of copies of chromosome 17 to the number of copies of HER-2/neu to be obtained; this enables quantification of low versus high amplification levels, and allows an estimate of the percentage of cells with HER-2/neu gene amplification. The clinically relevant distinction is whether the gene amplification is due to increased gene copy number on the two chromosome 17 homologues normally present or an increase in the number of chromosome 17s in the cells. In the majority of cases, ratio equivalents less than 2.0 are indicative of a normal/negative result, ratios of 2.1 and over indicate that amplification is present and to what degree. Interpretation of this data will be performed and reported from the Vysis-certified Cytogenet-ics laboratory at SHMC.

References

1. Wingo, P.A., Tong, T., Bolden, S., "Cancer Statistics", 1995;45:1:8-31.

2 "Cancer Rates and Risks", 4th ed., National Institutes of Health, National Cancer Institute, 1996, p. 120.

3 Slamon, D.J., Clark, G.M., Song, S.G., Levin, W.J., Ullrich, A., McGuire, W.L. "Human breast Cancer: Correlation of relapse and survival with amplification of the her-2/neu oncogene". Science, 235:177-182, 1987.

4 Xing, W.R., Gilchrist, K.W., Harris, C.P., Samson, W., Meisner, L.F. "FISH detection of HER-s/neu oncogene amplification in early onset breast cancer". Breast Cancer Res. And Treatment 39(2):203-212, 1996.

5. Press, M.F. Bernstein, L., Thomas, P.A., Meisner, L.F., Zhou, J.Y., Ma, Y., Hung, G., Robinson, R.A., Harris, C., El-Naggar, A., Slamon, D.J., Phillips, R.N., Ross, J.S., Wolman, S.R., Flom, K.J., "Her-2/neu gene amplification characterized by fluorescence in situ hybridization: poor prognosis in node-negative breast carcinomas", J. Clinical Oncology 15(8):2894-2904, 1997.

Variable expression of the translocated c-*abl* oncogene in Philadelphia-chromosome-positive B-lymphoid cell lines from chronic myelogenous leukemia patients

James B. Konopka[*‡], Steven Clark[*], Jami McLaughlin[*], Masakuzu Nitta[†], Yoshiro Kato[†], Annabel Strife[†], Bayard Clarkson[†], and Owen N. Witte[*§]

*Department of Microbiology and Molecular Biology Institute, University of California, Los Angeles, 405 Hilgard Avenue, Los Angeles, CA 90024; and †The Laboratory of Hematopoietic Cell Kinetics and The Laboratory of Cancer Genetics and Cytogenetics, Memorial Sloan-Kettering Cancer Center, 1275 York Avenue, New York, NY 10021

ABSTRACT   The consistent cytogenetic translocation of chronic myelogenous leukemia (the Philadelphia chromosome, Ph[1]) has been observed in cells of multiple hematopoietic lineages. This translocation creates a chimeric gene composed of breakpoint-cluster-region (*bcr*) sequences from chromosome 22 fused to a portion of the *abl* oncogene on chromosome 9. The resulting gene product (P210[c-abl]) resembles the transforming protein of the Abelson murine leukemia virus in its structure and tyrosine kinase activity. P210[c-abl] is expressed in Ph[1]-positive cell lines of myeloid lineage and in clinical specimens with myeloid predominance. We show here that Epstein–Barr virus-transformed B-lymphocyte lines that retain Ph[1] can express P210[c-abl]. The level of expression in these B-cell lines is generally lower and more variable than that observed for myeloid lines. Protein expression is not related to amplification of the *abl* gene but to variation in the level of *bcr-abl* mRNA produced from a single Ph[1] template.

Chronic myelogenous leukemia (CML) is a disease of the pluripotent stem cell (1). In greater than 95% of patients, the leukemic cells contain the cytogenetic marker known as the Philadelphia chromosome, or Ph[1] (2). This reciprocal translocation event between the long arms of chromosomes 9 and 22 has been used as a disease-specific marker for diagnosis and evaluation of therapy. Multiple hematopoietic lineages, including myeloid and B-lymphoid, contain Ph[1] in early or chronic phase, as well as in the more acute accelerated and blast crisis phases of the disease.

One molecular consequence of Ph[1] is the translocation of the chromosomal arm containing the c-*abl* gene on chromosome 9 into the middle of the breakpoint-cluster region (*bcr*) gene on chromosome 22 (3–6). Although the precise translocation breakpoints are variable, an RNA-splicing mechanism generates a very similar 8-kilobase (kb) mRNA in each case (5–9). The hybrid *bcr-abl* message encodes a structurally altered form of the *abl* oncogene product, called P210[c-abl] (10–13), with an amino-terminal segment derived from a portion of the exons of *bcr* on chromosome 22 and a carboxyl-terminal segment derived from a major portion of the exons of the c-*abl* gene on chromosome 9. The chimeric structure of *bcr-abl* and the resulting P210[c-abl] is similar to the structure of the Abelson murine leukemia virus *gag-abl* genome and resulting P160[v-abl] transforming gene product. Both proteins have very similar tyrosine kinase activities (10, 11, 14) which can be distinguished by their relative stability to denaturing detergents and by their ATP requirements from the recently described tyrosine kinase activity of the c-*abl* gene product (15).

In concert with structural modification of the amino-terminal portion of the *abl* gene, increased level of expression has been implicated in activation of c-*abl* oncogenic potential. Myeloid and erythroid cell lines and clinical samples derived from acute-phase CML patients contain about 10-fold higher levels of the 8-kb *bcr-abl* mRNA and P210[c-abl] than the c-*abl* mRNA forms (6 and 7 kb) and P145[c-abl] gene product (5, 8, 9, 11). The higher level of expression of the chimeric *bcr-abl* message in acute-phase cells is not likely to be solely due to the presence of the *bcr* promoter sequences at the 5' end of the gene, since the normal 4.5-kb and 6.7-kb *bcr*-encoded mRNA species are expressed at an even lower level than the normal c-*abl* messages (5, 6).

We have analyzed a series of Epstein–Barr virus-immortalized B-lymphoid cell lines derived from CML patients (16). With such *in vitro* clonal cell lines, we can evaluate whether the presence of Ph[1] always results in synthesis of the chimeric *bcr-abl* message and protein, and whether the quantitative expression varies for cells of B-lymphoid lineage as compared to previously examined myeloid cell lines. Our results show that cell lines that retain Ph[1] do express *bcr-abl* message and protein, but that the level is generally lower and more variable than previously seen for myeloid cell lines. The demonstration that the Ph[1] chromosomal template can vary in its level of expression of P210[c-abl] suggests that secondary mechanisms, beyond the translocation itself, contribute to the regulation of the *bcr-abl* gene in different cell types or subclones that derive from the affected stem cell.

MATERIALS AND METHODS

Cells and Cell Labelings. Epstein–Barr virus-transformed B-lymphoid cell lines were established from peripheral blood samples of chronic- and acute-phase CML patients as reported (16). The cell lines are designated according to patient number, karyotype, and lineage. For example, SK-CML7Bt(9,22)-33 refers to CML patient 7, B-lymphoid cell line, 9;22 translocation (Ph[1]), cell line 33; and SK-CML7BN-2 refers to B-cell line 2 with a normal karyotype derived from the same patient. Repeat karyotype analysis was performed to verify the retention of Ph[1] just prior to analysis for *abl* protein and RNA. Cells were maintained in RPMI 1640 medium with 20% fetal bovine serum. We have not observed any consistent pattern of *in vitro* growth rate that correlates to the stage of disease at the time of transformation with Epstein–Barr virus. Cells (1.5 × 10⁷) were washed twice with Dulbecco's modified Eagle's medium lacking phosphate and

---

supplemented with 5% dialyzed fetal bovine serum. Cells were then resuspended in 2 ml of the minimal medium. Labeling was started with the addition of [^{32}P]orthophosphate (1 mCi/ml; ICN; 1 Ci = 37 GBq) and continued at 37°C for 3–4 hr.

Immunoprecipitation and Immunoblotting. Immunoprecipitations were carried out as described (10). Cells (1.5 × 10^7) were washed with phosphate-buffered saline and extracted with 3–5 ml of phosphate lysis buffer (1% Triton X-100/0.1 NaDodSO$_4$/0.5% deoxycholate/10 mM Na$_2$HPO$_4$, pH 7.5/ 100 mM NaCl) with 5 mM EDTA and 5 mM phenylmethylsulfonyl fluoride. Extracts were clarified by centrifugation and precipitated with normal or rabbit anti-abl sera (anti-pEX-2 or anti-pEX-5) (17). The precipitated proteins were electrophoresed in a NaDodSO$_4$/8% polyacrylamide gel. ^{32}P-labeled proteins were detected by autoradiography. Alternatively, *abl* proteins were detected by immunoblotting. Extracts from unlabeled cells were clarified, and proteins were concentrated by immunoprecipitation with rabbit antisera against *abl*-encoded proteins [anti-pEX-2 and anti-pEX-5 combined (17)] and then fractionated in 8% acrylamide gels. The proteins were transferred from the gel to nitrocellulose filters, using protease-facilitated transfer (18). The *abl*-encoded proteins were detected using murine monoclonal antibodies as a probe and peroxidase-conjugated goat anti-mouse second stage antibody (Bio-Rad) for development. Rabbit antisera and mouse monoclonal antibodies to *abl* proteins were prepared using bacterially expressed regions of the v-*abl* protein as immunogens (17, 19). Anti-pEX-2 antibodies react with the internal tyrosine kinase domain and anti-pEX-5 antibodies react with the carboxyl-terminal segment of the *abl* proteins.

RNA Analysis. RNA was extracted from 10^8 cells by the NaDodSO$_4$/urea/phenol method (20). Polyadenylylated RNA was purified by oligo(dT) affinity chromatography. Samples were electrophoresed in a 1% agarose/formaldehyde gel and transferred to nitrocellulose. *abl* RNA species were detected by hybridization with a nick-translated v-*abl* fragment probe (21).

DNA Analysis. DNA was prepared from 5 × 10^7 cells of each cell line and processed for Southern blots with a v-*abl* probe as described (21).

RESULTS

Variable Levels of P210^{c-abl} Are Detected in Ph^1-Positive Cell Lines. Ph^1-positive and Ph^1-negative, Epstein–Barr virus-transformed B-lymphocyte cell lines derived from the same patient were examined for P210^{c-abl} synthesis by immunoprecipitation of [^{32}P]orthophosphate-labeled cell extracts with anti-abl sera (Fig. 1). The normal c-*abl* protein P145^{c-abl} was detected at a similar level in multiple Ph^1-positive and Ph^1-negative cell lines. P210^{c-abl} was only detected in the Ph^1-positive cell lines because the *bcr-abl* chimeric gene which encodes P210^{c-abl} resides on the Ph^1 (4, 5, 11, 13). The level of P210^{c-abl} was about 4- to 5-fold higher than the level of P145^{c-abl} in the SK-CML7Bt-33 cell line (Fig. 1A, +). The Ph^1-positive erythroid-progenitor cell line K562 (C) showed a level of P210^{c-abl} about 10-fold higher than P145^{c-abl}. However, the level of P210^{c-abl} was about one-fifth that of P145^{c-abl} in the Ph^1-positive SK-CML16Bt-1 cell line (Fig. 1B, +). Comparison of different autoradiographic exposures roughly indicated that the level of P210^{c-abl} varies over a 20-fold range between these Ph^1-positive B-cell lines. Analysis of four additional Ph^1-positive B-cell lines demonstrated that the level of P210^{c-abl} fell into two general classes; some cell lines had a level of P210^{c-abl} similar to SK-CML7Bt-33 and others had the low level similar to SK-CML16Bt-1 (Table 1). This differs from previous studies with Ph^1-positive myeloid cell lines and patient samples derived from acute-
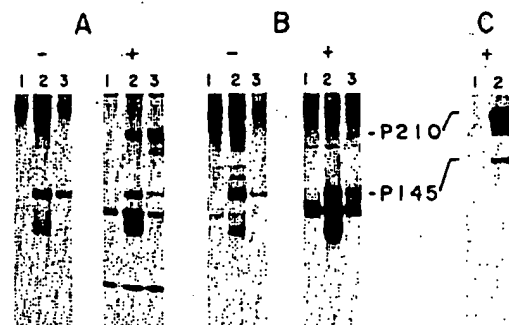

FIG. 1. Detection of variable levels of P210^{c-abl} in Ph^1-positive B-cell lines. Production of P145^{c-abl} and P210^{c-abl} in Epstein–Barr virus-transformed B-cell lines derived from a blast-crisis (A) and a chronic-phase (B) CML patient was examined by metabolic labeling with [^{32}P]orthophosphate and immunoprecipitation. Ph^1-negative (−) and Ph^1-positive (+) cell lines derived from each patient were analyzed. The Ph^1-negative cell line in A, − is SK-CML7BN-2 and in B, − is SK-CML16BN-1. The Ph^1-positive cell line in A, + is SK-CML7Bt-33 and in B, + is SK-CML16Bt-1. The K562 cell line, a Ph^1-positive erythroid progenitor cell line spontaneously derived from a blast-crisis patient (33), is represented in C. Cells (1.5 × 10^7) were metabolically labeled with 2 mCi of [^{32}P]orthophosphate for 3–4 hr and then were extracted and clarified by centrifugation. Samples were immunoprecipitated with control normal serum (lanes 1), anti-pEX-2 (lanes 2), or anti-pEX-5 (lanes 3) and analyzed by NaDodSO$_4$/8% PAGE followed by autoradiography with an intensifying screen (3 days for A and C, 10 days for B).

phase CML patients, in which P210^{c-abl} was detected at a 10-fold higher level than P145^{c-abl} (refs. 10 and 11; Table 1). There was no large difference in level of chimeric mRNA and P210^{c-abl} expressed in four myeloid/erythroid-lineage Ph^1-positive cell lines (K562, EM2, EM3, CML22, and BV173; refs. 9 and 11), despite a 4- to 5-fold amplification of *abl*-related sequences in the K562 cell line.

Detection of different levels of P210^{c-abl} in Fig. 1 could be due to decreased phosphorylation of P210^{c-abl}, a lower level of P210^{c-abl} synthesis, or altered stability of the protein. To help distinguish among these possibilities, the steady-state level of P210^{c-abl} in the cell lines was assayed by immunoblotting. The results show that SK-CML7Bt-33 (Fig. 2A, +) had a higher level of P210^{c-abl} than P145, similar to the results with metabolic labeling (Fig. 1). We did not detect P210^{c-abl} by immunoblotting with 2 × 10^7 cells of line SK-CML8Bt-3 (Fig. 2B, +). Reconstruction experiments using dilutions of cell extracts showed that we could detect about 5–10% the level of P210^{c-abl} expressed in the K562 cell line (data not shown). We infer that the steady-state level of P210^{c-abl} in SK-CML8Bt-3 is lower than the level in SK-CML7Bt-33 by a factor of at least 10. The level of P210^{c-abl} detected in these assays correlated with the amount of P210^{c-abl} tyrosine kinase activity that could be detected *in vitro* (data not shown).

Different Levels of P210^{c-abl} Are Reflected in the Amount of Stable *bcr-abl* mRNA. To identify the basis for detection of variable levels of P210^{c-abl}, we examined the production of the *abl* RNA. RNA blot hybridization analysis using a v-*abl* probe (Fig. 3) showed that the normal 6- and 7-kb c-*abl* mRNAs were present at a similar level in Ph^1-positive and -negative cell lines derived from different patients. However, the 8-kb mRNA that encodes P210^{c-abl} was detected at a 10-fold higher level in SK-CML7Bt-33 (Fig. 3A, +) than in SK-CML16Bt-1 (B, +), which correlated with the relative level of P210^{c-abl} detected in each cell line. Analysis of additional cell lines demonstrated that the level of 8-kb RNA directly correlated with the level of P210^{c-abl} (Table 1). The variation in level of 8-kb RNA detected in these cell lines was not due to loss or gain of Ph^1, because cytogenetic analysis confirmed the presence of Ph^1 in these cell lines (ref. 16 and

Medical Sciences: Konopka *et al.*

Proc. Natl. Acad. Sci. USA 83 (1986)   4051

Table 1.   Relative levels of *bcr-abl* expression in Epstein–Barr virus-immortalized B-cell lines and myeloid CML lines

Cell line*	CML phase†	Ph‡	P210§	8-kb mRNA¶
SK-CML7BN-2	BC	−	−	−
SK-CML8BN-10	Chronic	−	−	−
SK-CML8BN-12	Chronic	−	−	−
SK-CML16BN-1	Chronic	−	−	−
SK-CML35BN-1	Chronic	−	−	−
SK-CML7B5-33	BC	+	+++	+++
SK-CML21Bt-1	Acc	+	+++	+++
SK-CML21Bt-6	Acc	+	+++	+++
SK-CML8Bt-3	Chronic	+	+	±
SK-CML16Bt-1	Chronic	+	+	+
SK-CML35Bt-2	Chronic	+	+	+
K562	BC	+	+++++	+++++
BV173	BC	+	+++++	+++++
EM2	BC	+	+++++	+++++

*Cell lines derived from CML patients by transformation with Epstein–Barr virus as described (16). Names of cell lines indicate patient number and Ph¹ status: SK-CML7Bt indicates a cell line derived from patient 7 that carries the 9;22 Ph¹ translocation; N indicates a normal karyotype. Myeloid-erythroid cell lines (K562, EM2, and BV173) are described in previous publications (9, 11, 22, 33).

†Status of patient at the time cell line was derived. BC, blast crisis; Acc, accelerated phase.

‡Presence (+) or absence (−) of Ph¹ as demonstrated by karyotypic or Southern blot analysis.

§P210^{c-abl} detected as described in legend to Fig. 1. B-cell lines derived from blast-crisis and accelerated-phase patients had levels of P210 3- to 5-fold higher (+++) than levels of P145. Chronic-phase-derived cell lines had P210 levels lower than or just equivalent (+) to the level of P145. Myeloid and erythroid lines had levels of P210 5- to 10-fold higher than P145 (+++++).

¶Eight-kilobase *bcr-abl* mRNA detected as described in legend to Fig. 2. Symbols: ±, borderline detectable; +++++, level of 8-kb mRNA 5- to 10-fold higher than that of the 6- and 7-kb c-abl mRNA species; +++, level of 8-kb mRNA 3- to 5-fold higher than that of the 6- and 7-kb species; +, a level approximately equivalent to that of the 6- and 7-kb messages.

data not shown). There was no difference in the copy number of *abl*-related sequences as judged by Southern blot analysis (Fig. 4). Only the K562 cell line control showed an amplification of *abl* sequences, as previously reported (22, 23). These combined data suggest that differential *bcr-abl* mRNA expression from a single gene template is responsible for the variable levels of P210^{c-abl} detected. This could be mediated
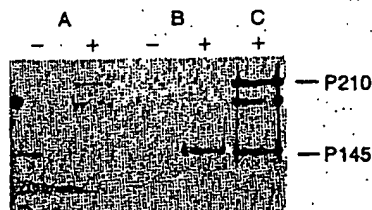
FIG. 2.   Analysis of steady-state *abl* protein levels by immunoblotting. Cell extracts prepared from 2 × 10⁷ cells of lines SK-CML7BN-2 (*A*,−), SK-CML7Bt-33 (*A*,+), SK-CML8BN-10 (*B*,−), and SK-CML8Bt-3 (*B*,+) were concentrated by immunoprecipitation with anti-pEX-2 plus anti-pEX-5. Samples were then electrophoresed in a NaDodSO₄/8% polyacrylamide gel and transferred to nitrocellulose, using protease-facilitated transfer (18). *abl* proteins were detected using a mixture of two monoclonal antibodies directed against the pEX-2 and pEX-5 *abl*-protein fragments produced in bacteria (19) as a probe and a peroxidase-conjugated goat anti-mouse second-stage antibody (Bio-Rad) for development.
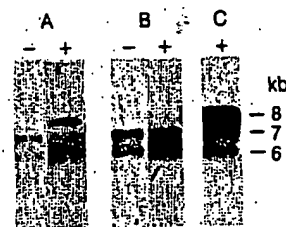
FIG. 3.   Comparison of *abl* RNA levels in Ph¹-positive and -negative B-cell lines. The levels of the normal 6- and 7-kb c-*abl* RNAs and the 8-kb *bcr-abl* RNA were analyzed by blot hybridization using a v-*abl* probe. RNA was extracted from Ph¹-negative lines SK-CML7BN-2 (*A*,−) and SK-CML16BN-1 (*B*,−), from Ph¹-positive lines SK-CML6Bt-33 (*A*,+) and SK-CML16Bt-3 (*B*,+), and from line K562 (*C*,+) by the NaDodSO₄/urea/phenol method (20). Polyadenylylated RNA was purified by oligo(dT) affinity chromatography, and 15 μg of each sample was electrophoresed in a 1% agarose/formaldehyde gel and then transferred to nitrocellulose. The blotted RNAs were hybridized with a nick-translated v-*abl* fragment probe (21) and then autoradiographed for 4 days.

by factors influencing the transcription rate of the *bcr-abl* gene or the stability of the mRNA.

DISCUSSION

Several lines of evidence suggest that formation of Ph¹ is not the primary event that affects the stem cell in CML. Patients have been identified that present with the clinical picture of CML but only later develop Ph¹ (1). This observation, coupled with studies of *G6PD* (glucose-6-phosphate dehydrogenase)-heterozygous females with CML that demonstrate stem-cell clonality by isozyme analysis among cell
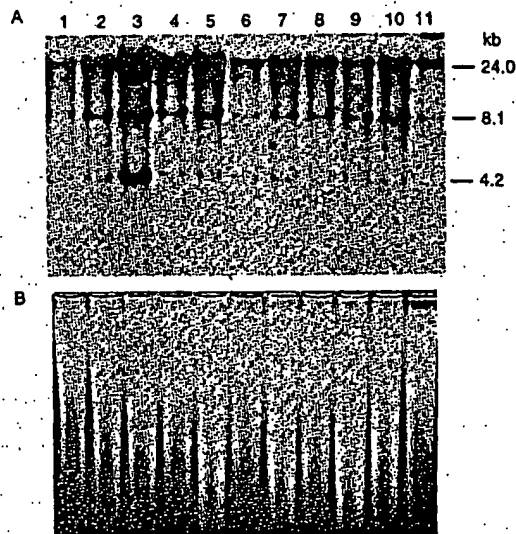
FIG. 4.   Southern blot analysis of *abl* sequences in Ph¹-positive and -negative B-cell lines. High molecular weight DNA (15 μg) was digested with restriction endonuclease *Bam*HI, separated in a 0.8% agarose gel, and then transferred to nitrocellulose. The blotted DNA fragments were hybridized with a nick-translated, 2.4-kb *Bgl* II v-*abl* fragment (1.5 × 10⁸ cpm/μg; ref. 21) and exposed for 4 days. (*A*) Autoradiogram of *abl*-specific fragments in cell lines HL-60 (lane 1), EM2 (lane 2), K562 (lane 3), SK-CML7Bt-33 (lane 4), SK-CML8Bt-3 (lane 5), SK-CML16Bt-1 (lane 6), SK-CML21Bt-6 (lane 7), SK-CML35Bt-2 (lane 8), SK-CML7BN-2 (lane 9), SK-CML8BN-2 (lane 10), and SK-CML35BN-1 (lane 11). (*B*) Ethidium bromide staining of agarose gel prior to transfer to nitrocellulose, showing the level of variation in amount of DNA loaded per lane.

populations that lack the Ph^1 marker, supports a secondary or complementary role for Ph^1 in the progression of the disease (24, 25). This chromosome marker is found in chronic, accelerated, and blast-crisis phases of the disease. It is likely that Ph^1 confers some growth advantage, since cells with the marker chromosome eventually predominate the marrow and peripheral blood even in chronic phase. During the phase of blast crisis, many patients develop additional chromosome abnormalities, including duplication of Ph^1, a variety of trisomies, and complex translocations (26). This is suggestive evidence for Ph^1 being a necessary but not sufficient genetic change for the full evolution of the disease.

The realization that one molecular result of Ph^1 is the generation of a chimeric *bcr-abl* protein with functional characteristics and structure analogous to the *gag-abl* transforming protein of the Abelson murine leukemia virus strengthens the argument for an important role of Ph^1 in the pathogenesis of CML. Although the Abelson virus is generally considered a rapidly transforming retrovirus, its effects can range from overcoming growth factor requirements, to cellular lethality, to induction of highly oncogenic tumors in a number of hematopoietic cell lineages (27, 28). Even in the transformation of murine cell targets, there are several lines of evidence that suggest that the growth-promoting activity of the v-*abl* gene product is complemented by further cellular changes in the production of the malignant-cell phenotype (29–31).

The regulation of *bcr-abl* gene expression is complex because the 5' end of the gene is derived from the non-*abl* sequences, *bcr*, normally found on chromosome 22 (6). The level of stable message for the normal *bcr* gene and the normal *abl* gene are both much lower than the level of the *bcr-abl* message and protein from cell lines and clinical specimens derived from myeloid blast-crisis patients (5, 6, 11). Therefore, the high level of *bcr-abl* expression cannot simply be attributed to the regulatory sequences associated with *bcr*. Possibly, creation of the chimeric gene disrupts the normal regulatory sequences and results in a higher level of expression. Variation in *bcr-abl* expression may result from secondary changes in the structure of the chimeric gene or function of *trans*-acting factors that occur during evolution of the disease. Our analysis of P210^{c-abl} and the 8-kb mRNA in Epstein–Barr virus-transformed Ph^1-positive B-cell lines demonstrates that stable message and protein levels from the *bcr-abl* gene can vary over a wide range. This variation does not result from a change in the number of *bcr-abl* templates secondary to gene amplification but more likely from changes in either transcription rate or mRNA stability. We suspect this range of *bcr-abl* expression is not limited to lymphoid cells. Analysis of peripheral blood leukocytes derived from an unusual CML patient who has been in chronic phase with myeloid predominance for 16 years showed a level of P210^{c-abl} one-fifth that of P145^{c-abl}, as detected by metabolic labeling with [^{32}P]orthophosphate and immunoprecipitation (S.C., O.N.W., and P. Greenberg, unpublished observations). Lower levels of expression of the chimeric mRNA have been demonstrated in clinical samples from chronic-phase CML patients compared to acute-phase CML patients (9). Others have reported chronic-phase patients with variable but, in some cases, relatively high levels of the *bcr-abl* mRNA (32). The sampling variation and the heterogenous mixture of cell types in clinical samples complicate such analyses. Further work is needed to evaluate whether there is a defined change in P210^{c-abl} expression during the progression of CML. It is interesting to note that among the limited sample of Ph^1-positive B-cell lines we have examined (Table 1), we have seen higher levels of P210^{c-abl} in those derived from patients at more advanced stages of the disease.

It will be important to search for cell-type-specific mechanisms that might regulate expression of *bcr-abl* from Ph^1.

1. Champlin, R. E. & Golde, D. W. (1985) *Blood* 65, 1039–1047.
2. Rowley, J. D. (1973) *Nature (London)* 243, 290–291.
3. Heisterkamp, N., Stephenson, J. R., Groffen, J., Hansen, P. F., de Klein, A., Bartram, C. R. & Grosveld, G. (1983) *Nature (London)* 306, 239–242.
4. Bartram, C. R., de Klein, A., Hagemeijer, A., van Agthoven, T., van Kessel, A. G., Bootsma, D., Grosveld, G., Ferguson-Smith, M. A., Davies, T., Stone, M., Heisterkamp, N., Stephenson, J. R. & Groffen, J. (1983) *Nature (London)* 306, 277–280.
5. Shtivelman, E., Lifshitz, B., Gale, R. P. & Canaani, D. (1985) *Nature (London)* 315, 550–554.
6. Heisterkamp, N., Stam, K. & Groffen, J. (1985) *Nature (London)* 315, 758–761.
7. Groffen, J., Stephenson, J. R., Heisterkamp, N., de Klein, A., Bartram, C. R. & Grosveld, G. (1984) *Cell* 36, 93–99.
8. Gale, R. P. & Canaani, E. (1984) *Proc. Natl. Acad. Sci. USA* 81, 5648–5652.
9. Collins, S., Kubonishi, L., Miyoshi, I. & Groudine, M. T. (1984) *Science* 225, 72–74.
10. Konopka, J. B., Watanabe, S. M. & Witte, O. N. (1984) *Cell* 7, 1035–1042.
11. Konopka, J. B., Watanabe, S. M., Singer, J., Collins, S. & Witte, O. N. (1985) *Proc. Natl. Acad. Sci. USA* 82, 1810–1814.
12. Kloetzer, W., Kurzrock, R., Smith, L., Talpaz, M., Spiller, M., Gutterman, J. & Arlinghaus, R. (1985) *Virology* 140, 230–238.
13. Kozbor, D., Giallongo, A., Sierzega, M. E., Konopka, J. B., Witte, O. N., Showe, L. C. & Croce, C. M. (1985) *Nature (London)*, in press.
14. Davis, R. L., Konopka, J. B. & Witte, O. N. (1985) *Mol. Cell. Biol.* 5, 204–213.
15. Konopka, J. B. & Witte, O. N. (1985) *Mol. Cell. Biol.* 5, 3116–3123.
16. Nitta, M., Kato, Y., Strife, A., Wachter, M., Fried, J., Perez, A., Jhanwar, S., Duigou, R., Chaganti, R. S. K. & Clarkson, B. (1985) *Blood* 66, 1053–1061.
17. Konopka, J. B., Davis, J. L., Watanabe, S. M., Ponticelli, A. S., Schiff-Maker, L., Rosenberg, N. & Witte, O. N. (1984) *Virology* 51, 223–232.
18. Gibson, W. (1981) *Anal. Biochem.* 118, 1–3.
19. Schiff-Maker, L., Konopka, J. B., Clark, S., Witte, O. N. & Rosenberg, N. (1986) *J. Virol.* 57, 1182–1186.
20. Schwartz, R. C., Sonenshein, G. E., Bothwell, A. & Gefter, M. L. (1981) *J. Immunol.* 126, 2104–2108.
21. Goff, S. P., Gilboa, E., Witte, O. N. & Baltimore, D. (1980) *Cell* 22, 777–785.
22. Collins, S. J. & Groudine, M. T. (1983) *Proc. Natl. Acad. Sci. USA* 80, 4813–4817.
23. Selden, J. R., Emanuel, B. S., Wang, E., Cannizzaro, L., Palumbo, A., Erikson, J., Nowell, P. C., Rovera, G. & Croce, C. M. (1983) *Proc. Natl. Acad. Sci. USA* 80, 7289–7292.
24. Fialkow, P. J., Martin, P. J., Najfeld, V., Penfold, G. K., Jacobson, R. J. & Hansen, J. A. (1981) *Blood* 58, 158–163.
25. Martin, P. J., Najfeld, V. & Fialkow, P. J. (1982) *Can. Gen. Cytogenet.* 6, 359–368.
26. Rowley, J. D. (1980) *Annu. Rev. Genet.* 14, 17–40.
27. Whitlock, C. A. & Witte, O. N. (1984) *Adv. Immunol.* 37, 74–98.
28. Pierce, J. H., Di Fiore, P. P., Aaronson, S. A., Potter, M., Pumphrey, J., Scott, A. & Ihle, J. N. (1985) *Cell* 41, 685–693.
29. Whitlock, C. A., Ziegler, S. & Witte, O. N. (1983) *Mol. Cell. Biol.* 3, 596–604.
30. Wolf, D., Harris, N. & Rotter, V. (1984) *Cell* 38, 119–126.
31. Klein, G. & Klein, E. (1985) *Nature (London)* 315, 190–195.
32. Stam, K., Jr., Heisterkamp, N., Grosveld, G., de Klein, A., Verma, R., Colemen, M., Dosik, H. & Groffen, J. (1985) *N. Engl. J. Med.* 313, 1429–1433.
33. Lozzio, C. B. & Lozzio, B. B. (1975) *Blood* 45, 321–334.

Genome-wide Study of Gene Copy Numbers, Transcripts, and Protein Levels in Pairs of Non-invasive and Invasive Human Transitional Cell Carcinomas*

Torben F. Ørntoft‡§, Thomas Thykjaer¶, Frederic M. Waldman‖, Hans Wolf**, and Julio E. Celis‡‡

Gain and loss of chromosomal material is characteristic of bladder cancer, as well as malignant transformation in general. The consequences of these changes at both the transcription and translation levels is at present unknown partly because of technical limitations. Here we have attempted to address this question in pairs of non-invasive and invasive human bladder tumors using a combination of technology that included comparative genomic hybridization, high density oligonucleotide array-based monitoring of transcript levels (5600 genes), and high resolution two-dimensional gel electrophoresis. The results showed that there is a gene dosage effect that in some cases superimposes on other regulatory mechanisms. This effect depended ($p < 0.015$) on the magnitude of the comparative genomic hybridization change. In general (18 of 23 cases), chromosomal areas with more than 2-fold gain of DNA showed a corresponding increase in mRNA transcripts. Areas with loss of DNA, on the other hand, showed either reduced or unaltered transcript levels. Because most proteins resolved by two-dimensional gels are unknown it was only possible to compare mRNA and protein alterations in relatively few cases of well focused abundant proteins. With few exceptions we found a good correlation ($p < 0.005$) between transcript alterations and protein levels. The implications, as well as limitations, of the approach are discussed. *Molecular & Cellular Proteomics 1:37–45, 2002.*

Aneuploidy is a common feature of most human cancers (1), but little is known about the genome-wide effect of this phenomenon at both the transcription and translation levels. High throughput array studies of the breast cancer cell line BT474 has suggested that there is a correlation between DNA copy numbers and gene expression in highly amplified areas (2), and studies of individual genes in solid tumors have revealed a good correlation between gene dose and mRNA or protein levels in the case of c-erb-B2, *cyclin d1, ems1*, and N-myc (3–5). However, a high cyclin D1 protein expression has been observed without simultaneous amplification (4), and a low level of c-myc copy number increase was observed without concomitant c-myc protein overexpression (6).

In human bladder tumors, karyotyping, fluorescent *in situ* hybridization, and comparative genomic hybridization (CGH)[1] have revealed chromosomal aberrations that seem to be characteristic of certain stages of disease progression. In the case of non-invasive pTa transitional cell carcinomas (TCCs), this includes loss of chromosome 9 or parts of it, as well as loss of Y in males. In minimally invasive pT1 TCCs, the following alterations have been reported: 2q−, 11p−, 1q+, 11q13+, 17q+, and 20q+ (7–12). It has been suggested that these regions harbor tumor suppressor genes and oncogenes; however, the large chromosomal areas involved often contain many genes, making meaningful predictions of the functional consequences of losses and gains very difficult.

In this investigation we have combined genome-wide technology for detecting genomic gains and losses (CGH) with gene expression profiling techniques (microarrays and proteomics) to determine the effect of gene copy number on transcript and protein levels in pairs of non-invasive and invasive human bladder TCCs.

EXPERIMENTAL PROCEDURES

Material—Bladder tumor biopsies were sampled after informed consent was obtained and after removal of tissue for routine pathology examination. By light microscopy tumors 335 and 532 were staged by an experienced pathologist as pTa (superficial papillary),

[1] The abbreviations used are: CGH, comparative genomic hybridization; TCC, transitional cell carcinoma; LOH, loss of heterozygosity; PA-FABP, psoriasis-associated fatty acid-binding protein; 2D, two-dimensional.
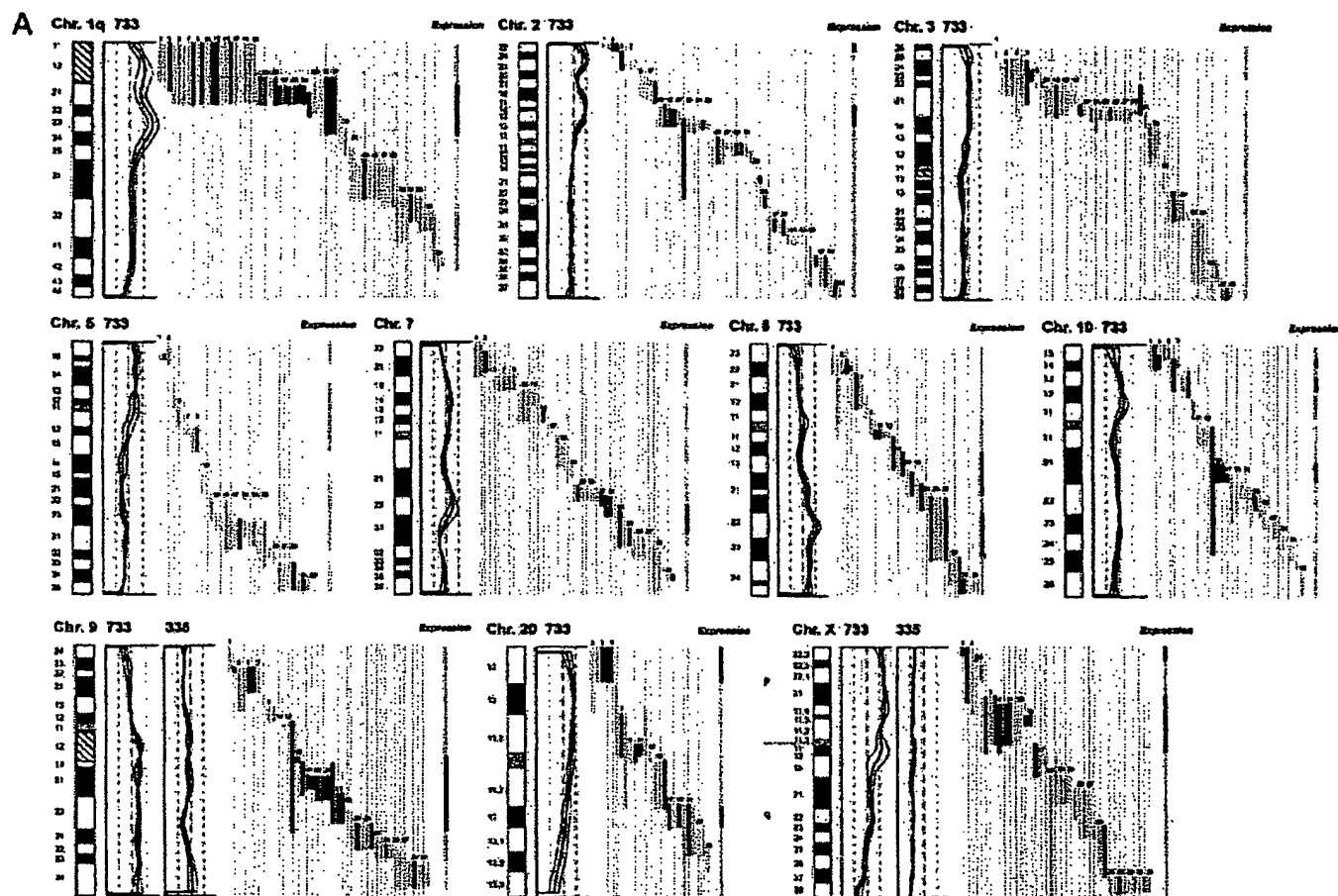
Fig. 1. **DNA copy number and mRNA expression level.** Shown from *left* to *right* are chromosome (*Chr.*), CGH profiles, gene location and expression level of specific genes, and overall expression level along the chromosome. *A*, expression of mRNA in invasive tumor 733 as compared with the non-invasive counterpart tumor 335. *B*, expression of mRNA in invasive tumor 827 compared with the non-invasive counterpart tumor 532. The average fluorescent signal ratio between tumor DNA and normal DNA is shown along the length of the chromosome (*left*). The *bold curve* in the ratio profile represents a mean of four chromosomes and is surrounded by *thin curves* indicating one standard deviation. The *central vertical line* (*broken*) indicates a ratio value of 1 (no change), and the *vertical lines* next to it (*dotted*) indicate a ratio of 0.5 (*left*) and 2.0 (*right*). In chromosomes where the non-invasive tumor 335 used for comparison showed alterations in DNA content, the ratio profile of that chromosome is shown to the *right* of the invasive tumor profile. The *colored bars* represents one gene each, identified by the running *numbers above* the *bars* (the name of the gene can be seen at www.MDL.DK/sdata.html). The *bars* indicate the purported location of the gene, and the *colors* indicate the expression level of the gene in the invasive tumor compared with the non-invasive counterpart; >2-fold increase (*black*), >2-fold decrease (*blue*), no significant change (*orange*). The *bar* to the *far right*, entitled *Expression* shows the resulting change in expression along the chromosome; the *colors* indicate that at least half of the genes were up-regulated (*black*), at least half of the genes down-regulated (*blue*), or more than half of the genes are unchanged (*orange*). If a gene was absent in one of the samples and present in another, it was regarded as more than a 2-fold change. A 2-fold level was chosen as this corresponded to one standard deviation in a double determination of ~1800 genes. Centromeres and heterochromatic regions were excluded from data analysis.

grade I and II, respectively, tumors 733 and 827 were staged as pT1 (invasive into submucosa), 733 was staged as solid, and 827 was staged as papillary, both grade III.

*mRNA Preparation—*Tissue biopsies, obtained fresh from surgery, were embedded immediately in a sodium-guanidinium thiocyanate solution and stored at −80 °C. Total RNA was isolated using the RNAzol B RNA isolation method (WAK-Chemie Medical GMBH). poly(A)[+] RNA was isolated by an oligo(dT) selection step (Oligotex mRNA kit; Qiagen).

*cRNA Preparation—*1 μg of mRNA was used as starting material. The first and second strand cDNA synthesis was performed using the SuperScript® choice system (Invitrogen) according to the manufacturer's instructions but using an oligo(dT) primer containing a T7 RNA polymerase binding site. Labeled cRNA was prepared using the ME-GAscrip® *in vitro* transcription kit (Ambion). Biotin-labeled CTP and

UTP (Enzo) was used, together with unlabeled NTPs in the reaction. Following the *in vitro* transcription reaction, the unincorporated nucleotides were removed using RNeasy columns (Qiagen).

*Array Hybridization and Scanning—*Array hybridization and scanning was modified from a previous method (13). 10 μg of cRNA was fragmented at 94 °C for 35 min in buffer containing 40 mM Tris acetate, pH 8.1, 100 mM KOAc, 30 mM MgOAc. Prior to hybridization, the fragmented cRNA in a 6× SSPE-T hybridization buffer (1 M NaCl, 10 mM Tris, pH 7.6, 0.005% Triton), was heated to 95 °C for 5 min, subsequently cooled to 40 °C, and loaded onto the Affymetrix probe array cartridge. The probe array was then incubated for 16 h at 40 °C at constant rotation (60 rpm). The probe array was exposed to 10 washes in 6× SSPE-T at 25 °C followed by 4 washes in 0.5× SSPE-T at 50 °C. The biotinylated cRNA was stained with a streptavidin-phycoerythrin conjugate, 10 μg/ml (Molecular Probes) in 6× SSPE-T
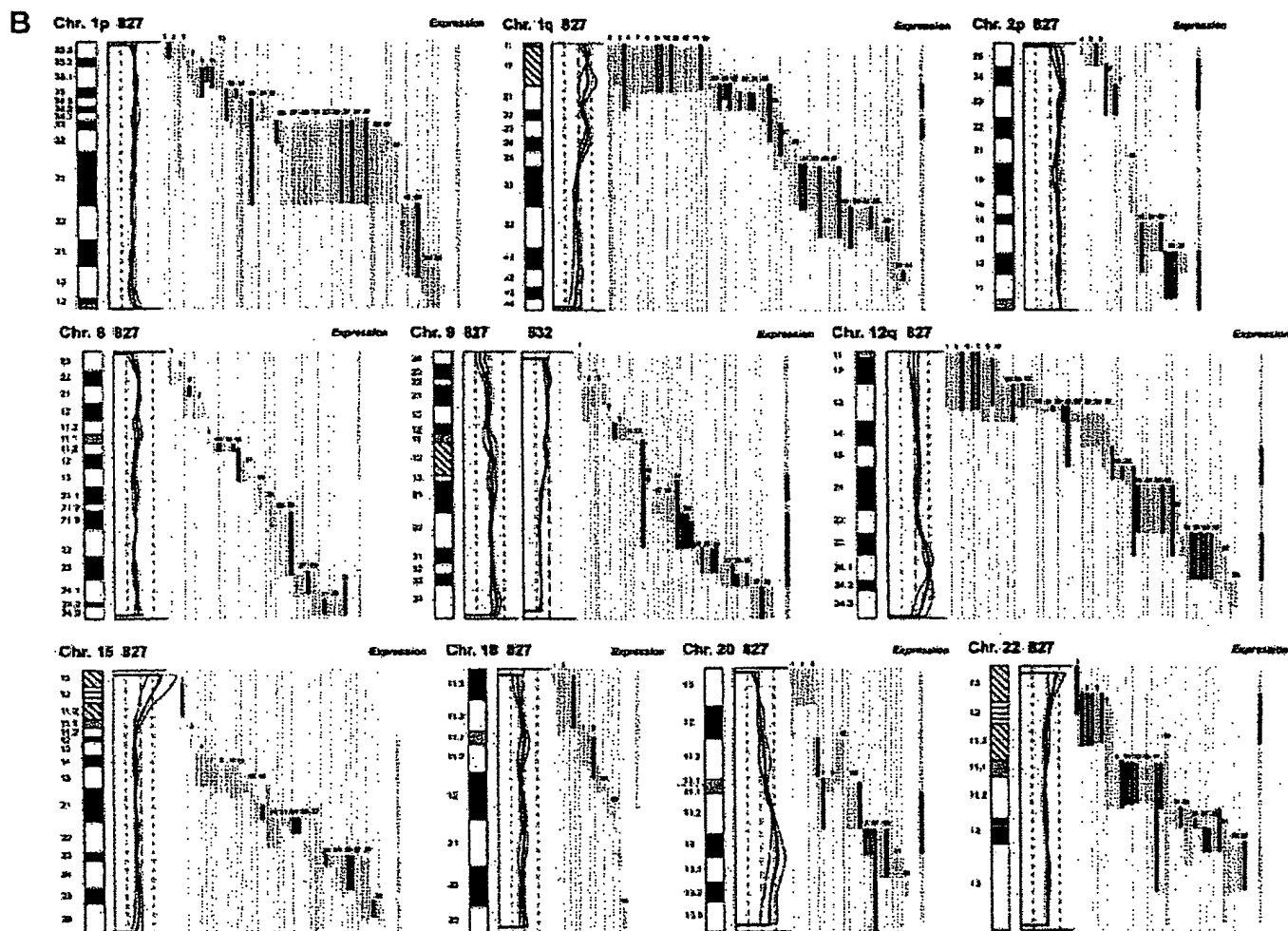
FIG. 1—continued

for 30 min at 25 °C followed by 10 washes in 6× SSPE-T at 25 °C. The probe arrays were scanned at 560 nm using a confocal laser scanning microscope (made for Affymetrix by Hewlett-Packard). The readings from the quantitative scanning were analyzed by Affymetrix gene expression analysis software.

Microsatellite Analysis—Microsatellite Analysis was performed as described previously (14). Microsatellites were selected by use of www.ncbi.nlm.nih.gov/genemap98, and primer sequences were obtained from the genome data base at www.gdb.org. DNA was extracted from tumor and blood and amplified by PCR in a volume of 20 μl for 35 cycles. The amplicons were denatured and electrophoresed for 3 h in an ABI Prism 377. Data were collected in the Gene Scan program for fragment analysis. Loss of heterozygosity was defined as less than 33% of one allele detected in tumor amplicons compared with blood.

Proteomic Analysis—TCCs were minced into small pieces and homogenized in a small glass homogenizer in 0.5 ml of lysis solution. Samples were stored at −20 °C until use. The procedure for 2D gel electrophoresis has been described in detail elsewhere (15, 16). Gels were stained with silver nitrate and/or Coomassie Brilliant Blue. Proteins were identified by a combination of procedures that included microsequencing, mass spectrometry, two-dimensional gel Western immunoblotting, and comparison with the master two-dimensional gel image of human keratinocyte proteins; see biobase.dk/cgi-bin/cells.

CGH—Hybridization of differentially labeled tumor and normal DNA to normal metaphase chromosomes was performed as described previously (10). Fluorescein-labeled tumor DNA (200 ng), Texas Red-labeled reference DNA (200 ng), and human Cot-1 DNA (20 μg) were denatured at 37 °C for 5 min and applied to denatured normal metaphase slides. Hybridization was at 37 °C for 2 days. After washing, the slides were counterstained with 0.15 μg/ml 4,6-diamidino-2-phenylindole in an anti-fade solution. A second hybridization was performed for all tumor samples using fluorescein-labeled reference DNA and Texas Red-labeled tumor DNA (inverse labeling) to confirm the aberrations detected during the initial hybridization. Each CGH experiment also included a normal control hybridization using fluorescein- and Texas Red-labeled normal DNA. Digital image analysis was used to identify chromosomal regions with abnormal fluorescence ratios, indicating regions of DNA gains and losses. The average green:red fluorescence intensity ratio profiles were calculated using four images of each chromosome (eight chromosomes total) with normalization of the green:red fluorescence intensity ratio for the entire metaphase and background correction. Chromosome identification was performed based on 4,6-diamidino-2-phenylindole banding patterns. Only images showing uniform high intensity fluorescence with minimal background staining were analyzed. All centromeres, p arms of acrocentric chromosomes, and heterochromatic regions were excluded from the analysis.

RESULTS

Comparative Genomic Hybridization—The CGH analysis identified a number of chromosomal gains and losses in the

TABLE I

Correlation between alterations detected by CGH and by expression monitoring

Top, CGH used as independent variable (if CGH alteration – what expression ratio was found); bottom, altered expression used as independent variable (if expression alteration – what CGH deviation was found).

| CGH alterations | Tumor 733 vs. 335 | Concordance | CGH alterations | Tumor 827 vs. 532 | Concordance |
	Expression change clusters			Expression change clusters	
13 Gain	10 Up-regulation 0 Down-regulation 3 No change	77%	10 Gain	8 Up-regulation 0 Down-regulation 2 No change	80%
10 Loss	1 Up-regulation 5 Down-regulation 4 No change	50%	12 Loss	3 Up-regulation 2 Down regulation 7 No change	17%

| Expression change clusters | Tumor 733 vs. 335 | Concordance | Expression change clusters | Tumor 827 vs. 532 | Concordance |
	CGH alterations			CGH alterations	
16 Up-regulation	11 Gain 2 Loss 3 No change	69%	17 Up-regulation	10 Gain 5 Loss 2 No change	59%
21 Down-regulation	1 Gain 8 Loss 12 No change	38%	9 Down-regulation	0 Gain 3 Loss 6 No change	33%
15 No change	3 Gain 3 Loss 9 No change	60%	21 No change	1 Gain 3 Loss 17 No change	81%

two invasive tumors (stage pT1, TCCs 733 and 827), whereas the two non-invasive papillomas (stage pTa, TCCs 335 and 532) showed only 9p−, 9q22-q33−, and X−, and 7+, 9q−, and Y−, respectively. Both invasive tumors showed changes (1q22–24+, 2q14.1-qter−, 3q12-q13.3−, 6q12-q22−, 9q34+, 11q12-q13+, 17+, and 20q11.2-q12+) that are typical for their disease stage, as well as additional alterations, some of which are shown in Fig. 1. Areas with gains and losses deviated from the normal copy number to some extent, and the average numerical deviation from normal was 0.4-fold in the case of TCC 733 and 0.3-fold for TCC 827. The largest changes, amounting to at least a doubling of chromosomal content, were observed at 1q23 in TCC 733 (Fig. 1A) and 20q12 in TCC 827 (Fig. 1B).

mRNA Expression in Relation to DNA Copy Number—The mRNA levels from the two invasive tumors (TCCs 827 and 733) were compared with the two non-invasive counterparts (TCCs 532 and 335). This was done in two separate experiments in which we compared TCCs 733 to 335 and 827 to 532, respectively, using two different scaling settings for the arrays to rule out scaling as a confounding parameter. Approximately 1,800 genes that yielded a signal on the arrays were searched in the Unigene and Genemap data bases for chromosomal location, and those with a known location (1096) were plotted as bars covering their purported locus. In that way it was possible to construct a graphic presentation of DNA copy number and relative mRNA levels along the individual chromosomes (Fig. 1).

For each mRNA a ratio was calculated between the level in the invasive *versus* the non-invasive counterpart. Bars, which represent chromosomal location of a gene, were color-coded according to the expression ratio, and only differences larger

than 2-fold were regarded as informative (Fig. 1). The density of genes along the chromosomes varied, and areas containing only one gene were excluded from the calculations. The resolution of the CGH method is very low, and some of the outlier data may be because of the fact that the boundaries of the chromosomal aberrations are not known at high resolution.

Two sets of calculations were made from the data. For the first set we used CGH alterations as the independent variable and estimated the frequency of expression alterations in these chromosomal areas. In general, areas with a strong gain of chromosomal material contained a cluster of genes having increased mRNA expression. For example, both chromosomes 1q21-q25, 2p and 9q, showed a relative gain of more than 100% in DNA copy number that was accompanied by increased mRNA expression levels in the two tumor pairs (Fig. 1). In most cases, chromosomal gains detected by CGH were accompanied by an increased level of transcripts in both TCCs 733 (77%) and 827 (80%) (Table I, *top*). Chromosomal losses, on the other hand, were not accompanied by decreased expression in several cases, and were often registered as having unaltered RNA levels (Table I, *top*). The inability to detect RNA expression changes in these cases was not because of fewer genes mapping to the lost regions (data not shown).

In the second set of calculations we selected expression alterations above 2-fold as the independent variable and estimated the frequency of CGH alterations in these areas. As above, we found that increased transcript expression correlated with gain of chromosomal material (TCC 733, 69% and TCC 827, 59%), whereas reduced expression was often detected in areas with unaltered CGH ratios (Table I, *bottom*). Furthermore, as a control we looked at areas with no alter-
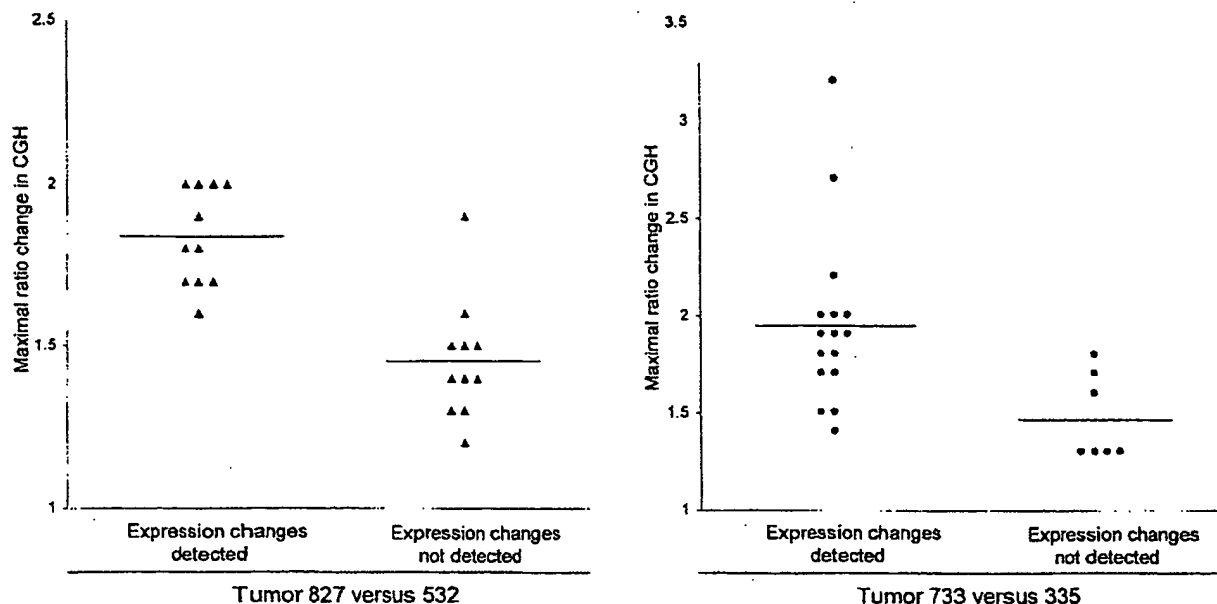
FIG. 2. **Correlation between maximum CGH aberration and the ability to detect expression change by oligonucleotide array monitoring.** The aberration is shown as a numerical -fold change in ratio between invasive tumors 827 (▲) and 733 (♦) and their non-invasive counterparts 532 and 335. The expression change was taken from the *Expression* line to the *right* in Fig. 1, which depicts the resulting expression change for a given chromosomal region. At least half of the mRNAs from a given region have to be either up- or down-regulated to be scored as an expression change. All chromosomal arms in which the CGH ratio plus or minus one standard deviation was outside the ratio value of one were included.

ation in expression. No alteration was detected by CGH in most of these areas (TCC 733, 60% and TCC 827, 81%; see Table I, *bottom*). Because the ability to observe reduced or increased mRNA expression clustering to a certain chromosomal area clearly reflected the extent of copy number changes, we plotted the maximum CGH aberrations in the regions showing CGH changes against the ability to detect a change in mRNA expression as monitored by the oligonucleotide arrays (Fig. 2). For both tumors TCC 733 ($p < 0.015$) and TCC 827 ($p < 0.00003$) a highly significant correlation was observed between the level of CGH ratio change (reflecting the DNA copy number) and alterations detected by the array based technology (Fig. 2). Similar data were obtained when areas with altered expression were used as independent variables. These areas correlated best with CGH when the CGH ratio deviated 1.6- to 2.0-fold (Table I, *bottom*) but mostly did not at lower CGH deviations. These data probably reflect that loss of an allele may only lead to a 50% reduction in expression level, which is at the cut-off point for detection of expression alterations. Gain of chromosomal material can occur to a much larger extent.

Microsatellite-based Detection of Minor Areas of Losses—In TCC 733, several chromosomal areas exhibiting DNA amplification were preceded or followed by areas with a normal CGH but reduced mRNA expression (see Fig. 1, TCC 733 chromosome 1q32, 2p21, and 7q21 and q32, 9q34, and 10q22). To determine whether these results were because of undetected loss of chromosomal material in these regions or

because of other non-structural mechanisms regulating transcription, we examined two microsatellites positioned at chromosome 1q25–32 and two at chromosome 2p22. Loss of heterozygosity (LOH) was found at both 1q25 and at 2p22 indicating that minor deleted areas were not detected with the resolution of CGH (Fig. 3). Additionally, chromosome 2p in TCC 733 showed a CGH pattern of gain/no change/gain of DNA that correlated with transcript increase/decrease/increase. Thus, for the areas showing increased expression there was a correlation with the DNA copy number alterations (Fig. 1A). As indicated above, the mRNA decrease observed in the middle of the chromosomal gain was because of LOH, implying that one of the mechanisms for mRNA down-regulation may be regions that have undergone smaller losses of chromosomal material. However, this cannot be detected with the resolution of the CGH method.

In both TCC 733 and TCC 827, the telomeric end of chromosome 11p showed a normal ratio in the CGH analysis; however, clusters of five and three genes, respectively, lost their expression. Two microsatellites (D11S1760, D11S922) positioned close to MUC2, IGF2, and cathepsin D indicated LOH as the most likely mechanism behind the loss of expression (data not shown).

A reduced expression of mRNA observed in TCC 733 at chromosomes 3q24, 11p11, 12p12.2, 12q21.1, and 16q24 and in TCC 827 at chromosome 11p15.5, 12p11, 15q11.2, and 18q12 was also examined for chromosomal losses using microsatellites positioned as close as possible to the gene loci
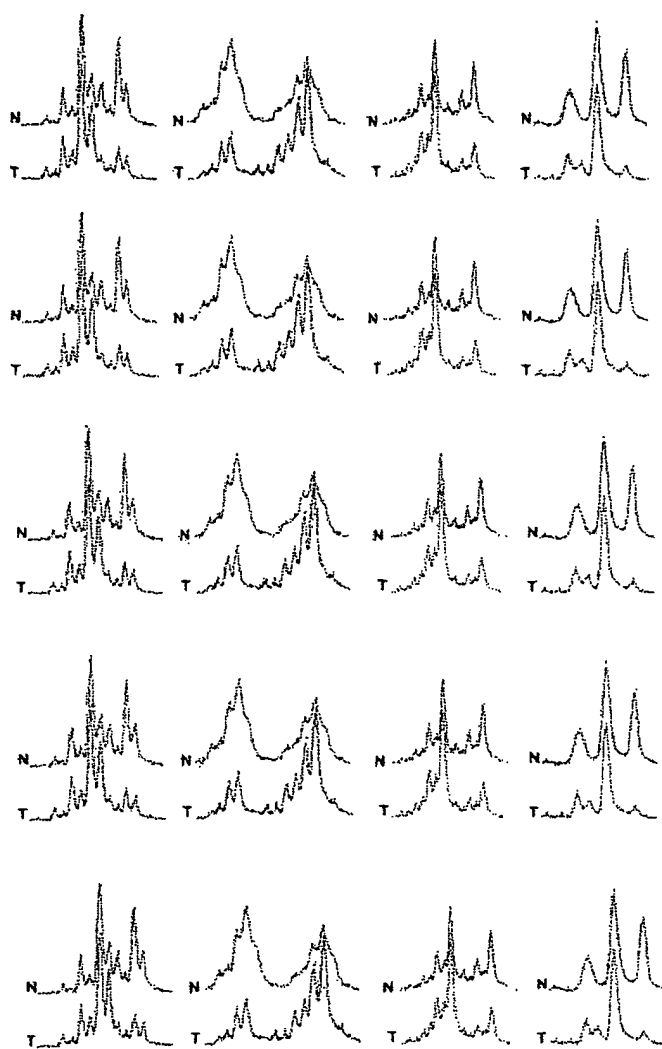
Fig. 4. **Correlation between protein levels as judged by 2D-PAGE and transcript ratio.** For comparison proteins were divided in three groups, unaltered in level or up- or down-regulated (*horizontal axis*). The mRNA ratio as determined by oligonucleotide arrays was plotted for each gene (*vertical axis*). ▲, mRNAs that were scored as present in both tumors used for the ratio calculation; △, mRNAs that were scored as absent in the invasive tumors (along *horizontal axis*) or as absent in non-invasive reference (*top* of figure). Two different scalings were used to exclude scaling as a confounder, TCCs 827 and 532 (▲△) were scaled with background suppression, and TCCs 733 and 335 (●○) were scaled without suppression. Both comparisons showed highly significant ($p < 0.005$) differences in mRNA ratios between the groups. Proteins shown were as follows: Group A (from *left*), phosphoglucomutase 1, glutathione transferase class μ number 4, fatty acid-binding protein homologue, cytokeratin 15, and cytokeratin 13; *B* (from *left*), fatty acid-binding protein homologue, 28-kDa heat shock protein, cytokeratin 13, and calcyclin; *C* (from *left*), α-enolase, hnRNP B1, 28-kDa heat shock protein, 14-3-3-ε, and pre-mRNA splicing factor; *D*, mesothelial keratin K7 (type II); *E* (from *top*), glutathione *S*-transferase-π and mesothelial keratin K7 (type II); *F* (from *top* and *left*), adenylyl cyclase-associated protein, E-cadherin, keratin 19, calgizzarin, phosphoglycerate mutase, annexin IV, cytoskeletal γ-actin, hnRNP A1, integral membrane protein calnexin (IP90), hnRNP H, brain-type clathrin light chain-a, hnRNP F, 70-kDa heat shock protein, heterogeneous nuclear ribonucleoprotein A/B, translationally controlled tumor protein, liver glyceraldehyde-3-phosphate dehydrogenase, keratin 8, aldehyde reductase, and Na,K-ATPase β-1 subunit; *G*, (from *top* and *left*), TCP20, calgizzarin, 70-kDa heat shock protein, calnexin, hnRNP H, cytokeratin 15, ATP synthase, keratin 19, triosephosphate isomerase, hnRNP F, liver glyceraldehyde-3-phosphatase dehydrogenase, glutathione *S*-transferase-π, and keratin 8; *H* (from *left*), plasma gelsolin, autoantigen calreticulin, thioredoxin, and NAD+-dependent 15 hydroxyprostaglandin dehydrogenase; *I* (from *top*), prolyl 4-hydroxylase β-subunit, cytokeratin 20, cytokeratin 17, prohibition, and fructose 1,6-biphosphatase; *J* annexin II; *K*, annexin IV; *L* (from *top* and *left*), 90-kDa heat shock protein, prolyl 4-hydroxylase β-subunit, α-enolase, GRP 78, cyclophilin, and cofilin.

Fig. 3. **Microsatellite analysis of loss of heterozygosity.** Tumor 733 showing loss of heterozygosity at chromosome 1q25, detected (a) by D1S215 close to Hu class I histocompatibility antigen (gene number 38 in Fig. 1), (b) by D1S2735 close to cathepsin E (gene number 41 in Fig. 1), and (c) at chromosome 2p23 by D2S2251 close to general β-spectrin (gene number 11 on Fig. 1) and of (d) tumor 827 showing loss of heterozygosity at chromosome 18q12 by S18S1118 close to mitochondrial 3-oxoacyl-coenzyme A thiolase (gene number 12 in Fig. 1). The *upper curves* show the electropherogram obtained from normal DNA from leukocytes (*N*), and the *lower curves* show the electropherogram from tumor DNA (*T*). In all cases one allele is partially lost in the tumor amplicon.

showing reduced mRNA transcripts. Only the microsatellite positioned at 18q12 showed LOH (Fig. 3), suggesting that transcriptional down-regulation of genes in the other regions may be controlled by other mechanisms.

Relation between Changes in mRNA and Protein Levels— 2D-PAGE analysis, in combination with Coomassie Brilliant Blue and/or silver staining, was carried out on all four tumors using fresh biopsy material. 40 well resolved abundant known proteins migrating in areas away from the edges of the pH
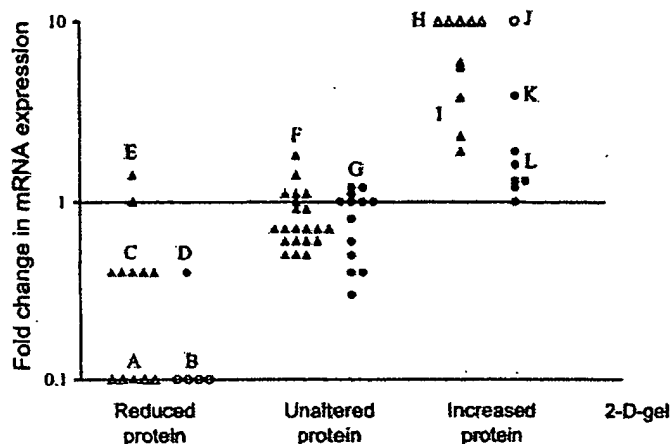
gradient, and having a known chromosomal location, were selected for analysis in the TCC pair 827/532. Proteins were identified by a combination of methods (see "Experimental Procedures"). In general there was a highly significant correlation ($p < 0.005$) between mRNA and protein alterations (Fig. 4). Only one gene showed disagreement between transcript alteration and protein alteration. Except for a group of cyto-
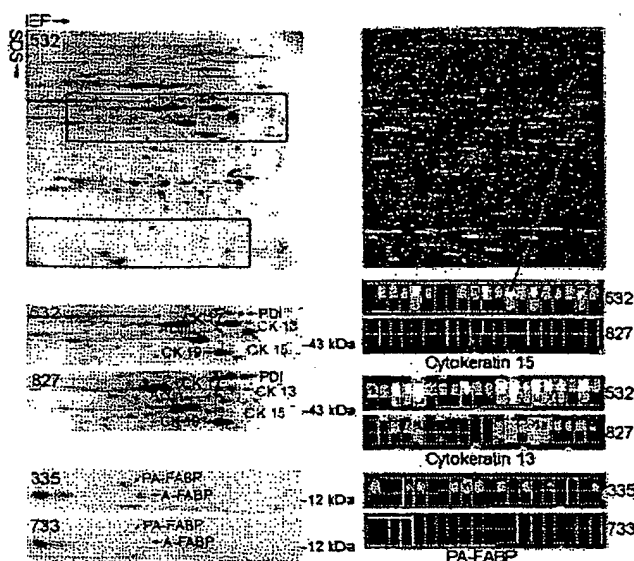
FIG. 5. **Comparison of protein and transcript levels in invasive and non-invasive TCCs.** The *upper part* of the figure shows a 2D gel (*left*) and the oligonucleotide array (*right*) of TCC 532. The *red rectangles* on the *upper gel* highlight the areas that are compared below. Identical areas of 2D gels of TCCs 532 and 827 are shown below. Clearly, cytokeratins 13 and 15 are strongly down-regulated in TCC 827 (*red annotation*). The tile on the array containing probes for cytokeratin 15 is enlarged *below* the array (*red arrow*) from TCC 532 and is compared with TCC 827. The *upper row* of *squares* in each tile corresponds to perfect match probes; the *lower row* corresponds to mismatch probes containing a mutation (used for correction for unspecific binding). Absence of signal is depicted as *black*, and the higher the signal the lighter the color. A high transcript level was detected in TCC 532 (6151 units) whereas a much lower level was detected in TCC 827 (absence of signals). For cytokeratin 13, a high transcript level was also present in TCC 532 (15659 units), and a much lower level was present in TCC 827 (623 units). The 2D gels at the *bottom* of the figure (*left*) show levels of PA-FABP and adipocyte-FABP in TCCs 335 and 733 (invasive), respectively. Both proteins are down-regulated in the invasive tumor. To the *right* we show the array tiles for the PA-FABP transcript. A medium transcript level was detected in the case of TCC 335 (1277 units) whereas very low levels were detected in TCC 733 (166 units). *IEF*, isoelectric focusing.

keratins encoded by genes on chromosome 17 (Fig. 5) the analyzed proteins did not belong to a particular family. 26 well focused proteins whose genes had a know chromosomal location were detected in TCCs 733 and 335, and of these 19 correlated ($p < 0.005$) with the mRNA changes detected using the arrays (Fig. 4). For example, PA-FABP was highly expressed in the non-invasive TCC 335 but lost in the invasive counterpart (TCC 733; see Fig. 5). The smaller number of proteins detected in both 733 and 335 was because of the smaller size of the biopsies that were available.

11 chromosomal regions where CGH showed aberrations that corresponded to the changes in transcript levels also showed corresponding changes in the protein level (Table II). These regions included genes that encode proteins that are found to be frequently altered in bladder cancer, namely cytokeratins 17 and 20, annexins II and IV, and the fatty acid-binding proteins PA-FABP and FBP1. Four of these proteins were encoded by genes in chromosome 17q, a frequently amplified chromosomal area in invasive bladder cancers.

DISCUSSION

Most human cancers have abnormal DNA content, having lost some chromosomal parts and gained others. The present study provides some evidence as to the effect of these gains and losses on gene expression in two pairs of non-invasive and invasive TCCs using high throughput expression arrays and proteomics, in combination with CGH. In general, the results showed that there is a clear individual regulation of the mRNA expression of single genes, which in some cases was superimposed by a DNA copy number effect. In most cases, genes located in chromosomal areas with gains often exhibited increased mRNA expression, whereas areas showing losses showed either no change or a reduced mRNA expression. The latter might be because of the fact that losses most often are restricted to loss of one allele, and the cut-off point for detection of expression alterations was a 2-fold change, thus being at the border of detection. In several cases, how-

TABLE II

Proteins whose expression level correlates with both mRNA and gene dose changes

Protein	Chromosomal location	Tumor TCC	CGH alteration	Transcript alteration[a]	Protein alteration
Annexin II	1q21	733	Gain	Abs to Pres[a]	Increase
Annexin IV	2p13	733	Gain	3.9-Fold up	Increase
Cytokeratin 17	17q12-q21	827	Gain	3.8-Fold up	Increase
Cytokeratin 20	17q21.1	827	Gain	5.6-Fold up	Increase
(PA-)FABP	8q21.2	827	Loss	10-Fold down	Decrease
FBP1	9q22	827	Gain	2.3-Fold up	Increase
Plasma gelsolin	9q31	827	Gain	Abs to Pres	Increase
Heat shock protein 28	15q12-q13	827	Loss	2.5-Fold up	Decrease
Prohibitin	17q21	827/733	Gain	3.7-/2.5-Fold up[b]	Increase
Prolyl-4-hydroxyl	17q25	827/733	Gain	5.7-/1.6-Fold up	Increase
hnRNPB1	7p15	827	Loss	2.5-Fold down	Decrease

[a] Abs, absent; Pres, present.
[b] In cases where the corresponding alterations were found in both TCCs 827 and 733 these are shown as 827/733.

ever, an increase or decrease in DNA copy number was associated with *de novo* occurrence or complete loss of transcript, respectively. Some of these transcripts could not be detected in the non-invasive tumor but were present at relatively high levels in areas with DNA amplifications in the invasive tumors (*e.g.* in TCC 733 transcript from cellular ligand of annexin II gene (chromosome 1q21) from absent to 2670 arbitrary units; in TCC 827 transcript from small proline-rich protein 1 gene (chromosome 1q12-q21.1) from absent to 1326 arbitrary units). It may be anticipated from these data that significant clustering of genes with an increased expression to a certain chromosomal area indicates an increased likelihood of gain of chromosomal material in this area.

Considering the many possible regulatory mechanisms acting at the level of transcription, it seems striking that the gene dose effects were so clearly detectable in gained areas. One hypothetical explanation may lie in the loss of controlled methylation in tumor cells (17–19). Thus, it may be possible that in chromosomes with increased DNA copy numbers two or more alleles could be demethylated simultaneously leading to a higher transcription level, whereas in chromosomes with losses the remaining allele could be partly methylated, turning off the process (20, 21). A recent report has documented a ploidy regulation of gene expression in yeast, but in this case all the genes were present in the same ratio (22), a situation that is not analogous to that of cancer cells, which show marked chromosomal aberrations, as well as gene dosage effects.

Several CGH studies of bladder cancer have shown that some chromosomal aberrations are common at certain stages of disease progression, often occurring in more than 1 of 3 tumors. In pTa tumors, these include 9p−, 9q−, 1q+, Y− (2, 6), and in pT1 tumors, 2q−,11p−, 11q−, 1q+, 5p+, 8q+, 17q+, and 20q+ (2–4, 6, 7). The pTa tumors studied here showed similar aberrations such as 9p− and 9q22-q33− and 9q− and Y−, respectively. Likewise, the two minimal invasive pT1 tumors showed aberrations that are commonly seen at that stage, and TCC 827 had a remarkable resemblance to the commonly seen pattern of losses and gains, such as 1q22–24 amplification (seen in both tumors), 11q14-q22 loss, the latter often linked to 17 q+ (both tumors), and 1q+ and 9p−, often linked to 20q+ and 11 q13+ (both tumors) (7–9). These observations indicate that the pairs of tumors used in this study exhibit chromosomal changes observed in many tumors, and therefore the findings could be of general importance for bladder cancer.

Considering that the mapping resolution of CGH is of about 20 megabases it is only possible to get a crude picture of chromosomal instability using this technique. Occasionally, we observed reduced transcript levels close to or inside regions with increased copy numbers. Analysis of these regions by positioning heterozygous microsatellites as close as possible to the locus showing reduced gene expression revealed loss of heterozygosity in several cases. It seems likely that multiple and different events occur along each chromosomal

arm and that the use of cDNA microarrays for analysis of DNA copy number changes will reach a resolution that can resolve these changes, as has recently been proposed (2). The outlier data were not more frequent at the boundaries of the CGH aberrations. At present we do not know the mechanism behind chromosomal aneuploidy and cannot predict whether chromosomal gains will be transcribed to a larger extent than the two native alleles. A mechanism as genetic imprinting has an impact on the expression level in normal cells and is often reduced in tumors. However, the relation between imprinting and gain of chromosomal material is not known.

We regard it as a strength of this investigation that we were able to compare invasive tumors to benign tumors rather than to normal urothelium, as the tumors studied were biologically very close and probably may represent successive steps in the progression of bladder cancer. Despite the limited amount of fresh tissue available it was possible to apply three different state of the art methods. The observed correlation between DNA copy number and mRNA expression is remarkable when one considers that different pieces of the tumor biopsies were used for the different sets of experiments. This indicate that bladder tumors are relatively homogenous, a notion recently supported by CGH and LOH data that showed a remarkable similarity even between tumors and distant metastasis (10, 23).

In the few cases analyzed, mRNA and protein levels showed a striking correspondence although in some cases we found discrepancies that may be attributed to translational regulation, post-translational processing, protein degradation, or a combination of these. Some transcripts belong to undertranslated mRNA pools, which are associated with few translationally inactive ribosomes; these pools, however, seem to be rare (24). Protein degradation, for example, may be very important in the case of polypeptides with a short half-life (*e.g.* signaling proteins). A poor correlation between mRNA and protein levels was found in liver cells as determined by arrays and 2D-PAGE (25), and a moderate correlation was recently reported by Ideker *et al.* (26) in yeast.

Interestingly, our study revealed a much better correlation between gained chromosomal areas and increased mRNA levels than between loss of chromosomal areas and reduced mRNA levels. In general, the level of CGH change determined the ability to detect a change in transcript. One possible explanation could be that by losing one allele the change in mRNA level is not so dramatic as compared with gain of material, which can be rather unlimited and may lead to a severalfold increase in gene copy number resulting in a much higher impact on transcript level. The latter would be much easier to detect on the expression arrays as the cut-off point was placed at a 2-fold level so as not to be biased by noise on the array. Construction of arrays with a better signal to noise ratio may in the future allow detection of lesser than 2-fold alterations in transcript levels, a feature that may facilitate the analysis of the effect of loss of chromosomal areas on transcript levels.

In eleven cases we found a significant correlation between DNA copy number, mRNA expression, and protein level. Four of these proteins were encoded by genes located at a frequently amplified area in chromosome 17q. Whether DNA copy number is one of the mechanisms behind alteration of these eleven proteins is at present unknown and will have to be proved by other methods using a larger number of samples. One factor making such studies complicated is the large extent of protein modification that occurs after translation, requiring immunoidentification and/or mass spectrometry to correctly identify the proteins in the gels.

In conclusion, the results presented in this study exemplify the large body of knowledge that may be possible to gather in the future by combining state of the art techniques that follow the pathway from DNA to protein (26). Here, we used a traditional chromosomal CGH method, but in the future high resolution CGH based on microarrays with many thousand radiation hybrid-mapped genes will increase the resolution and information derived from these types of experiments (2). Combined with expression arrays analyzing transcripts derived from genes with known locations, and 2D gel analysis to obtain information at the post-translational level, a clearer and more developed understanding of the tumor genome will be forthcoming.

REFERENCES

1. Lengauer, C., Kinzler, K. W., and Vogelstein, B. (1998) Genetic instabilities in human cancers. *Nature* 17, 643–649
2. Pollack, J. R., Perou, C. M., Alizadeh, A. A., Eisen, M. B., Pergamenschikov, A., Williams, C. F., Jeffrey, S. S., Botstein, D., and Brown, P. O. (1999) Genome-wide analysis of DNA copy-number changes using cDNA microarrays. *Nat. Genet.* 23, 41–46
3. de Cremoux, P., Martin, E. C., Vincent-Salomon, A., Dieras, V., Barbaroux, C., Liva, S., Pouillart, P., Sastre-Garau, X., and Magdelenat, H. (1999) Quantitative PCR analysis of c-erb B-2 (HER2/neu) gene amplification and comparison with p185(HER2/neu) protein expression in breast cancer drill biopsies. *Int. J. Cancer* 83, 157–161
4. Brungier, P. P., Tamimi, Y., Shuuring, E., and Schalken, J. (1996) Expression of cyclin D1 and EMS1 in bladder tumors; relationship with chromosome 11q13 amplifications. *Oncogene* 12, 1747–1753
5. Slavc, I., Ellenbogen, R., Jung, W. H., Vawter, G. F., Kretschmar, C., Grier, H., and Korf, B. R. (1990) *myc* gene amplification and expression in primary human neuroblastoma. *Cancer Res.* 50, 1459–1463
6. Sauter, G., Carroll, P., Moch, H., Kallioniemi, A., Kerschmann, R., Narayan,

P., Mihatsch, M. J., and Waldman, F. M. (1995) c-*myc* copy number gains in bladder cancer detected by fluorescence *in situ* hybridization. *Am J. Pathol.* 146, 1131–1139
7. Richter, J., Jiang, F., Gorog, J. P., Sartorious, G., Egenter, C., Gasser, T. C., Moch, H., Mihatsch, M. J., and Sauter, G. (1997) Marked genetic differences between stage pTa and stage pT1 papillary bladder cancer detected by comparative genomic hybridization. *Cancer Res.* 57, 2860–2864
8. Richter, J., Beffa, L., Wagner, U., Schraml, P., Gasser, T. C., Moch, H., Mihatsch, M. J., and Sauter, G. (1998) Patterns of chromosomal imbalances in advanced urinary bladder cancer detected by comparative genomic hybridization. *Am. J. Pathol.* 153, 1615–1621
9. Bruch, J., Wohr, G., Hautmann, R., Mattfeldt, T., Bruderlein, S., Moller, P., Sauter, S., Hameister, H., Vogel, W., and Paiss, T. (1998) Chromosomal changes during progression of transitional cell carcinoma of the bladder and delineation of the amplified interval on chromosome arm 8q. *Genes Chromosomes Cancer* 23, 167–174
10. Hovey, R. M., Chu, L., Balazs, M., De Vries, S., Moore, D., Sauter, G., Carroll, P. R., and Waldman, F. M. (1998) Genetic alterations in primary bladder cancers and their metastases. *Cancer Res.* 15, 3555–3560
11. Simon, R., Burger, H., Brinkschmidt, C., Bocker, W., Hertle, L., and Terpe, H. J. (1998) Chromosomal aberrations associated with invasion in papillary superficial bladder cancer. *J. Pathol.* 185, 345–351
12. Koo, S. H., Kwon, K. C., Ihm, C. H., Jeon, Y. M., Park, J. W., and Sul, C. K. (1999) Detection of genetic alterations in bladder tumors by comparative genomic hybridization and cytogenetic analysis. *Cancer Genet. Cytogenet.* 110, 87–93
13. Wodicka, L., Dong, H., Mittmann, M., Ho, M. H., and Lockhart, D. J. (1997) Genome-wide expression monitoring in *Saccharomyces cerevisiae*. *Nat. Biotechnol.* 15, 1359–1367
14. Christensen, M., Sunde, L., Bolund, L., and Orntoft, T. F. (1999) Comparison of three methods of microsatellite detection. *Scand. J. Clin. Lab. Invest.* 59, 167–177
15. Celis, J. E., Ostergaard, M., Basse, B., Celis, A., Lauridsen, J. B., Ratz, G. P., Andersen, I., Hein, B., Wolf, H., Orntoft, T. F., and Rasmussen, H. H. (1996) Loss of adipocyte-type fatty acid binding protein and other protein biomarkers is associated with progression of human bladder transitional cell carcinomas. *Cancer Res.* 56, 4782–4790
16. Celis, J. E., Ratz, G., Basse, B., Lauridsen, J. B., and Celis, A. (1994) in *Cell Biology: A Laboratory Handbook* (Celis, J. E., ed) Vol. 3, pp. 222–230, Academic Press, Orlando, FL
17. Ohlsson, R., Tycko, B., and Sapienza, C. (1998) Monoallelic expression: 'there can only be one'. *Trends Genet.* 14, 435–438
18. Hollander, G. A., Zuklys, S., Morel, C., Mizoguchi, E., Mobisson, K., Simpson, S., Terhorst, C., Wishart, W., Golan, D. E., Bhan, A. K., and Burakoff, S. J. (1998) Monoallelic expression of the interleukin-2 locus. *Science* 279, 2118–2121
19. Brannan, C. I., and Bartolomei, M. S. (1999) Mechanisms of genomic imprinting. *Curr. Opin. Genet. Dev.* 9, 164–170
20. Ohlsson, R., Cui, H., He, L., Pfeifer, S., Malmikumpa, H., Jiang, S., Feinberg, A. P., and Hedborg, F. (1999) Mosaic allelic insulin-like growth factor 2 expression patterns reveal a link between Wilms' tumorigenesis and epigenetic heterogeneity. *Cancer Res.* 59, 3889–3892
21. Cui, H., Hedborg, F., He, L., Nordenskjold, A., Sandstedt, B., Pfeifer-Ohlsson, S., and Ohlsson, R. (1997) Inactivation of H19, an imprinted and putative tumor repressor gene, is a preneoplastic event during Wilms' tumorigenesis. *Cancer Res.* 57, 4469–4473
22. Galitski, T., Saldanha, A. J., Styles, C. A., Lander, E. S., and Fink, G. R. (1999) Ploidy regulation of gene expression. *Science* 285, 251–254
23. Tsao, J., Yatabe, Y., Markl, I. D., Hajyan, K., Jones, P. A., and Shibata, D. (2000) Bladder cancer genotype stability during clinical progression. *Genes Chromosomes Cancer* 29, 26–32
24. Zong, Q., Schummer, M., Hood, L., and Morris, D. R. (1999) Messenger RNA translation state: the second dimension of high-throughput expression screening. *Proc. Natl. Acad. Sci. U. S. A.* 96, 10632–10636
25. Anderson, L., and Seilhamer, J. (1997) Comparison of selected mRNA and protein abundances in human liver. *Electrophoresis* 18, 533–537
26. Ideker, T., Thorsson, V., Ranish, J. A., Christmas, R., Buhler, J., Eng, J. K., Bumgarner, R., Goodlett, D. R., Aebersold, R., and Hood, L. (2001) Integrated genomic and proteomic analyses of a systematically perturbed metabolic network. *Science* 292, 929–934

Overexpression of a DEAD Box Protein (DDX1) in Neuroblastoma and Retinoblastoma Cell Lines*

Roseline Godbout‡, Mary Packer, and Wenjun Bie

From the Department of Oncology, Cross Cancer Institute and University of Alberta, 11560 University Ave., Edmonton, Alberta T6G1Z2, Canada

The DEAD box gene, *DDX1*, is a putative RNA helicase that is co-amplified with *MYCN* in a subset of retinoblastoma (RB) and neuroblastoma (NB) tumors and cell lines. Although gene amplification usually involves hundreds to thousands of kilobase pairs of DNA, a number of studies suggest that co-amplified genes are only overexpressed if they provide a selective advantage to the cells in which they are amplified. Here, we further characterize *DDX1* by identifying its putative transcription and translation initiation sites. We analyze DDX1 protein levels in *MYCN/DDX1*-amplified NB and RB cell lines using polyclonal antibodies specific to DDX1 and show that there is a good correlation with *DDX1* gene copy number, *DDX1* transcript levels, and DDX1 protein levels in all cell lines studied. DDX1 protein is found in both the nucleus and cytoplasm of *DDX1*-amplified lines but is localized primarily to the nucleus of nonamplified cells. Our results indicate that DDX1 may be involved in either the formation or progression of a subset of NB and RB tumors and suggest that DDX1 normally plays a role in the metabolism of RNAs located in the nucleus of the cell.

DEAD box proteins are a family of putative RNA helicases that are characterized by eight conserved amino acid motifs, one of which is the ATP hydrolysis motif containing the core amino acid sequence DEAD (Asp-Glu-Ala-Asp) (1–3). Over 40 members of the DEAD box family have been isolated from a variety of organisms including bacteria, yeast, insects, amphibians, mammals, and plants. The prototypic DEAD box protein is the translation initiation factor, eukaryotic initiation factor 4A, which, when combined with eukaryotic initiation factor 4B, unwinds double-stranded RNA (4). Other DEAD box proteins, such as p68, Vasa, and An3, can effectively and independently destabilize/unwind short RNA duplexes *in vitro* (5–7). Although some DEAD box proteins play general roles in cellular processes such as translation initiation (eukaryotic initiation factor 4A (4)), RNA splicing (PRP5, PRP28, and SPP81 in yeast (8–10)), and ribosomal assembly (SrmB in *Escherichia coli* (11)), the function of most DEAD box proteins remains unknown. Many of the DEAD box proteins found in higher eukaryotes are tissue- or stage-specific. For example, *PL10* mRNA is expressed only in the male germ line, and its product

has been proposed to have a specific role in translational regulation during spermatogenesis (12). Vasa and ME31B are maternal proteins that may be involved in embryogenesis (13, 14). p68, found in dividing cells (15), is believed to be required for the formation of nucleoli and may also have a function in the regulation of cell growth and division (16, 17). Other DEAD box proteins are implicated in RNA degradation, mRNA stability, and RNA editing (18–20).

The human DEAD box protein gene *DDX1*[1] was identified by differential screening of a cDNA library enriched in transcripts present in the two RB cell lines Y79 and RB522A (21). The longest *DDX1* cDNA insert isolated from this library was 2.4 kb with an open reading frame from position 1 to 2201. All eight conserved motifs characteristic of DEAD box proteins are found in the predicted amino acid sequence of DDX1 as well as a region with homology to the heterogeneous nuclear ribonucleoprotein U, a protein believed to participate in the processing of heterogeneous nuclear RNA to mRNA (22, 23). The region of homology to heterogeneous nuclear ribonucleoprotein U spans 128 amino acids and is located between the first two conserved DEAD box protein motifs, 1a and 1b.

The proto-oncogene *MYCN* encodes a member of the MYC family of transcription factors that bind to an E box element (CACGTG) when dimerized with the MAX protein (24, 25). The *MYCN* gene is amplified and overexpressed in approximately one-third of all NB tumors (26, 27). Amplification of *MYCN* is associated with rapid tumor progression and a poor clinical prognosis (26, 27). MYCN overexpression is usually achieved by increasing gene copy number rather than by up-regulating basal expression of MYCN (27, 28). Because gene amplification involves hundreds to thousands of kilobase pairs of contiguous DNA (29–32), it is possible that co-amplification of a gene located in proximity to *MYCN* may contribute to the poor clinical prognosis of *MYCN*-amplified tumors. The *DDX1* gene maps to the same chromosomal band as *MYCN*, 2p24, and is located ~400 kb telomeric to the *MYCN* gene (33–36). All four *MYCN*-amplified RB tumor cell lines tested to date are amplified for *DDX1* (21),[2] while approximately two-thirds of NB cell lines and 38–68% of NB tumors are co-amplified for both genes (37–39). George *et al.* (39) found a significant decrease in the mean disease-free survival of patients with *DDX1/MYCN*-amplified NB tumors compared with *MYCN*-amplified tumors. Similarly, Squire *et al.* (38) observed a trend toward a worse clinical prognosis when both genes were amplified in the tumors of NB patients. To date, there have been no reports of a

---

[1] The abbreviations used are: DDX1, DEAD box 1; NB, neuroblastoma; RB, retinoblastoma; RACE, rapid amplification of cDNA ends; PAGE, polyacrylamide gel electrophoresis; nt, nucleotide(s); MOPS, 4-morpholinepropanesulfonic acid; bp, base pair(s); kb, kilobase(s) or kilobase pair(s).

[2] R. Godbout, unpublished results.

tumor amplified only for *DDX1*, and the role that this gene plays in cancer formation and progression is not known.

Because of the high rate of rearrangements in amplified DNA (31, 40), it is unlikely that a gene located ~400 kb from the *MYCN* gene will be consistently amplified as an intact unit unless its product provides a growth advantage to the cell. Based on Southern blot analysis, the *DDX1* gene extends over more than 30 kb, and there are no gross rearrangements of this gene in *DDX1*-amplified tumors (21, 38). Furthermore, there is a good correlation between *DDX1* transcript levels and gene copy number in the tumors analyzed to date. However, we need to show that DDX1 protein is overexpressed in *DDX1*-amplified tumors if we are to entertain the possibility that this protein plays a role in the tumorigenic process. Here, we isolate and characterize the 5'-end of *DDX1* mRNA and extend the *DDX1* cDNA sequence by ~300 nt. We identify the predicted initiation codon of DDX1 and generate antisera that specifically recognize DDX1 protein. We analyze levels of DDX1 protein in both *DDX1*-amplified and nonamplified RB and NB tumors and study the subcellular location of this protein in the cell.

MATERIALS AND METHODS

Library Screening—A human fetal brain cDNA library (Stratagene) was screened using a 320-bp DNA fragment from the 5'-end of the 2.4-kb *DDX1* cDNA previously described (23). Phagemids containing positive inserts were excised from λ ZAP II following the supplier's directions. The ends of the cDNA inserts were sequenced using the dideoxynucleotide chain termination method with T7 DNA polymerase (Amersham Pharmacia Biotech).

A human placenta genomic library (CLONTECH) was screened with the 5'-end of *DDX1* cDNA. Positive plaques were purified, and the genomic DNA was analyzed using restriction enzymes and Southern blotting. *Eco*RI-digested DNA fragments from these clones were subcloned into pBluescript and digested with exonuclease III and mung bean nuclease to obtain sequentially deleted clones. The exon/intron map of the 5' portion of the *DDX1* gene was obtained by comparing the sequence of *DDX1* cDNA with that of the genomic DNA.

Rapid Amplification of cDNA Ends (RACE)—We used the Ampli-FINDER RACE kit (CLONTECH) to extend the 5'-end of *DDX1* cDNA. Briefly, two μg of poly(A)+ RNA isolated from RB522A was reverse transcribed at 52 °C using either primer P1 or P3 (Fig. 1A). The RNA template was hydrolyzed, and excess primer was removed. A single-stranded AmpliFINDER anchor containing an *Eco*RI site was ligated to the 3'-end of the cDNA using T4 RNA ligase. The cDNA was amplified using either primer P2 or P4 (Fig. 1A) and AmpliFINDER anchor primer. RACE products were cloned into pBluescript.

Primer Extension—Poly(A)+ RNAs were isolated from RB and NB cell lines as described previously (21, 38). The 21-nt primers 5'-TTCGT-TCTGGGCACCATGTGT-3' (primer P4 in Fig. 1A) and 5'-TGGGAC-CTAGGGCTTCTGGAC-3' (primer P3 in Fig. 1A) were end-labeled with [γ-32P]ATP (3000 Ci/mmol; Mandel Scientific) and T4 polynucleotide kinase. Each of the labeled primers was annealed to 2 μg of poly(A)+ RNA at 45 °C for 90 min, and the cDNA was extended at 42 °C for 60 min using avian myeloblastosis virus reverse transcriptase (Promega). The primer extension products were heat-denatured and run on a 8% polyacrylamide gel containing 7 M urea in 1× TBE buffer. A G + A sequencing ladder served as the size standard.

S1 Nuclease Protection Assay—The S1 nuclease protection assay to map the transcription initiation site of *DDX1* was performed as described by Favaloro *et al.* (41). The DNA probe was prepared by digesting genomic DNA spanning the upstream region of *DDX1* and exon 1 with *Ava*I, labeling the ends with [γ-32P]ATP (3000 Ci/mmol) and polynucleotide kinase, and removing the label from one of the ends by digesting the DNA with *Sph*I (Fig. 4). The RNA samples were resuspended in a hybridization mixture containing 80% formamide, 40 mM PIPES, 400 mM NaCl, 1 mM EDTA, and the heat-denatured *Sph*I–*Ava*I probe labeled at the *Ava*I site. The samples were incubated at 45 °C for 16 h and digested with 3000 units/ml S1 nuclease (Boehringer Mannheim) for 60 min at 37 °C. The samples were precipitated with ethanol; resuspended in 80% formamide, TBE buffer, 0.1% bromphenol blue, xylene cyanol; denatured at 90 °C for 2 min; and electrophoresed in a 7 M urea, 8% polyacrylamide gel in TBE buffer.

Northern and Southern Blot Analysis—Poly(A)+ RNAs were isolated from RB and NB cell lines as described previously (21, 38). Two μg of

poly(A)+ RNA/lane were electrophoresed in a 6% formaldehyde, 1.5% agarose gel in MOPS buffer (20 mM MOPS, 5 mM sodium acetate, 1 mM EDTA, pH 7.0) and transferred to nitrocellulose filter in 3 M sodium chloride, 0.3 M sodium citrate. The filters were hybridized to the following DNA probes, 32P-labeled by nick translation: (i) a 1.6-kb *Eco*RI insert from *DDX1* cDNA clone 1042 (21), (ii) a 260-bp cDNA fragment spanning the 3'-end of *DDX1* exon 1 as well as exons 2 and 3, (iii) a 160-bp fragment derived from the 5'-end of *DDX1* exon 1, and (iv) α-actin cDNA to control for lane to lane variation in RNA levels. Filters were hybridized and washed under high stringency. Southern blot analysis was as described previously (21).

Preparation of Anti-DDX1 Antiserum—To prepare antiserum to the C terminus of the DDX1 protein, we inserted a 1.8-kb *Eco*RI fragment from bp 848 to 2668 of *DDX1* cDNA (Fig. 1B) into *Eco*RI-digested pMAL-c2 expression vector (New England Biolabs). DH5α cells transformed with this vector were grown to mid-log phase and induced with 0.1 mM isopropyl-1-thio-β-D-thiogalactoside. The cells were harvested 3–4 h postinduction and lysed by sonication. Soluble maltose binding protein-DDX1 fusion protein was affinity-purified using amylose resin, and the maltose-binding protein was cleaved with factor Xa. The DDX1 protein was purified on a SDS-PAGE gel, electroeluted, and concentrated. Approximately 100 μg of protein was injected into rabbits at 4–6-week intervals. For the initial injection, the protein was dispersed in complete Freund's adjuvant (Sigma), while subsequent injections were prepared in Freund's incomplete adjuvant. Blood was collected from each rabbit 10 days after injection, and the specificity of the antiserum was tested using cell extracts from RB522A. To prepare antiserum to the N terminus of DDX1 protein, a *DDX1* cDNA fragment from bp 268 to 851 (Fig. 1B) was inserted into pGEX-4T2 (Amersham Pharmacia Biotech). The recombinant protein produced from this construct contains the first 186 amino acids of the predicted DDX1 sequence. Soluble glutathione *S*-transferase-DDX1 fusion protein was purified with glutathione-Sepharose 4B (Amersham Pharmacia Biotech). The glutathione *S*-transferase component of the fusion protein was cleaved with thrombin.

Subcellular Fractionations and Western Blot Analysis—We used two different procedures for subcellular fractionations. First, we isolated nuclear and S100 (soluble cytoplasmic) fractions from RB522A, IMR-32, Y79, RB(E)-2, HeLa, and HL60 using the procedure of Dignam (42). On average, we obtained 5–6 times more protein in the cytosolic fractions than in the nuclear fractions. Second, 10^8 RB522A cells were lysed and fractionated into S4 (soluble cytoplasmic components), P2 (heavy mitochondria, plasma membrane fragments), P3 (mitochondria, lysozymes, peroxisomes, and Golgi membranes), and P4 fractions (membrane vesicles from rough and smooth endoplasmic reticulum, Golgi, and plasma membrane) by differential centrifugation (43). We obtained 8 mg of protein in the S4 fraction, 1 mg in P2, 0.5 mg in P3, and 2 mg in P4 fraction. The procedures related to the immunoelectron microscopy have been previously described (44).

For Western blot analysis, proteins were electrophoresed in polyacrylamide-SDS gels and electroblotted onto nitrocellulose using the standard protocol for protein transfer described by Schleicher and Schuell. The filters were incubated with a 1:5000 dilution of DDX1 antiserum, a 1:200 dilution of anti-MYCN monoclonal antibody (Boehringer Mannheim), or a 1:200 dilution of anti-actin (Santa Cruz Biotechnology, Inc., Santa Cruz, CA). For the colorimetric analysis, antigen-antibody interactions were visualized using either alkaline phosphatase-linked goat anti-rabbit IgG (for DDX1) or goat anti-mouse IgG (for MYCN) at a 1:3000 dilution. For the ECL Western blotting analysis (Amersham Pharmacia Biotech), we used a 1:100,000 dilution of peroxidase-linked secondary anti-rabbit IgG antibody (for DDX1) or secondary anti-goat IgG antibody (Jackson ImmunoResearch Laboratories).

RESULTS

Identification of the 5'-End of the DDX1 Transcript—We have previously reported the sequence of *DDX1* cDNA isolated from an RB cDNA library (21, 23). This 2.4-kb *DDX1* cDNA contains an open reading frame spanning positions 1–2201 with a methionine encoded by the first three nucleotides (Fig. 1A). There is a polyadenylation signal and poly(A) tail in the 3'-untranslated region, indicating that the sequence is complete at the 3'-end. Manohar *et al.* (37) have also isolated *DDX1* cDNA from the NB cell line LA-N-5. Their cDNA extended the 5'-end of our sequence by 42 bp and included an additional in frame methionine (*double underlined* in Fig. 1A). The possibil-

A

```
                                                    +1
                                              ┌──→ primer extension
                                        5'   TTCCTT    6
                                             ↑↑  ↑
    ┌──→RACE ┌──→S1 nuclease
   *CTCTGTAGCTGTGACCCTGATACCGCGTGGTGTGCTCCGAACACATGGT    55
   ↑
   GCCCAGAACGAAGGCGGCGTCCAGAAGCCCTAGGTCCCAGAGGTCCGCTC   105
                      P3
   AGCGGCAGGCGCATAAGGCGGGGCCGGCGCGGGCCTTTCCTTCCATCGGA   155

   ACCGTTCTCCCGGGGCTGAGTCCCTGCCCGGACTCCGAACGCCGAAGACC   205
                              ┌──→ cDNA screening (this study)
   AGGGGCCGGAAGCGCGCGCCGCCACTGCCACGCCGTGTCAGTCGGGAGGG   255
                          ┌──→ published sequence - Manohar et al. (24)
   AGGGAGCGAGCAGGCGAAGCCGCGGAGGACGGGGTGAAGATGGCGGCCTT   305
       exon 1 ┌──→ exon 2
            ┌──┬ published sequence - Godbout et al. (23)
   CTCCGAGATGGGTGTAATGCCTGAGATTGCACAAGCTGTGGAAGAGATGG   355
       exon 2 ┌──→ exon 3
   ATTGGCTCCTCCCAACTGATATCCAGGCTGAATCTATCCCATTGATCTTA   405
                              P2
   GGAGGAGGTGATGTACTTATGGCTGCAGAA...3'    435
       P1
```

B

```
 5'  ┌──────┬─────────────────────────┬────────┐  3'
     │ 5' UTR │    OPEN READING FRAME   │ 3' UTR │
     └──────┴─────────────────────────┴────────┘
     1     295                      2515    2711
```

FIG. 1. **Partial sequence and structure of DDX1 cDNA.** A, the sequence of the 5'-end of DDX1 cDNA. The sequence in *boldface type* starting at the *asterisk* was obtained using the RACE strategy. The additional 6 bp in *italic boldface type* at the 5'-end of the cDNA are predicted based on the known DDX1 genomic sequence and primer extension analysis. P1, P2, P3, and P4 are primers used in the RACE experiments (the complementary sequence was used in each case). Primers P3 and P4 were also used for the primer extension analysis. Three in frame methionine codons are indicated by the *double underline*. An in frame stop codon is indicated by the *boldface double underline*. The three major transcription initiation sites identified by primer extension are indicated by the *single arrows*, while a minor site is represented by the *broad arrow*. The predicted DDX1 transcription initiation sites obtained by RACE, S1 nuclease, and primer extension are indicated as well as the 5'-ends of DDX1 cDNA sequences obtained by screening cDNA libraries. The sequences transcribed from exons 1, 2, and 3 are also shown. B, the structure of the 2711-bp DDX1 cDNA is shown with an open reading frame from position 295 to 2515.

FIG. 2. **Identification of the 5'-end of the DDX1 transcript by primer extension.** Radioactively labeled primer P4 was annealed to 2 μg of poly(A)$^+$ RNA from RB522A (*lane 1*), 1 μg of poly(A)$^+$ RNA from RB522A (*lane 2*), and 2 μg of poly(A)$^+$ RNA from RB(E)-2 cells (*lane 3*), and extended using reverse transcriptase. The products were run on an 8% denaturing polyacrylamide gel with a G + A sequencing ladder as size marker. The primer extension products are indicated on the *left*. The sizes of the products (in nt) are presented as the distance from primer P4.

ity of additional in frame methionines located further upstream could not be excluded, because there were no predicted stop codons in the upstream region of the cDNA.

Northern blot analysis indicated a DDX1 transcript size of ~2800 nt, suggesting that the DDX1 cDNAs isolated to date were lacking ~300–350 bp of 5' sequence. We have used different approaches to identify the transcription start site of DDX1. First, we exhaustively screened a commercial fetal brain cDNA library with the 5'-end of DDX1 cDNA. Although numerous clones were analyzed, only one extended the sequence (by 35 bp) beyond that published by Manohar *et al.* (37) (Fig. 1A).

We next used the RACE procedure in an attempt to isolate additional 5' sequence. The nested primers used to amplify the 5'-end of the DDX1 transcript are labeled as primers P1 and P2 in Fig. 1A and are located downstream of the three in frame methionines (*double underlined* in Fig. 1A). Poly(A)$^+$ RNA from RB522A was reverse transcribed at 52 °C using primer P1, and the reverse transcribed cDNA was amplified using the nested primer P2 and the 5'-RACE primer. Using this approach, we generated a product that was 230 bp longer than any of the cDNAs obtained by screening libraries (Fig. 1A). Sequencing of this 230-bp cDNA revealed an in frame stop codon (*boldface double underline* in Fig. 1A) located 123 bp
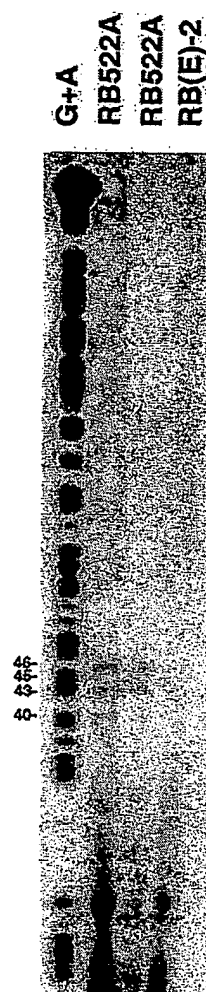
upstream of the predicted translation initiation site. We then prepared primers P3 and P4, located near the 5'-end of the RACE cDNA (Fig. 1A) and repeated the RACE procedure to see if additional 5' sequences could be obtained. The resulting RACE products did not extend the DDX1 cDNA sequence further.

The location of the DDX1 transcription initiation site was verified by primer extension. Poly(A)$^+$ RNA was prepared from the following two cell lines: DDX1-amplified RB cell line RB522A and a nonamplified RB cell line RB(E)-2. RB522A has elevated levels of DDX1 mRNA, while RB(E)-2 has at least 20-fold lower levels of this transcript. Three products of 40, 43, and 46 nt (with a weak signal at 45 nt) were detected in RB522A using primer P4 (Figs. 1A and 2). The 40-nt product corresponded exactly with the 5'-end of the RACE-derived cDNA while the 43- and 46-nt products extended the predicted size of the DDX1 transcript by 3 and 6 nt, respectively. None of these products were observed in RB(E)-2. Bands of identical sizes to those obtained with RB522A mRNA were also observed in the DDX1-amplified NB cell line BE(2)-C but not in the DDX1-amplified NB cell line IMR-32 (data not shown). The same predicted DDX1 transcription initiation site was identified with primer P3 except that the bands were of weaker
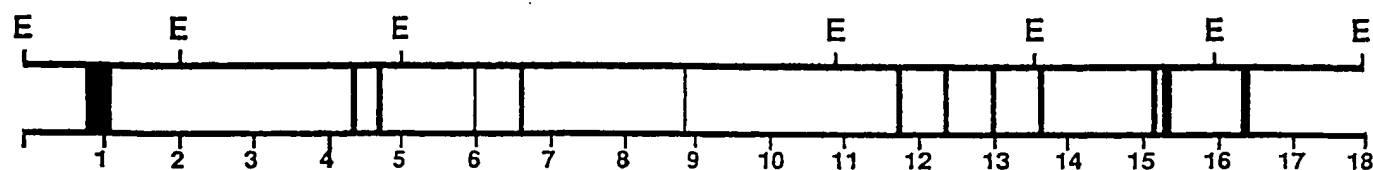
FIG. 3. **Genomic map of the 5'-end of *DDX1*.** The exons are represented by the *black boxes*, and distances are in kilobase pairs. The locations of *Eco*RI (*E*) sites are indicated.

intensity (data not shown). We have designated the transcription start site identified by primer extension as +1 (Fig. 1A).

The sequence of the 6 nt extending beyond the RACE cDNA was obtained by comparison of the cDNA sequence with that of *DDX1* genomic DNA. Bacteriophages containing *DDX1* genomic DNA were isolated by screening a human placenta library with 5' *DDX1* cDNA. Eighteen kb of DNA were sequenced from two bacteriophages with overlapping *DDX1* genomic DNA. Thirteen exons were identified within this 18-kb region (Fig. 3) corresponding to cDNA sequences from position 1 to 1249. The 310-bp exon 1 was by far the longest of the 13 exons sequenced, corresponding to the entire 5'-untranslated region of *DDX1* as well as the first in frame methionine. The sequences transcribed from exons 1, 2, and 3 are indicated in Fig. 1A.

Knowledge of the genomic structure of *DDX1* allowed us to use the S1 protection assay, a technique that is independent of reverse transcriptase, to further define the 5'-end of the *DDX1* transcript. Poly(A)$^+$ RNAs from six *DDX1*-amplified lines (RB lines: Y79 and RB522A; NB lines: BE(2)-C, IMR-32, LA-N-1, and LA-N-5) and six nonamplified lines (RB lines: RB(E)-2 and RB412; NB lines, GOTO, NB-1, NUB-7, and SK-N-MC) were hybridized to a DNA probe that extended from position −745 in the 5'-flanking *DDX1* DNA to position +164 in exon 1. This DNA probe was labeled at position +164 as indicated in Fig. 4. Nonhybridized DNA was digested with S1 nuclease, and the sizes of the protected fragments were analyzed on a denaturing polyacrylamide gel. Bands of 150–153 nt were observed in *lane 2* (RB522A), *lane 5* (BE(2)-C), and *lane 8* (LA-N-1) with bands of much weaker intensity in *lane 7* (IMR-32) (Fig. 4). Specific bands were not detected in either *DDX1*-amplified Y79 and LA-N-5 or the nonamplified lines. Although the sizes of the S1 protected bands in RB522A, BE(2)-C, and LA-N-1 were 5 and 11 nt shorter than predicted based on RACE and primer extensions, respectively, there was general agreement with all three techniques regarding the location of the *DDX1* transcription initiation site (Fig. 1A). The smaller S1 nuclease protected products could have arisen as the result of S1 digestion of the 5'-end of the RNA:DNA heteroduplex because of its relatively high rU:dA content (45).

Identification of the same transcription initiation site in three *DDX1*-amplified lines suggests that this represents the bona fide start site of *DDX1* transcription. However, it was not clear why this start site was either very weak or not detected in three other amplified lines. To determine whether the 5'-end of exon 1 is transcribed in all *DDX1*-amplified lines, we carried out a direct analysis of the 5'-end of the *DDX1* transcript by Northern blotting. Two probes were used for this analysis: the 5' probe contained a 160-bp fragment from bp 1 to 160 (5'-half of exon 1), and the 3' probe contained a 260-bp fragment from bp 160 to 420 (3'-half of exon 1 as well exons 2 and 3) (Fig. 1A). With the 3' probe, we obtained bands of similar size and intensity in four *DDX1*-amplified lines (RB522A, BE(2)-C, IMR-32, and LA-N-5). Band intensity was somewhat weaker in Y79 and stronger in LA-N-1 in comparison with the other lines (Fig. 5). No signal was detected in the non-*DDX1*-amplified line RB412. With the 5' probe, a relatively strong signal was observed in RB522A, BE(2)-C, and LA-N-1, while a considerably weaker

but readily apparent signal was detected in Y79, IMR-32, and LA-N-5. The signal obtained with actin indicates that, with the exception of LA-N-1, similar amounts of RNA were loaded in each lane and that the RNA was not degraded. These results indicate that at least a portion of the 160-bp 5'-end of exon 1 is transcribed in all *DDX1*-amplified lines.

Based on primer extension, S1 nuclease protection assay, Northern blot analysis and the sequencing of the RACE products, we conclude that the *DDX1* transcript is 2.7 kb with an open reading frame spanning nucleotides 295–2515 encoding a predicted protein of 740 amino acids with an estimated molecular weight of 82.4 (Fig. 1B). An in frame stop codon is located 123 nt upstream of the predicted translation initiation site, at positions 172–174. The first in frame methionine following the stop codon is in agreement with the Kozak consensus sequence (46). Furthermore, the predicted start methionine codon for human DDX1 corresponds perfectly with that of *Drosophila* DDX1 (47). A stop codon is located 15 nt upstream of the initiation codon in *Drosophila* DDX1.

Analysis of DDX1 Protein Levels in Neuroblastoma and Retinoblastoma—We and others have previously shown that there is a good correlation between gene copy number and RNA levels in *DDX1*-amplified RB and NB cell lines (37, 38). To determine whether the correlation extends to DDX1 protein levels, we prepared antiserum to two nonoverlapping recombinant DDX1 proteins. First, we prepared a C terminus recombinant protein construct by inserting a 1.8-kb *Eco*RI fragment from bp 848 to 2668 (amino acids 185–740) (Fig. 1B) into the pMAL-c2 expression vector. Recombinant protein expression was induced with isopropyl-1-thio-β-D-thiogalactoside, and the 110-kDa maltose-binding protein-DDX1 fusion product was purified by affinity chromatography using amylose resin, followed by electrophoresis on a SDS-PAGE gel after cleaving the maltose-binding protein fusion partner with factor Xa. Second, we prepared an N terminus construct by ligating a DNA fragment from bp 268 to 851 (amino acids 1–186) into pGEX-4T2. The 50-kDa glutathione S-transferase-DDX1 fusion protein was purified by affinity chromatography on a glutathione column. This N terminus fusion protein contains only the first of the eight conserved motifs found in all DEAD box proteins, while the C terminus fusion protein includes the remaining seven motifs.

We measured DDX1 protein levels in total cell extracts of three RB and 10 NB cell lines. Using antiserum to the N terminus fusion protein, we observed a strong signal in all *DDX1*-amplified cell lines: the RB cell lines Y79 (*lane 1*) and RB522A (*lane 2*) and the NB cell lines BE(2)-C (*lane 4*), IMR-32 (*lane 6*), LA-N-1 (*lane 8*), and LA-N-5 (*lane 9*) (Fig. 6). Two bands were observed in the majority of extracts. Of the amplified lines, Y79 produced the weakest signal, with the most intense signal observed in LA-N-1. There was an excellent correlation with DDX1 protein and mRNA levels in these cell lines, with lower levels of DDX1 mRNA observed in Y79 and higher levels in LA-N-1 (Fig. 7A). As shown in Fig. 7B, this correlation extended to *DDX1* gene copy number. No gross DNA rearrangements were seen in the *DDX1*-amplified lines; however, three small bands of altered size were observed in the RB412 lane. Although the nature of the DNA alteration is not known, it is noteworthy that *DDX1* transcript levels in RB412

FIG. 4. S1 nuclease mapping of the 5'-end of the *DDX1* transcript. Two μg of poly(A)$^+$ RNA from four RB lines (*DDX1*-amplified Y79 and RB522A and nonamplified RB(E)-2 and RB412), eight NB lines (*DDX1*-amplified BE(2)-C, IMR-32, LA-N-1, and LA-N-5 and nonamplified GOTO, NB-1, NUB-7, and SK-N-MC), and tRNA as a negative control were hybridized to a *SphI–AvaI* fragment labeled at the *AvaI* site with [γ-^{32}P]ATP and polynucleotide kinase. Bands of 150–153 nt are shown in *lanes 2* (RB522A), *5* (BE(2)-C), and *8* (LA-N-1) with much weaker bands in *lane 7* (IMR-32). A map of the probe indicating the transcription initiation site identified by primer extension (+*1*), the labeling site (*), and exons 1 and 2, is shown at the *bottom*.
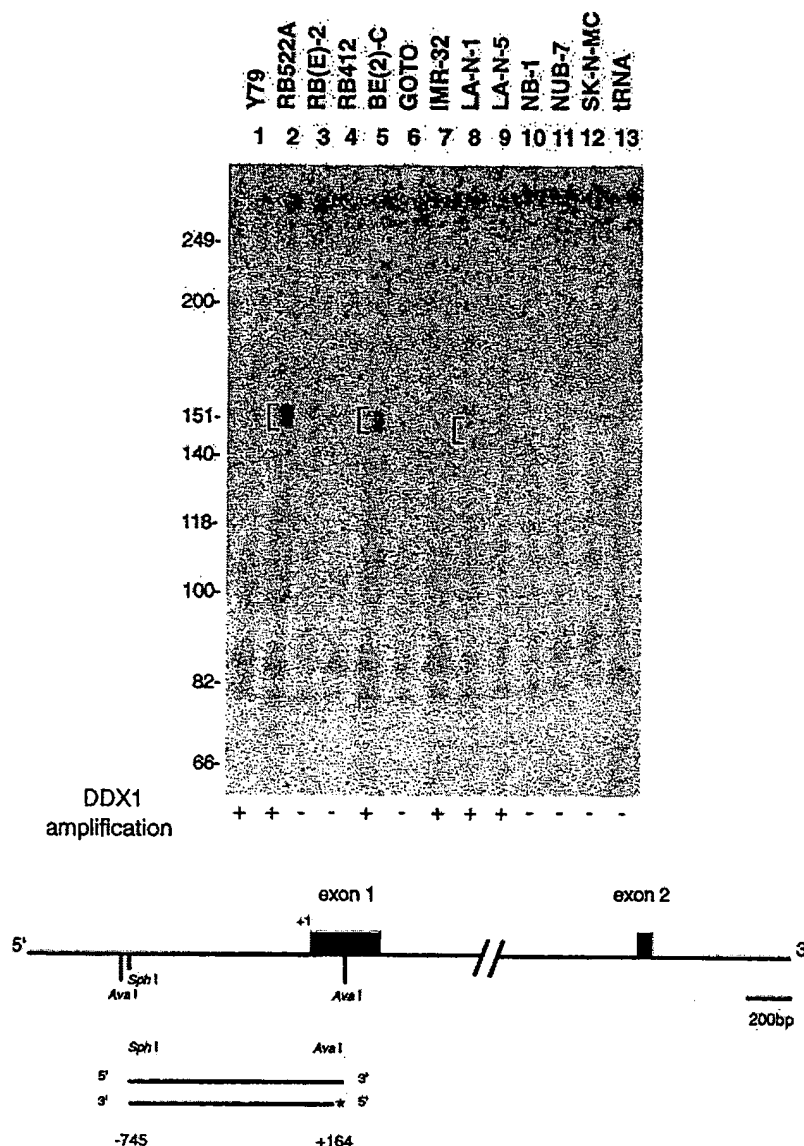
are extremely low (Fig. 7A) and that the top DDX1 protein band in RB412 cell extracts is smaller in size than the top band from the other cell extracts (Fig. 6).

Two DDX1 protein bands were present in most of the lanes in Fig. 6. The same two bands were detected with antiserum to the C terminus of the DDX1 protein, as well as a third band at ~60 kDa (data not shown). There was no variation in the intensity of the 60-kDa band in *DDX1*-amplified and nonamplified cell extracts. The 60-kDa band probably represents another member of the DEAD box protein family, because the C terminus DDX1 protein used to prepare this antiserum contained seven of the eight conserved motifs found in all DEAD box proteins. To obtain an estimate of the size of the two DDX1 bands, we ran cellular extracts from RB522A on a 7% SDS-PAGE gel with the BenchMark protein ladder (Life Technologies, Inc.). The size of the DDX1 protein was determined using the Alpha Imager 2000 documentation and analysis system for molecular weight calculation. Based on this analysis, the estimated molecular mass of the top band is 89.5 kDa, while that of the bottom band is 83.5 kDa. The 84-kDa band may represent the unmodified product encoded by the DDX1 transcript (capable of encoding a protein with a predicted molecular mass of 82.4 kDa), while the top band may represent post-translational modification of DDX1 protein (*e.g.* phosphorylation). Another possibility is that the top band represents intact DDX1
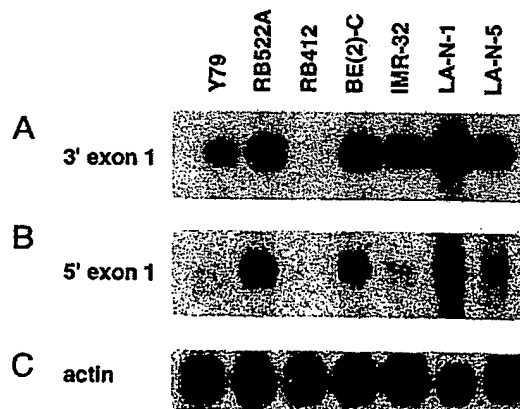
FIG. 5. Northern blot analysis of the 5'-end of the *DDX1* transcript. Two μg of poly(A)$^+$ RNA isolated from *DDX1*-amplified Y79, RB522A, BE(2)-C, IMR-32, LA-N-1, and LA-N-5 and nonamplified RB412 were electrophoresed in a 1.5% agarose-formaldehyde gel. The RNA was transferred to a nitrocellulose filter and sequentially hybridized with a 260-bp fragment from *DDX1* cDNA from bp +160 to +420 (3'-end of exon 1 as well as exons 2 and 3) (*A*), a 160-bp fragment from *DDX1* cDNA from bp +1 to +160 (5'-end of exon 1) (*B*), and actin cDNA (*C*). The DNA was labeled with [^{32}P]dCTP by nick translation. The blots were hybridized and washed under high stringency.
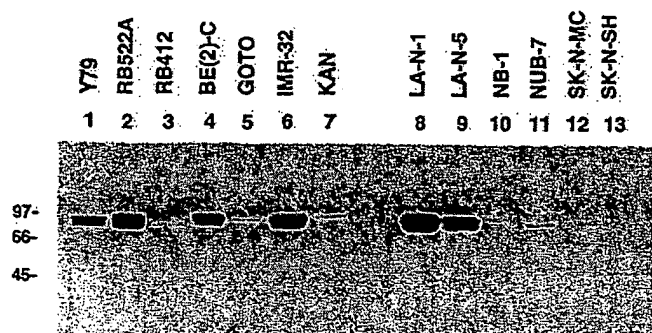
FIG. 6. **DDX1 protein expression in RB and NB cell lines.** Western blots were prepared using total cellular extracts from three RB (Y79, RB522A, and RB412) and 10 NB cell lines (BE(2)-C, GOTO, IMR-32, KAN, LA-N-1, LA-N-5, NB-1, NUB-7, SK-N-MC, and SK-N-SH). The lines that are amplified for the *DDX1* gene are Y79, RB522A, BE(2)-C, IMR-32, LA-N-1, and LA-N-5. Twenty μg of protein were loaded in each lane and electrophoresed in a 10% SDS-PAGE gel. DDX1 was detected using a 1:5000 dilution of the antiserum to the amino terminus of DDX1 protein. Size markers in kilodaltons are indicated on the *side.*
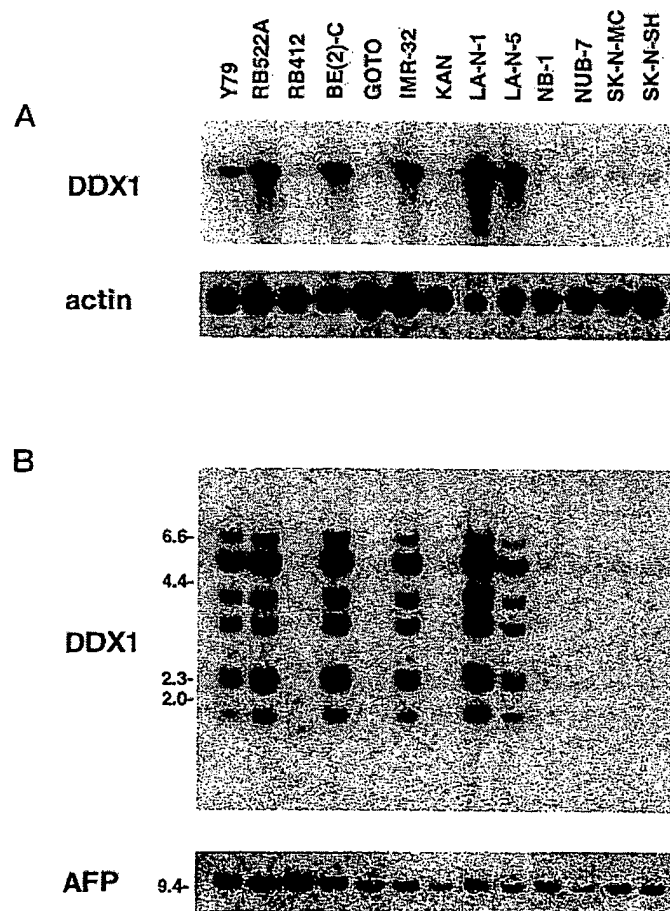
FIG. 7. **Northern and Southern blot analyses of *DDX1* in RB and NB cell lines.** *A*, 2 μg of poly(A)$^+$ RNA were loaded in each lane, electrophoresed in a 1.5% agarose-formaldehyde gel, and transferred to a nitrocellulose filter. The filter was first hybridized to a ^{32}P-labeled 1.6-kb DDX1 cDNA (clone 1042) (21), stripped, and rehybridized to actin DNA. *B*, 10 μg of genomic DNA from each of the indicated cell lines were digested with *Eco*RI, electrophoresed in a 1% agarose gel, and transferred to a nitrocellulose filter. The filter was hybridized to ^{32}P-labeled clone 1042 *DDX1* cDNA, stripped, and reprobed with labeled α-fetoprotein cDNA. Markers (in kilobase pairs) are indicated on the *side.*

and the lower band is a specific truncated or degradation product of DDX1. Yet a third possibility is that the two bands represent the products of differentially spliced transcripts or
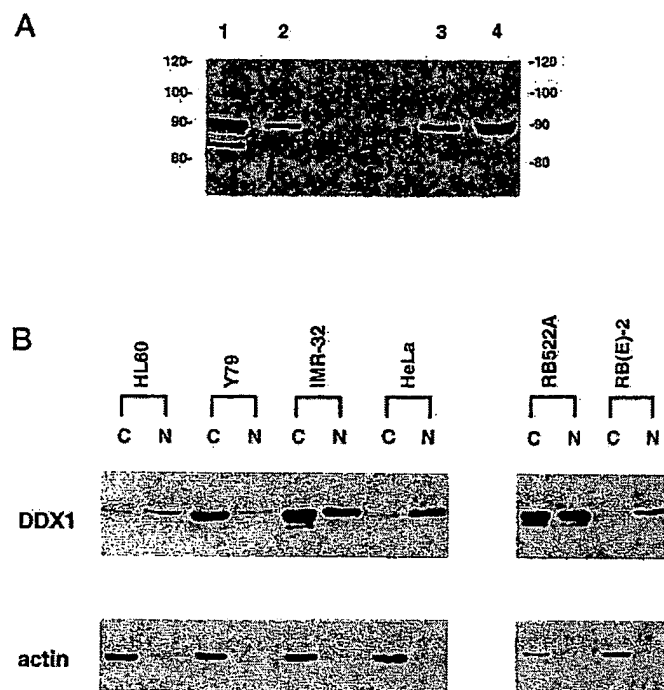

FIG. 8. **Distribution of DDX1 in the nucleus and cytoplasm.** *A*, cytosolic and nuclear extracts were prepared from RB522A and electrophoresed in a 7% SDS-PAGE gel. Cytosolic extracts were loaded in *lanes 1* (20 μg of protein) and *2* (10 μg), while nuclear extracts were loaded in *lanes 3* (10 μg) and *4* (20 μg). DDX1 was visualized using a 1:5000 dilution of the antiserum to the N terminus. The BenchMark protein ladder size markers (kilodaltons) are indicated on the *left*. *B*, cytosolic and nuclear extracts were prepared from HL60, Y79, IMR-32, HeLa, RB522A, and RB(E)-2 and electrophoresed in an 8% SDS-PAGE gel. Twenty μg of proteins were loaded in each *lane* marked *C* (cytosolic) and *N* (nuclear). DDX1 was visualized using a 1:5000 dilution of the antiserum to the N terminus. Actin levels were analyzed using a 1:200 dilution of anti-actin antibody (Santa Cruz Biotechnology).

different translation initiation sites. However, the lack of any obvious differences in *DDX1* transcript sizes in the three RB and 10 NB lines analyzed in Fig. 7*A* does not support the latter possibility (*e.g.* compare the *DDX1* transcript size in NUB-7 (which produces the lower DDX1 protein band) and in NB-1 (which produces the higher DDX1 protein band)).

Subcellular Localization of DDX1 Protein—DEAD box proteins have been implicated in a variety of cellular functions including RNA splicing in the nucleus, translation initiation in the cytoplasm, and ribosome assembly in the nucleolus. To obtain an indication of the possible role of DDX1, we studied its subcellular location. Nuclear and cytosolic extracts were prepared from *DDX1*-amplified RB522A and run on a 7% SDS-PAGE gel. Although there was more DDX1 protein in the cytosol than in the nucleus on a per cell basis, the proportion of DDX1 protein relative to total protein was similar in both cellular compartments (Fig. 8*A*). Both the 90- and 84-kDa bands were present in cytosol and nuclear extracts, although the bottom band was more readily apparent in the cytosol. By running the gel for an extended period of time (twice as long as usual), we were able to detect an additional weak band at ~88 kDa in both nuclear and cytosolic extracts.

To determine whether DDX1 consistently localizes to both the cytoplasm and nucleus, we prepared cytosol and nuclear extracts from two additional *DDX1*-amplified lines, Y79 and IMR-32, as well as from nonamplified RB(E)-2, HL60, and HeLa. DDX1 protein was found in both the nucleus and cytoplasm of IMR-32, primarily in the cytoplasm of Y79, and mainly in the nucleus of the three nonamplified lines (Fig. 8*B*). In addition, DDX1 was almost exclusively found in nuclear
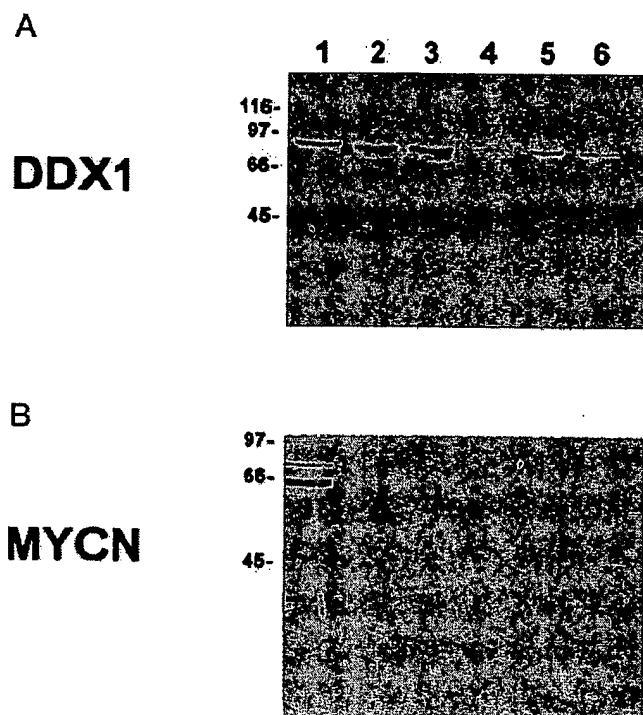
A

DDX1

B

MYCN

FIG. 9. **Subcellular location of DDX1 protein.** RB522A cells were fractionated into nuclear (*lane 1*), S100 and S4 cytosol (*lanes 2 and 3*), P2 membrane (*lane 4*), P3 membrane (*lane 5*), and P4 membrane (*lane 6*) fractions. Twenty μg of protein were loaded in each lane and run on a 10% SDS-PAGE gel. *A*, DDX1 protein was detected using a 1:5000 dilution of the antiserum to the N terminus of DDX1. *B*, MYCN protein was detected using a commercially available antibody at a 1:200 dilution. Size markers (kilodaltons) are indicated on the *side*.

extracts prepared from normal GM38 fibroblasts (data not shown). We used anti-actin antibody to ensure that our nuclear and cytosolic extracts were not cross-contaminated (Fig. 8*B*).

We next carried out a more detailed analysis of DDX1 subcellular location using two different approaches: (i) fractionation of cellular components into nuclei; S100 or S4 cytosol (containing soluble cytoplasmic components, including 40 S ribosomes); P2 (heavy mitochondria, plasma membrane fragments plus material trapped by these membranes); P3 (mitochondria, lysosomes, peroxisomes, Golgi membranes, some rough endoplasmic reticulum); and P4 (microsomes from smooth and rough endoplasmic reticulum, Golgi and plasma membranes) (43); and (ii) immunogold electron microscopy. The *DDX1*-amplified RB522A cell line was used for both experiments. The fractionation procedures indicate that DDX1 is mainly in the nucleus and in the cytosol (S4 and S100 fractions) of RB522A cells (Fig. 9*A*). As a control, we used anti-human MYCN antibody to determine the location of MYCN (also amplified in RB522A) in our subcellular fractions. As shown in Fig. 9*B*, MYCN was primarily found in the nucleus, as one would expect of a transcription factor.

For the electron microscopy analysis, antiserum to the N terminus of DDX1 was coupled to protein A gold particles, and the distribution of DDX1 was examined in RB522A cells fixed in paraformaldehyde and glutaraldehyde. DDX1 was present in both the cytoplasm and nucleus (data not shown). There was no association with either cell organelles or with nuclear or plasma membranes.

DISCUSSION

There are presently few clues as to the function of DDX1 in normal and cancer cells. Our earlier data indicate that *DDX1* mRNA is present at higher levels in fetal tissues of neural origin (retina and brain) compared with other fetal tissues (21).

There may therefore be a requirement for elevated levels of this putative RNA helicase for the efficient production or processing of neural specific transcripts. A role in cancer formation or progression is an intriguing possibility, because overexpression of an RNA unwinding protein could affect the secondary structure of RNAs in such a way as to alter the expression of specific proteins in tumor cells. *DDX1* is co-amplified with *MYCN* in a subset of RB and NB cell lines and tumors (37–39). *MYCN* amplification is common in stage IV NB tumors and is a well documented indicator of poor prognosis. A general trend toward a poorer clinical prognosis is observed when both the *MYCN* and *DDX1* genes are amplified compared with when only *MYCN* is amplified (38, 39), suggesting a possible role for DDX1 in NB tumor formation or progression.

It is generally accepted that co-amplified genes are not overexpressed unless they provide a selective growth advantage to the cell (48, 49). For example, although *ERBA* is closely linked to *ERBB2* in breast cancer and both genes are commonly amplified in these tumors, *ERBA* is not overexpressed (48). Similarly, three genes mapping to 12q13–14 (*CDK4*, *SAS*, and *MDM2*) are overexpressed in a high percentage of malignant gliomas showing amplification of this chromosomal region, while other genes mapping to this region (*GADD153*, *GLI*, and *A2MR*) are rarely overexpressed in gene-amplified malignant gliomas (50, 51). The first three genes are probably the main targets of the amplification process, while the latter three genes are probably incidentally included in the amplicons. The data shown here indicate that DDX1 is overexpressed at both the protein and RNA levels in *DDX1*-amplified RB and NB cell lines and that there is a strong correlation between *DDX1* gene copy number, *DDX1* RNA levels, and DDX1 protein levels in these lines. Our results are therefore consistent with DDX1 overexpression playing a positive role in some aspect of NB and RB tumor formation or progression. Recently, Weiss *et al.* (52) have shown that transgenic mice that overexpress MYCN develop NB tumors several months after birth. They conclude that MYCN overexpression can contribute to the initiation of tumorigenesis but that additional events are required for tumor formation. Amplification of *DDX1* may represent one of many alternative pathways by which a normal precursor "neuroblast" or "retinoblast" cell gains malignant properties.

The function of the majority of tissue-specific or developmentally regulated DEAD box genes remains unknown. However, some members of this protein family have been either directly or indirectly implicated in tumorigenesis. For example, the p68 gene has been found to be mutated in the ultraviolet lightinduced murine tumor 8101 (53), while DDX6 (also known as RCK or p54) is encoded by a gene located at the breakpoint of the translocation involving chromosomes 11 and 14 in a cell line derived from a B-cell lymphoma (54, 55). Similarly, the production of a chimeric protein between *DDX10* and the nucleoporin gene *NUP98* has been proposed to be involved in the pathogenesis of a subset of myeloid malignancies with inv(11) (p15q22) (56). Interestingly, Grandori *et al.* (57) have shown that MYCC interacts with a DEAD box gene called *MrDb*, suggesting that the transcription of some DEAD box genes could be regulated through interaction with members of the MYC family. Future work will involve determining whether DDX1 represents another member of the DEAD box family with a role in the tumorigenic process.

DEAD box proteins have been implicated in translation initiation, RNA splicing, RNA degradation, and RNA stability (3, 18, 19). We carried out subcellular localization studies in an attempt to obtain a general indication of the function of DDX1. We found DDX1 protein in both the cytoplasm and nucleus of *DDX1*-amplified NB and RB lines. In contrast, DDX1 was

mainly located in the nucleus of nonamplified cell lines and normal fibroblast cultures. DDX1 was not associated with cellular organelles or with membranes based on immunoelectron microscopy. We therefore propose that the primary role of DDX1 is in the nucleus. The presence of DDX1 in the cytoplasm of *DDX1*-amplified cells may indicate that the amount of DDX1 protein that is allowed in the nucleus is tightly regulated. Alternatively, DDX1 may play a dual role in the nucleus and cytoplasm of *DDX1*-amplified cells.

An important component of our analysis was to identify the translation and transcription initiation sites of *DDX1*. We used a combination of techniques to identify the transcription start site: screening of RB and fetal brain libraries, RACE, primer extension, genomic DNA sequencing, S1 nuclease mapping, and Northern blot analysis using probes to the predicted 5′-end of the transcript. The transcription start site identified using these techniques is located ~300 nt upstream of the predicted translation initiation codon and was readily detected in three *DDX1*-amplified lines and barely detectable in a fourth amplified line. The 5′-untranslated region as well as the first in frame methionine are encoded within the first exon of *DDX1*. An in frame stop codon is located 123 nt upstream of the predicted initiation codon. We were unable to identify the transcription initiation site of *DDX1* in two of the six amplified lines tested as well as in nonamplified lines. Although it remains possible that there are different transcription start sites in different cell lines, detection of lower levels (rather than the absence) of the 5′-most 160 nt of the *DDX1* transcript in IMR-32, Y79, and LA-N-5 compared with RB522A, BE(2)-C, and LA-N-1 supports a quantitative rather than a qualitative difference in the 5′-end of this transcript in these cells. Our results suggest that the 5′-end of *DDX1* mRNA is rarely intact, even in mRNA preparations that otherwise appear to be of high quality based on analysis of control transcripts. The 5′-end of *DDX1* mRNA may therefore be especially susceptible to degradation, perhaps because of its sequence and/or secondary structure.

In conclusion, we have mapped the 5′-end of the 2.7-kb *DDX1* transcript and have identified the predicted translation initiation site of DDX1 protein. We have found that *DDX1*-amplified RB and NB tumor lines overexpress DDX1 protein and that there is a good correlation between gene copy number and both transcript and protein levels in these cells. We have shown that DDX1 protein is primarily located in the nucleus of cells that are not *DDX1*-amplified. In contrast, DDX1 is present in both the nucleus and cytoplasm of *DDX1*-amplified NB and RB lines. A cytoplasmic location in *DDX1*-amplified lines may indicate that the amount of nuclear DDX1 is tightly regulated or that DDX1 plays a dual role in the cytoplasm and nucleus of these cells.

REFERENCES

1. Linder, P., Lasko, P. F., Ashburner, M., Leroy, P., Nielsen, P. J., Nishi, K., Schnier, J., and Slonimski, P. P. (1989) *Nature* 337, 121–122
2. Wassarman, D. A., and Steitz, J. A. (1991) *Nature* 349, 463–464
3. Schmid, S. R., and Linder, P. (1992) *Mol. Microbiol.* 6, 283–292
4. Rozen, F., Edery, I., Meerovitch, K., Dever, T. E., Merrick, W. C., and Sonenberg, N. (1990) *Mol. Cell. Biol.* 10, 1134–1144
5. Hirling, H., Scheffner, M., Restle, T., and Stahl, H. (1989) *Nature* 339, 562–564
6. Liang, L., Diehl-Jones, W., and Lasko, P. (1994) *Development* 120, 1201–1211
7. Gururajan, R., Mathews, L., Longo, F., and Weeks, D. L. (1994) *Proc. Natl. Acad. Sci. U. S. A.* 91, 2056–2060
8. Dalbadie-McFarland, G., and Abelson, J. (1990) *Proc. Natl. Acad. Sci. U. S. A.* 87, 4236–4240
9. Jamieson, D. J., Rahe, B., Pringle, J., and Beggs, J. D. (1991) *Nature* 349, 715–717
10. Strauss, E. J., and Guthrie, C. (1994) *Nucleic Acids Res.* 22, 3187–3193
11. Nishi, K., Morel-Deville, F., Hershey, J. W. B., Leighton, T., and Schnier, J. (1988) *Nature* 336, 496–498
12. Leroy, P., Alzari, P., Sassoon, D. Wolgemuth, D., and Fellous, M. (1989) *Cell* 57, 549–559
13. Hay, B., Jan, L. Y., and Jan, Y. N. (1988) *Cell* 55, 577–587
14. De Valoir, T., Tucker, M., Belikoff, E. J., Camp, L. A. Bolduc, C., and Beckingham, K. (1991) *Proc. Natl. Acad. Sci. U. S. A.* 88, 2113–2117
15. Ford, M. J., Anton, I. A., and Lane, D. P. (1988) *Nature* 332, 736–738
16. Iggo, R. D., and Lane, D. P. (1989) *EMBO J.* 8, 1827–1831
17. Buelt, M. K., Glidden, B. J., and Storm, D. R. (1994) *J. Biol. Chem.* 269, 29367–29370
18. Iost, I., and Dreyfus, M. (1994) *Nature* 372, 193–196
19. Py, B., Higgins, C. F., Krisch, H. M., and Carpousis, A. J. (1996) *Nature* 381, 169–172
20. Missel, A., Souza, A. E., Nörskau, G., and Göringer, H. U. (1997) *Mol. Cell. Biol.* 17, 4895–4903
21. Godbout, R., and Squire, J. (1993) *Proc. Natl. Acad. Sci. U. S. A.* 90, 7578–7582
22. Kiledjian, M., and Dreyfuss, G. (1992) *EMBO J.* 11, 2655–2664
23. Godbout, R., Hale, M., and Bisgrove, D. (1994) *Gene (Amst.)* 138, 243–245
24. Blackwood, E. M., and Eisenman, R. N. (1991) *Science* 251, 1211–1217
25. Amati, B., Dalton, S., Brooks, M. W., Littlewood, T. D., Evan, G. I., and Land, H. (1992) *Nature* 359, 423–426
26. Brodeur, G. M., Seeger, R. C., Schwab, M., Varmus, H. E., and Bishop, J. M. (1984) *Science* 224, 1121–1124
27. Seeger, R. C., Brodeur, G. M., Sather, H., Dalton, A., Siegel, S. E., Wong, K. Y., and Hammond, D. (1985) *N. Engl. J. Med.* 313, 1111–1116
28. Cohn, S. L., Salwen, H., Quasney, M. W., Ikegaki, N., Cowan, J. M., Herst, C. V., Sharon, B., Kennett, R. H., and Rosen, S. T. (1991) *Prog. Clin. Biol. Res.* 366, 21–27
29. Cowell, J. K. (1982) *Annu. Rev. Genet.* 16, 21–59
30. Zehnbauer, B. A., Small, D., Brodeur, G. M. Seeger, R., and Vogelstein, B. (1988) *Mol. Cell. Biol.* 8, 522–530
31. Akiyama, K., and Nishi, Y. (1991) *Nucleic Acids Res.* 19, 6887–6894
32. Schneider, S. S., Hiemstra, J. L., Zehnbauer, B. A., Taillon-Miller, P., Le Paslier, D., Vogelstein, B., and Brodeur, G. M. (1992) *Mol. Cell. Biol.* 12, 5563–5570
33. Amler, L. C., Schürmann, J., and Schwab, M. (1996) *Genes Chromosomes Cancer* 15, 134–137
34. Kuroda, H., White, P. S., Sulman, E. P., Manohar, C., Reiter, J. L., Cohn, S. L., and Brodeur, G. M. (1996) *Oncogene* 13, 1561–1565
35. Noguchi, Y., Akiyama, K., Yokoyama, M., Kanda, N., Matsunaga, T., and Nishi, Y. (1996) *Genes Chromosomes Cancer* 15, 129–133
36. Pandita, A., Godbout, R., Zielenska, M., Thorner, P., Bayani, J., and Squire, J. A. (1997) *Genes Chromosomes Cancer* 20, 243–252
37. Manohar, C. F., Salwen, H. R., Brodeur, G. M., and Cohn, S. L. (1995) *Genes Chromosomes Cancer* 14, 196–203
38. Squire, J. A., Thorner, P. S., Weitzman, S., Maggi, J. D., Dirks, P., Doyle, J., Hale, M., and Godbout, R. (1995) *Oncogene* 10, 1417–1422
39. George, R. E., Kenyon, R. M., McGuckin, A. G., Malcolm, A. J., Pearson, A. D. J., and Lunec, J. (1996) *Oncogene* 12, 1583–1587
40. Reiter, J. L., and Brodeur, G. M. (1996) *Genomics* 32, 97–103
41. Favaloro, J., Treisman, R., and Kamen, R. (1980) *Methods Enzymol.* 65, 718–745
42. Dignam, J. D. (1990) *Methods Enzymol.* 182, 194–203
43. Graham, J. (1984) in *Centrifugation: A Practical Approach* (Rickwood, D. ed.) 2nd Ed., pp. 161–182, IRL Press, Oxford
44. Godbout, R., Marusyk, H., Bisgrove, D., Dabbagh, L., and Poppema, S. (1995) *Exp. Eye Res.* 60, 645–657
45. Miller, K. G., and Sollner-Webb, B. (1981) *Cell* 27, 165–174
46. Kozak, M. (1988) *Nucleic Acids Res.* 15, 8125–8132
47. Rafti, F., Scarvelis, D., and Lasko, P. F. (1996) *Gene (Amst.)* 171, 225–229
48. Van de Vijver, M., van de Bersselaar, R., Devilee, P., Cornelisse, C., Peterse, J., and Nusse, R. (1987) *Mol. Cell. Biol.* 7, 2019–2023
49. Gaudray, P., Szepetowski, P., Escot, C., Birnbaum, D., and Theillet, C. (1992) *Mutat. Res.* 276, 317–328
50. Forus, A., Florence, V. A., Maelandsmo, G. M., Meltzer, P. S., Fodstad, O., and Myklebost, O. (1993) *Cell Growth Differ.* 4, 1065–1070
51. Reifenberger, G., Reifenberger, J., Ichimura, K., Meltzer, P. S., and Collins, V. P. (1994) *Cancer Res.* 54, 4299–4303
52. Weiss, W. A., Aldape, K., Mohapatra, G., Feuerstein, B. G., and Bishop, J. M. (1997) *EMBO J.* 16, 2985–2995
53. Dubey, B. P., Hendrickson, R. C., Meredith, S. C., Siegel, C. T., Shabanowitz, J., Skipper, J. C. A., Engelhard, V. H., Hunt, D. F., and Schreiber, H. (1997) *J. Exp. Med.* 185, 695–705
54. Akao, Y., Seto, M., Yamamoto, K., Iida, S., Nakazawa, S., Inazawa, J., Abe, T., Takahashi, T., and Ueda, R. (1992) *Cancer Res.* 52, 6083–6087
55. Lu, D., and Yunis, J. J. (1992) *Nucleic Acids Res.* 20, 1967–1972
56. Arai, Y., Hosoda, F., Kobayashi, H., Arai, K., Hayashi, Y., Kamada, N., Kaneko, Y., and Ohki, M. (1997) *Blood* 89, 3936–3944
57. Grandori, C., Mac, J., Siëbelt, F., Ayer, D. E., and Eisenman, R. N. (1996) *EMBO J.* 15, 4344–4357

ORIGINAL ARTICLE

Identification of putative oncogenes in lung adenocarcinoma by a comprehensive functional genomic approach

R Li[1], H Wang[1], BN Bekele[2], Z Yin[3], NP Caraway[1], RL Katz[1], SA Stass[4] and F Jiang[4]

[1]Department of Pathology, The University of Texas MD Anderson Cancer Center, Houston, TX, USA; [2]Department of Biostatistics & Applied Mathematics, The University of Texas MD Anderson Cancer Center, Houston, TX, USA; [3]Department of Internal Medicine, The University of Texas Houston Medical School, Houston, TX, USA and [4]Department of Pathology, The University of Maryland School of Medicine, Baltimore, MD, USA

Amplification and overexpression of putative oncogenes confer growth advantages for tumor development. We used a functional genomic approach that integrated simultaneous genomic and transcript microarray, proteomics, and tissue microarray analyses to directly identify putative oncogenes in lung adenocarcinoma. We first identified 183 genes with increases in both genomic copy number and transcript in six lung adenocarcinoma cell lines. Next, we used two-dimensional polyacrylamide gel electrophoresis and mass spectrometry to identify 42 proteins that were overexpressed in the cancer cells relative to normal cells. Comparing the 183 genes with the 42 proteins, we identified four genes – PRDX1, EEF1A2, CALR, and KCIP-1 – in which elevated protein expression correlated with both increased DNA copy number and increased transcript levels (all r > 0.84, two-sided P < 0.05). These findings were validated by Southern, Northern, and Western blotting. Specific inhibition of EEF1A2 and KCIP-1 expression with siRNA in the four cell lines tested suppressed proliferation and induced apoptosis. Parallel fluorescence in situ hybridization and immunohistochemical analyses of EEF1A2 and KCIP-1 in tissue microarrays from patients with lung adenocarcinoma showed that gene amplification was associated with high protein expression for both genes and that protein overexpression was related to tumor grade, disease stage, Ki-67 expression, and a shorter survival of patients. The amplification of EEF1A2 and KCIP-1 and the presence of overexpressed protein in tumor samples strongly suggest that these genes could be oncogenes and hence potential targets for diagnosis and therapy in lung adenocarcinoma. Oncogene (2006) 25, 2628–2635. doi:10.1038/sj.onc.1209289; published online 12 December 2005

Keywords: lung cancer; microarrays; proteomics; tissue microarray

Correspondence: Assistant Professor F Jiang, Department of Pathology, The University of Maryland School of Medicine, 10 South Pine Street, MSTF 7th floor, Baltimore, MD 21201-1192, USA.
E-mail: fjiang@som.umaryland.edu

Introduction

In lung adenocarcinoma, as in other types of cancer, gene amplification and the consequent overexpression of the amplified oncogene play an important role in the development of tumors, because their overexpression confers a growth advantage. The ability to identify putative oncogenes that are activated during tumorigenesis could facilitate the choice of molecular genetic targets for diagnosis and therapy of the disease. This concept has been exemplified by HER-2, which was first found to be amplified in neuroblastomas and subsequently shown to be associated with poor prognosis in breast cancer (Ross and Fletcher, 1999). Now, HER-2 aberrations are used as a predictor of response to therapy, and treatment of HER-2-positive breast cancer with the monoclonal anti-HER-2 antibody trastuzumab has been shown to improve prognosis (Ross and Fletcher, 1999). Emerging evidence of common amplicons in lung adenocarcinomas (Luk et al., 2001; Jiang et al., 2004; Tonon et al., 2005) suggests that additional oncogenes remain to be identified; however, conventional techniques are ineffective in pinpointing such oncogenes. Parallel measurement of DNA copy number and mRNA levels in cDNA microarrays permits changes in copy number to be compared with transcription levels on a gene-by-gene basis to generate lists of candidate genes within the defining amplicons (Hyman et al., 2002; Pollack et al., 2002). However, use of transcript patterns does not allow assessment of the expression of protein products or identification of proto-oncogenes. Another approach, identifying differentially expressed proteins by proteomic analysis and then comparing the proteins present with mRNA expression in cDNA microarrays from the same specimens, can clarify the extent to which changes in transcript patterns reflect changes in their cognate proteins and post-transcriptional mechanisms (Chen et al., 2002), but this approach cannot be used to identify oncogenes driven by extensive increases of their gene copy number. Moreover, using individual microarrays or proteomic approaches alone cannot distinguish the cancer-driving oncogenes that directly propel tumor progression from the larger number of passenger genes that may be concurrently over-represented but are not biologically relevant in tumor development.

In this study, we used a comprehensive approach that integrated simultaneous comparative genomic hybridization (CGH) and transcript microarray with proteomic analyses of six lung adenocarcinoma cell lines. We directly and specifically identified four putative oncogenes that could have been activated through amplification and consequent elevation of transcript expression. We used small interfering RNA (siRNA) to inhibit the expression of two of these four genes in the lung cancer cell lines, which further implicated them in oncogenesis. We then explored the clinical significance of these findings by assessing the expression of these two genes in tissue microarrays of human lung cancer specimens. Our findings underscore the power of integrated functional genomic analyses for identifying putative oncogenes in tumorigenesis; such activated genes could be useful as targets for diagnosis or therapy in lung cancer.

Results

Simultaneous global genomic and transcript analyses identify 183 genes with increases in genomic copy numbers and transcript expression levels

To identify genes in which increased DNA copy number might contribute to increased transcript in lung adenocarcinomas, first we used CGH with microarrays of six lung adenocarcinoma cell lines. We identified 587 genes showing increases in DNA copy number across all six cell lines (Supplementary Table 1S), which were distributed as 90 amplicons on all chromosomes except for chromosomes 13 and Y (Supplementary Table 2S). A subsequent transcript test with the identical arrays of the same cell lines revealed 275 genes that showed increased mRNA levels (Supplementary Table 3S). Using random permutation tests across all cancer cell lines, we identified 183 genes (31%) that showed elevated transcript levels from the 587 genes that were over-represented in the genome (Table 1), suggesting that elevated transcript levels of the 183 genes may reflect their genomic over-representation in the cancer cells. These findings are consistent with previous reports linking genomic changes with altered transcript patterns in breast cancer (Hyman et al., 2002; Pollack et al., 2002). However, our finding that only 31% of the genes showing increased DNA copy numbers had cognate increases in transcript expression in lung adenocarcinomas is different from the overall rates of 40–60% reported for breast cancer (Hyman et al., 2002; Pollack et al., 2002). This discordance may reflect methodologic differences between studies or biological differences between breast cancer and lung adenocarcinoma.

Proteomic analyses identify four genes for which protein abundance was associated with increases in the cognate gene and transcript levels

Analysis of transcript patterns is insufficient for understanding the expression of protein products and the effect of genomic over-representation on the expression

of their cognate proteins. To extend these findings beyond genomic over-representation to expression of the protein products of those genes, we next assessed protein expression in the same cell lines by two-dimensional polyacrylamide gel electrophoresis (PAGE) and found that 42 different proteins, representing 42 individual genes, were significantly increased in the cancer cell lines (Table 2; Supplementary Figures 1S and 2S). Some of these proteins were identified as having multiple isoforms, and all individual isoforms exhibited increases in expression ranging from 4.6 to 12.8 times their expression in normal lung tissue cells. In comparing protein level of the 42 genes with changes in their cognate genomic and mRNA expression from the global microarray analyses, we found that four (9.5%) of those 42 genes – PRDX1, EEF1A2, CALR, and KCIP-1 – showed statistically significant correlations between elevated protein expression and increases in both copy number and mRNA expression (all $r > 0.84$; $P < 0.05$) (Table 2) in the cancer cell lines. These findings imply that the abundance of these four proteins is attributable to the amplification and consequent elevated transcription of their cognate genes.

Validation of copy number, transcript, and protein expression of PRDX1, EEF1A2, CALR, and KCIP-1 in lung cancer cell lines

To confirm our findings from the high-throughput analyses, we next used Southern, Northern, and Western blotting to assess DNA, RNA, and protein levels for the four genes identified in the six cell lines. For comparison, we arbitrarily chose one gene, NFKB1, in which an increase in protein level did not correlate with genetic changes. Overall, we found excellent concordance between the CGH microarray and Southern blotting analyses, transcript array and Northern blotting analyses, and proteomic and Western blotting analyses for all five genes (Figure 1). For example, KCIP-1 showed fivefold amplification in five of the six cancer cell lines, whereas NFKB1 showed no such increase in any of the cell lines. As for transcript expression, Northern blotting of EEF1A2 showed high expression in five of the six cancer cell lines; again, levels of NFKB1 transcript were not increased in any cancer cell line as compared with normal bronchial epithelial cells. The results of Western blotting were also consistent with the results of the proteomic experiments; for example, five of the cancer cell lines exhibited strong protein bands for PRDX1 as compared with normal cells. These findings provide strong support for the validity of the results derived from the high-throughput techniques in this study.

These parallel analyses also revealed close correlations in the extent of changes in gene copies, transcript, and protein of each of the four genes in the cancer cell lines. For example, in the five cancer cell lines that showed at least fourfold increases in EEF1A2 copy number, expression of transcript and protein was also increased by at least a factor of four as well (relative to their expression in normal cells) (Supplementary Figure 3S). The protein abundance of the four genes showing

2630

Table 1 List of 183 genes with statistically significant correlation (0.05) between genomic copy number and transcript level

Gene symbol	Chro.	Distance from p arm of each chromosome (Mb)	α
ENO1	1	8.5	0.0085
DDOST	1	20.1	0.0111
SFN	1	26.4	0.0113
MLP	1	32.2	0.0114
AKR1A1	1	45.4	0.0128
PRDX1	1	45.4	0.0122
UQCRH	1	46.2	0.0125
RPL7	1	96.4	0.0127
COL11A1	1	102.6	0.0129
MCL1	1	147.3	0.0222
PSMB4	1	148.1	0.0131
JTB	1	150.7	0.0134
RPS27	1	150.7	0.0135
HAX1	1	151	0.0266
MUC1	1	151.9	0.0143
CCT3	1	153.1	0.0167
CRABP2	1	153.4	0.0148
TKT	1	159.3	0.0152
ATP1B1	1	165.8	0.0234
CHIT1	1	199.7	0.0154
SNRPE	1	200.2	0.0165
YWHAQ	2	9.6	0.0159
ODC1	2	10.60	0.0119
RPL31	2	101.20	0.0161
BENE	2	110.40	0.0169
STAT1	2	191.80	0.0175
HSPD1	2	198.30	0.0277
HSPE1	2	198.30	0.0185
RPL37A	2	217.30	0.0388
IGFBP2	2	217.50	0.0189
RPS7	2	3.30	0.0193
RAB1A	2	65.30	0.0204
IGKC	2	89.00	0.0285
LTF	3	46.3	0.0455
PFN2	3	151	0.0207
KPNA4	3	161.5	0.0211
S100P	4	6.7	0.1122
UGDH	4	39.3	0.0215
UCHL1	4	41.1	0.0222
SPP1	4	89.3	0.0227
TRIM2	4	154.7	0.0231
FGB	4	156	0.0235
FGG	4	156	0.0441
SDHA	5	0.251	0.0243
PDCD6	5	0.305	0.0245
CCT5	5	10.3	0.0446
PTPRF	5	14.2	0.0248
RPL37	5	40.8	0.0251
ENC1	5	74	0.0336
QP-C	5	132.2	0.0466
SPINK1	5	147.2	0.0256
CANX	5	179.2	0.0263
SOX4	6	21.7	0.0321
HDGF	6	22.6	0.0362
RPS10	6	34.6	0.0177
RPL10A	6	35.4	0.0369
VEGF	6	43.7	0.0372
OSF-2	6	45.4	0.0173
FSCN1	7	5.3	0.038
CYCS	7	24.9	0.0381
CBX3	7	25.9	0.0289
IGFBP3	7	45.7	0.0389
CLDN4	7	72.7	0.0403
HSPB1	7	75.5	0.0433
CALR	7	92.7	0.0425
COL1A2	7	93.6	0.0457
ATP5J2	7	98.7	0.0475
AKR1B10	7	133.6	0.0481

Table 1 (continued)

Gene symbol	Chro.	Distance from p arm of each chromosome (Mb)	α
RPS20	8	56.7	0.0482
TCEB1	8	74.6	0.0486
LAPTM4B	8	98.5	0.0497
RPL30	8	98.7	0.0054
KCIP-1	8	101.6	0.0093
PABPC1	8	101.78	0.0119
EEF1D	8	144.4	0.0121
TSTA3	8	144.5	0.0122
RPL8	8	145.6	0.0128
TRA1	9	117.1	0.0136
RPL35	9	121.1	0.0133
HSPA5	9	121.5	0.0135
LCN2	9	124.4	0.0137
DPP7	9	133.4	0.0139
PFKP	10	3.2	0.0223
AKR1C1	10	5.1	0.0146
PLAU	10	75.6	0.0356
DSP	10	76.7	0.0289
TALDO1	11	0.434	0.0143
SLC22A1L	11	2.9	0.0151
TSSC3	11	2.9	0.0611
RPL27A	11	8.7	0.0156
ST5	11	8.8	0.0162
LDHA	11	18.5	0.0168
MDK	11	46.4	0.0162
DOC-1R	11	67.5	0.0167
MMP12	11	102.8	0.0177
HYOU1	11	118.9	0.0183
SCNN1A	12	6.3	0.0185
LDHB	12	21.7	0.0193
KRT7	12	52.3	0.0196
KRT5	12	52.6	0.0197
KRT6E	12	52.6	0.0201
ERBB3	12	56.2	0.0212
NACA	12	56.8	0.0218
TM4SF3	12	71.2	0.0401
NTS	12	86.2	0.0215
ASCL1	12	103.3	0.0219
TXNRD1	12	104.6	0.0223
CKAP4	12	106.6	0.0124
COX6A1	12	120.7	0.0435
BGN	12	122.5	0.0235
RAN	12	129.88	0.0238
RPL36A	14	48.1	0.0243
PGD	14	50.7	0.0248
THBS2	15	37.5	0.0251
TRAF4	15	38.3	0.0253
SPINT1	15	38.7	0.0254
RPL17	15	45.26	0.0411
PKM2	15	70.1	0.0258
IDH2	15	88.2	0.0211
RPL23A	16	0.377	0.0264
MSLN	16	0.753	0.0366
UBE2I	16	1.3	0.0271
RPS2	16	1.95	0.0281
CLDN9	16	3.1	0.0329
ARL6IP	16	18.7	0.0412
EIF3S8	16	28.3	0.0336
TUFM	16	28.9	0.0377
ALDOA	16	30.1	0.038
NME4	16	53.6	0.0381
GPR56	16	57.4	0.0386
CDH1	16	68.5	0.0289
NQO1	16	69.5	0.0396
SLC7A5	16	87.6	0.0397
APRT	16	88.6	0.0411
GALNS	16	88.6	0.0255
RPL13	16	89.3	0.0431
MCP	17	32.4	0.0465

Table 1 (continued)

Gene symbol	Chro.	Distance from p arm of each chromosome (Mb)	α
ERBB2	17	35.11	0.0483
JUP	17	39.8	0.0495
CRF	17	40.39	0.0505
RPL27	17	41.1	0.0046
NME1	17	46.59	0.0082
COL1A1	17	48.6	0.0108
ABCC3	17	49.1	0.0326
NME2	17	49.6	0.0111
RPL38	17	72.7	0.0117
SMT3H2	17	73.6	0.0119
SYNGR2	17	76.6	0.0122
LGALS3BP	17	77.4	0.0127
P4HB	17	80.3	0.0126
PPAP2C	19	0.221	0.0228
GPI	19	39.55	0.0145
HPN	19	40.2	0.0129
ZNF146	19	41.4	0.0131
SPINT2	19	43.4	0.0238
PSMD8	19	43.5	0.0132
YIF1P	19	43.5	0.0135
RPS16	19	44.6	0.0144
CEACAM5	19	46.9	0.0145
CEACAM6	19	46.9	0.0143
GIPR	19	50.8	0.0259
SNRPD2	19	50.9	0.0413
KDELR1	19	53.6	0.0152
RPL28	19	60.6	0.0156
RPS5	19	63.6	0.0267
TRIM28	19	63.7	0.0158
DAP	20	35.6	0.0166
TOP1	20	40.3	0.0172
UBE2C	20	45.1	0.0174
RPS21	20	61.6	0.0268
EEF1A2	20	62.8	0.0185
TFF3	21	42.6	0.0186
TFF1	21	42.7	0.0192
CSTB	21	44.1	0.0201
MIF	22	22.6	0.0202
XBP1	22	27.5	0.0204
PRDX4	X	22.9	0.0198
SYN1	X	46.3	0.0204
TIMP1	X	46.3	0.0209
PLP2	X	47.8	0.0212
MAGED1	X	50.3	0.0331
RPS4X	X	71	0.0124
SSR4	X	152.6	0.0232

corresponding increases in both DNA copy number and mRNA provides further evidence that these could be oncogenes, the activation of which is reflected by genomic amplification and consequent increases in transcript level in lung adenocarcinoma cell lines.

Specific inhibition of EEF1A2 and KCIP-1 expression by siRNAs led to decreased cell proliferation and induction of apoptosis

To further prove the oncogenic function of the identified genes in lung tumorigenesis, we used siRNAs to inhibit the endogenous expression of EEF1A2 and KCIP-1 protein in four lung cancer cell lines (H1563, H229, H522, and SK-LU). Transfection of the cancer cells with specific siRNAs reduced the level of EEF1A2 and KCIP-1 protein by 70–90% 48 h after transfection

(Supplementary Figure 4S). In contrast, EEF1A2 and KCIP-1 protein levels remained unchanged in mock-treated control cells and in cells transfected with a scrambled siRNA sequence. At 48 h after siRNA transfection, the percentage of proliferation of the transfected cancer cells was reduced to 15–30% as compared with 91–100% of cell proliferation of the same cell lines treated with PBS or scrambled siRNA (Supplementary Figure 5S). Apoptosis of siRNA-transfected cells was 27–34%, whereas only 4% of the same cell lines treated with PBS or scrambled siRNA showed apoptosis. These results strongly support an oncogenic role for the identified genes in lung cancer and confirm their potential usefulness as therapeutic targets for the disease.

Amplification and protein expression of KCIP-1 and EEF1A2 in lung tissue

To further validate these findings and to assess the possible clinical significance of the four potential putative oncogenes identified from the cell lines, we first applied fluorescence *in situ* hybridization and immuno-histochemical analysis, in parallel, to commercially available human lung tissue microarrays (Ambion, Austin, TX, USA) to evaluate the status of two of these four genes in lung cancer tissue specimens. (Commercially available antibodies to PRDX1 or CALR were not suitable for use in immunohistochemical analysis when this report was written.) Overexpression of KCIP-1 and EEF1A2 protein in the tumors was concordant with amplification of the corresponding genes ($P = 0.0003$ for KCIP-1 and $P = 0.0011$ for EEF1A2). For example, 16 (35%) of the 46 lung adenocarcinomas in the microarray showed amplification of *KCIP-1*, and strong cytoplasmic staining for KCIP-1 protein was seen in 18 tumors (39%) (Figure 2). We next examined whether overexpression of these genes was associated with increased cell proliferation by analysing Ki-67 expression in contiguous sections of the tissue micro-arrays. Positive Ki-67 expression was found to correlate with positive expression of both KCIP-1 ($P = 0.02$) and EEF1A2 ($P = 0.01$). To extend these findings, we then studied 11 tissue microarray blocks comprising normal and tumor tissue specimens from 113 patients with pathologic stage I non-small-cell lung cancer who had undergone curative surgery (Wang et al., 2005). Immunohistochemical analysis showed that EEF1A2 was expressed in 32 cases (28%) and KCIP-1 in 29 cases (26%). Univariate and multivariate Cox proportional hazards models were used to detect possible associations between EEF1A2 and KCIP-1 expression and clinico-pathologic variables. Expression of EEF1A2 or KCIP-1 was associated with short overall survival time ($P = 0.0012$ for EEF1A2 and $P = 0.0026$ for KCIP-1) (Supplementary Figure 6S). Age at diagnosis, histologic type of cancer, degree of tumor differentiation, and smoking history were not associated with survival time.

Although only two genes were validated in the lung tissue microarrays (because available antibodies to the other two genes were not suitable for use in

Table 2 Proteins showing significant overexpression in cancer cell lines relative to those in normal bronchial epithelial cell lines and their correlation coefficients with increased DNA copy number or mRNA values*

Acc. no.	Gene ID	Gene	Mw/pI	Description	r with genomic copy changes[b]	r with mRNA changes[b]
Q06830	5052	PRDX1	48.4/5.4	Peroxiredoxin 1	0.92364	0.91892
Q05639	1917	EEF1A2	50.5/5.7	Eukaryotic translation elongation factor 1 alpha 2	0.90218	0.89456
P27797	811	CALR	61/5.5	Calreticulin	0.84128	0.86434
P63104	7534	KCIP-1	27/6.5	Tyrosine 3-monooxygenase activation protein, zeta	0.84467	0.85499
P07237	5034	P4HB	54/6.2	Procollagen-proline, 2-oxoglutarate 4-dioxygenase	0.91884	0.76786
Q04695	3872	KRT17	48.0/4.9	Keratin 17	0.00236	0.86892
P09211	2950	GSTP1	23.2/4.7	Glutathione S-transferase pi	0.84218	0.69456
P17936	3486	IGFBP-3	31.6/5.8	Insulin-like growth-factor binding protein 3	0.06412	0.16434
P26641	1937	EEF1G	50/6.4	Eukaryotic translation elongation factor 1 gamma	0.00446	0.85549
P08727	3880	KRT19	44.1/5.2	Keratin 19	−0.04884	0.86786
P04792	3315	HSPB1	22/6.5	Heat shock 27 kDa protein 1	0.00364	0.31892
P00558	5230	PGK1	44.5/4.2	Phosphoglycerate kinase 1	0.50402	0.79456
Q01995	5876	TAGLN	22.5/4.3	Transgelin	−0.34128	−0.26434
P08631	3055	JTK9	59.5/6.8	Hemopoietic cell kinase	−0.01446	0.02549
P09382	3956	LGALS1	16/5.5	Galectin-1, galactoside-binding, soluble, 1	0.026623	0.01123
Q92784	8110	DPF3	25.8/4.8	D4, zinc and double PHD fingers, family 3	0.094884	−0.03214
P54257	9001	HAP1	75.5/6.5	Huntington-associated protein 1	0.12364	−0.08108
P05783	3875	KRT18	48/5.3	Keratin 18	0.010218	0.60544
P05787	3856	KRT8	9.2/4.4	Keratin 8	0.041280	0.84566
P00738	3240	HP	55.2/6.2	Haptoglobin	0.044679	−0.14501
P09769	2268	FGR	59.5/5.2	Gardner-Rasheed feline sarcoma viral oncogene homolog	0.031264	−0.13789
P19838	4790	NFKB1	50.4/6.3	Nuclear factor of kappa light gene enhancer in B-cells 1	0.04467	−0.14501
P29034	6273	S100A2	10.9/4.6	S100 calcium-binding protein A2	0.87964	0.243214
Q13105	7709	ZBTB17	87.9/5.3	Zinc-finger and BTB domain containing 17	−0.17636	0.048108
Q00987	4193	MDM2	75.2/4.8	Transformed 3T3 cell double minute 2	−0.19782	−0.50544
P27816	4134	MAP4	111/5.4	Microtubule-associated protein 4	0.25872	−0.05356
P52732	3832	KIF11	119.2/6.2	Kinesin family member 11	−0.25778	−0.53444
P25205	4172	MCM3	90.9/5.5	Minichromosome maintenance deficient 3	0.25644	0.053666
P08631	3055	HCK	59.5/5.7	Hemopoietic cell kinase	0.65533	0.054501
P09237	4316	MMP7	22.6/5.8	Matrix metalloproteinase 7	0.234987	0.876820
P30305	994	CDC25B	64.9/4.5	Cell division cycle 25B	0.045116	0.283214
P50290	998	CDC42	21.3/6.1	Cell division cycle 42 (GTP-binding protein, 25 kDa)	−0.47636	0.088108
P61586	387	RHOA	19.8/6.9	Ras homolog gene family, member A	−0.49782	−0.00544
P63000	5879	RAC1	21.5/6.8	Ras-related C3 botulinum toxin substrate 1	−0.05583	−0.03566
P07437	203068	TUBB	49.6/6.5	Tubulin, beta polypeptide	0.255533	0.145010
P24864	898	CCNE1	47.1/4.3	Cyclin E1	−0.65116	0.232149
P04141	1437	CSF2	16.9/6.3	Colony stimulating factor 2 (granulocyte-macrophage)	−0.64636	−1.28108
P28072	5694	PSMB6	25.3/5.2	Proteasome (prosome, macropain) subunit, beta type, 6	−0.69782	−1.30544
P00352	216	ALD-H1A1	54.7/4.3	Aldehyde dehydrogenase 1 family, member A1	−0.75872	0.03356
Q03013	2948	GTM4	25.3/5.0	Glutathione S-transferase M4	−0.78533	0.134501
P63241	1984	EIF5A	10/4.4	Eukaryotic translation initiation factor 5A	−0.97893	−1.44321
Q01469	2171	EFABP	18.0/4.2	Fatty acid-binding protein 5	0.25684	−0.36432

*Only the gene showing statistically significant increased protein expression with increases in both genomic copy number and transcript simultaneously will be considered as potential putative oncogene in lung adenocarcinoma cells. [b]r, Spearman correlation coefficients between proteins and genomic or mRNA values are based on all six cancer cell lines; bold indicates P<0.05, if r>0.84000. Mw, molecular weight; pI, isoelectric point.

immunohistochemical analysis), these findings are consistent with those from our cell lines, demonstrating again that genomic amplification and consequent increases in amounts of transcript may be, at least in part, driving the abundance of proteins in these lung tumors. The association between expression of these genes and that of Ki-67, a known indicator of poor prognosis in lung cancer (Martin et al., 2004), suggests that activation of these genes may be an indicator of tumor aggressiveness. These results also suggest that expression of EEF1A2 and KCIP-1 proteins in stage I non-small-cell lung cancer may be useful as a marker for distinguishing patients with relatively poor prognosis from those who might benefit from adjuvant treatment.

Discussion

Our current study illustrates the power of integrated functional genomic analyses for identifying putative oncogenes and for evaluating their potential clinical significance. Among the four identified oncogenes, three genes (PRDX1, CALR, and KCIP-1) have been implicated in lung tumorigenesis. PRDX1 is an antioxidant protein involved in regulating cell proliferation, differentiation, and apoptosis. Kim et al. (2003) found PRDX1 expression to be elevated in both lung cancer and adjacent normal lung tissue, suggesting that activation of PRDX1 may enhance proliferation in lung cancer. CALR has a major role in Ca^{2+} binding and the
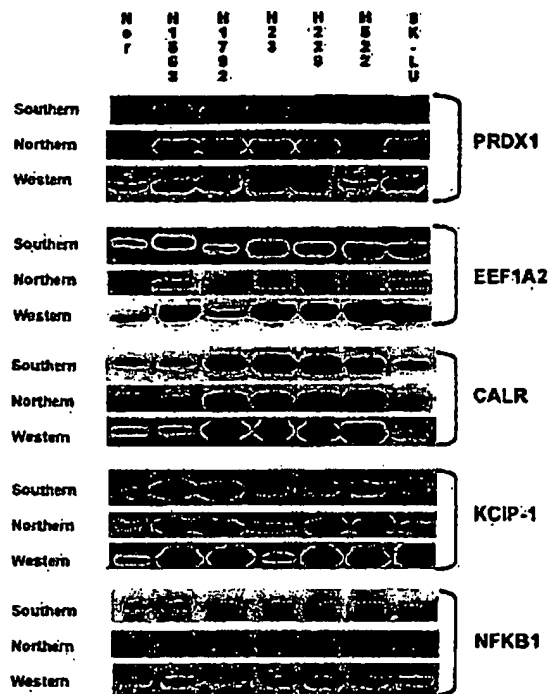
Figure 1 Confirmation by Southern, Northern, and Western blot analyses of increased DNA copies, transcript levels, and protein levels in the four genes identified in high-throughput analyses. For comparison, we arbitrarily chose one gene, *NFKB1*, in which an increased protein level did not correlate with genetic changes. The blotting results are consistent with the results from the CGH array, transcript array, and proteomic analyses. Nor, indicates normal bronchial epithelial cell line. All the experiments were repeated at least three times with each cell line. Means of normalized to β-actin signal intensities on Southern, Northern, and Western blots, along with 95% confidence intervals, were calculated (β-actin signals are not shown in the figure; two different normal bronchial epithelial cell lines were used in the confirmation and only one normal cell line is shown in the figure).

transcriptional regulation of other genes and was recently found to be overexpressed in 73% of 40 lung adenocarcinomas (Oates and Edwards, 2000). *KCIP-1* belongs to the 14-3-3 family, which participates via the MAPK and Wnt signaling pathways in the regulation of many cellular processes including cell proliferation and differentiation as well as tumorigenesis (Thomas *et al.*, 2005). *KCIP-1* was recently found to be expressed in all 12 lung tumors tested in a single-institution study (Qi *et al.*, 2005). Interestingly, *EEF1A2* was originally considered a putative oncogene in ovarian cancer on the basis of its being amplified in 25% and over-expressed in 30% of the same set of ovarian tumors (Anand *et al.*, 2002); functional analyses have established its oncogenic role in cellular transformation (Lee, 2003). Our discovery that *EEF1A2* may be a putative oncogene in lung adenocarcinoma demonstrates the power of our functional genomic strategy for rapidly identifying potential oncogenes.

Although the main focus of this study was to specifically identify putative oncogenes, it should be

noted that 90.7% of the genes showing high protein expression did not show corresponding increases in both DNA copy number and transcript, a finding consistent with that of others that transcriptional, translational, and post-translational regulatory mechanisms can greatly influence the abundance of protein in lung tumorigenesis (Chen *et al.*, 2002). For example, *NFKB1* is a critical arbiter of immune responses, cell survival, and transformation and is often activated in several types of tumors (Chen *et al.*, 2002). Deregulation of *NFKB1* is thought to be modulated through phosphorylation of Ser337 by protein kinase A (Chen *et al.*, 2002). In our study, 68.8% of the genes showing over-representation in the genome did not show elevated transcript levels, implying that at least some of these genes are 'passenger' genes that are concurrently amplified because of their location with respect to amplicons but lack biological relevance in terms of the development of lung adenocarcinoma.

Although the potential oncogenes we identified here are likely to be important, certainly other oncogenes could be involved in the development of lung adenocarcinoma. The oligo microarray we used consists of 22 000 probes, which represent only about 60% of the human genome. Moreover, each probe was designed for the 3′ region of expressed sequence tags of the selected genes. Also, our results were initially derived from cancer cell lines, although the findings were later confirmed in human tissue samples. Our ongoing study using microarrays with information on more genes and the development of high-resolution proteomic analyses for use with larger numbers of specimens will allow more comprehensive analyses of the molecular consequences of gene amplifications. Such expanded analyses will very likely lead to the identification of additional oncogenes.

Some of the results of our current study were comparable to those of other studies of lung cancer. For example, genomic copy number and protein levels of KCIP-1 were previously found to be amplified and overexpressed in primary lung cancers by cDNA clone-based CGH array analysis (Jiang *et al.*, 2004) and proteomic analysis (Chen *et al.*, 2002), respectively. Our functional genomic approach, which integrates simultaneous CGH, transcript microarrys, proteomic analyses, and siRNA, allows us not only to quickly identify potential oncogenes but also to explore their significance as diagnostic and therapeutic targets in tumor progression – more than could be achieved by any technique alone.

Genes identified in this way may serve as promising targets for diagnosis and therapy in lung adenocarcinoma. Further research on the clinical implications of such genes is needed; experiments now underway in our laboratory include overexpression of the genes in normal cells, disruption of the function of these genes in cancer cells, and investigation of how interactions among these genes (or interactions with other known oncogenes) may mediate the expression of the transformed phenotype.
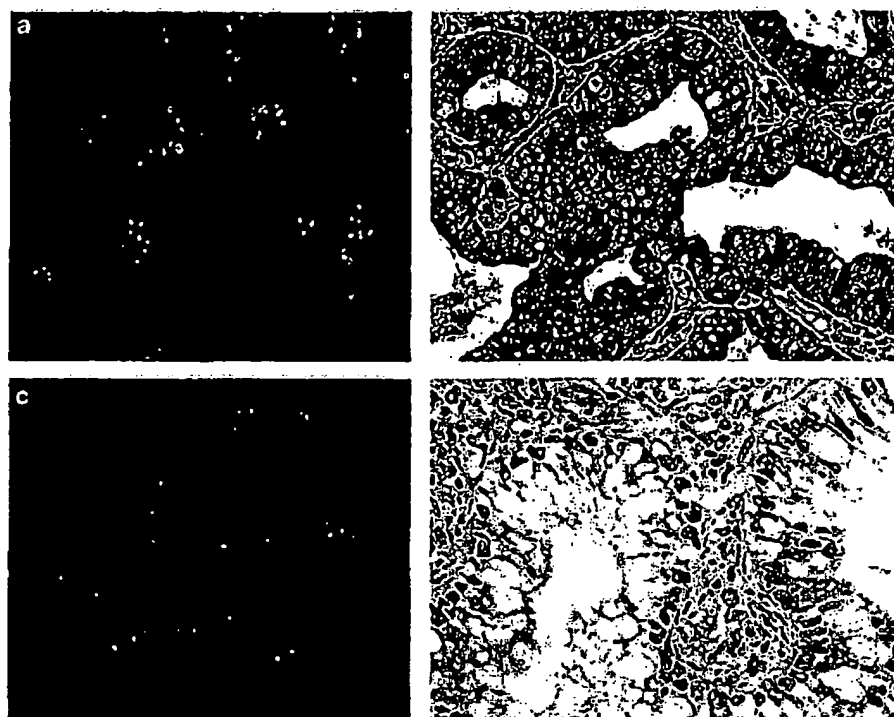
Figure 2   *EEF1A2* amplification is associated with high EEF1A2 protein expression in lung adenocarcinomas. (a) Cells from a lung adenocarcinoma sample in which *EEF1A2* is amplified show more green signals (*EEF1A2*) than red signals (chromosome 20 centromeric probe) (original magnification, x 400). (b) Immunohistochemical staining of cells from the same tissue sample as in panel a shows strong EEF1A2 staining in the cytoplasm. (c) A lung adenocarcinoma sample with two copies of *EEF1A2* and chromosome 20 centromeric probe, indicating no *EEF1A2* amplification (original magnification, x 400). (d) Immunohistochemical staining of cells from the same tissue sample as in panel c shows negative staining for EEF1A2.

Materials and methods

Cell lines

Six human lung adenocarcinoma cell lines (H23, H229, H1792, SK-LU-1, H522, and H1563) were obtained from the American Type Culture Collection (Manassas, VA, USA). Two normal bronchial epithelial cell lines were obtained from Clontech (Palo Alto, CA, USA). Genomic DNA, mRNA, and protein were derived from a single harvest of these cells.

DNA and RNA profiles by microarray analysis

Genomic DNA labeling and hybridization were performed as described previously (Barrett *et al.*, 2004) with Agilent's Human 1A Oligo Microarray (V2) (Agilent Technologies, Palo Alto, CA, USA), which contains 22 000 unique 60-mer oligos. Details of the protocol for analysing transcripts are available at http://www.chem.agilent.com. Map positions for arrayed genes were assigned by identifying the DNA sequence represented in the UniGene cluster and matching it with the Golden Path genome assembly (http://genome.ucsc.edu/; Mat 7, 2004 Freeze). Microarray images of DNA copy number and expression were analysed by using AgilentCGH Analytics and Feature Extraction software. DNA copy number profiles that deviated significantly from background signal ratios (measured from normal control cell hybridization, as described elsewhere; Barrett *et al.*, 2004) were interpreted as evidence of true differences in DNA copy number. The criteria for defining genomic over-representation and amplicons are described elsewhere (Hyman *et al.*, 2002); details are given in the

Supplementary Information. An increase in mRNA level was defined as a twofold increase in signal ratio relative to that of the control ($\log_2 > 1$).

Quantitative two-dimensional PAGE and mass spectrometry

Analysis of proteins by two-dimensional PAGE and their identification by mass spectrometry were performed as previously described (Shen *et al.*, 2004). Briefly, protein pellets were solubilized in rehydration buffer, after which the first-dimension isoelectric focusing was carried out with a Protean IEF Cell (Bio-Rad Laboratories) and the second-dimension separation was carried out with Bio-Rad's Ready Gel Precast Gels and the Bio-Rad Criterion Cell apparatus. Protein spots were visualized by silver-based staining, and all gels were assessed with Bio-Rad's PDQuest 2D gel image analysis software. Selected spots were subjected to in-gel tryptic digestion and analysed on a Voyager-DE PRO matrix-assisted laser desorption ionization/time-of-flight mass spectrometer (Applied Biosystems, Foster City, CA, USA). The mass list of the 20 most intense monoisotopic peaks for each sample was entered in the MS-Fit search program (v3.2.1) (http://prospector.ucsf.edu/ucsfhtml4.0/msfit.htm) and searched in the National Center for Biotechnology Information protein database.

Southern, Northern, and Western blot analyses

Southern, Northern, and Western blot hybridizations were performed according to standard protocols. cDNA clones for the tested genes were purchased from Invitrogen (Carlsbad,

CA, USA) and prepared as probes for the blot hybridizations. Antibodies used were obtained as follows: PRDX1, CALR, NFKB1, KCIP-1, and β-actin from Santa Cruz Biotechnology (Santa Cruz, CA, USA); and EEF1A2 from Upstate Biotechnology (Waltham, MA, USA).

Fluorescence in situ hybridization and immunohistochemical analyses of lung tissue microarrays

Fluorescence *in situ* hybridizations and immunohistochemical analyses of KCIP-1 and EEF1A2 were carried out as described elsewhere (Jiang *et al.*, 2002; Wang *et al.*, 2005) with Lung Tissue Microarrays (Ambion, Austin, TX, USA) and 11 homemade microarray blocks containing tissue samples from 113 patients with pathologic stage I non-small-cell lung cancer (Wang *et al.*, 2005). DNA probes specific for *KCIP-1* and *EEF1A2* were obtained by screening a Human BAC Clone library (Invitrogen) by polymerase chain reaction as described previously (Jiang *et al.*, 2002). The antibodies used for the immunohistochemical analyses were the same as those used for the Western blotting. Cell proliferation of the lung tissues was assessed with a Ki-67 monoclonal antibody from Santa Cruz Biotechnology. Definitions of the cutoff value for a positive result of each antibody are shown in Supplementary Information.

siRNA transfection, cellular proliferation assay, and apoptosis analysis

Transfections were carried out by using siPORT Lipid Transfection Agent (Ambion) with siRNAs targeting KCIP-1 or EEF1A2 or with a scrambled siRNA duplex (siControl) (Dharmacon Inc., Lafayette, CO, USA), with PBS used as a negative control (Jiang *et al.*, 2002). Cells were fixed 24, 48, or 96 h later and subjected to further tests. All siRNAs were prepared by using a transcription-based method with Silencer siRNA according to the manufacturer's instructions (Ambion). Sequences of the individual siRNAs are listed in Supplementary Table 4S. Inhibition of cell growth by the

siRNAs was determined by MTT staining, and cell growth rate was plotted against the percentage of viable cells in the saline-treated controls (a value arbitrarily set at 100%) (Jiang *et al.*, 2002). Apoptosis was analysed by fluorescence cell cycle analysis of terminal deoxynucleotidyl transferase-mediated dUTP nick-end labeling with FITC-labeled dUTP (Boehringer Mannheim Biochemicals, Mannheim, Germany) (Jiang *et al.*, 2005).

Statistical analyses

Relationships between gene copy number and mRNA level were examined as described elsewhere (Hyman *et al.*, 2002, Supplementary Information). Correlations between protein abundance and DNA copy number and mRNA expression of the corresponding genes were evaluated with the Spearman correlation coefficient. Fisher's exact test and χ^2-tests were used to analyse associations between amplification and expression of the candidate genes with various histopathologic variables of the samples in the tissue microarrays. Univariate and multivariate analyses were carried out with Cox's proportional hazards model to determine which independent factors might have a joint significant influence on survival. A P-value $\leqslant 0.05$ was considered statistically significant; all statistical tests were based on a two-sided significance level.

References

Anand N, Murthy S, Amann G, Wernick M, Porter LA, Cukier IH *et al.* (2002). *Nat Genet* **31**: 301–305.

Barrett MT, Scheffer A, Ben-Dor A, Sampas N, Lipson D, Kincaid R *et al.* (2004). *Proc Natl Acad Sci USA* **101**: 17765–17770.

Chen G, Gharib TG, Huang CC, Taylor JM, Misek DE, Kardia SL *et al.* (2002). *Mol Cell Proteomics* **1**: 304–313.

Hyman E, Kauraniemi P, Hautaniemi S, Wolf M, Mousses S, Rozenblum E *et al.* (2002). *Cancer Res* **62**: 6240–6245.

Jiang F, Caraway NP, Li RY, Katz RL. (2005). *Oncogene* **24**: 3409–3418.

Jiang F, Lin F, Price R, Gu J, Medeiros LJ, Zhang HZ *et al.* (2002). *J Mol Diagn* **4**: 144–149.

Jiang F, Yin Z, Caraway NP, Li R, Katz RL. (2004). *Neoplasia (New York)* **6**: 623–635.

Kim HJ, Chae HZ, Kim YJ, Kim YH, Hwangs TS, Park EM *et al.* (2003). *Cell Biol Toxicol* **19**: 285–298.

Lee JM. (2003). *Reprod Biol Endocrinol* **1**: 69–73.

Luk C, Tsao MS, Bayani J, Shepherd F, Squire JA. (2001). *Cancer Genet Cytogenet* **125**: 87–99.

Martin B, Paesmans M, Mascaux C, Berghmans T, Lothaire P, Meert AP *et al.* (2004). *Br J Cancer* **91**: 2018–2225.

Oates J, Edwards C. (2000). *Histopathology* **36**: 341–347.

Pollack JR, Sorlie T, Perou CM, Rees CA, Jeffrey SS, Lonning PE *et al.* (2002). *Proc Natl Acad Sci USA* **99**: 12963–12968.

Qi W, Liu X, Qiao D, Martinez JD. (2005). *Int J Cancer* **113**: 359–363.

Ross JS, Fletcher JA. (1999). *Semin Cancer Biol* **9**: 125–138.

Shen J, Person MD, Zhu J, Abbruzzese JL, Li D. (2004). *Cancer Res* **64**: 9018–9026.

Thomas D, Guthridge M, Woodcock J, Lopez A. (2005). *Curr Top Dev Biol* **67**: 285–303.

Tonon G, Wong KK, Maulik G, Brennan C, Feng B, Zhang Y *et al.* (2005). *Proc Natl Acad Sci USA* **102**: 9625–9630.

Wang H, Zhang Z, Li R, Ang KK, Zhang H, Caraway NP *et al.* (2005). *Int J Cancer* **116**: 285–290.

Supplementary Information accompanies the paper on Oncogene website (http://www.nature.com/onc)